



Advanced Fuels Campaign 2022 Accomplishments

November 2022

Changing the World's Energy Future

Phyllis L King, Heather D Medema



INL is a U.S. Department of Energy National Laboratory operated by Battelle Energy Alliance, LLC

DISCLAIMER

This information was prepared as an account of work sponsored by an agency of the U.S. Government. Neither the U.S. Government nor any agency thereof, nor any of their employees, makes any warranty, expressed or implied, or assumes any legal liability or responsibility for the accuracy, completeness, or usefulness, of any information, apparatus, product, or process disclosed, or represents that its use would not infringe privately owned rights. References herein to any specific commercial product, process, or service by trade name, trade mark, manufacturer, or otherwise, does not necessarily constitute or imply its endorsement, recommendation, or favoring by the U.S. Government or any agency thereof. The views and opinions of authors expressed herein do not necessarily state or reflect those of the U.S. Government or any agency thereof.

Advanced Fuels Campaign 2022 Accomplishments

Phyllis L King, Heather D Medema

November 2022

**Idaho National Laboratory
Idaho Falls, Idaho 83415**

<http://www.inl.gov>

**Prepared for the
U.S. Department of Energy
Under DOE Idaho Operations Office
Contract DE-AC07-05ID14517**



ADVANCED FUELS CAMPAIGN 2022 Accomplishments





15 TON

NET 460 LBS

CAUTION
PINCH HAZARD
DO NOT ENTER
AREA
WHEN UNCHARGED
EQUIPMENT IS IN
MOTION

Nuclear Fuels Cycle & Supply Chain

Advanced Fuels Campaign 2022 Accomplishments

INL/MIS-22-69876


November 15, 2022

Compiled and edited by:



Phyllis King

11-17-2022



Heather Medema

11-17-2022

Approved by:



Daniel Wachs, FCRD AFC National Technical Director

11-17-2022



TABLE OF CONTENTS

1

ADVANCED FUELS COMPLEX MANAGEMENT AND INTEGRATION

1.1	Advanced Fuels Campaign Leadership Team.....	10
1.2	From the Director	12
1.3	Accident Tolerant Fuels — A Perspective by Frank Goldner	14
1.4	Capabilities	20
	ATF-2 Historical Accomplishments	20

2

ADVANCED LIGHT WATER REACTOR FUELS OVERVIEW

2.1	LWR Fuel Fabrication and Properties	24
2.2	LWR Core Materials	26
	Microstructure evaluation of pre and post LOCA HBU fuel	26
	Summarizing Effect of Coating Thickness and Condition on Behavior of Zr Cladding	30
	Microstructure-Based Benchmarking for Nano/Microscale Tension and Ductility Testing of Irradiated Steels.....	34
	Bridging the Length Scales on Mechanical Property Evaluation.....	40
	Bridging Microscale to Macroscale Mechanical Property Measurements and Predication of Performance Limitation for FeCrAl Alloys Under Extreme Reactor Applications	44
	Benchmarking Microscale Ductility Measurements.....	48
	Understanding of degradation of SiC/SiC materials in nuclear systems and development of mitigation strategies	52
	Multiaxial Failure Envelopes and Uncertainty Quantification of Nuclear-Grade SiCf/SiC Woven Ceramic Matrix Tubular Composites.....	56

TABLE OF CONTENTS - *CONTINUED*

	Mechanistic Understanding of Radiolytically Assisted Hydrothermal Corrosion of SiC in LWR Coolant Environments	60
	Probabilistic Failure Criterion of SiC/SiC Composites Under Multi-Axial Loading	66
	Development of Multi-Axial Failure Criteria for Nuclear Grade SiCf-SiCm Composites	70
	Advanced Coating and Surface Modification Technologies for SiC-SiC Composite for Hydrothermal Corrosion Protection in LWR	72
2.3	LWR Irradiation Testing and PIE Techniques	78
	Ring Tension Testing	78
2.4	LWR Fuel Safety Testing	82
	Resumption of Water-based RIA Testing in the U.S.	82
	Combined TREAT-SATS LOCA Test Plan with Industry Consensus	86
	Design of Severe Accident Test Station Fission Gas Release Capability	88
	Report Summarizing Progress in Digital Image Correlation Analysis of Burst Phenomenon	92
	Demonstration of a Transient Heating and Visualization System to Collect and Characterize Fission Gas Release on Irradiated Nuclear Fuel	96
2.5	LWR Computational Analysis	100
2.6	Accident Tolerant Fuel Industry Advisory Committee	102
2.7	ATF Industry Teams	104
	Westinghouse Electric Company LLC	106
	Framatome	110
	General Electric	114
	GA	118

3 ADVANCED REACTOR FUELS

Thermal Conductivity of Irradiated Binary Metallic Fuels	122
AFC-FAST Irradiation and Initial PIE	126
Initial Fast Reactor Fuel Transient Irradiations: In-Pile Data and Initial Findings	130
AR Computational Analysis	134
Results of a Trade Study on Design and Fabrication Candidates for Sodium Free Metallic Fuel	136

4 CAPABILITY DEVELOPMENT

In-reactor LOCA Testing Capability	142
Summary of I-Loop Status and Accomplishments	144
Refabrication of fuel rods for follow-on testing	148
Final design of the LOCA test commissioning series in TREAT	152
Remote Handling and Assembly of the THOR Capsule for Transient Testing Irradiated Fast Reactor Fuels	156
A Strategy for Establishing a Fast Reactor Testbed without a Domestic Fast Spectrum Test Reactor	160

5 APPENDIX

5.1 Publications	164
5.2 FY-22 Level 2 Milestones	172
5.3 AFC Nuclear Energy University Projects (NEUP) Grants	174
5.4 Acronyms	180
5.5 Divider Photo Captions	190



FUEL
HANDLING CASE

CTFW-D
T-MWH-0007

NST
T-MWH-0201

MWH-0002

CAUTION RADIOACTIVE MATERIAL
FUEL HANDLING CASE



AFC MANAGEMENT AND INTEGRATION

- 1.1 Advanced Fuels Campaign Leadership Team
- 1.2 From the Director
- 1.3 Accident Tolerant Fuels –
A Perspective by Frank Goldner
- 1.4 Capabilities

1.1 ADVANCED FUELS CAMPAIGN LEADERSHIP TEAM

Daniel Wachs

National Technical Director
(208) 526-6393
daniel.wachs@inl.gov



Edward Mai

Deputy National Technical Director
(208) 526-2141
edward.mai@inl.gov



Todd Pavey

TREAT Project Management
(208) 526-9023
todd.pavey@inl.gov



Kory Linton

ORNL Project Management
(865) 241-2767
lintonkd@ornl.gov



David Kamerman

ATF Qualification Lead
(208) 526-3128
david.kamerman@inl.gov



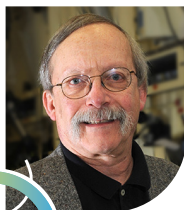
Nathan Capps

High Burnup Qualification Lead
(865) 341-0458
cappsna@ornl.gov



Douglas Porter

Advanced Reactors Focus Lead
(208) 533-7659
douglas.porter@inl.gov



Josh White

Fabrication and Properties Technical Lead
(505) 667-3879
jtwhite@lanl.gov



Pavel Medvedev
Performance Assessment
Technical Lead
(208) 526-7299
pavel.medvedev@inl.gov



Colby Jensen
Safety Testing Technical Lead
(208) 526-4294
colby.jensen@inl.gov



Michael Todosow
Technology Assessment
Strategic Lead
(631) 344-2445
todosowm@bnl.gov



Ed Beverly
Project Controls
(208) 533-7709
edward.beverly@inl.gov



Nicolas Woolstenhulme
Irradiation Testing Technical Lead;
Advanced Fuel Design Strategic Lead
(208) 526-1412
nicolas.woolstenhulme@inl.gov



Tarik Saleh
Core Materials Technical Lead
(505) 665-1670
tsaleh@lanl.gov



Fabiola Cappia
Nuclear Fuel Science Strategic Lead
(208) 533-7091
fabiola.cappia@inl.gov



Phyllis King
Systems Engineering Lead
(208) 526-4348
phyllis.king@inl.gov



Rebekah Thompson
Program Admin. & Executive Admin.
Assistant to the National Technical Lead
(208) 526-7956
rebekah.thompson@inl.gov

1.2 FROM THE DIRECTOR



Daniel Wachs
National Technical Director
(208) 526-6393
daniel.wachs@inl.gov

It's a great pleasure to open the 2022 Advanced Fuels Campaign (AFC) Accomplishments Report. While a report of this type is, by necessity, unable to comprehensively capture all the accomplishments made by this long standing, nationally relevant research and development (R&D) program, it is my hope that it reflects the quality and talent of the remarkable people that staff it and the world class scientific facilities they wield. Even in the face of a pandemic that curtailed many of our personal and collective routines for the two years prior and much of FY22, impactful research continued and the summaries that follow in this report provide clear evidence.

The mission of the AFC is to perform or support research, development, and demonstration activities that identify and mature innovative fuels, cladding materials, and associated technologies with the potential to improve the performance and enhance the safety of current and future reactors; increase the efficient utilization of nuclear energy resources; contribute to enhancing proliferation resistance of the nuclear fuel cycle; and address challenges related to waste management and ultimate disposal.

AFC pursues its mission objectives using a goal-oriented, science-based approach that seeks to establish a fundamental understanding of fuel and cladding behaviors under conditions that arise during fabrication, normal steady-state irradiation,

off-normal transient scenarios, and storage/disposal. This approach includes advancing the theoretical understanding of fuel behavior, conducting fundamental and integral experiments, and supporting the mechanistic, multi-scale modeling of nuclear fuels to inform and guide fuel development projects, advance the technological readiness of promising fuel candidates, and ultimately support fuel qualification and licensing initiatives.

This methodology is built on a foundation of 'analytical experiments' that merge advanced modeling and simulation with modern data-rich experimental methods to investigate the dominant physical phenomena associated with a given fuel system as necessary to drive its development to completion. AFC researchers utilize and evolve the nation's most important nuclear materials research capabilities, a comprehensive nuclear fuels testbed that spans multiple national laboratories, to serve this mission. These capabilities range from the world's premier nuclear materials test reactors - Advanced Test Reactor (ATR), High Flux Isotope Reactor (HFIR), and Transient Reactor Test Facility (TREAT) to state-of-the-art materials science instruments and manufacturing technologies. AFC works in close partnership with the Nuclear Energy Advanced Modeling and Simulation (NEAMS) program to implement advanced tools for modeling and simulation by collaborating on development of mechanistic fuel behavior models and conducting

experimental studies that inform and support assessment of its most advanced tools. AFC will also work closely with the Advanced Sensors and Instruments (ASI) program to develop and deploy new sensors and instruments in experiments that will allow researchers to directly observe the evolution of materials in representative severe environments. This represents a massive leap beyond the irradiate and observe model used historically to develop and qualify nuclear fuels (colloquially referred to as ‘cook and look’).

As an early adopter of these methodologies and tools, AFC is applying them to a variety of fuel development and qualification initiatives that crosscut the national nuclear research enterprise. Specifically, AFC objectives in the coming five-year horizon include:

1. Support the industry-led development of Accident Tolerant Fuel (ATF) technologies with improved reliability and performance under normal operations and enhanced tolerance to design basis and severe accident scenarios. This effort is expected to culminate with implementation of batch reloads of one or more near-term ATF concept(s) in commercial reactor(s) in the mid-2020’s;
2. Collaborate with industry and regulatory community to perform the R&D necessary to support extending the burnup of current commercial light water

reactor fuels from 62 to 75 GWd/MTU by 2026;

3. Lead research and development on innovative fuel and cladding technologies with applications to future advanced reactors, especially metallic fuels for fast-spectrum reactors, including reactors that utilize both once-through and recycle approaches to the fuel cycle;
4. Continue the development and demonstration of a multi-scale, science-based approach to fuel development and testing, and contribute to the establishment of a state-of-the-art R&D infrastructure necessary to accelerate the development of new fuel concepts; and
5. Collaborate with NEAMS and ASI on the execution of ‘analytical experiments’ that result in mechanistic fuel behavior and subsequent development and validation of multi-scale, multi-physics. Ultimately leading to increasingly predictive fuel performance models and codes.

Considering these critical missions, the AFC program is clearly a foundational component of the nuclear energy community’s response to increasing clean energy demand.

Sincerely,



Dan Wachs

1.3 ACCIDENT TOLERANT FUELS — A PERSPECTIVE BY FRANK GOLDNER

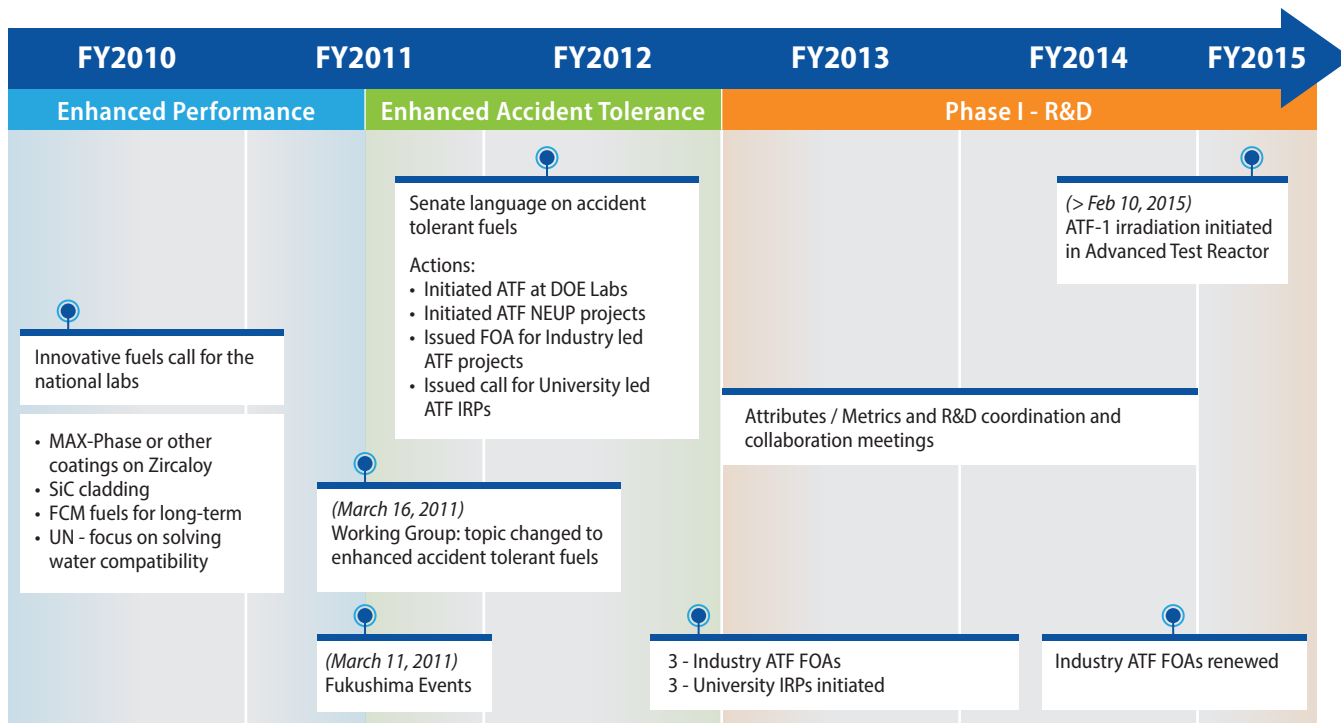
Before ATF

In 2009, at the suggestion of Kemal Pasamehmetoglu, our National Technology Director at that time, we issued a call to our nuclear laboratories for innovative nuclear fuels proposals. This started a two-year effort in which we evaluated quite a few very interested ideas and ultimately funded a few, but which also had significant industrial participation via a working group set up to effect the performance aspect of the effort. Fortuitously, this working group included the three light water reactor (LWR) fuel supply companies who later became the industry mainstay of our Accident Tolerant Fuel (ATF) program.

On March 16, 2011, a week after the Fukushima accident, during a routine working group status meeting, we unanimously agreed to change the focus of our working group from enhanced fuel performance to enhanced accident tolerance. Therefore, we were fortunate to be able to hit the ground running when Congress in 2012 gave Department of Energy (DOE) guidance to “... report to the Committee, within 90 days of enactment of the act, on its plan for development of meltdown resistant fuels leading to reactor testing and utilization by 2020.”

And Then There Was ATF

Although it was not until March 2015 before we delivered a fully government cleared report back to Congress, in 2013 we were able to effect a fully active ATF program with involvement of our key national laboratories, three key LWR fuel vendors, as well as effect important national and international cooperations. A 2014 Nuclear Regulatory Commission (NRC)–DOE Nuclear Safety Research MOU (ML14072A366) was modified with an addendum in 2017 to cover ATF safety research (ML17130A815). In 2014, under guidance of Kemal Pasamehmetoglu, Shannon Bragg-Sitton, and Jon Carmack we initiated socializing our ATF strategy with the Paris based Organisation for Economic Co-operation and Development (OECD) Nuclear Energy Agency (NEA), which resulted in a 367-page 2018 state-of-the art report on Light Water Reactor Accident-Tolerant Fuels (OECD 2018, NEA No. 7317). Significant involvement was also initiated in the US with the Nuclear Energy Institute, and the Electric Power Research Institute. In the last 10 years we have also had major involvement with numerous US universities as well as involvement with several important international nuclear energy initiatives in Europe, Russia, China, and Japan.



We Have Accomplished Much in Ten Years

I think we can all be very proud of how much we have accomplished since inception of the ATF program, a mere 10 years ago, including:

- ATF vendor candidates having effected lead rods irradiations in 8 commercial reactors, including one fully loaded Lead Test Assembly (LTA).
- Affected testing facility expansions at our main nuclear laboratories, including reactivation of Transient Reactor Test Facility (TREAT) and

significant capability expansions of Advanced Test Reactor (ATR) and High Flux Isotope Reactor (HFIR).

- Influenced the creation of ATF programs in most major nuclear countries, and continued support of ATF programs in the International Atomic Energy Agency (IAEA) and the Nuclear Energy Agency (NEA).
- Support of US universities via the Nuclear Energy University Project (NEUP) process, benefitting many students in their degree work and future job possibilities, while providing useful info to our program.

Figure 1. Accident Tolerant Fuel Related Activities Around the Time of the Fukushima Event



U.S. DEPARTMENT OF
ENERGY

Development of Light Water Reactor Fuels with Enhanced Accident Tolerance

Report to Congress
April 2015

United States Department of Energy
Washington, DC 20585

Figure 2. 2015 Report To Congress (RTC)



Figure 3. Strategic Overview in the RTC

- Success via the Small Business Innovation Research (SBIR) process of several Small Business Industrial developments, especially in the advanced clad development areas, such as related to silicon carbide and deposition of advanced clad coatings.
- Direct support of computer code modelling development at our national laboratories, the NRC and US industries.

The Future - Full of Possibilities for ATF Ideas to Impact LWR and non-LWR Developed Needs:

LWR Fuels:

Long-term advanced LWR fuel designs, s.a. non-zircaloy-clad concepts.

- Coolant chemistry issues, such as corrosion and crud formation.
- Reactor power uprates with associated fuel assembly design improvements.

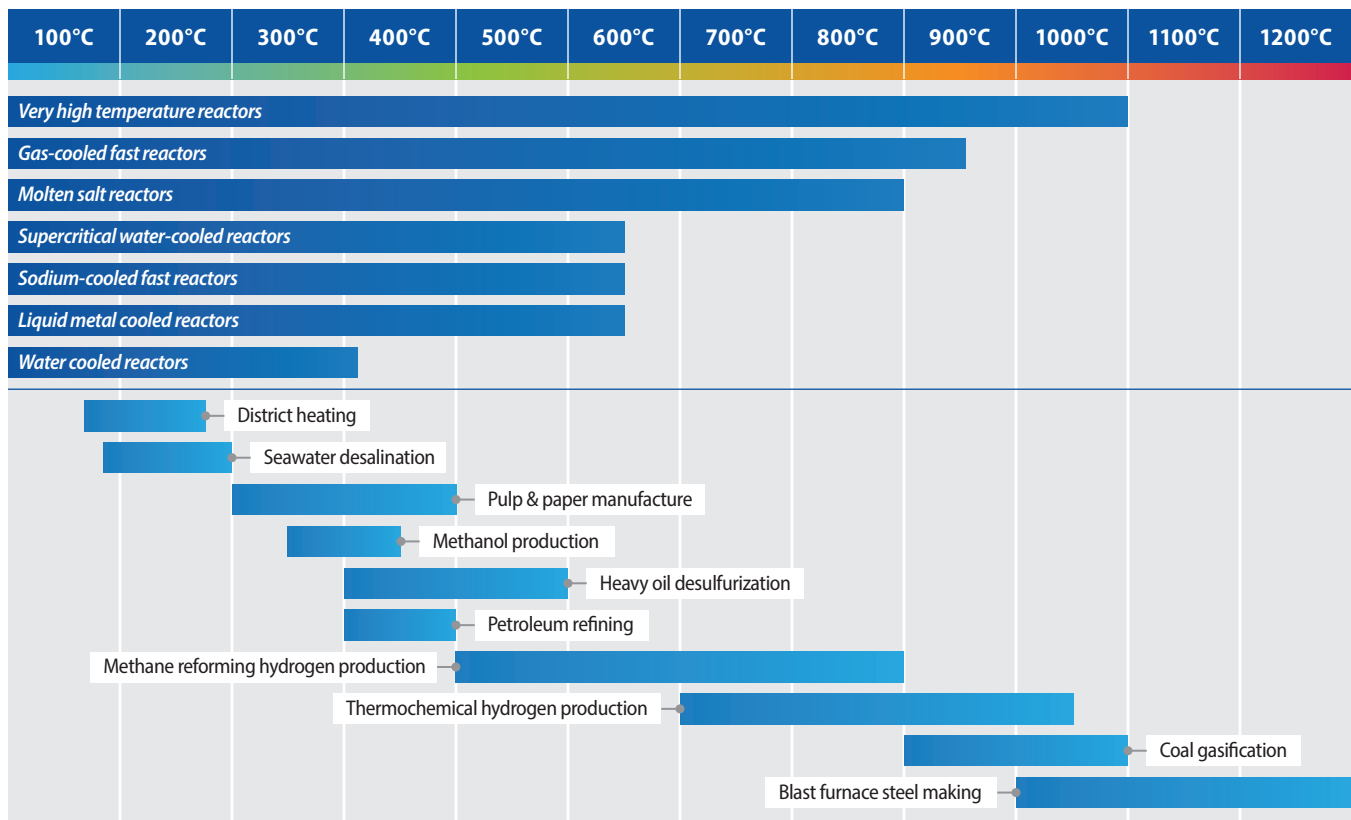


Figure 4. Temperature Ranges of Small Modular Reactor (SMR) Designs & Corresponding Non-Electric Applications (Ref: IAEA Advances in Small Modular Reactor Technology Developments, 2020)

- Advanced Fuel Cycle possibilities to further improve resource utilization.
- And always, safety enhancing feature developments.

Nuclear Reactors Fuels in General:

When one looks at the plethora of advanced reactor types and potential applications it seems intuitively obvious that ATF developments with associated lab capabilities and computer models can have a significant impact on our nation's energy development needs, in areas we are only now beginning to explore, or dream of.

Reference:

IAEA Advances in Small Modular Reactor Technology Developments, 2020

End Note:

I am honored to have been associated with this impressive program and the wonderful and brilliant people that have been, are currently, and will be involved in, as it continues to develop its possibilities and contribution to the sustainability and beneficial use of nuclear energy.

FG, 2022



1.4 CAPABILITIES

ATF-2 Historical Accomplishments

Principal Investigator: David Kamerman

Team Members/ Collaborator: Brian Durtschi, Nicolas Woolstenhulme, Bryon Curnutt, Travis Labossiere-Hickman, Richard Skifton, Fabiola Cappia

With less than half of the reactors that were available in the past, the United States LWR Testbed stands poised to support the same diversity of test conditions and data needs to support development of advanced LWR fuels and materials.

A fully prototypic testing platform for testing new light water reactor (LWR) accident tolerant fuel (ATF) designs has been established in a pressurized water loop in the center flux trap of Idaho National Laboratory's (INL's) Advanced Test Reactor (ATR). The irradiation experiment, named ATF-2, has completed seven cycles of prototypic steady-state irradiation of 45 test pins to burnups as high as 30 MWd/kgU. Irradiation conditions have been maintained via the Loop-2A pressurized water coolant loop and power and fast-neutron flux histories of each of the fueled forty-one test pins has been calculated using a combined Monte Carlo N-Particle (MCNP) and ORIGEN methodology.

Project Description:

The experiment design was required to support the irradiation testing needs of multiple ATF developers (e.g., fuel vendors)—all of whom have slightly different technologies, development timetables, and irradiation testing needs. To accommodate these changing test plans, the ATF-2 test train was designed with six tiers that are arranged axially over the length of the core. The incore portion of the Loop-2A in-pile tube is approximately 122 cm tall, with a maximum test train diameter of 4.34 cm. The ATF-2 test train fills this diameter and consists of six tiers that are arranged axially in the core, each of which

contains a 2×3 array of test pins. The tiers are numbered 1–6, with Tier 1 at the bottom and Tier 6 at the top. At various times, two of the tiers are combined so that longer test pins can be irradiated. The six tiers are joined together with dovetail joints and held in place by spring clamps. The flow area in the tiers when configured with standard 17×17 pressurized water reactor (PWR)-sized fuel pins is $\sim 2.677 \text{ cm}^2$. This arrangement allows for the disassembly of the test train in the ATR canal so that individual test pins can be removed at various times in their irradiation life and be replaced with new fresh pins. The entire design is modular, thus allowing for large reconfigurable test matrixes.

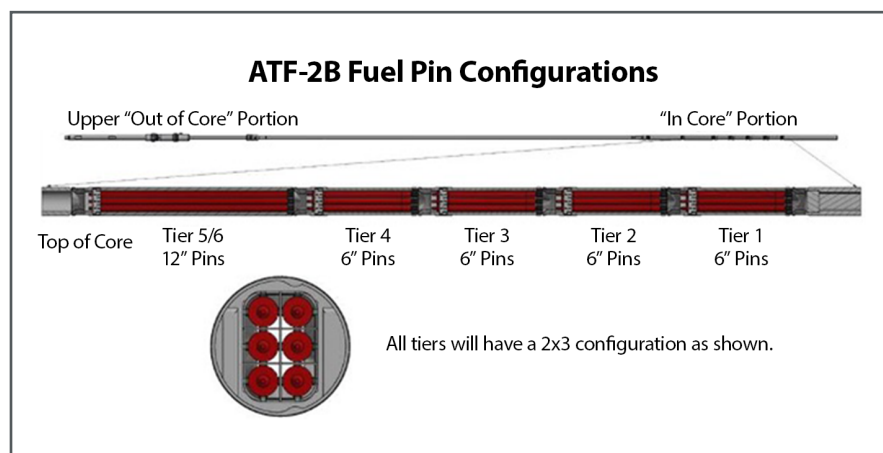
Accomplishments:

ATF-2 has irradiated 41 integral fuel test pins and 4 unfueled test pins for a total of 45 test pins. The irradiation involved 16 test pins with baseline Zr alloys, 23 coated-Zr alloys, and 6 test pins with iron-chromium-aluminum (FeCrAl) alloys. All the integral fueled test pins contained UO_2 fuel pellets enriched to between 4.9 and 4.95% U-235 and heavy metal densities between 10.4 and 10.5 grams/ cm^3 . Some UO_2 pellets contained sintering additives to increase their grain size and provide both improved fission-gas retention and better pellet plasticity at high-temperature.

The ATF-2 irradiation has completed seven steady-state ATR cycles,

beginning with Cycle 164A on June 12, 2018, and concluding with Cycle 169A on April 23, 2021. The first two cycles were irradiated with lower coolant temperatures ($\sim 250^{\circ}\text{C}$) and pressures (13.5 MPa) on the lower end of prototypic PWR operating conditions. These were increased to their present values of 285°C and 15.5 MPa in cycle 166A in July of 2019. At the start of Cycle 166B irradiation (November 2019), 7 of the baseline Zr alloy pins and 3 of the coated Zr alloy pins were removed. These were replaced with boiling water reactor (BWR)-sized pins. Prior to the start of Cycle 168A in April of 2020, another minor reconfiguration was made to remove two additional baseline Zr alloy pins and three Cr-coated Zr alloy test pins. After Cycle 169A in April of 2021, three baseline Zr alloy pins, 13 coated Zr alloy pins, and 12 BWR-sized FeCrAl pins all were removed from the ATF-2 test train. Following their removal, the test pins were shipped to INL's Hot Fuels Examination Facility (HFEF), where they were subjected to nondestructive and destructive examination to determine how they performed in-pile.

Power histories, neutron fluxes, and test pin depletions were calculated for each cycle using a coupled MCNP and ORIGEN methodology. An MCNP Type 7 fission-energy (F7) tally is used to calculate an energy deposition value in terms of MeV/g per source neutron. MCNP Type 4 flux (F4) tallies are used to calculate the total flux, thermal flux ($<0.625\text{ eV}$), and fast flux ($>1\text{ MeV}$). The MCNP-calculated heat rates are fed into an ORIGEN input file and depleted over a given time interval.



Linear heat rates for the test varied from 200 W/cm to 450 W/cm . Peak burnups reached were 30 GWd/MTU and peak fast fluences in the cladding were $4.9\text{e}25\text{ n/cm}^2$. Test pin examination data has been sent to all three U.S. fuel vendors and is being used in the development of their ATF products including licensing activities.

Many ATF developers have begun to rely more heavily on lead test assembly (LTA) irradiations in commercial reactors of their coated Zircaloy ATF technology. Thus, the goals of the ATF-2 mission are evolving again to: (1) provide continued irradiation of the small number of pins from the initial irradiation that require continued irradiation to high burnup; (2) support the irradiation of more novel ATF technologies, such as silicon carbide composite (SiC-SiC) cladding; and (3) provide test space for the conditioning of refabricated pins from commercial reactor irradiations prior to transient testing in INL's Transient Reactor Test Facility (TREAT).

Figure 1. In-Core portion of the ATF-2 test train

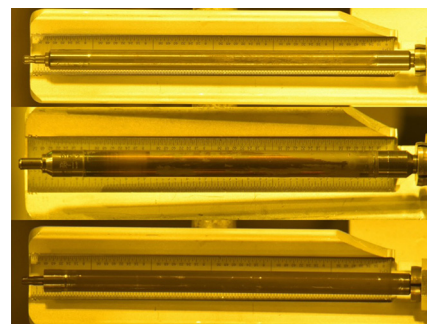
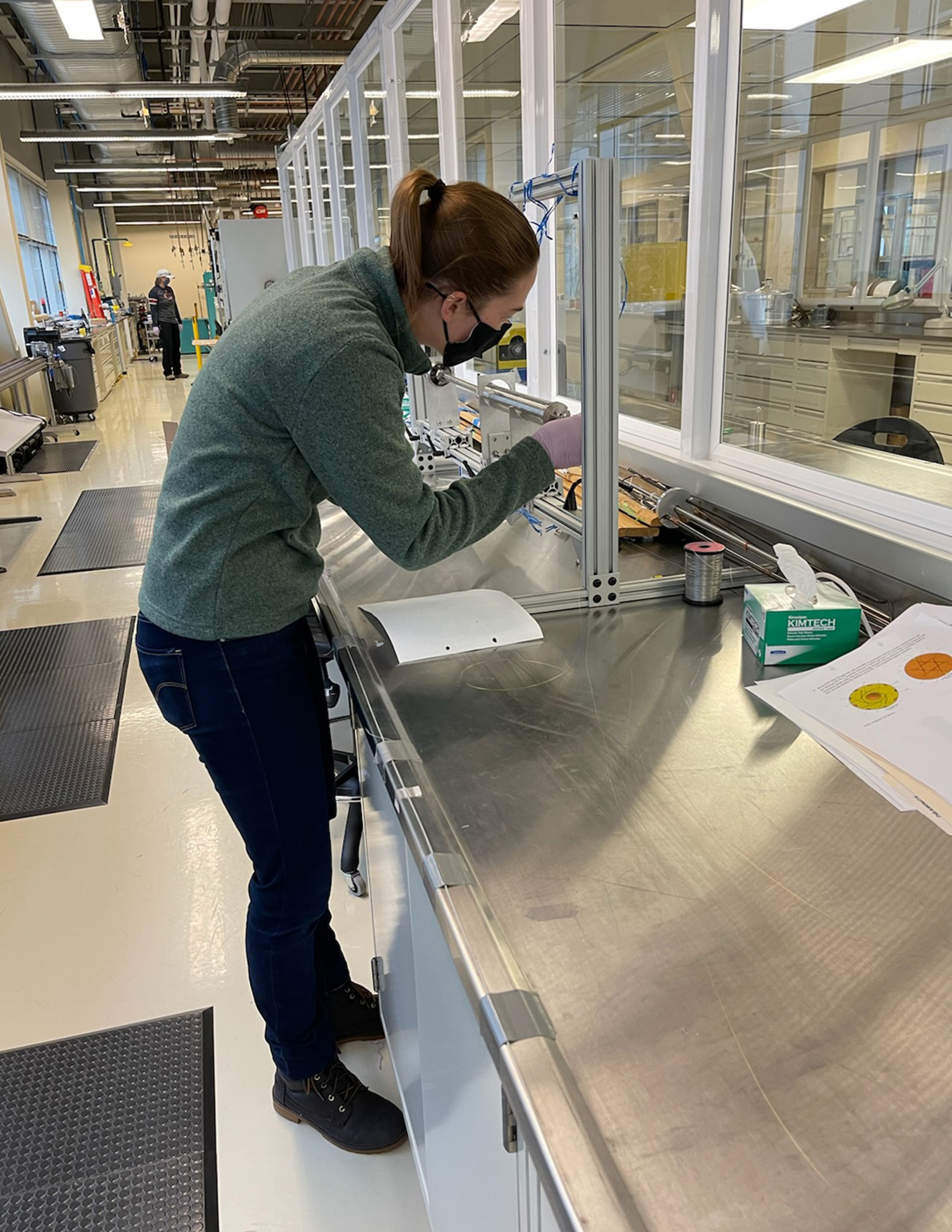


Figure 2. Irradiated ATF-2 test pins prior to destructive PIE





ADVANCED LWR FUELS OVERVIEW

- 2.1 LWR Fuel Fabrication and Properties
- 2.2 LWR Core Materials
- 2.3 LWR Irradiation Testing and PIE Techniques
- 2.4 LWR Fuel Safety Testing
- 2.5 LWR Computational Analysis
- 2.6 ATF Industry Advisory Committee
- 2.7 ATF Industry Teams

2.1 LWR FUEL FABRICATION AND PROPERTIES

Fabrication and Thermophysical Properties Evolution in Chromium-doped UO_2

Principal Investigator: Adrien J. Terricabras

Team Members/ Collaborator: Joshua T. White, Scarlett Widgeon Paisner, Darrin D. Byler

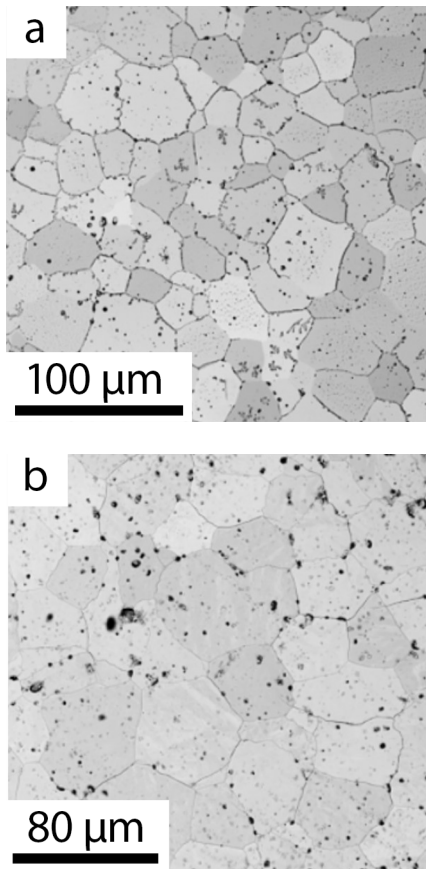


Figure 1. Grain morphologies of a) 750 ppm and b) 2500 ppm Cr-doped UO_2 as observed under SEM following thermal etching

Chromium-doped UO_2 fuels is an industrially important Accident Tolerant Fuel (ATF) due to the ability to increase the average grain size relative to standard UO_2 . However, there is a lack of knowledge of the thermophysical properties of these doped fuels, which is necessary for accurately modeling the in-pile performance. The work accomplished this fiscal year focused on developing large grain Cr-doped UO_2 pellets as a function of Cr content and subsequently measuring the thermophysical and mechanical properties. The microstructural variations were also investigated to evaluate chromium formation within the microstructure of the sintered pellets.

Project Description:

Both the Nuclear Regulatory Commission (NRC) and the Nuclear Energy Advanced Modeling and Simulations (NEAMS) program need thermophysical and thermomechanical data of the Cr-doped UO_2 system in order to validate information provided by industry. Because the data provided by industry is controlled as proprietary information, NEAMS is not able to use these data sets to develop codes to study the performance. To make this data widely available, Los Alamos National Laboratory (LANL) is working on fabricating Cr-doped, large grain UO_2 pellets and has collected measurements on

the thermophysical properties. In particular, the thermal conductivity is of interest due to the high importance of this property for the safety of light water reactor (LWR) fuels. Although the fabrication of the industry doped fuel concepts is proprietary, LANL has spent significant efforts in past years to develop a fabrication procedure to produce analogous samples. This includes carefully controlling the sintering atmosphere and chromium content to fabricate fuels with large average grain sizes, which has been found to be $> 28 \mu\text{m}$ and is dependent on the Cr concentration. The information from these measurements will be fed into modeling efforts through NEAMS to understand the performance of these fuels under irradiation.

There has been particular interest on the location of the Cr after sintering, which has been hypothesized to either accumulate at the grain boundaries or may be incorporated into the UO_2 lattice. The former has been inferred from X-ray diffraction (XRD) patterns, which is seen as a contraction of the lattice parameter. The Cr content, oxidation state, and location have implications on the fission gas release of the doped fuels upon irradiation. The work accomplished here will be unified into fuel performance code simulations of the doped fuels to assist in validating commercial codes provided by industry partners.

Accomplishments:

The work supported under this work package has resulted in three milestone reports, M3FT-22LA020201018 (submitted March 2022), M3FT-22LA020201013 (submitted March 2022) and M2FT-22LA020201011 (to be submitted September 2022). The work accomplished here involves sintering of Cr-doped UO_2 pellets with Cr concentrations ranging from 750 to 7800 ppm Cr. Inductively coupled plasma mass spectrometry (ICP-MS) was collected before and after sintering to determine any Cr loss during sintering. The sintered pellets have densities > 94.5 percent theoretical density (%TD) and post sintering XRD patterns show only peaks from UO_2 . There is a small shift towards lower angles with increasing Cr content, which indicates a contraction of the lattice with higher Cr contents. This indicates that Cr is being dissolved into the UO_2 lattice as opposed to forming a secondary phase. Scanning electron microscopy (SEM) images and energy dispersive X-Ray (EDX) spectroscopy show that at higher Cr contents, Cr_2O_3 does precipitate out as a secondary phase and indicates that Cr is only dissolved into the lattice up until a threshold level, after which the secondary phase is seen. The precipitates are found within the grains as opposed to being located at the grain boundaries.

The average grain size in the doped UO_2 sintered pellets was measured and show increases in the grain sizes with increasing Cr content, as is shown in Figure 1. The 750 and 2500 ppm Cr-doped pellets

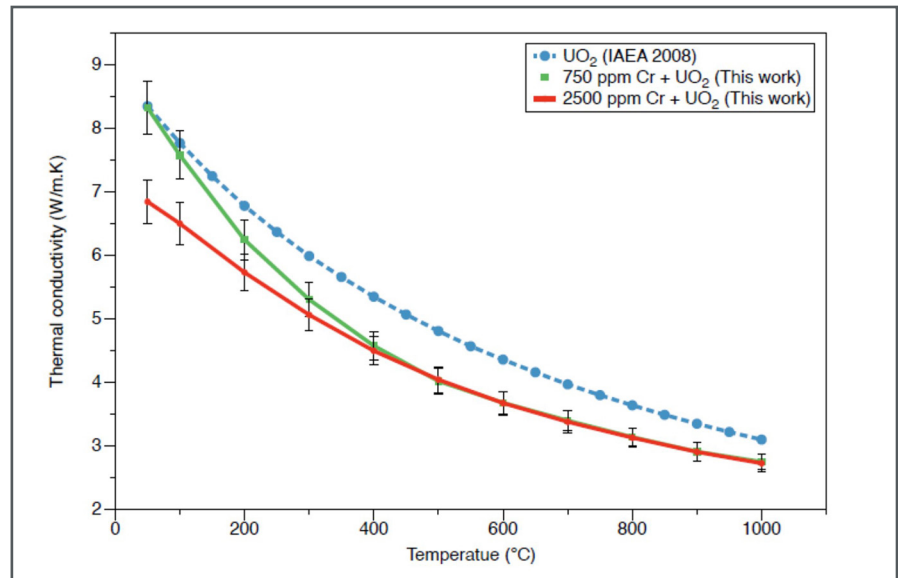


Figure 2. Thermal conductivity evolution of 750 ppm and 2500 ppm Cr-doped UO_2 from 50 to 1000 °C

revealed grain sizes of $28.2 \pm 2.3 \mu\text{m}$ and $41.5 \pm 3.8 \mu\text{m}$, respectively. For comparison, the average grain size of standard, undoped UO_2 is $\sim 10 \mu\text{m}$. The sintered pellets were used to measure heat capacity, thermal expansion, density, and thermal diffusivity of the Cr-doped materials. These measurements were used to calculate the thermal conductivity as a function of temperature and were compared to that of standard UO_2 published in 2008 by Fink. The results show that the thermal conductivity decreases at higher temperature and likely results from the phonon scattering due to Cr dopants in the UO_2 lattice. The results are shown in the attached Figure 2. Doped and undoped large grain UO_2 were fabricated and shipped to High Flux Isotope Reactor (HFIR) for irradiation tests.

Cr-doped UO_2 shows an increase in grain size and also shows changes in the thermal conductivity relative to UO_2 , which will be used to model in-pile performance.

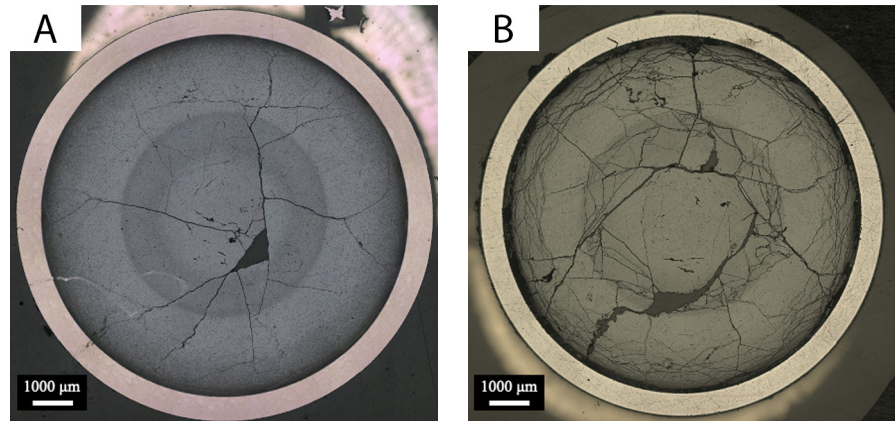
2.2 LWR CORE MATERIALS

Microstructure Evaluation of Pre and Post LOCA HBU Fuel

Principal Investigator: Rachel L. Seibert

Team Members/ Collaborator: Nathan Capps, Casey McKinney, Chad Parish, Tyler Gerczak, Jason Harp, Jesse Werden

Figure 1. Optical micrographs of two fuel rods under examination (a) as-irradiated and (b) post-simulated LOCA testing. Fuel fragmentation is clearly observed in the before and after, and the different radial zones of the HBU structure are also observable as observed under SEM following thermal etching



High burnup (HBU) fuel rods using uranium dioxide under loss-of-coolant accident (LOCA) testing present a phenomenon known as fuel fragmentation relocation and dispersal (FFRD), in which LOCA-tested fuel with sufficiently HBU suffer fragmentation and pulverization. Also called high burnup fuel fragmentation (HBFF), pulverized fuel results in a sand-like consistency and could prove dangerous due to its ability to relocate into the cladding balloon region of the fuel and potentially disperse from cladding under rupture conditions. Previous engineering scale studies determined cladding behavior, pellet history, and LOCA test conditions all directly impact pulverization severity, but do not explain the mechanism driving pulverization. Additional studies

indicate microstructure and fission gas release play a role in HBFF, as experimental results indicate Fission Gas Release (FGR) leads to fuel fragmentation and pulverization. To better understand the role microstructure plays in HBFF, advanced microscopy techniques are used to assess HBU fuel before and after simulated LOCA testing.

Project Description:

Commercial UO_2 fuel rods before and after simulated LOCA testing were explored using advanced microscopy. Samples were selected material irradiated in the North Anna powerplant and experienced average burnups greater than 63 GWd/tU. Different burnup structures were observed across the radial cross sections of the fuel. Scanning electron microscopy (SEM) was

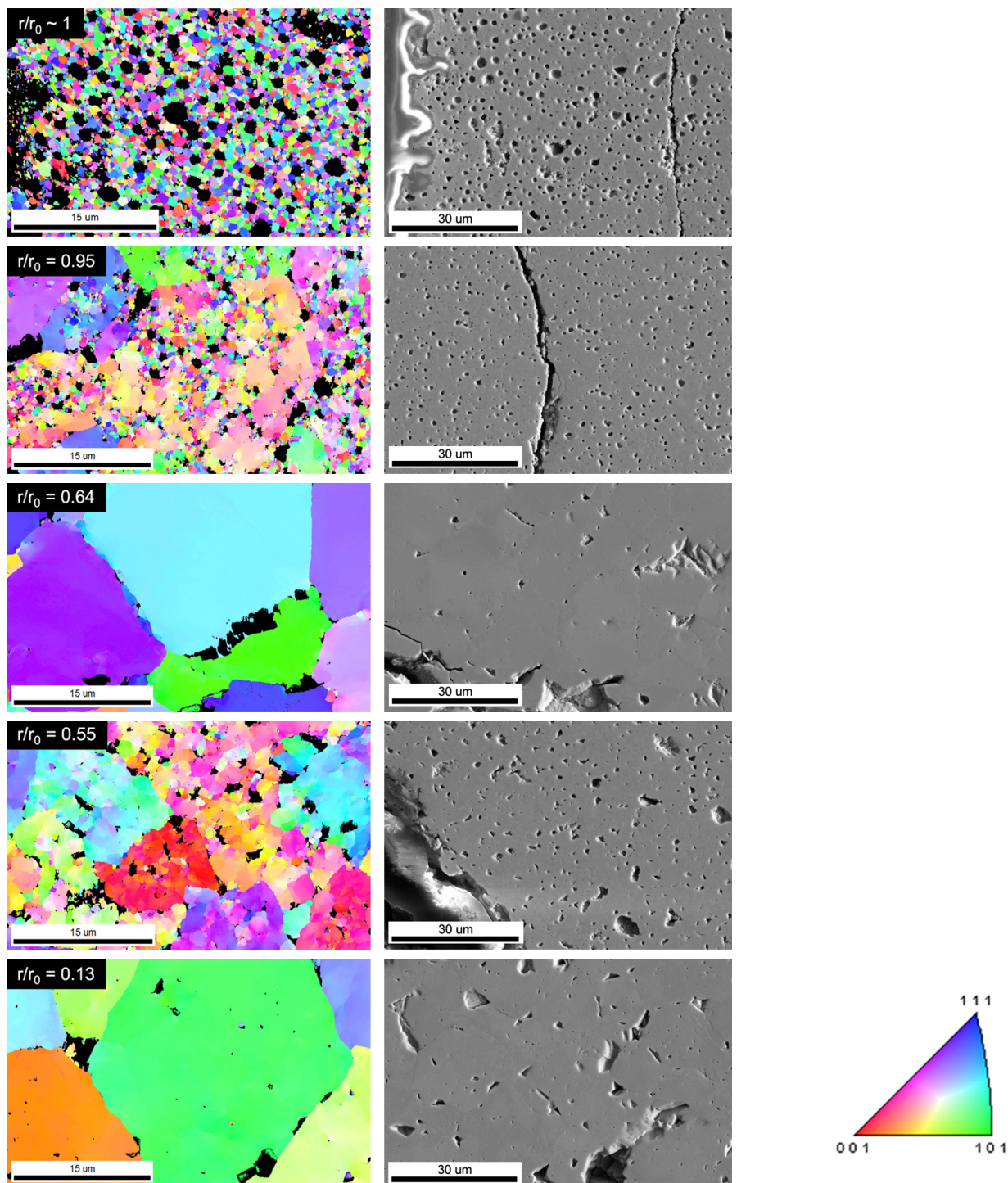


Figure 2. Inverse pole figure maps from each primary region in the HfB₂ structure from the as-irradiated sample showing the microstructural and pore variation across the pellet radius

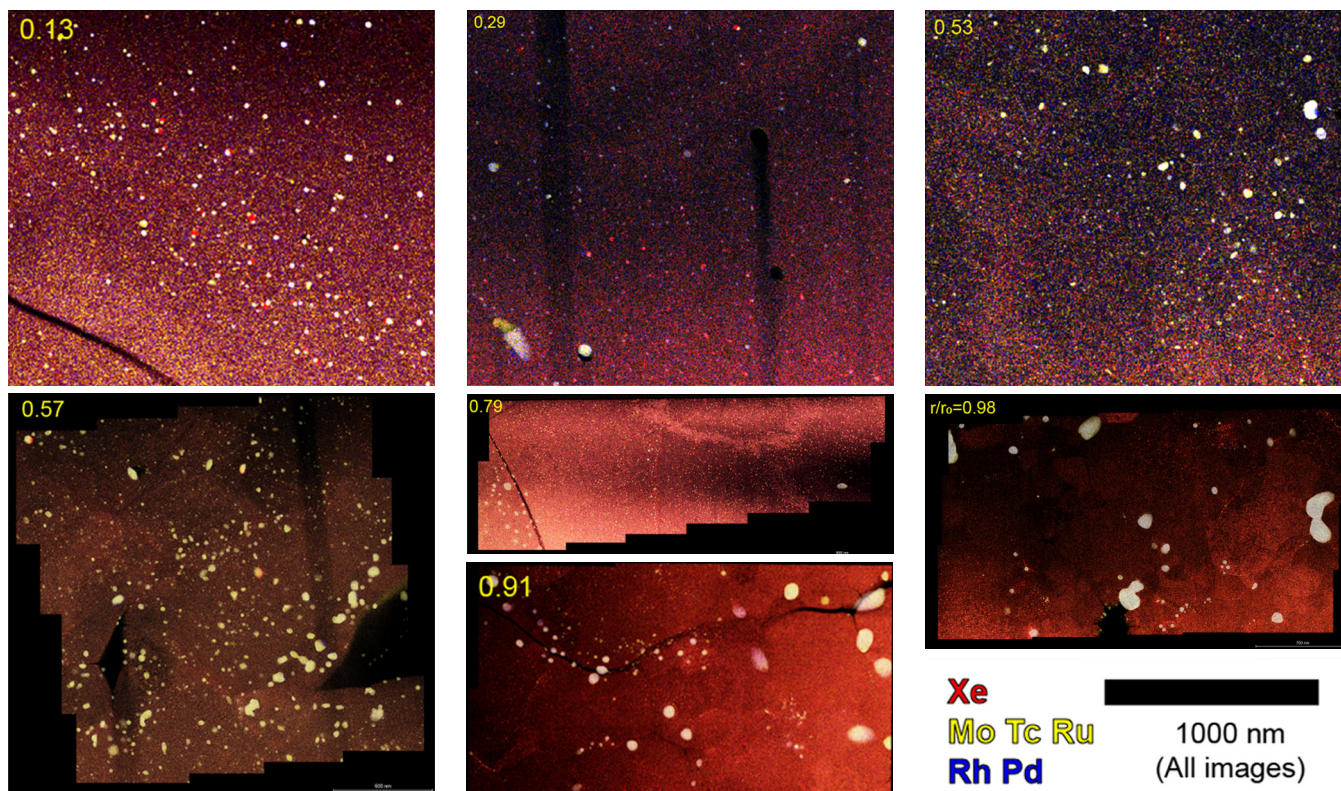


Figure 3. STEM/EDS map from the as-irradiated sample indicating Xe bubbles (red) along grain boundaries and intragranularly along the sample liftout at various distances from the fuel/cladding interface. Yellow precipitates are Mo+Tc+Ru, Blue are Rh+Pd, and White are five metal particles

evaluate porosity and to facilitate energy dispersive x-ray spectroscopy (EDS) mapping for fission product precipitates and electron backscatter diffraction (EBSD) to study grain structure changes in the material. Scanning transmission electron microscopy (STEM) coupled with EDS was used to assess microstructure and Xe gas bubble evolution on a nanometer scale at selected regions across the fuel pin. Microscopy was conducted to better understand HBU structure and its effect on fragmentation, and to better understand the possible driving mechanisms of HBU structure restructuring.

Accomplishments:

Restructuring found in the fuel central region is suggested to be partially caused by the bubbles in the region. This is supported by the strong correlation between low angle grain boundaries (LAGBs) and porosity size and shape. It is suggested that temperature has a stronger effect than burnup across an individual fuel pin, making it probable that the clean-grained central region of the fuel is the result of higher temperatures wiping out the LAGBs and LAGB-forming structures (dislocations) from this region. Future work intends to run simulations to assess the impact of

Analytical microscopy on pre- and post-LOCA tested fuel rods has revealed insight on how microstructure may affect post-LOCA fuel fragmentation.

burnup and temperature on these samples. A SEM survey of all samples showed trends in porosity as a function of the radial position along the fuel pin. The position is defined by the ratio of the radial position (r) to the radius of the fuel pellet (r_0) such that the fuel cladding interface is defined as $r/r_0 \sim 1$. The samples examined showed a decreasing number of pores at the fuel/cladding interface as a function of LOCA testing. Pores are more dense but smaller close to the cladding, then again at around $r/r_0 \sim 0.5$. Between this at $r/r_0 \sim 0.75$ and again close to the fuel center at $r/r_0 \sim < 0.3$, there is an increase in average pore area, but a decrease in the total pore numbers in that region. In the regions where the pores are smaller but denser, pores are highly circular. Five metal precipitates (FMPs) were observable in the HBU structure of some of the as-irradiated and post-LOCA samples via SEM, but due to resolution deficiencies was not seen in all samples. The FMPs in the central regions of the fuel began appearing in the restructured central region. The results from SEM support the theory that there is increased diffusion of FMPs at higher temperatures. It appears defects and FMPs in the hotter central region of the fuel have higher mobility

and allow for mobilization of FMPs and the formation of LAGBs. While results are still under reinvestigation due to resolution, they suggest burnup also effects distribution and mobility of FMPs across the central region of the fuel. Additionally, the largest FMPs were found near the fuel/cladding interface, and again at approximately $r/r_0 \sim 0.5$ (central restructured region of the fuel). Work has been done to quantify Xe bubbles in STEM maps taken at select regions across the fuel pin. Xe bubbles are distributed non-uniformly across the fuel pin, often appearing at or near grain boundaries. No obvious monotonic relationship was observed between FMPs and Xe bubbles in the samples tested. Taken broadly, however, FMPs are often associated with fine Xe bubbles. Xe bubbles are larger farther from the cladding, likely due to the higher temperature profile and lower generation rate driving the nucleation and growth process differently. A model has been developed to quantify the number of atoms in Xe bubbles to aid with future fuel modeling efforts of Xe evolution and safety testing responses.

Summarizing Effect of Coating Thickness and Condition on Behavior of Zr Cladding

Principal Investigator: Tim Graening

Team Members/ Collaborator: Mackenzie Ridley, Caleb P. Massey, Ben Garrison, Kory Linton, Andrew Nelson

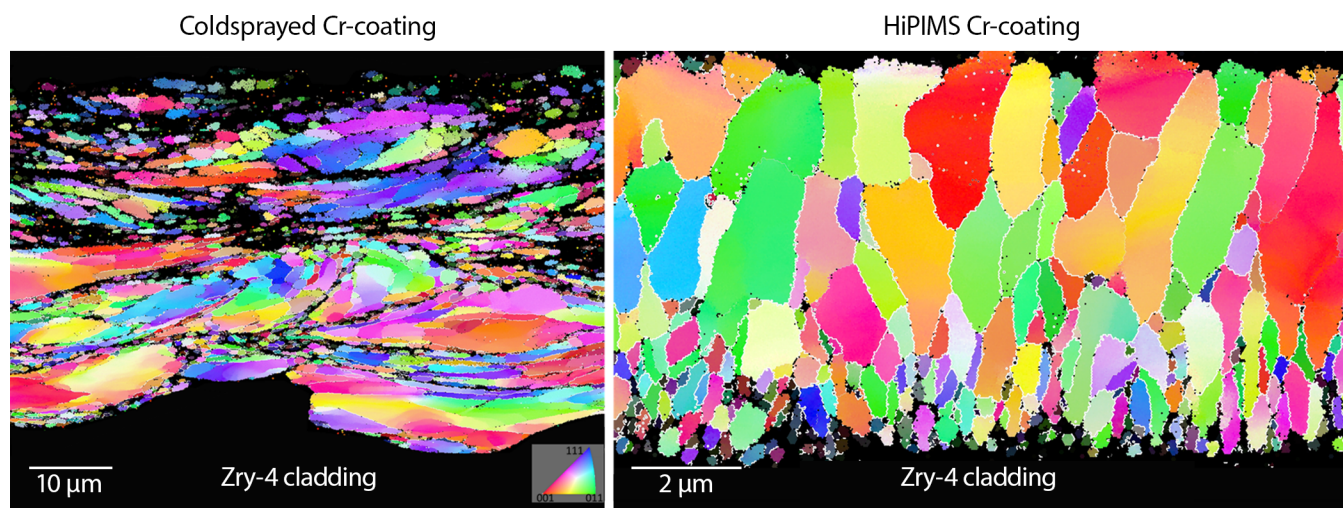
Accurate TEM investigations of the interface bonding between Cr-coating and Zry-4 cladding provide valuable information to simulation models.

Accident-tolerant fuel (ATF) concepts have been developed and tested in diverse research programs around the world. Industry teams have developed proprietary coating compositions and geometries, but knowledge gaps exist in terms of the resulting properties of the coating and the cladding and how those properties affect each other in reactor conditions. Steady-state and transient BISON coated Zr models have improved in recent years, but fundamental datasets to validate performance predictions are limited. The ability of the Advanced Fuel Campaign (AFC) to produce high-quality Cr coatings of varying thicknesses now allows for testing of Cr-coated Zr cladding under a range of representative conditions to expand these datasets. The milestone document gives a comprehensive summary of the range of mechanical testing of coated Zr performed in FY 2022.

Project Description:

The AFC augmented the proprietary activities undertaken by commercial fuel vendors by supporting fundamental activities intended to understand fundamental performance and delineate underlying dependencies such as coating geometry and integrity effect on performance. Having data available in the open literature is important

to inform and benchmark ongoing modeling efforts and to facilitate dialogue both within AFC, independent regulators, and the broader international community. The work presented compares different Cr coating microstructures and thicknesses on conventional Zry-4 claddings. Evaluating the impact of thickness, microstructure and adherence at the interface is crucial to understand how thin coatings may impact cladding performance under normal operating condition. The interface of as-coated claddings was characterized to assess coating anisotropic texture, grain sizes, and chemical composition. Two different coating application processes were assessed as well as coating thickness. Burst tests were performed to simulate a loss-of-coolant accident on each coating thickness to link coating thickness and microstructure to the mechanical performance. Another activity highlighted by the Nuclear Regulatory Commission's (NRC) Phenomena Identification and Ranking Tables (PIRT) is to evaluate the impact of a coating flaw on performance. Furthermore, the resulting data in the milestone report offers guidance to tailor coating thickness and microstructure to improve corrosion resistance and accident performance, without interfering from a neutronic



perspective. The data generated herein will be used to develop mechanistic models used to predict the mechanical response of coated claddings for code-qualification, safe application, and lead to additional margin of ATFs.

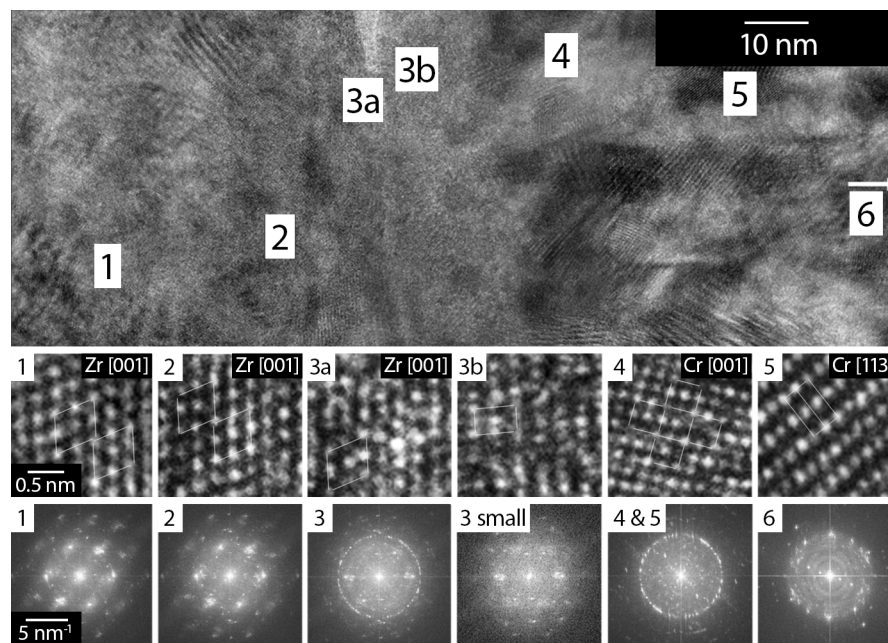
Accomplishments:

A second batch of High-power impulse magnetron sputtering (HiPIMS) coating claddings were produced. Zry-4 cladding surface preparation was performed and coating parameters were optimized to apply an adhesive coating on the cladding material to ensure reproducibility. Scanning electron microscopy (SEM) and transmission electron microscopy (TEM) were performed to characterize the microstructure properties of coldsprayed and

HiPIMS Cr on Zircaloy-4 cladding. Electron backscatter diffraction (EBSD) was performed on the coated material to identify as fabricated grain sizes and grain orientation. The two application processes were compared and the microstructure is shown as inverse pole figures in Figure 1. Take note of the different scale bars. Those results could be used to simulate and understand the mechanical behavior of coated cladding concepts. However, to understand how the coating and the cladding interaction, the direct interface requires additional detailed investigation. High Resolution Transmission Electron Microscopy (HRTEM) methods in particular were used to investigate the interface region between coating and cladding

Figure 1. Inverse pole figure maps of cold-sprayed (left) and HiPIMS (right) Cr-coating show a microstructure dependence on the coating process. The Zry-4 substrate is shown in black on the bottom of the micrograph. The rest of the image contains Cr coating. Because of the highly deformed small grains, some areas within the Cr coating and on the top could not be indexed

Figure 2. Magnified regions of the stitched HRTEM image across the interface are shown for the highlighted areas (1, 2, 3a, 3b, 4, 5, and 6). FFT images of the surrounding areas of around 2,500 nm² are shown for areas 1 through 5. FFT “3 small” is taken from a reduced area of 225 nm² in the transition area shown around 3a and 3b. FFT 6 was taken from an area around 50 nm to the right of this image. Scale bars are applicable for each row



to identify potential laves phase formation $(\text{Cr}(\text{Fe})_2\text{Zr})$. No Laves phase formations were identified in the as-coated conditions, even though Fe was found at the interface. A stitched high-resolution image is shown in Figure 2. The Cr lattice structure was identified with grain sizes of a few ten nanometers in area 3 directly located at the interface. Fast Fourier Transformation (FFT) images of the surrounding areas for each numbered areas were used to identify Zr and Cr phases. To provide measurable data, modified burst tests were performed on both materials to assess the impact of coating thickness on mechanical properties. Preliminary

results suggest minimal impact of coating thickness but instead a larger impact from the application process itself. Those findings need to be verified. One important aspect is the impact of potential flaws in the coating. A simple method to create a generic flaw in the coating was developed using laser engraving on the coating surface. A study of 27 engraving parameters was conducted and parameter sets for successful engravings were determined. Some of those flaws are highlighted in Figure 3. The method can now be applied to prepare coated cladding with pre-existing flaws before future tests.

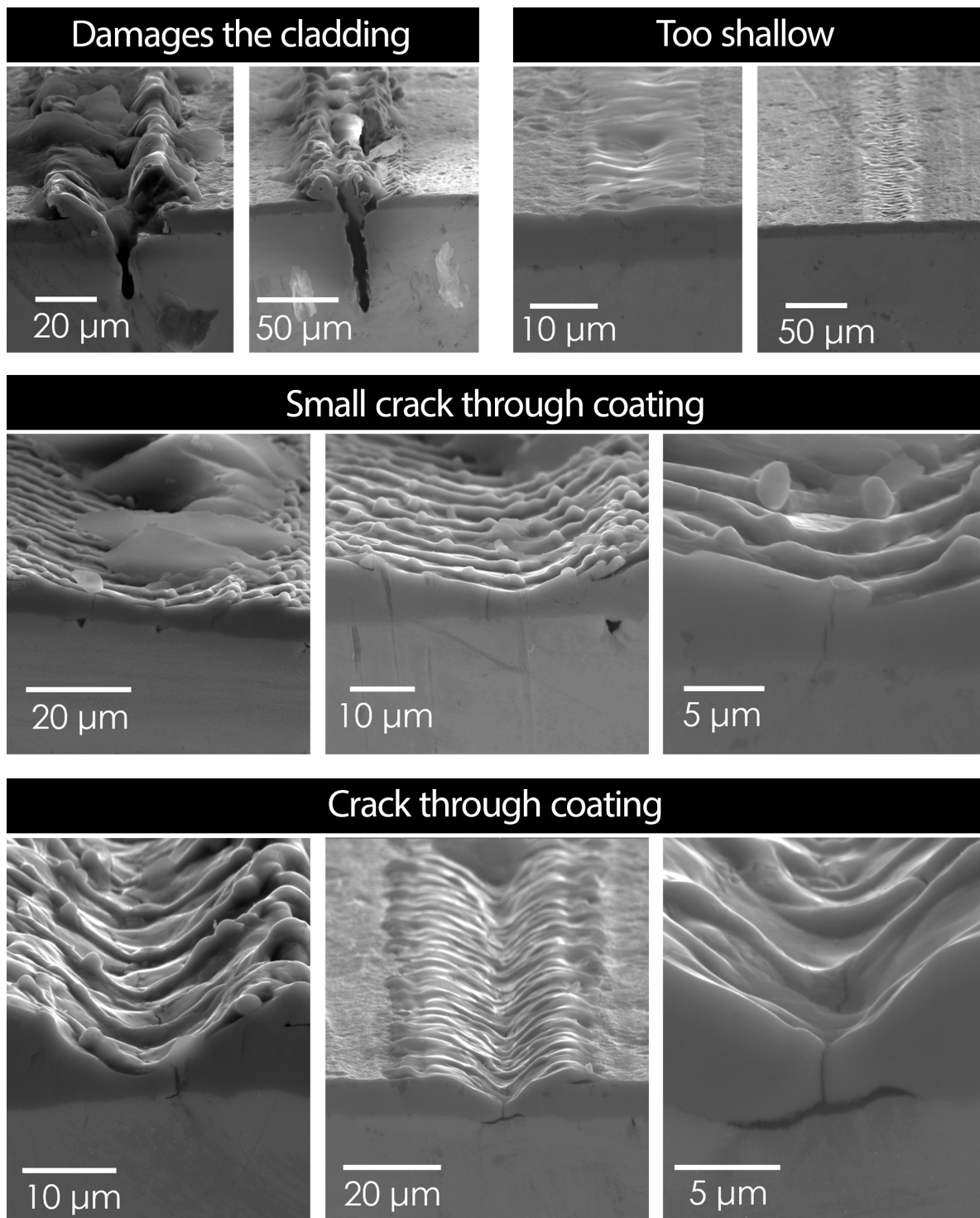


Figure 3. SEM images of laser engravings in the axial direction of the cladding tube showing different damage profiles

Microstructure-Based Benchmarking for Nano/Microscale Tension and Ductility Testing of Irradiated Steels

Principal Investigator: Janelle P. Wharry (Purdue University)

Team Members/ Collaborator: Anter El-Azab (Purdue University), Maxim Gushev (Oak Ridge National Laboratory)

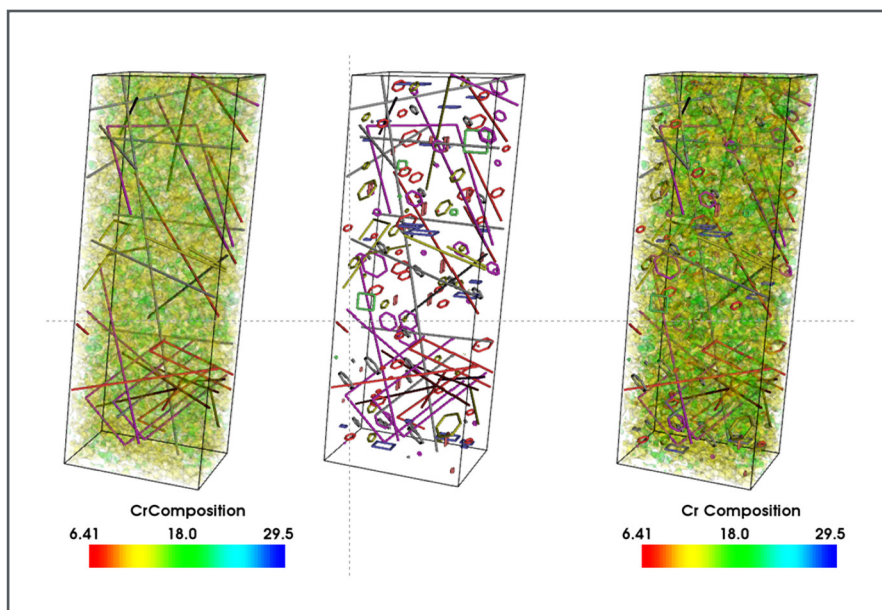


Figure 1. Integration of different irradiation induced defects in discrete dislocation dynamics simulations: (i) fluctuating composition fields showing the composition of Cr along with glide dislocations, (b) irradiation induced defects along with glide dislocations, and (c) both composition fields and irradiation induced loops along with the glide dislocations which are expected to change the mechanical behavior of the irradiated alloys

The objective of this study is to develop standardized methods for nano/micro-scale tensile and ductility testing of irradiated Fe-Cr steels. This project is carrying out microstructure-based benchmarking to ensure that the nano/micro-scale tests deform by the same mechanisms as macro-scale tests. Transmission electron microscopic (TEM) in situ mechanical testing enables direct observation of plastic phenomena concurrent to mechanical loading, in the region where failure will occur. Coupling these experiments with multiscale models, we will identify the approaches that provide consistent deformation mechanisms between the nano/micro-scale and

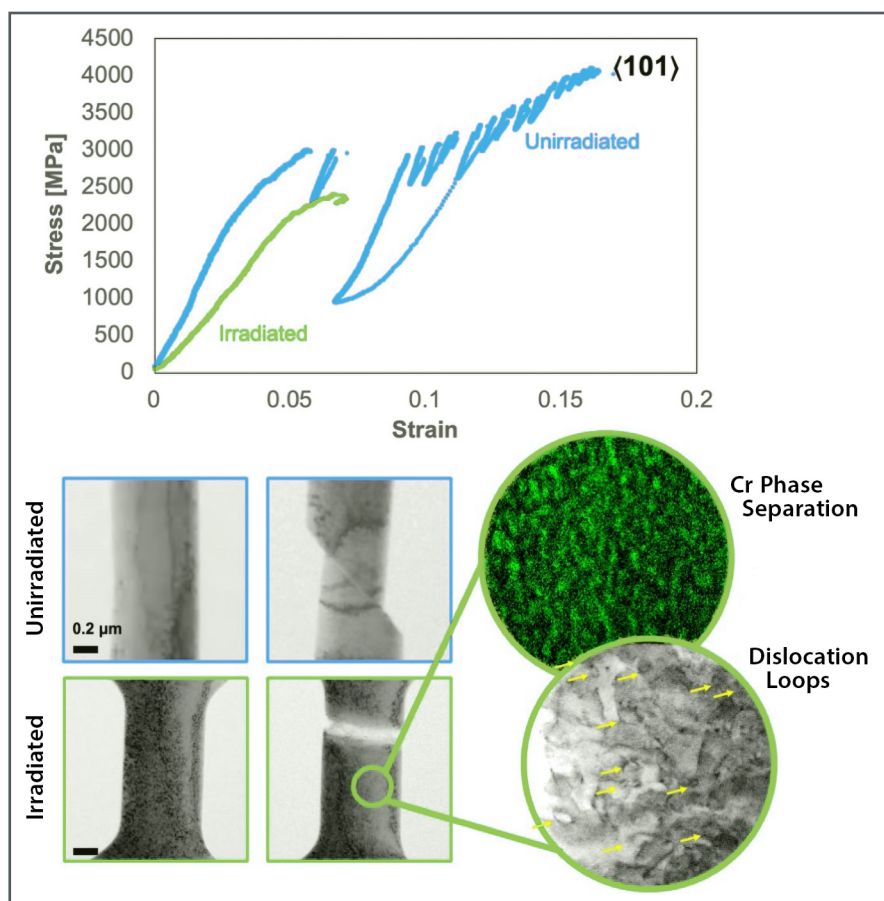
macro-scale tests, from which we will suggest standard practices. We focus on FeCrAl alloys and use the irradiated microstructure to inform finite element and dislocation dynamics models, which are then used to respectively design and interpret the macro-scale and nano/micro-scale tensile and ductility tests. Achieving consistent deformation mechanisms will enable establishment of standard practices for nano/micro-mechanical testing.

Project Description:

This project carries out microstructure-based benchmarking. The only scientifically correct way to “benchmark” mechanical tests is to ensure that the nano/micro-scale tests deform by the same mechanisms as do the macro-scale tests. As such, the most effective (and cost- and time-efficient) method for ensuring consistent deformation mechanisms is to observe plastic phenomena concurrent to mechanical loading, and to do so precisely in the region where failure will occur. TEM in situ mechanical testing enables exactly this. It is also especially well-suited for ductility studies, which rely on high-precision displacement measurements at regular time intervals throughout the test – here, the microstructure (from TEM video) can itself serve as displacement indicators. We are conducting “microstructure-based” benchmarking by investigating key process parameters for TEM in

situ tension and ductility testing. Coupling experimental studies with dislocation dynamics models, we will identify the approaches that provide consistent deformation mechanisms between the nano/micro-scale and macro-scale tests, from which we will suggest standard practices.

This project utilizes a multiscale, integrated feedback loop between models and experiments, to ascertain the effects of key experiment parameters on mechanical properties. We focus on a ferritic Generation II FeCrAl alloy, under equivalent neutron and Fe²⁺ self-ion irradiation conditions. Macroscopic dogbone tensile specimens exposed to 15 displacements per atom (dpa) of neutron irradiation are available to the team in the necessary geometries, along with virgin material for ion irradiation. We use the irradiated microstructure to inform finite element and dislocation dynamics models, which are then used to respectively design and interpret the macro-scale and nano/micro-scale tensile and ductility tests. Achieving consistent deformation mechanisms will lead to establishment of standard practices for nano/micro-mechanical testing. The primary project outcome, which is a set of recommended guidelines for nano/micro-scale mechanical testing, will lead to unprecedented reductions in the time and cost to qualifying materials



for in-reactor service, across all Department of Energy-Nuclear Energy programs.

Accomplishments:

Specimens of C35M and C37M have been ion irradiated also to 7 dpa at 375°C. We have characterized the as-received and ion irradiated microstructures using TEM, to reveal a high density of dislocation loops and no voids.

Figure 2. TEM in situ tensile testing results from unirradiated and irradiated (7 dpa, 357°C) C35M FeCrAl specimens in (101)101 oriented grains. Stress-strain curves show that irradiated specimens exhibit lower yield than unirradiated specimens, which may be attributed to the size effect given the high number densities of dislocation loop and Cr-rich nanophase separation defects in the irradiated material. Still-frames from TEM in situ videos are shown upon initial loading and at fracture

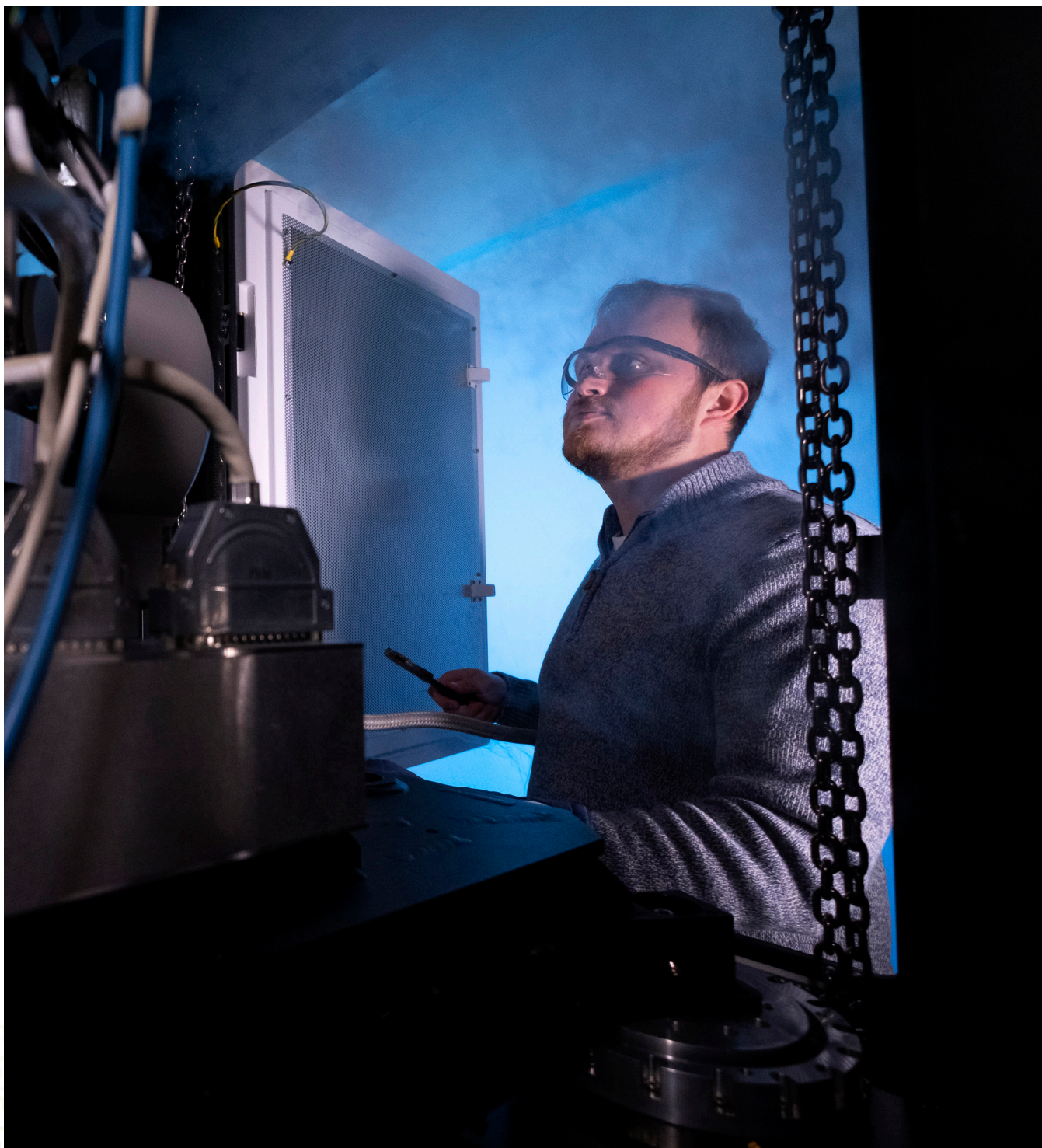


Figure 3. Ph.D. student Caleb Clement loading a specimen into the FEI Themis scanning transmission electron microscopy at Purdue

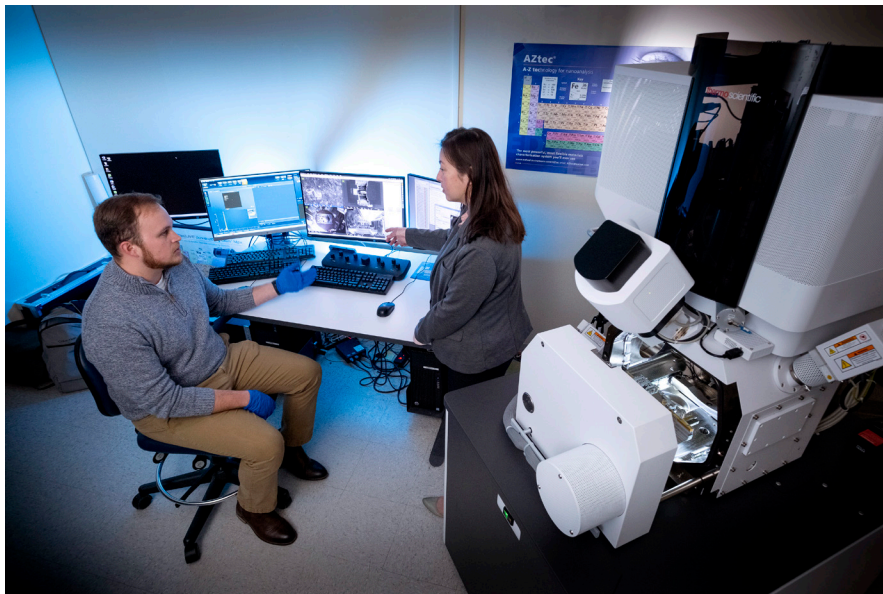


Figure 4. Ph.D. student Caleb Clement and PI Janelle Wharry working on the FEI Helios dual-beam focused ion beam (FIB) /scanning electron microscopy (SEM) at Purdue

We have carried out TEM in situ tensile testing on unirradiated C37M on the three primary grain orientations: [100], [110], and [111]. Two tensile tests were conducted from [100], two from [110], and one from [111]. The TEM in situ tests show clear evidence of dislocation slip in all three grain orientations. However, in the [111] test, even though dislocation slip appears to occur, the slip does not ultimately cause failure of the tensile bar. Instead, at a stress ~ 3.7 GPa, nano-twin needles appear to form in the specimen. With further strain, a twin nucleates then widens. The tensile bar ultimately fractures in the larger twin. We have also carried out TEM in situ tensile loading on the ion irradiated C37M on [100], [110], and [111] grains. All of these tensile tests have shown clear evidence of dislocation slip, with no evidence of deformation twinning in the irradiated C37M. Surprisingly, however, plastic yield

appears to occur at a lower stress than in the unirradiated material. This appearance of irradiation softening is inconsistent with the irradiated microstructure evolution and is merely an artifact of specimen size effects.

Yield stress, ductility, and elastic modulus values appear size-effected in the tested specimens. However, a notable difference in yield stress is observed across the two grain orientations, again consistent with models. The strain hardening coefficient is determined to be 0.48 in [100] grains, and 0.68 in [110] grains. These values are also consistent with our deformation mechanism observations, indicative that slip occurs more readily in the [110] grains. The stress-strain curve of the ion irradiated TEM in situ tensile bar on the [111] grain orientation shows considerable ductility, but a significant number of load drops, each of which correspond to clear evidence of dislocation-mediated

Figure 5. Ph.D. student Haozheng Joseph Qu and PI Janelle Wharry preparing a specimen for TEM at Purdue

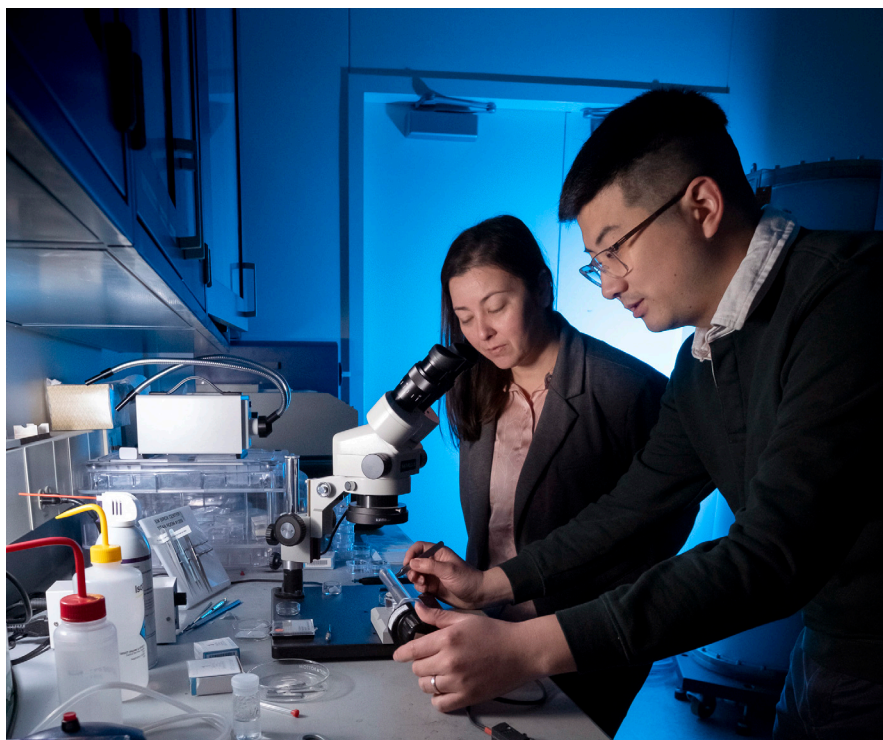
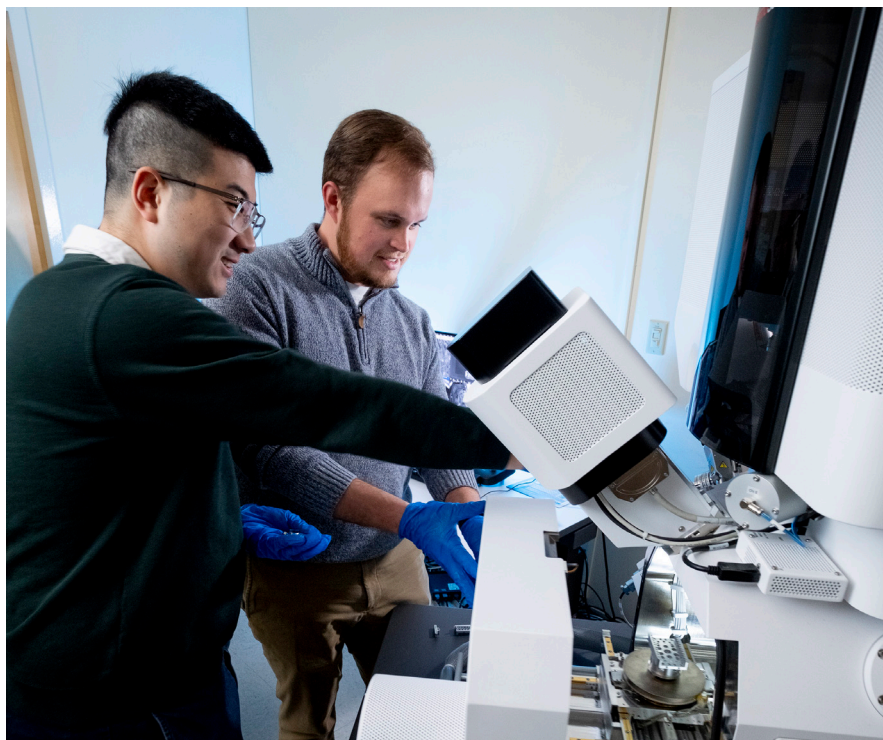


Figure 6. Ph.D. students Haozheng Joseph Qu and Caleb Clement loading a specimen into the FEI Helios dual-beam FIB/SEM at Purdue



events in the TEM in situ video. These results confirm the activity of dislocation slip.

We have established a simulated annealing algorithm for the reconstruction of the composition maps in irradiated FeCrAl, which show irradiation-induced α - α' phase separation. This composition reconstruction algorithm has ability to be extended to other systems that undergo irradiation-induced or thermally-induced phase separation; a manuscript has just been submitted for peer review. This algorithm has been coupled to a dislocation dynamics model, which can now simulate the deformation of the irradiated alloy.

Additionally, we developed a composition-sensitive discrete dislocation dynamic based numerical framework for predicting the mechanical behavior of irradiated FeCrAl alloys. The methodology is capable of taking into consideration the composition fluctuations associated with α - α' phase separation behaviors, as well as irradiation loops which are typically observed during the irradiation of FeCrAl alloys. These dislocation dynamics models inform how microchemistry and microstructure introduce spatial variations in dislocation mobility, and results will be compared against TEM in situ tensile tests of irradiated samples. Dislocation dynamics simulations are currently being executed using input parameters supplied by TEM in situ tensile experiments, including specimen dimensions, strain rate, and irradiated microstructure.

On a parallel front, we have also been investigating the deformation mechanisms in FeCrAl alloys using molecular dynamics (MD). MD work involves investigating the atomistic origins of changes in the mechanical behavior of irradiated FeCrAl alloys. As part of the MD efforts, we are trying to set up simulations with irradiation induced prismatic loops to compare the deformation mechanisms as compared to the pristine FeCrAl alloys. We have also run MD simulations of FeCrAl simulation boxes of varying sizes, to model specimen size variations. These MD simulations have been tested with Fe and FeCrAl potentials. During deformation, MD predicts dislocation slip activity in the [110] and [111] loading directions, with dislocation glide leading to nucleation of residual mobile dislocation loops near the eventual fracture surface. On the other hand, the [100] loading direction exhibits a volumetric shift that appears to suggest a twinning type mechanism. The MD simulations have also generated dislocation velocity results, which are also key input parameters for dislocation dynamics calculations.

All experimental efforts have been conducted by graduate student George Warren, under supervision from principal investigator (PI) Wharry and Co-PI Gushev. All computational efforts have been conducted by graduate student Yash Pachaury, under supervision from Co-PI El-Azab.

Coupling TEM in situ mechanical testing with dislocation dynamics modeling enables us to ascertain tensile properties from irradiated material volumes too small for existing standard mechanical testing configurations, dramatically reducing the cost of qualifying materials.

Bridging the Length Scales on Mechanical Property Evaluation

Principal Investigator: Peter Hosemann

Team Members/ Collaborator: Andrew Dong, Hi Vo, Jason Duckering, Eric Olivas, Assel Aitkaliyeva, Tanvi Ajantiwalay

Micromechanical testing is becoming a part of the nuclear materials examination toolbox and this research shows the scaling effects associated with specific microstructural features.

The development of small-scale mechanical testing in combination with microstructural investigation is of great interest to the nuclear materials community for both materials development and monitoring applications. This research aims to bridge the length scale of material property evaluation and thus enhance the confidence in using data obtained from microscale testing to macroscale applications. Work performed involves micromechanical testing of a wide variety of nuclear-relevant material microstructures as well as developing novel testing and analysis techniques to bridge work across length scales.

Project Description:

Small scale mechanical testing ($<100\mu\text{m}$, commonly $<10\mu\text{m}$) has significant advantages for materials research. It enables isolation and probing of specific microstructural regions and features of interest. Furthermore, it increases the

number of samples and tests that can be performed for a finite volume of material. This is particularly relevant to the monitoring of reactor components as in-service surveillance testing has limited material due to both space constraints as well as representative sampling conditions. Ex-service components similarly have constraints over the amount of volume available to examine. Through increased statistics and targeted investigations into material properties, small scale testing can therefore be invaluable to continued operation of the nation's current reactor fleet and the design of next generation reactors.

However, much work needs to be done in order to establish confidence in drawing application scale conclusions from small scale data. This involves the development of data collection and analysis techniques at the small scale as well as demonstrating the fidelity in derived micro- to macroscale scaling relationships. It is the objective of this research to obtain small scale mechanical data from a variety of different materials and microstructural features and expand the state-of-knowledge on how these smaller scale features influence the properties of a material. Simultaneous development of testing and analysis techniques aim to bridge gaps length scale examinations.

Accomplishments:

A major aspect of this research is to obtain micromechanical data from materials spanning a wide range of material conditions and microstructures. To this end, micromechanical testing has been performed on materials containing different degrees of dislocation densities (pure nickel and various heats of Alloy 600), precipitates (different heats of CuCrZr provided by the United Kingdom Atomic Energy Agency), and grain sizes (different heats of 304SS). Results from this work includes the introduction of the "blocked volume" concept evaluating the effect of constraint on micromechanical testing results (Hi Vo, University of California, Berkeley). This concept is detailed in Figure 1.

Furthermore, testing of ion-irradiated HT-9 (from Idaho National Laboratory obtained via Los Alamos National Laboratory) was performed. A subset of the samples tested include HT-9 samples that were irradiated at Sandia National Laboratory using 4MeV protons to doses levels of $7\text{E-}5$, $7\text{E-}4$ and $7\text{E-}3$ dpa (Tanvi Ajantiwalay, University of Florida). These results are shown in Figure 2 comparing unirradiated HT-9 to the ion-irradiated HT-9.

Also performed is a thickness study on tensile properties for a variety of the aforementioned materials

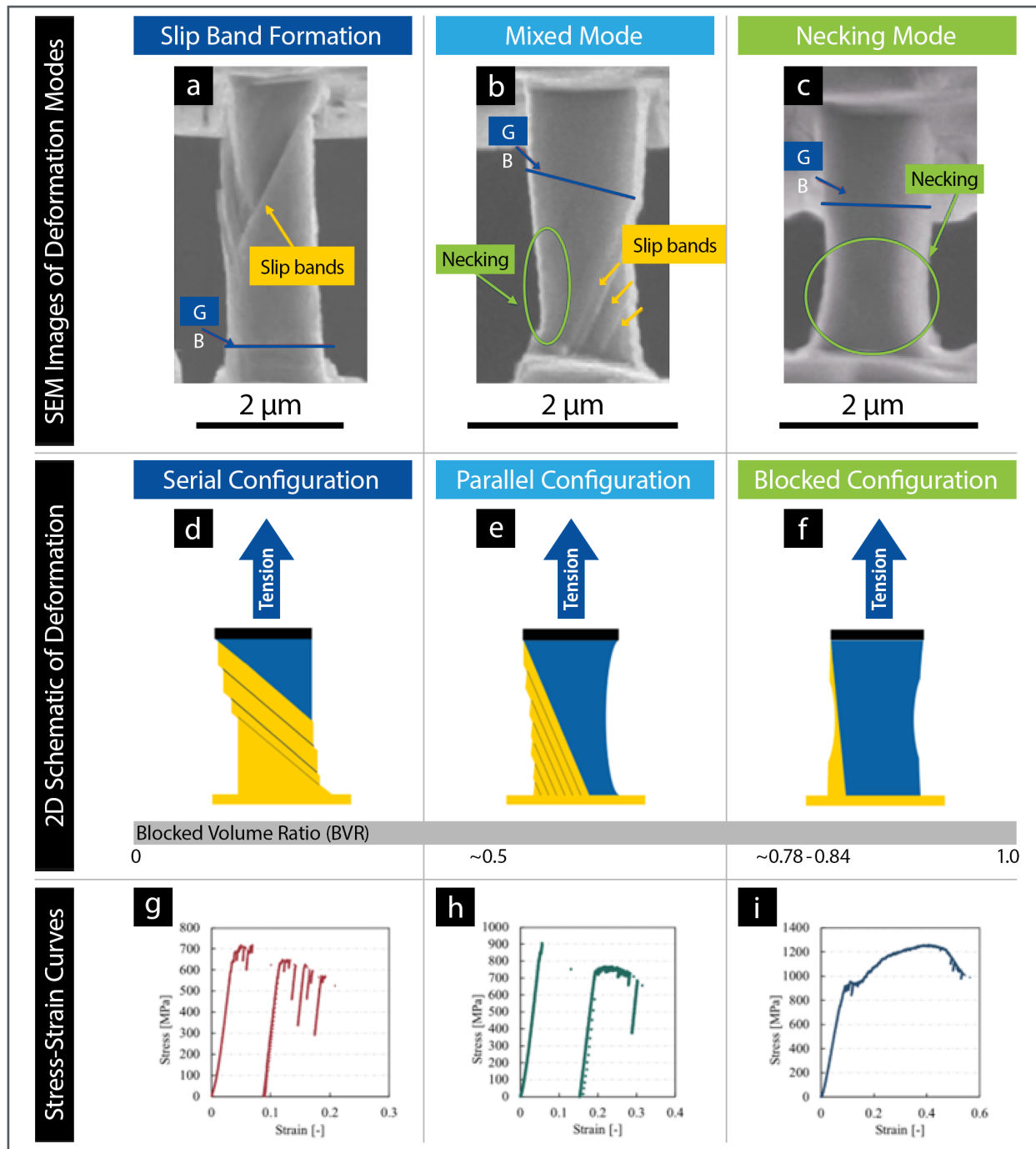


Figure 1. 2D schematics of the influence of multi-slip system constraint. A) The blocked and free volumes are in serial configuration, observed when the blocked volume ratio is low. B) The blocked and free volume are in parallel configuration, observed the blocked volume ratio is intermediate. C) The blocked volume is much greater than the free volume region. D) The serial configuration A deforms by forming multiple slip bands in the free volume. E) The parallel configuration B deforms by simultaneous strain bursts in the free volume and necking in the blocked volume. F) The blocked configuration F exhibits high level of work-hardening and subsequent necking

Figure 2. Stress vs. strain curves for unirradiated (U) and ion-irradiated HT-9 specimens at three different doses: 7×10^{-5} dpa (L), 7×10^{-4} dpa (M), and 7×10^{-3} dpa (H)

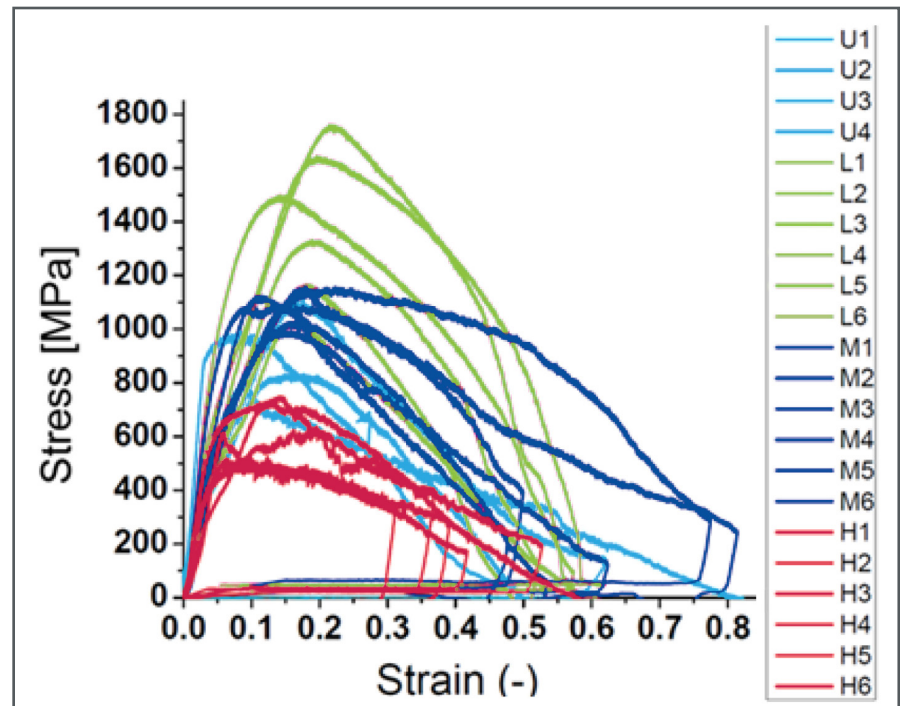
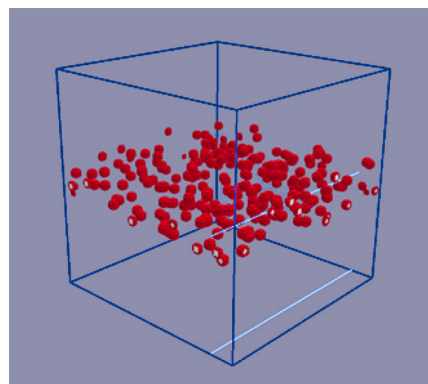


Figure 3. Example of a simulation used to calculate hardening due to microstructural features. This specific simulation volume involves a single dislocation (light blue) interacting with a random distribution of precipitates or voids (red)

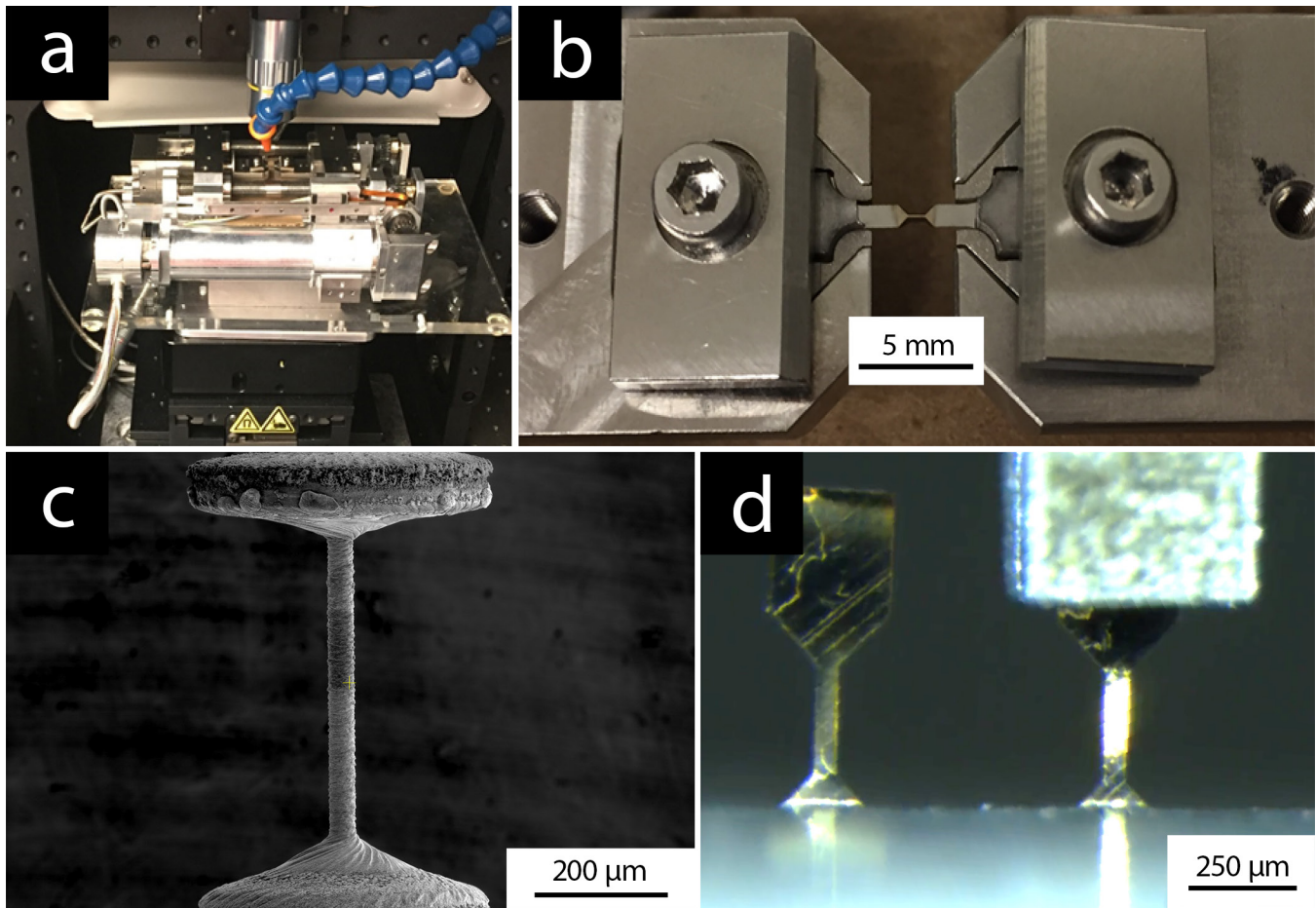


(304SS, CuCrZr, and HT-9) where samples ranged in thickness from $800\mu\text{m}$ down to $30\mu\text{m}$ using the SS-J sample geometry (Andrew Dong, University of California, Berkeley). Across the three alloys and seven total variants examined, bulk tensile properties were generally preserved down to thicknesses around $200\mu\text{m}$. As thickness reduced below $200\mu\text{m}$, strength and ductility values began

to significantly differ from bulk, with the magnitude of change depending on the alloy and variant.

Overlapping of a portion of the micromechanical testing was purposefully performed across institutions (University of California, Berkeley and University of Florida) in efforts to probe the fidelity of testing results. This blind testing and data analysis resulted in generally good agreement between instruments and analysis techniques at the different institutions as well as led to identification of areas where disagreement can exist and potential magnitude of discrepancies.

Beyond mechanical testing, development into multiscale modelling and analysis has also been performed. This includes using discrete dislocation dynamics to determine models and fitting parameters for radiation-



induced defects (Hi Vo, University of California, Berkeley). Figure 3 shows an example of a simulation performed to calculate hardening from various microstructural features. Finite element modelling of a tensile testing setup used throughout this research has also been successful (Eric Olivas, Los Alamos National Laboratory).

Finally, development of micro-mesoscale sample preparation and testing techniques has also been performed as part of this work. A femtosecond laser was employed to machine tensile samples of various geometries including of a reduced

geometry while pre-mounted in a tensile tester, a round dogbone via a laser lathe technique, and a series of samples along a thin sheet edge (Andrew Dong and Jason Duckering, University of California, Berkeley). Examples of each are shown in Figure 4. This shows promise in being able to rapidly and consistently manufacture testing specimens between the 10-100+ μ m length range.

Figure 4. Examples of micro-mesoscale samples manufactured via femtosecond laser machining. a) The femtosecond laser machining workstation with a tensile testing machine placed inside. b) A reduced geometry SS-J sample machined while mounted in a tensile tester. c) A round dogbone machined via a laser lathe process imaged within an SEM. d) A sheet edge sample being pulled in a tensile tester with an adjacent as-machined sample on the same sheet to the left

Bridging Microscale to Macroscale Mechanical Property Measurements and Predication of Performance Limitation for FeCrAl Alloys Under Extreme Reactor Applications

Principal Investigator: Jian Wang (University of Nebraska-Lincoln)

Team Members/ Collaborator: Dongyue Xie, Mingyu Gong, Bingqian Wei (University of Nebraska-Lincoln); Tianyi Sun, Jiangyuan Fan (Purdue University); Tianyao Wang (Texas A&M University / Xinghang Zhang (Purdue University), Lin Shao (Texas A&M University)

Microscale mechanical testing has greatly benefited nuclear materials studies in at least two aspects: one is its feasibility to integrate with scanning electron microscopy (SEM) and transmission electron microscopy (TEM) microscopes for in situ atomic scale or microscale structural characterization to reveal fundamental details, and the other is its significance in development of accelerator-based ion irradiation technique as a surrogate method to simulate neutron damage. However, limited ion penetration depths, which are about a few microns for MeVs heavy ions and 10s microns for MeV light ions, make microscale mechanical tests a necessity. But, there is a great challenge to bridge microscale tests to macroscale tests because a bulk specimen of irradiated nuclear materials for high dose applications cannot be obtained in laboratory. This project is facing this inexorable challenge. We aim to develop an integrated theoretical, modeling, and experimental platform that enables predicting the ductility of nuclear structural materials based on microscale mechanical tests.

Project Description:

To utilize micro-scale measurements for prediction of macro-scale properties, there is a need to transform the knowledge obtained

from micro-scale measurements and characterizations of deformed and/or high-dose irradiated materials into predictions of the macro-scale mechanical properties (especially for ductility) of irradiated materials. Mechanical properties of a structural material are primarily controlled by the overall micro-structure and the character and distribution of microstructural defects induced by deformation and/or irradiation, all of which can be observed and quantified using microscopy. Combining micro-scale characterization of microstructural defects and in-situ micro-mechanical testing, we can explore the correlation of mechanical properties with contributions of individual microstructural defect ensembles. These correlations will enable us to develop the Mechanisms-based Single Crystal Plasticity Model (MSCP) at the meso-scale. Implementing the MSCP into the Visco-Plastic Self-Consistent (VPSC) model for polycrystalline aggregates, we are able to describe the Constitutive Law for Polycrystals (CLP) at the micro-scale (texture and the distribution of grain size are known). Comparing with the results of various macro-mechanical tests we can validate the micro-scale CLP. Lastly, we implement the CLP into finite element analysis and

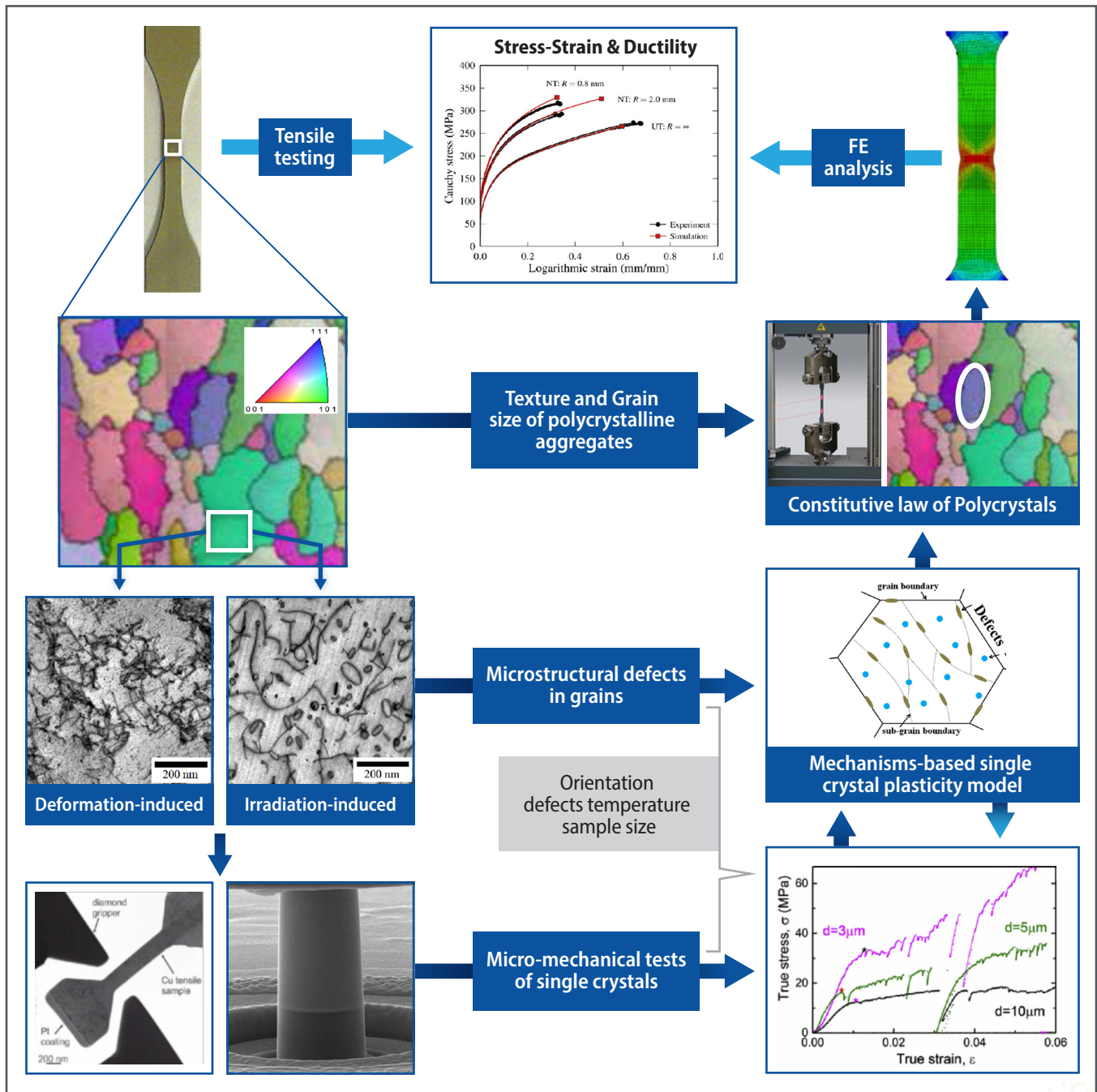


Figure 1. Schematic of objectives: Bridging micro-scale to macro-scale mechanical property measurements and prediction of performance limitations for FeCrAl alloys under extreme reactor applications. At the meso/micro-scale, we explore the correlation of microstructural defects with micro-mechanical properties of FeCrAl alloys and thereby develop the Mechanisms-based Single Crystal Plasticity model (MSCP); At the micro/macro-scale, we develop the Constitutive Law for Polycrystals (CLP) by implementing the MSCP into the Visco-Plastic Self-Consistent (VPSC) model and validating the CLP by comparing macro-mechanical tests; Lastly at the macro-scale, we implement the CLP into finite element analysis to predict the ductility of FeCrAl alloys following mechanical deformation and/or radiation

perform macro-scale tensile testing to calibrate the localization criterion for predicting the ductility at the macro-scale.

The project selects FeCrAl as the primary testing materials since FeCrAl alloys have attracted increased interests in the nuclear community as a promising candidate for accident tolerant fuel cladding for light water reactors. Along with its wide applications and excellent properties, we aim at developing an integrated theoretical, modeling, and experimental platform (Figure 1) that enables prediction of the macro-ductility of FeCrAl alloys based on micro-scale mechanical tests. The technologies and modeling capabilities developed from this project, however, are generally applicable to alloys other than FeCrAl. This project will establish such a framework that combines mechanical testing and modeling techniques at various length scales to understand the mechanical properties of small specimens and predict the strength and ductility of large-scale specimens with similar internal microstructures and microchemistry. The project will have direct impact on understanding the mechanical behavior of a suite of irradiated small-scale metallic materials for applications in various nuclear reactors.

Accomplishments:

Temperature dependence of the mechanical property of polycrystalline FeCrAl alloys was evaluated

at University of Nebraska-Lincoln by tension testing at room temperature, 500 °C, and 700 °C, respectively. When the temperature was increased to 700 °C, the stress decreases immediately after yield, there is no strain hardening. Slip resistance for {112} and {110} slips are measured by using micropillars at University of Nebraska-Lincoln and Purdue University. There is no obvious size effect as the pillar diameter is greater than 5.5 μm. The critical resolved shear stress of FeCrAl single crystals associated with dominant slip system of {110} <111> and {112} <111> are 220 MPa and 230 MPa at room temperature, 142 and 141 MPa at 200°C, 137 and 139 MPa at 350 °C, and 115 MPa for both slip systems at 500 °C.

Hardening behaviors of micropillars were investigated at University of Nebraska-Lincoln by using micropillars with specific orientations which favor the type and number of activated slip systems. The strain hardening rates derived from these tests clearly indicated that the weakest hardening is associated with pillars with one activated slip system, the largest hardening is observed in pillars with multiple activated slip systems. The critical strain for reaching a stable strain hardening rate increases with the number of activated slip systems. For the bi-crystal pillars, the strain hardening rate is related to the geometrical compatibility factor, the higher the factor is, the lower the strain hardening rate is.

This project enables the development of an integrated theoretical, modeling, and experimental platform that can predict mechanical response of ion irradiated structural materials based on microscale mechanical tests.

We conducted proton radiation and Fe ion radiation tests on the 800 °C annealed FeCrAl alloys at Texas A&M University. Proton irradiation experiments provide plateau damage of 0.01 dpa and 0.1 dpa. Fe ions energy is 5 MeV, producing a peak damage of 100 dpa at 350 °C. Based on micropillar compression tests at University of Nebraska-Lincoln and Purdue University, the critical resolved shear stress (CRSS) to activate the {110} <111> and {112} <111> slip system in the 0.1 dpa proton irradiated FeCrAl alloy is 195 MPa and 210 MPa at 200 °C, 160 MPa and 182 MPa at 350 °C, respectively. At 500 °C, the CRSS for both slip systems are 105 MPa. It is noted that the CRSS increases with the damage, and the increase in the CRSS for {112} <111> is higher than {110} <111>. Nanoindentations with different strain rates were conducted on the unirradiated sample and the Fe ion irradiated samples with peak damages of 1 dpa and 10 dpa. The hardness increases with dose and strain rate. The strain rate sensitivity m is measured to be 0.0216, 0.0226, and 0.0216 for the sample with no damage, 1 dpa, and 10 dpa respectively, indicating that the strain rate sensitivity barely changes after Fe³⁺ ion irradiation.

We employ a crystal plasticity model to predict the mechanical response of FeCrAl alloys at different deformation temperatures. First, a MSCP model is developed based on generation and motion of dislocations which is significantly affected by the microstructures and temperatures. The MSCP is then implemented into the crystallographic VPSC framework for polycrystalline aggregates. The MSCP-VPSC model is employed for unirradiated materials, and reveals the effects of texture, dislocation density and temperature on the mechanical response. The predictions show fairly good correlation to experiments which is shown in previous reports. Furthermore, we considered the evolution of damage in materials during deformation to capture features of both hardening and softening stages during loading FeCrAl alloys.

Benchmarking Microscale Ductility Measurements

Principal Investigator: Owen T. Kingstedt (University of Utah)

Team Members/ Collaborator: Ashley Spear (University of Utah), Jiyoung Chang (University of Utah), Ryan Berke (Utah State University)

The simulation tools and experimental techniques developed through this project enable informed macroscale ductility predictions to be obtained from a limited number of microscale specimens.

Ion bombardment is an attractive technique to efficiently induce damage that mimics that produced during prolonged in-service irradiation exposure. However, the damaged material layer is limited to a few micrometers in depth. To evaluate the mechanical performance of this damaged layer improvements are necessary in our approaches to microscale tension testing, particularly when attempting to assess ductility. Ductility is a material performance metric directly tied to structural health. Multi-length scale experimentation and a non-local damage large strain elasto-viscoplastic fast Fourier transform (LS-EVP-FFT) based crystal plasticity model are combined to develop approaches to enable the upscaling of ductility measurements obtained from microscale specimens to predict macroscale component ductility.

Project Description:

The technical objectives of the research are 1) to establish practices for obtaining tensile microscale ductility measurements and 2) to identify methodologies for comparing microscale ductility measurements to macroscale ductility measurements.

In achieving these objectives, the experimental mechanics community will be provided with straightforward, economical approaches to multi-lengthscale specimen production, new grid-based full-field techniques translated to the microscale, and methods for obtaining high-quality tensile mechanical behavior measurements at reduced length scales. While the proposed approaches have traditional throughput capabilities, informed LS-EVP FFT frameworks are leveraged to simulate thousands of representative microstructure instantiations for specimens of different geometric ratios. In addition, incorporating non-localized damage allows for close correspondence between microstructurally driven deformation heterogeneities and failure processes observed in experiments.

Meeting these objectives directly supports the needs of Department of Energy (DOE) to meet its goal of continued safe, reliable, and economic operation of the nation's reactor fleet. By providing techniques that can be used to assess the structural health of legacy and next-generation nuclear materials, the DOE will be better able to make informed decisions as to when nuclear

reactors should be decommissioned and improve understanding of the mechanical performance of next-generation materials.

Accomplishments:

The research team achieved multiple accomplishments during the project execution. First, a variable-length virtual extensometer technique was developed to obtain thousands of ductility measurements from a single tension experiment (Ryan Berke, Utah State University). The advancement in data analysis allows for just a handful of experiments to be conducted when quantifying material ductility, thereby significantly improving throughput. Furthermore, the technique is length scale agnostic and can be applied to microscale and macroscale full-field displacement data. From the ductility data point cloud obtained using the variable extensometer technique, a unifying ductility law was proposed that merges Barba's Law and the Bertella-Oliver equation.

Advances were also made to the grid method (GM) full-field deformation technique, enabling it to be imple-

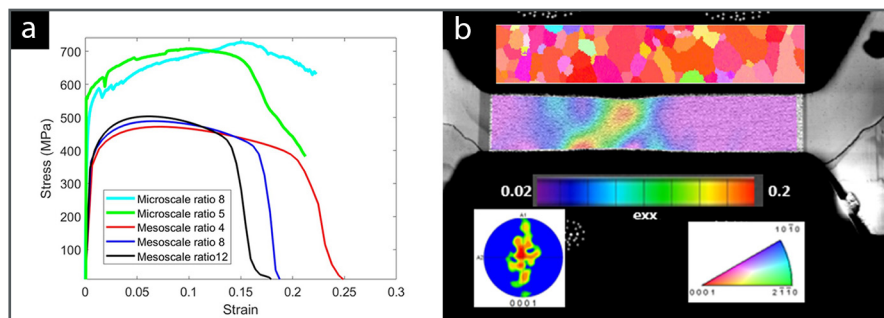


Figure 1. a) A multi-length scale comparison of the mechanical behavior of Zircaloy-2 using different specimen geometric ratios, b) representative data captured during each experiment including electron back scatter diffraction inverse pole figure orientation mapping and full field deformation fields as a function of strain

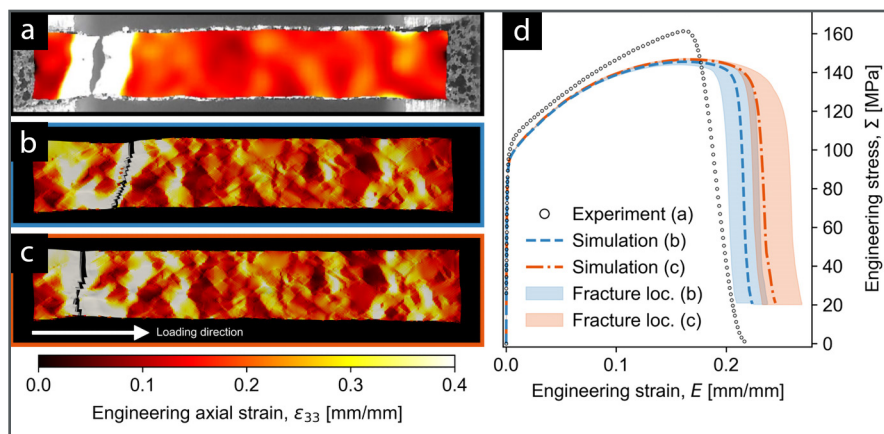


Figure 2. Comparison between an experimental oxygen-free high thermal conductivity (OFHC) copper tensile test and simulations with semi-synthetic microstructures (i.e., surface microstructure that directly matches the OIM map from the experimental test coupon but with variable subsurface microstructures). a) Axial strain field of the experimental coupon collected at final fracture using digital image correlation. b, c) Axial strain fields at final fracture from two of the 15 simulations representing the two predicted fracture locations. d) Macroscopic stress-strain responses from the experiment and 15 simulations; simulations are color-coded based on the two predicted fracture locations, and the color-filled regions correspond to the full range of simulated responses for a given predicted fracture location. In a)-c), visible surface crystallographic orientation maps are identical

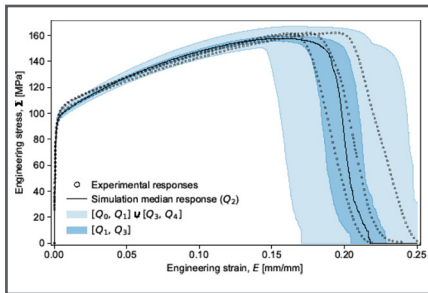


Figure 3. Macroscopic stress-strain distributions from 100 simulations of statistically similar microstructure instantiations compared to experimental stress-strain curves for OFHC copper. The shaded regions span the quartiles (where Q_n indicates the n -th quartile) of the engineering stresses from the 100 microstructural instantiations at each strain point

mented at the microscale (Owen Kingstedt, University of Utah). Focus-ion beam patterning techniques and spectral analysis were leveraged to provide full-field Scanning Electron Microscopy (SEM)-distortion corrected displacement and strain fields. This new technique, the SEM-GM, can resolve intra-granular and inter-granular slip processes, enabling further understanding of deformation mechanism communication and transmission across grain boundaries.

Existing ductility laws fail to account for the contribution of microstructural features, testing environment, and the length scale at which material testing occurs. Before these laws can be modified to account for these contributors to observed material behavior, practical improvements to testing are needed. With respect to this need, a high-temperature micro-tensile stage capable of providing controlled temperature profiles was fabricated and utilized to conduct tension experiments on specimens whose thicknesses are comparable to the penetration depths achieved during ion bombardment (just a few microns) (Owen Kingstedt and Jiyoung Chang, University of Utah). During testing, the grain

orientations are mapped, deformation fields are captured, and stress-strain behavior up to failure is captured. Using these tools, the effect of specimen geometric ratio on mechanical behavior at the mesoscale and the microscale for copper and Zircaloy-2 at ambient and elevated temperatures were quantified (Owen Kingstedt, University of Utah).

Additionally, the capabilities of an LS-EVP-FFT framework were extended to incorporate a triaxiality-based continuum damage mechanics (CDM) formulation within a crystal-plasticity constitutive model (Ashley Spear, University of Utah). The CDM formulation was augmented with an integral-based nonlocal regularization approach that correctly handles gas-phase material necessary to model unconstrained surfaces. The improved model is capable of predicting microstructurally driven deformation and failure processes. The modified modeling framework is leveraged to assess the variability in ductility that can be expected when small-scale specimens have a number of grains in their gauge section below the representative volume element (RVE) limit.

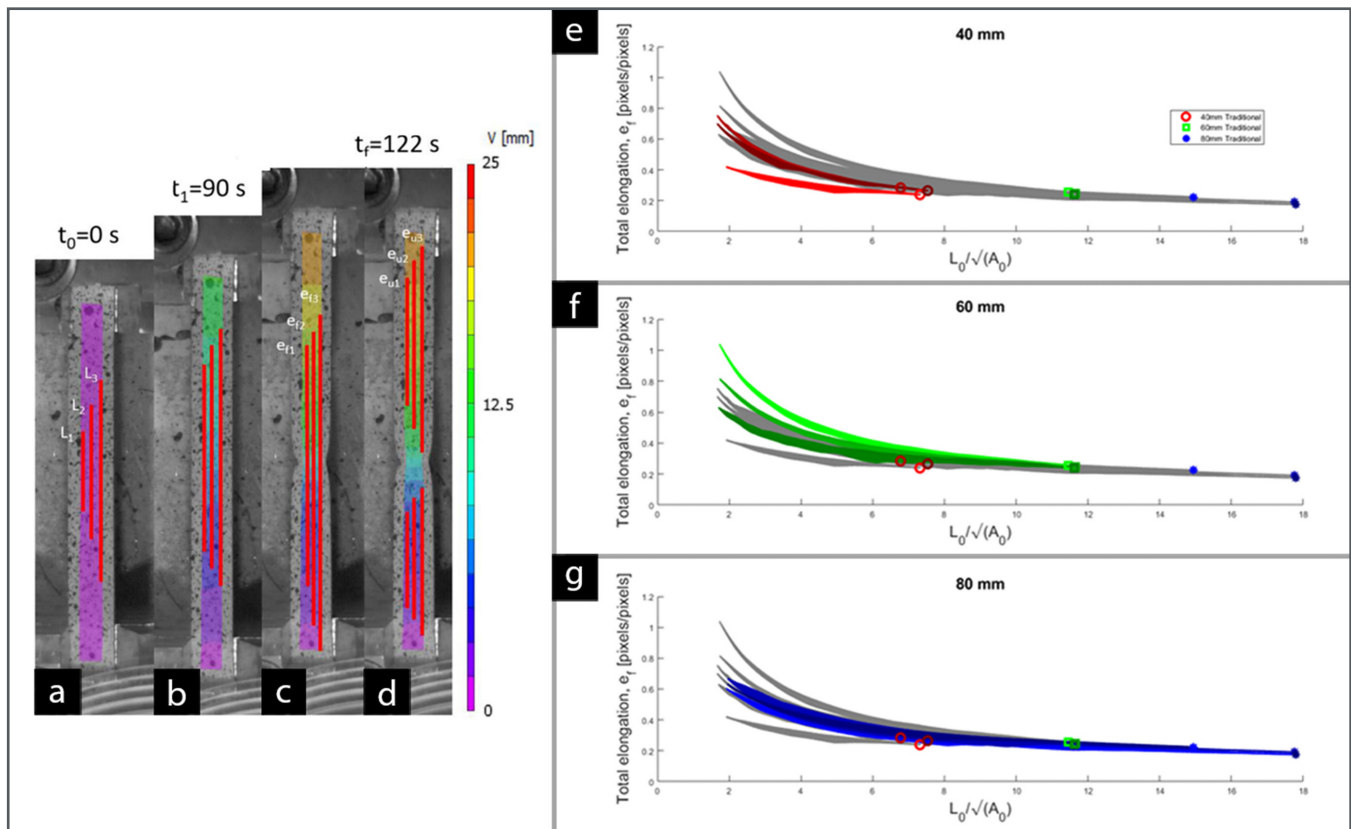


Figure 4. Visualization of the variable extensometer to a macroscale experiment a) initial reference image to obtain initial gauge lengths only three of the thousands of extensometers are shown for clarity b) increasing displacement of the virtual extensometers as axial strain accumulates, c) final image captured before failure used to calculate the final elongation of each extensometer. Note the onset of necking near the middle of the gauge section d) the virtual extensometers that do not span the necking region are used to calculate the uniform specimen elongation. e-g) Comparison of the point clouds obtained across nine macroscale ductility experiments conducted on copper. Red point clouds are for specimens with a gauge length of 40mm, green is for 60mm gauge length specimens, and blue is for 80 mm gauge length specimens

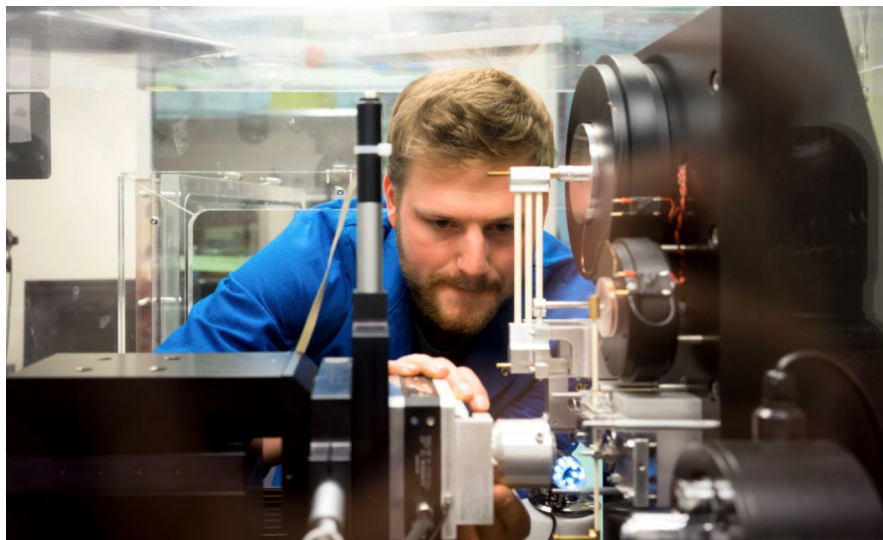
Understanding of Degradation of SiC-SiC Materials in Nuclear Systems and Development of Mitigation Strategies

Principal Investigator: Peter Hosemann

Team Members/ Collaborator: Joey Kabel, Ryan Schoell, Sebastian Lam, Djamel Kaoumi, Christian Deck, Kirill Shapovalov, Julie Tucker, Yongqiang Wang, Enguerrand Buckel, Aaron Mengel, Jia-Hong Ke

Our results show that PVD based techniques can be used to identify suitable coatings and CVD processes can be introduced to the manufacturing process of SiC/SiC composites.

Figure 1. Joey Kabel performing hardness measurements



Silicon carbide has been studied as an accident tolerant fuel (ATF) cladding to combat ongoing challenges with zirconium-based alloys. SiC_{fiber}/PyC_{interphase}/SiC_{matrix} composites were chosen initially due to their favorable properties regarding oxidation, neutron irradiation tolerance, high temperature strength, and neutronics, however, two feasibility challenges still have inhibited development of a nuclear grade SiC composite. Hydrothermal corrosion on the surface of the composite occurs at concerning rates within boiling water reactor (BWR) environments with the oxide layer dissolving at $>10\mu\text{m}/\text{year}$. Hermeticity also is another point of

discussion as micro-crack evolution within the matrix material can lead to fission gas release and further oxidation. The development of a barrier coating would mitigate these issues and hopefully bring SiC composites to nuclear feasibility.

Project Description:

This research aims to develop a dual-purpose barrier coating which can be commercially applied to SiC matrix composites to enhance their corrosion and mechanical properties within nuclear environments. The first technical objective of this project was to identify coating systems which would enhance SiC performance. This includes

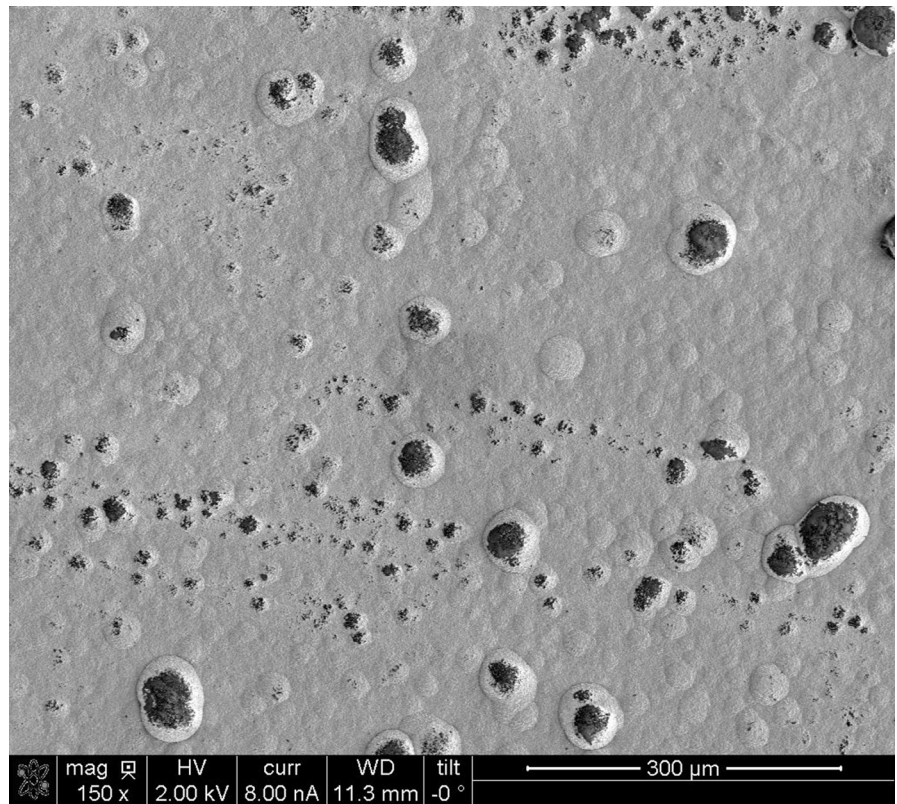


Figure 2. Autoclave setup for corrosion experiments at NCSU

modeling of the oxide layer's stability to choose candidate elements and coating methods which would optimize oxide stability, adherence to substrate, and fuel performance. Once chosen, the selected coatings would be deposited onto SiC and tested by heat treating and corroding the coatings in a simulated BWR environment. Once corroded, a combination of scanning electron microscopy (SEM), energy dispersive spectroscopy (EDS), x-ray photoelectron spectroscopy (XPS) and tunneling electron microscopy (TEM) would be utilized to characterize the quality and adherence of the coatings. In parallel, nanoindentation will be used to verify the mechanical

integrity of the coatings. With this, a comprehensive view of the effectiveness of each coating will be developed and recommendations can be made on future coating systems. While current literature of SiC as an ATF rod cladding material remains extensive, metallic coatings on SiC have been rarely investigated and this research, if successful, would bolster the feasibility of SiC within nuclear environments. SiC composites coated with an extremely resistant metallic coating have the potential to solve many of the safety concerns related to the current generation of cladding, enhancing the safety and reliability of the next generation of reactors.

Figure 3. SEM image of the best performing PVD combinatorial alloy coating with a composition of Zr(30%) Cr(50%)Ti(20%) as-received



Accomplishments:

The first step in developing a commercially available, corrosion resistant, high temperature barrier coating for SiC was performing computer simulations and developing models for expected performance of different coating systems. Oregon State University lead the effort to simulate which coatings would excel at oxide stability, adherence to substrate, and fuel performance when deposited onto SiC. Ultimately titanium, chromium, and zirconium-based coatings were chosen to be coated onto the SiC composites using physical vapor deposition (PVD) and chemical vapor deposition (CVD). With this, commercial vendors were found to produce SiC wafers and

subsequently coat them with our desired compositions. To test this, a total of 19 different coatings were extensively investigated for corrosion and mechanical properties. Among them were TiN, TiCN, CrN, and ZrN CVD coatings from two different suppliers, Ionbond and Diffusion Alloys, 3 different layered PVD coatings produced by collaborators at General Atomics using an in-house system, and 8 different combinatorial and layered PVD coatings produced by the Swiss Federal Laboratories for Materials Science and Technology (EMPA). A combination of heat treatments performed by the University of California, Berkeley (UCB) and corrosion in simulated BWR environments performed by North Carolina State University (NCSU) were tested

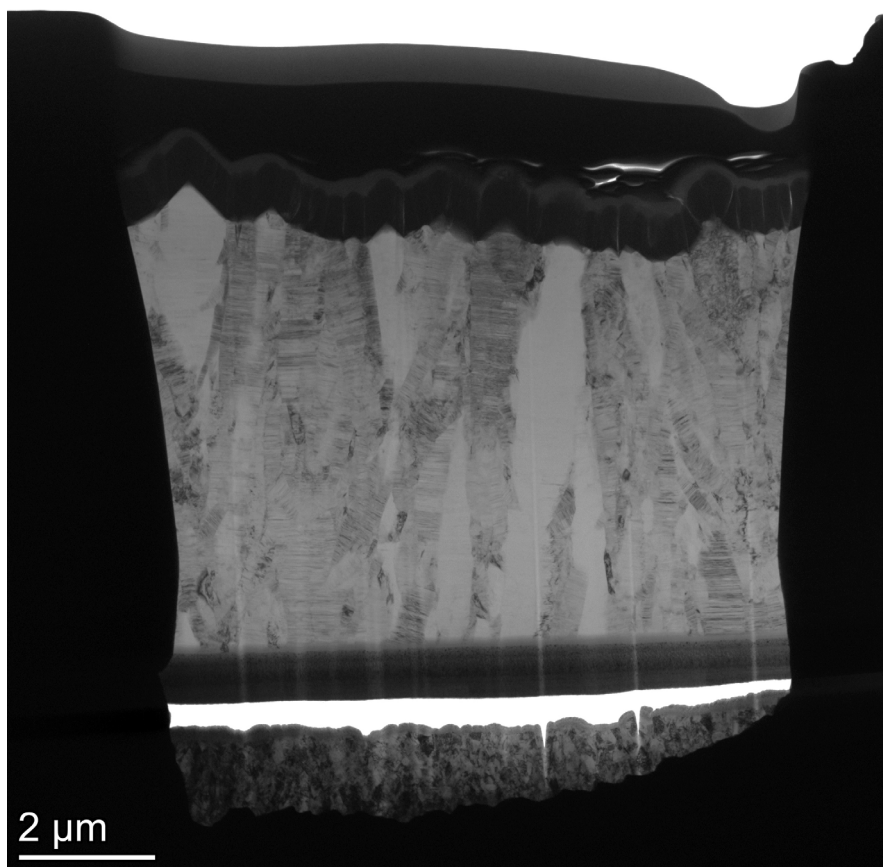


Figure 4. TEM view of cross section of the best performing PVD combinatorial alloy coating with a composition of Zr(30%)Cr(50%)Ti(20%) as-received

on each coating to various results however generalized trends started to appear with each coating. SEM, EDS, XPS, TEM, and nanoindentation performed by UCB and NCSU were employed to further investigate the interfaces of the coatings before and after testing. As a result of this study, major conclusions were found about the performance of each coating system. We found that the CVD coatings didn't perform well in the corrosion environment with mass losses being reported for all samples through a 2-week experiment primarily through delamination and spallation. However, the PVD samples show promising results with 5 different coating systems

gaining mass through the 7-day experiment. The best coating which was investigated was a combinatorial PVD coating produced by EMPA with a composition of Zr(30%)Cr(50%)Ti(20%) which showed positive mechanical properties, no delamination or cracking, and mass gain. In total, a comprehensive look on a variety of metallic coatings on SiC substrates has been gained through the project as well as promising results for future investigation.

Multiaxial Failure Envelopes and Uncertainty Quantification of Nuclear-Grade SiCf/SiCm Woven Ceramic Matrix Tubular Composites

Principal Investigator: Ghatu Subhash

Team Members/ Collaborator: Bhavani Sankar (Co-PI, University of Florida (UF), Nam-Ho Kim (Co-PI, UF), Nance James (former UF student, currently at Sandia National Laboratories, New Mexico), Hemanth Thandaga Nagaraju (current UF PhD student), Christian Deck (Collaborator, General Atomics (GA)) and Sarah Oswald (Collaborator, GA)

This research directly addresses the uncertainty arising from manufacturing process by not only developing multi-axial failure criteria for SiCf/SiC tubes under complex stress states, but also provides failure envelopes for any combination of loads and a phenomenological failure criterion which can be easily applied for design optimization by the industry without the need for interpolation or extrapolation from limited experimental data (i.e., the procedure developed here can be used as an analytical laboratory that can replace the actual testing and thereby saving considerable amount of time and money).

Silicon carbide (SiC) fiber-reinforced ceramic matrix (SiCf/SiCm) composite tubes are being considered for nuclear fuel cladding. However, their microstructure is highly heterogeneous consisting of fibers of different diameters, braids woven at slightly different angles, porosity of various sizes, wall thickness variations and such. These variabilities introduce uncertainty in mechanical properties and failure strengths, even when the tubes are manufactured under nominally same conditions. Hence the technical objectives of the research were to quantify statistical variability in the prominent properties in SiCf/SiCm composites, experimentally determine failure strengths under various combination of loads, develop constitutive relations and failure envelopes for complex multi-axial loading conditions, and propose a phenomenological failure criterion which is easily adoptable in industry.

Project Description:

The proposal aims to quantify the uncertainty (or variability) in properties (Elastic moduli and strength) of SiCf/SiCm woven composite tubes arising from the heterogeneity in their microstructural variables and geometrical features. The variability

in fiber diameter, braid angle, wall thickness of the tube, and porosity has been experimentally measured and a micromechanical model was developed to estimate the uncertainty in modulus and strength of the woven composites. We have utilized finite element (FE) based micromechanics to develop constitutive models for woven composites and determined the failure envelopes under multi-axial loading using the Direct Micromechanics Method (DMM). Concurrently, the composite tubes were tested under flexure, compression, and hoop loading to determine their failure strengths. Analyses was then performed to propagate uncertainties in the material properties and strength to establish variability in failure envelopes under multi-axial loading. Finally, the failure envelopes were validated using a variety of experiments at static and dynamic strain rates in addition to experimental data available in the literature for the SiCf/SiCm composites.

For safe design of nuclear reactors, uncertainty in properties and failure behavior in all possible scenarios must be quantified. However, investigation of failure behavior under such complex scenarios is cost

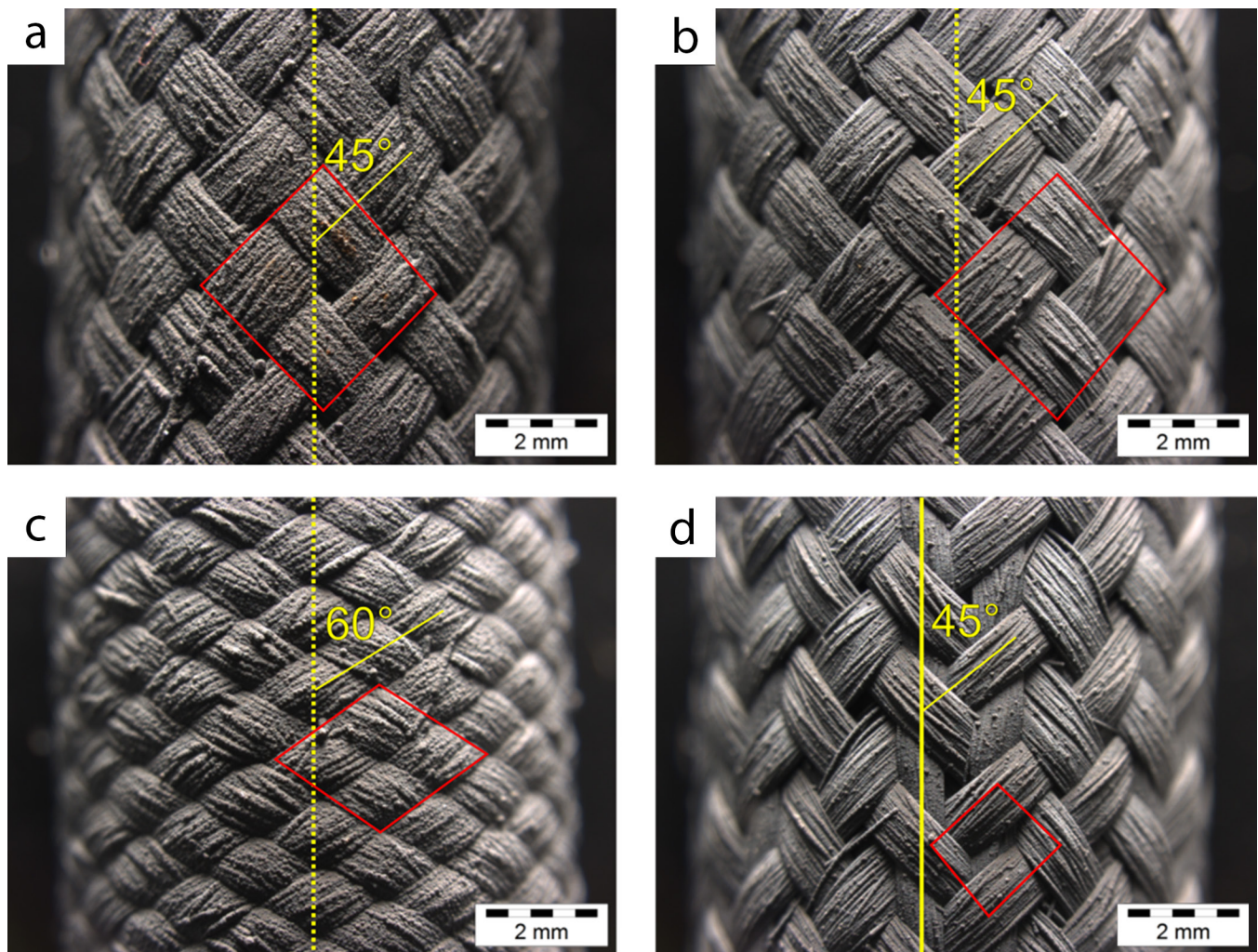


Figure 1. SiCf-SiCm tubular composite architectures used in this investigation. The dashed line represents the vertical axis and the solid lines represent the yarn orientation. The red outline is the unit cell. (a) 45° 2-ply biaxial; (b) 45° 3-ply biaxial; (c) 60° 2-ply biaxial (hoop biased); and (d) 45° 2-ply biaxial

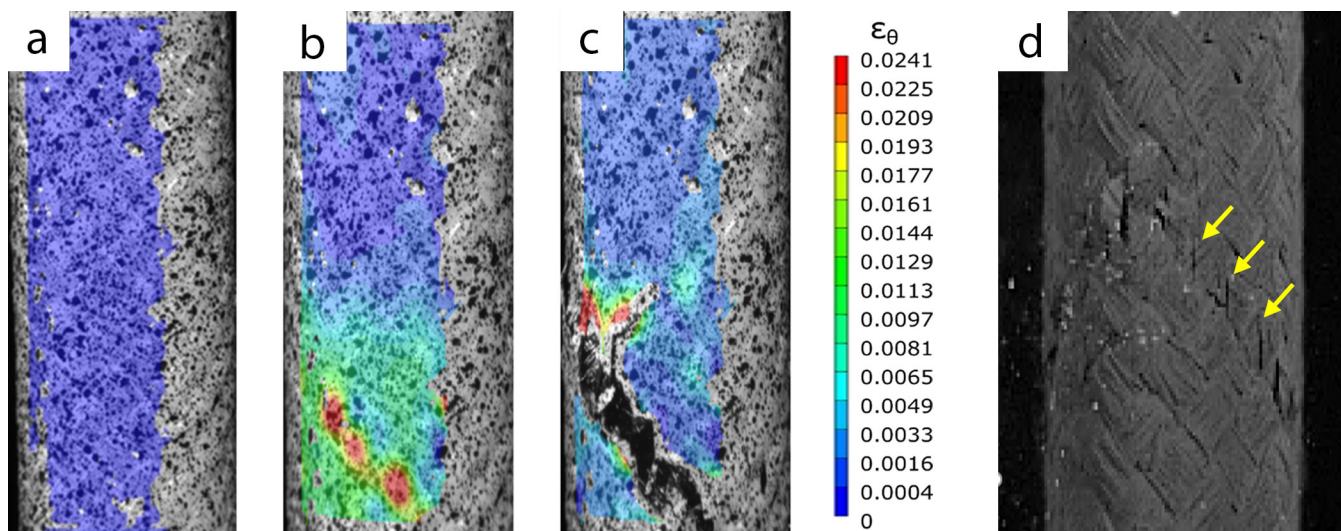


Figure 2. Sequence of digital image correlation images from a typical hoop burst test: (a) Initial uniform hoop strain, (b) a frame just final fracture showing highly localized increase in strain (red regions) where fracture is about to occur in a single yard over its width, and (c) frame after final fracture. (d) Failure mode of crack initiation in a single yarn is shown from a separate test

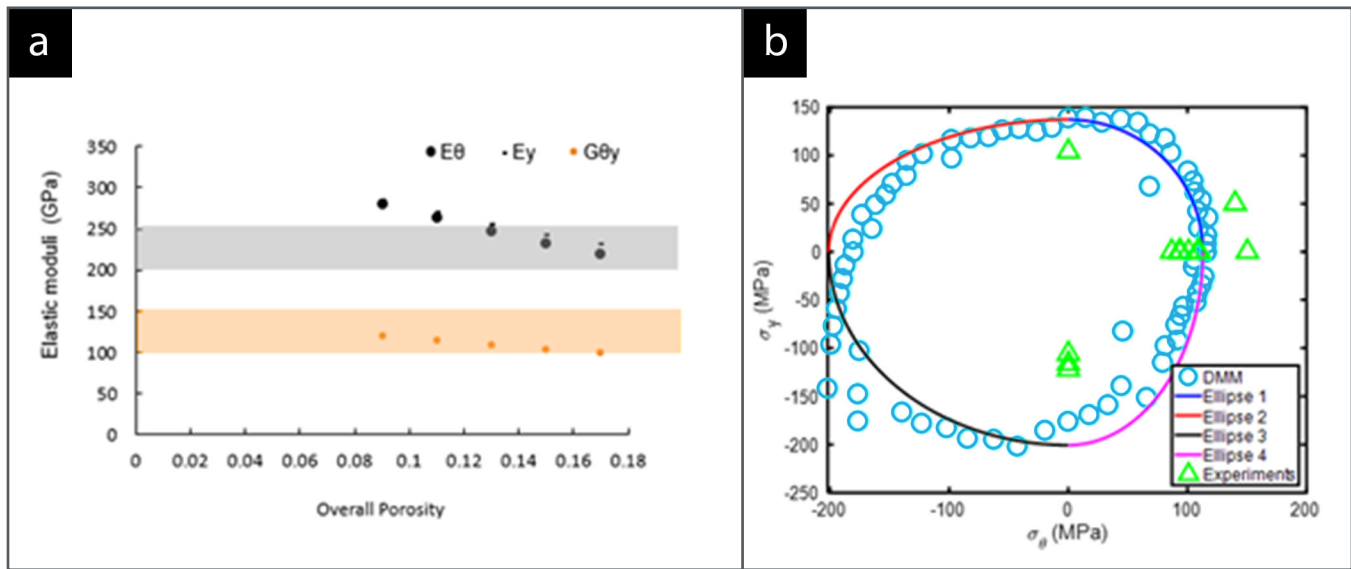
prohibitive and an experimental impossibility. The proposed innovative approach combines new modeling schemes verified by well characterized experiments to quantify uncertainty in the predicted results. By quantifying the influence of heterogeneity and variability in performance, one can successfully predict the reliability of operation under extreme conditions and hence safety assessment can be made with confidence.

Accomplishments:

We have experimentally determined the strength and failure behavior of four SiCf/SiCm composite architectures (Figure 1) with biaxial and triaxial weave orientations at 45° and 60°, under various stress states (axial compression, internal pressure, and rotating flexure). It was found that the braiding angle had the most significant influence on the strength under tensile hoop burst and flexural loading, whereas the effect of fiber angle was not significant for compression loading. These results point to the importance of customizing the

design of tube architecture for enhanced performance in specified nuclear applications. In addition, these experiments revealed a unique failure mode with microcrack nucleation and growth only up to the width of a single yarn (Figure 2). This crack growth behavior is reflected as periodic oscillations in the load-displacement response.

Computationally, elastic constants in various orientations were calculated by using a curved repeatable unit cell (RUC) to account for curved geometry of the tube. This analysis, once for all, settles the issue of using homogenization methods for composites with curved geometries and quantifies the degree of difference in elastic properties between curved and planar geometries. To account for the high-volume fraction of yarns in the SiCf/SiCm composites, a new method called 'chipped-away model' was developed. A multi-scale model using Mori-Tanaka method was implemented to account for high porosity and calculate degradation in Young's modulus of the SiC matrix. The appropriate boundary conditions



were imposed on the FE model to predict elastic constants, which were in good agreement with the experiments as evidenced by Figure 3(a). In this figure, E_θ , E_y and $G_{\theta y}$ refer to stiffnesses along hoop (θ), axial (y), and shear modulus in θ - y plane.

To quantify uncertainty in elastic constants and reduce the computational cost associated with complex FE analyses, polynomial equations that best approximate the FE predictions were constructed. Initially, global sensitivity analysis was conducted to determine dominant variables that influence the elastic constants. They were identified as porosity, Young's modulus of SiC matrix, and Young's modulus of SiC fiber. The developed polynomial equations were then used in Monte Carlo Simulations (MCS) to quickly generate large data of elastic constants for SiCf/SiCm tubes. The uncertainty in elastic constants was determined by calculating the coefficient of variation (COV) from MCS-generated data. The COV in

each of the elastic constants was about 10%. A statistical distribution was also fit to MCS-generated data which is helpful in evaluating 'what-if' scenarios for the performance of SiCf/SiCm tubes.

In the next step, failure envelopes were constructed in stress space by considering the proportional limit stress (PLS) as a failure mode. We used DMM to predict failure for a given loading condition, knowing the strength of the constituent materials. An example failure envelope for one combination of stresses is shown in Figure 3(b). The predicted PLS is in reasonable agreement with the experiments (green triangles). For industrial applications, we proposed a phenomenological failure criterion by fitting ellipse equations (regression fit) in each quadrant as the failure criterion. The COV was found to vary between 25%-48% indicating high variability in PLS.

Figure 3. (a) The predicted elastic constants (symbols) of SiCf/SiCm tubes and the reported range of experiments (shaded region). (b) The PLS values from DMM (cyan symbols) and the curve (ellipses) fit to data in each quadrant. The ellipse equation can be used as a phenomenological failure criterion to assess the performance of SiCf/SiCm tubes

Mechanistic Understanding of Radiolytically Assisted Hydrothermal Corrosion of Silicon Carbide in Light Water Reactor Coolant Environments

Principal Investigator: Dr. Peng Wang, University of Michigan

Team Members/ Collaborators: Dr. Gary S. Was, University of Michigan; Dr. Izabela Szlufarska, University of Wisconsin-Madison; Dr. Keyou Mao, Oak Ridge National Laboratory; Dr. Luke Czerniak, Westinghouse Electric Company LLC

This project will provide a fundamental understanding of the hydrothermal corrosion mechanisms of Silicon Carbide (SiC) in light water reactors (LWRs) under the condition where displacement damage and radiolysis products are present. This project also addresses the need for ongoing accident tolerant fuel (ATF) program research and development (R&D) on SiC/SiC composite cladding. The key feasibility issue of hydrothermal corrosion of SiC was assessed in this project, which is critical for designing a reliable fuel cladding. Currently, radiolytically assisted dissolution of SiC in the LWR environment is still unknown territory. The in-situ ion irradiation-corrosion experiments in this study offer a rapid and cost-effective means to evaluate materials and study the corrosion mechanisms under irradiation conditions comparable to test reactor conditions. It will also extend our knowledge of the degradation mode of SiC-based materials under the influence of irradiation, especially at high doses, which is critically important to the durability of the cladding. By coupling with the model study, this research also provides a broader picture of the long-term corrosion and dissolution behavior of SiC with and without irradiation and

radiolysis products. This research can transfer knowledge to other applications involving SiC in a water environment at high temperatures. Corrosion kinetics of SiC in reactor operation is critical to constructing a corrosion model for SiC cladding in fuel performance codes. This work will directly impact the application of SiC as LWR fuel cladding in commercial reactors.

Project Description:

This project aims to apply ion beam irradiation with in-situ pressurized water reactor water corrosion in combination with modeling and simulation to develop a mechanistic understanding of the hydrothermal corrosion behavior for SiC. A series of ion beam irradiation was performed on the chemical vapor deposition (CVD) SiC sample, and long-term autoclave exposure and in-situ proton irradiation-corrosion experiments were conducted. The modeling team studied the dynamic corrosion processes of the water/SiC system by using ab initio molecular dynamics (AIMD) within the density functional theory (DFT) framework. The modeling results indicate that the initial hydrogen scission reactions play an essential role in the surface corrosion processes, regardless of the surface orientation. In addition, kinetic studies identified that the soluble silicic acid would be

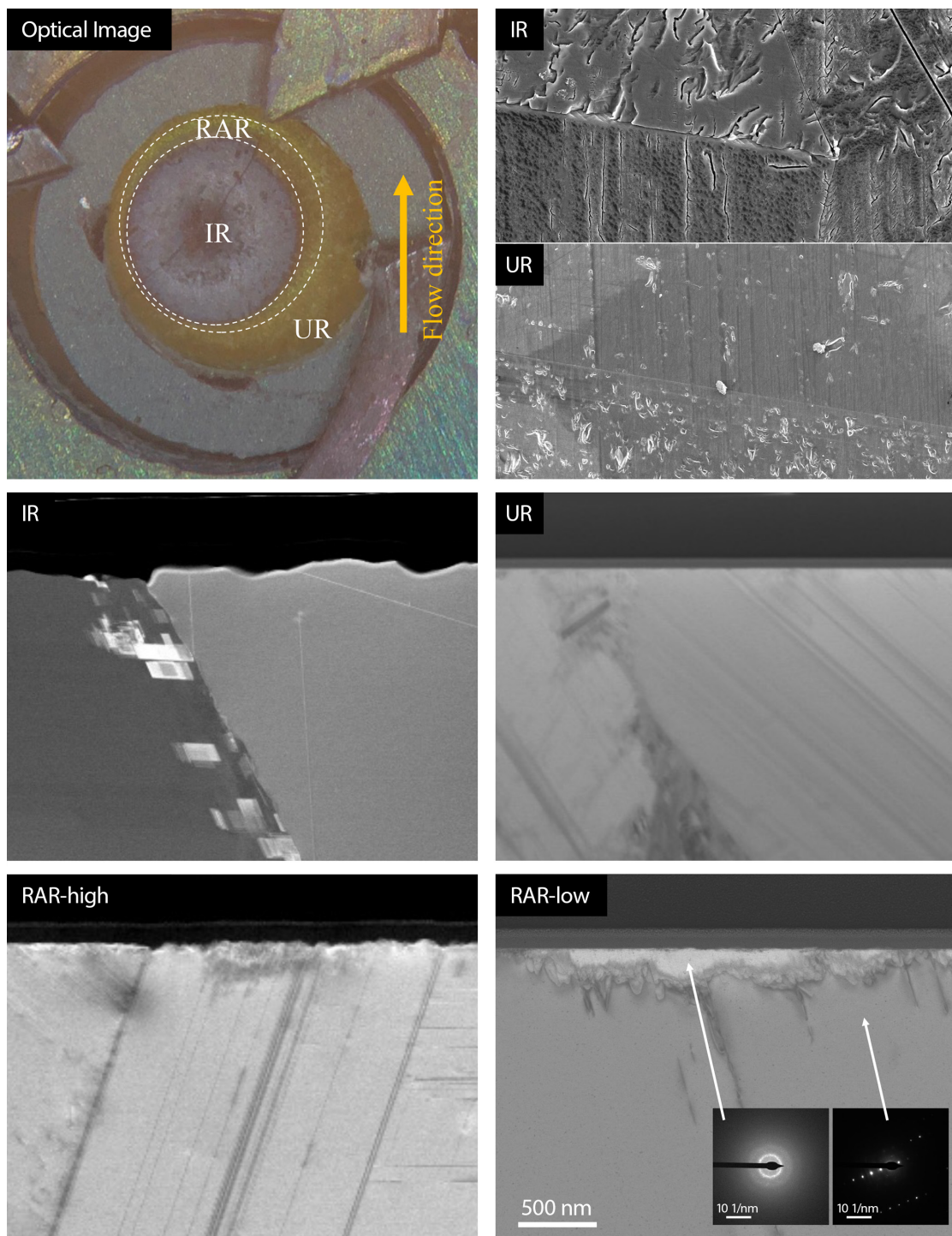


Figure 1. Optical and scanning electron microscopy (SEM) images of SiC sample after the in-situ irradiation-corrosion experiment in hydrogenated water chemistry. The transmission electron microscopy (TEM) bright field micrograph shows the cross-section views of the distinguished individual regions on the sample

Figure 2. Schematic structure of $\text{SiO}(\text{OH})_2$ motif dissolution from a classical MD simulation at 2000K after the surface attack

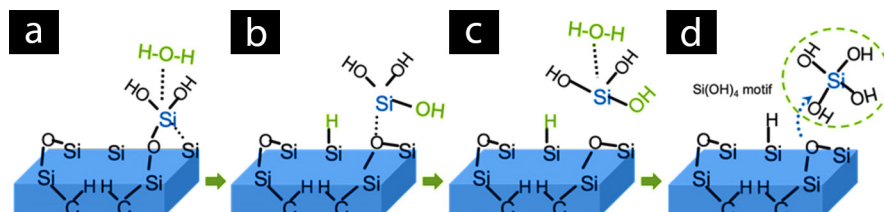
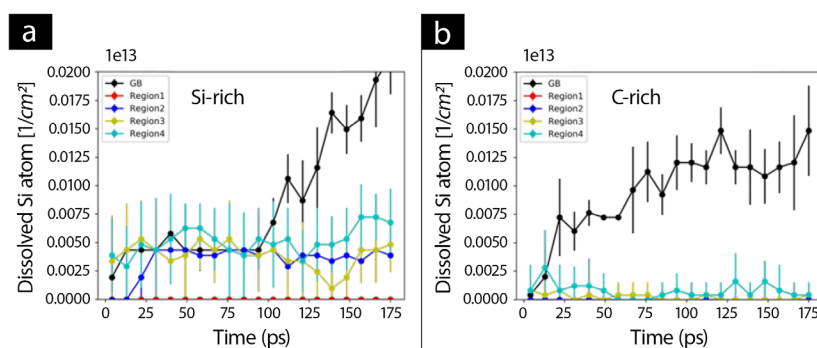
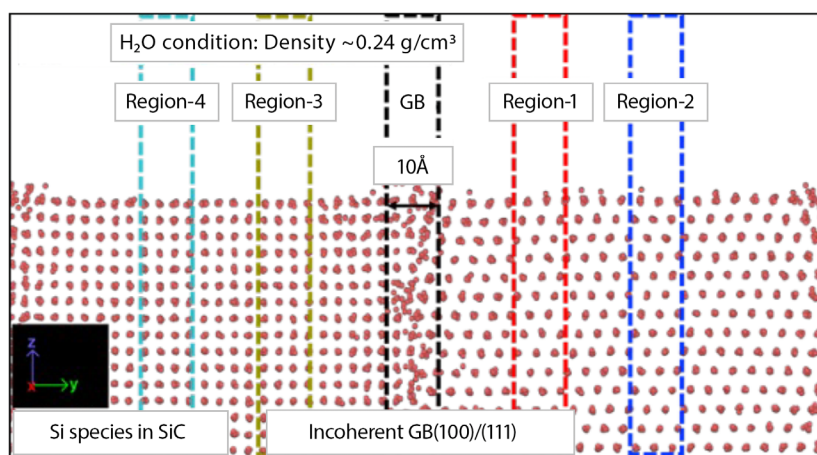


Figure 3. Comparison of SiC dissolution rate using simulated cells with stoichiometric lattice and an incoherent grain boundary. (a) and (b) compare the dissolution rate of Si species in GB and stoichiometric regions. (a) and (b) displays the dissolved Si atom for the Si-rich and C-rich GB, respectively



directly dissolved from intermediate motifs instead of forming a stable silica layer on the SiC surface. When barriers are considered, the preferred reaction path for SiC dissolution goes through the intermediate H_2SiO_3 motif, followed by hydrolysis and deprotonation reactions.

Furthermore, the surface orientation effects on corrosion processes have been identified by considering a set of low-index surfaces, and the team found that the (110) surface would be the most corrosion-resistant surface compared with others, which could provide some strategies for the design of high corrosion-resistant SiC materials for hydrothermal applications. However, it should be noted that besides the interfacial corrosion, the microstructure in materials, such as grain boundaries (GB), is another essential factor to affect the corrosion behavior of materials, as reported in other experimental work. Incoherent grain boundaries corrosion was accelerated under strain and the presence of under-coordinated Si within the GB region, both of which reduce the positive charge on silicon atoms, making them more reactive with oxygen.

Accomplishments:

1. Constructed a portable long-term exposure autoclave (LEXA) for hydrothermal corrosion study of irradiated SiC samples and completed a 90-day exposure on the ion irradiated and neutron irradiated samples.
2. Designed and conducted in-situ irradiation-corrosion experiment on SiC sample with and without pre-irradiation and observed enhanced corrosion under active proton irradiation where both displacement damage and radiolysis products affected the corrosion rate of SiC (example shown in Figure 1).
3. The microstructure of proton irradiated SiC is comparable with neutron irradiated samples in black spot defects, stacking faults (SFs), and Frank loops.
4. Modeling work revealed that as the oxygen concentration in the environment increases, accompanied by the increased redox potential of water, the corrosion mechanism switches from a Si reaction-driven condition to a condition where both Si and C reactions are possible. Hence, accelerated corrosion behavior can be modeled as a function of corrosion potential and oxygen content.

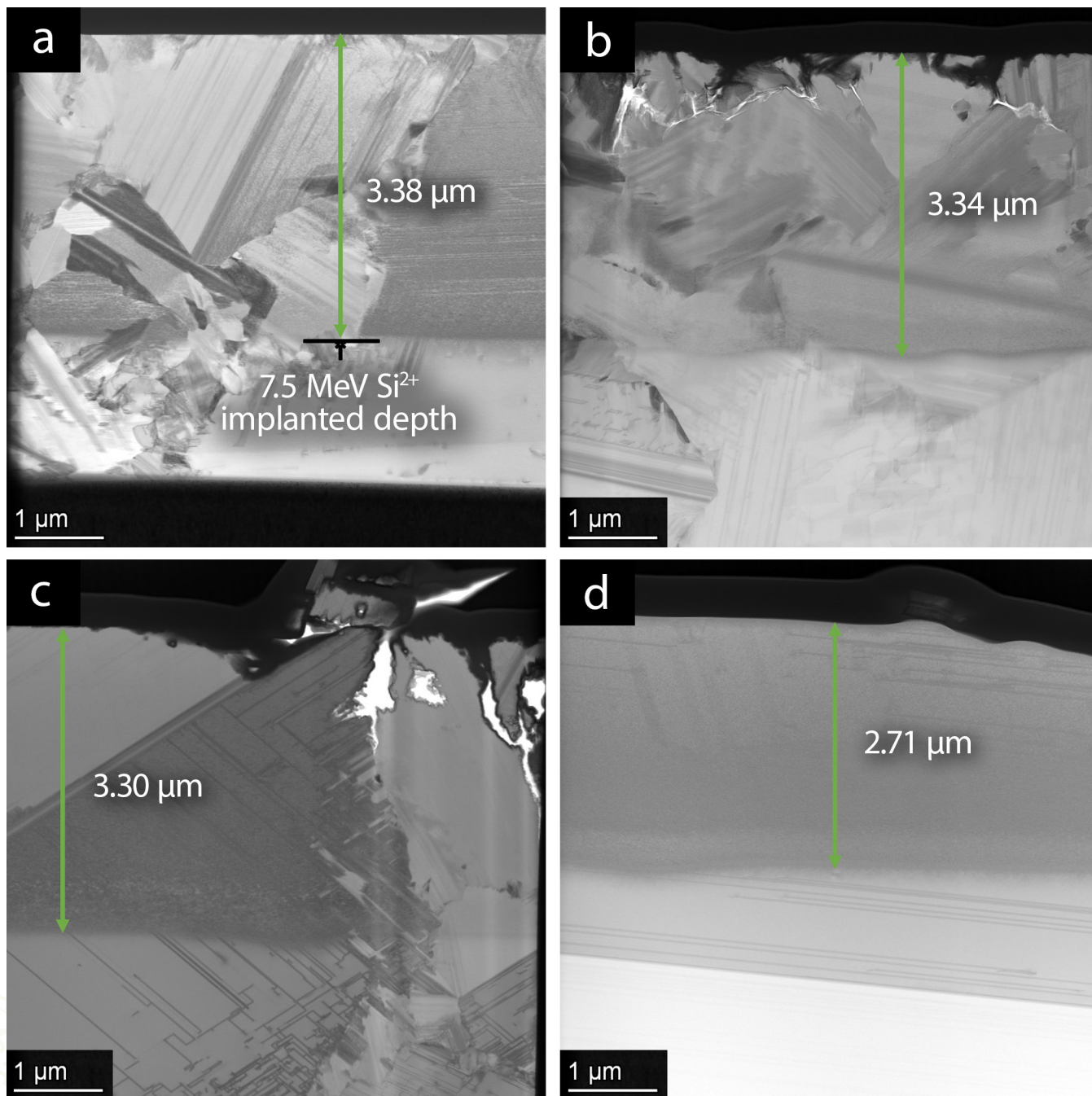


Figure 4. TEM bright field micrograph of a SiC sample implanted with 7.5 MeV Si²⁺ after 24 h in-situ irradiation-corrosion test in pure water with 200 ppb dissolved oxygen, (a) hydrothermal corrosion region; (b) hydrothermal corrosion with a low level of radiolysis products present; (c) and (d) hydrothermal corrosion under active proton irradiation, with a low and high level of radiolysis products, respectively

The accelerated hydrothermal dissolution of SiC was observed under active proton irradiation in simulated LWR water chemistry on CVD 3C-SiC.

5. Molecular dynamic (MD) simulations were performed and determined that the H species dissociated from H₂O molecules can break Si-C bonds and displace Si atoms from the surface, thus resulting in the local disorder of the surface. In addition to AIMD simulations, we demonstrated that oxidation of Si-terminated surface produces motifs, like SiO(OH)₂, which are known precursors to silica and silicic acid formation (example shown in Figure 2).
6. AIMD simulation indicated that the radiation induced chemical changes at grain boundaries could modify the corrosion resistance of SiC (example shown in Figure 3). Specifically, the radiation induced C-rich grain boundary regions can suppress the intergranular corrosion. The corrosion suppression is due to extra C-C networks, which can impede the H scission reaction at the grain boundaries.
7. Experimental results suggest that hydrothermal corrosion of SiC is preferential at the crystallographically discontinuous boundaries having large misorientation, e.g., incoherent GBs. Selective corrosion at planar defects (i.e., SFs) under active irradiation is also likely to enhance corrosion. SiC also shows an accelerated corrosion rate and enhanced GB attacks under higher oxygen activity w/wo the active irradiation due to the already high corrosion potential induced by the considerable oxygen activity (example shown in Figure 4).

Probabilistic Failure Criterion of SiC/SiC Composites Under Multi-Axial Loading

Principal Investigator: Jia-Liang Le

Team Members/ Collaborators: Joseph F. Labuz, Takaaki Koyanagi, Chen Hu, Anna Gorgogianni

An integrated experimental and analytical framework is developed for reliability analysis of SiC/SiC composite claddings under multiaxial loading.

Owing to its excellent mechanical properties and stability under high temperature and neutron irradiation conditions, SiC/SiC composites have emerged as a promising material for light water reactors (LWRs) in the development of accident-tolerant fuel (ATF) systems. Structural integrity and retention of hermeticity are two crucial requirements for SiC/SiC claddings during normal operations, and both of them are closely related to the proportional limit stress (PLS) of the material. Understanding the behavior of SiC/SiC composites under multi-axial stress states and developing a probabilistic approach for evaluating the structural vulnerability are of paramount importance for reliability-based analysis and design of SiC/SiC composite claddings. So far, there has been very limited effort towards experimental and analytical investigations of probabilistic failure of SiC/SiC claddings. This critical knowledge gap motivates this research.

Project Description:

The proposed research is to develop a probabilistic failure criterion for SiC/SiC composites under multi-axial loading, and to incorporate the criterion into reliability analysis of the structural integrity of SiC/SiC fuel cladding. The research consists of two parts: 1) experimental investigation of multiaxial failure behavior of SiC/SiC composites, and 2) theoretical modeling of

time-dependent probabilistic failure of SiC/SiC cladding. In the experimental investigation, the PLS is determined through the examination of stress-strain response, the acoustic emission measurement, as well as the X-ray computed tomography. The theoretical framework is derived by combining the finite weakest-link statistical model and the subcritical damage growth model. This theoretical model captures the time-dependent failure mechanism of the material, which has a major consequence for predicting the lifetime distribution of the cladding. Meanwhile, the model also predicts that the failure statistics of the cladding depend strongly on the cladding length.

The results of the multiaxial experiments reveal the level of statistical variation of the PLS of SiC/SiC materials under different stress states. The theoretical model provides a robust analytical tool for extrapolation of small-scale laboratory test results to the behavior of full-scale claddings. These findings lay down a scientific foundation for the development of reliability-based design of SiC/SiC fuel claddings, which will play an essential role in improving the structural safety and integrity of LWRs.

Accomplishments:

The overarching goal of this research is to develop a probabilistic failure model for SiC/SiC composites

and to apply it to assess the structural reliability of SiC/SiC composite claddings. Toward this goal, the objectives of this project are: 1) design a new testing system, which is capable of producing different multi-axial stress states. 2) Use acoustic emission and X-ray tomography analyses to examine the damage status of specimens. 3) Develop a finite weakest-link statistical model for SiC/SiC composites under multi-axial loading. The model will be calibrated by the multi-axial tests.

In this research, a robust multi-axial testing systems was developed for generating various load combinations of axial force and internal pressure, as depicted in Figure 1. To provide the effective isolation (jacketing) from the internal fluid pressure, viton membranes of a special shape were manufactured to seal both the internal surface of specimen and interface between the specimen and apparatus. High strength epoxy was used in-between the contracted surface of specimen and apparatus to transmit axial loading. With this design, the system is able to load the specimen up to ultimate failure. Figure 2 shows the failure pattern of a specimen in the multi-axial experiment.

During the test, strain gage readings and acoustic emission signal rates were recorded and subsequently used to determine the PLS. The current experiments involved five load paths: pure axial tension, pure hoop tension, and 1:1, 2:1 and 1:2 ratios between the hoop stress and axial stress. These test results (both the PLS and the ultimate limit states, ULS) were presented in terms of failure surfaces with statistical variability

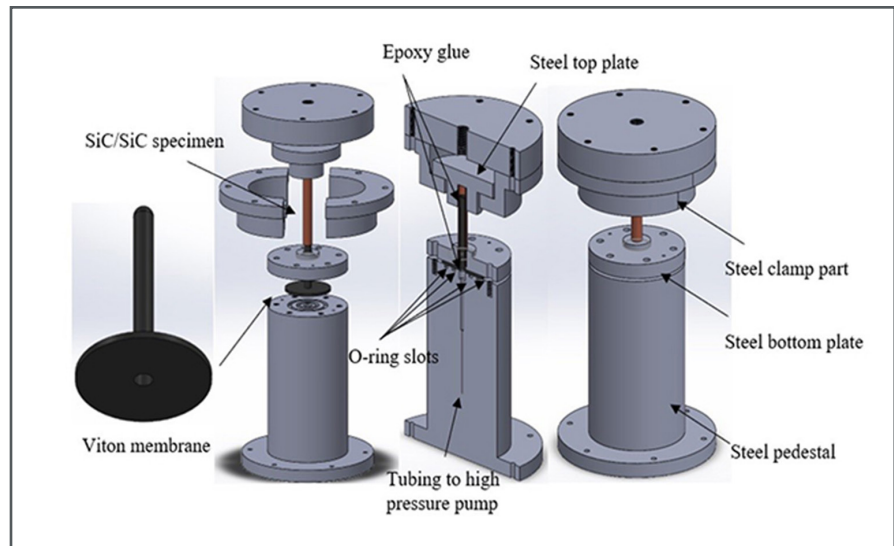


Figure 1. Multiaxial test apparatus

(Figure 3). The convex shape of the failure surface indicated an enhancement in material resistance under biaxial tension.

In parallel with the experimental investigation, a mechanistic probabilistic model was developed to predict the lifetime distribution of SiC/SiC claddings corresponding to the PLS limit. The model takes into account the mechanism of subcritical damage growth. The direct consequence is that the failure probability of the cladding at any given time is governed not only by the current loading state, but also by the previous loading history. The analysis also showed that a long cladding would experience a considerably higher failure risk as compared to a short one (Figure 4). Such a size effect is expected to play a crucial role in design extrapolation from laboratory test results to full-length cladding.

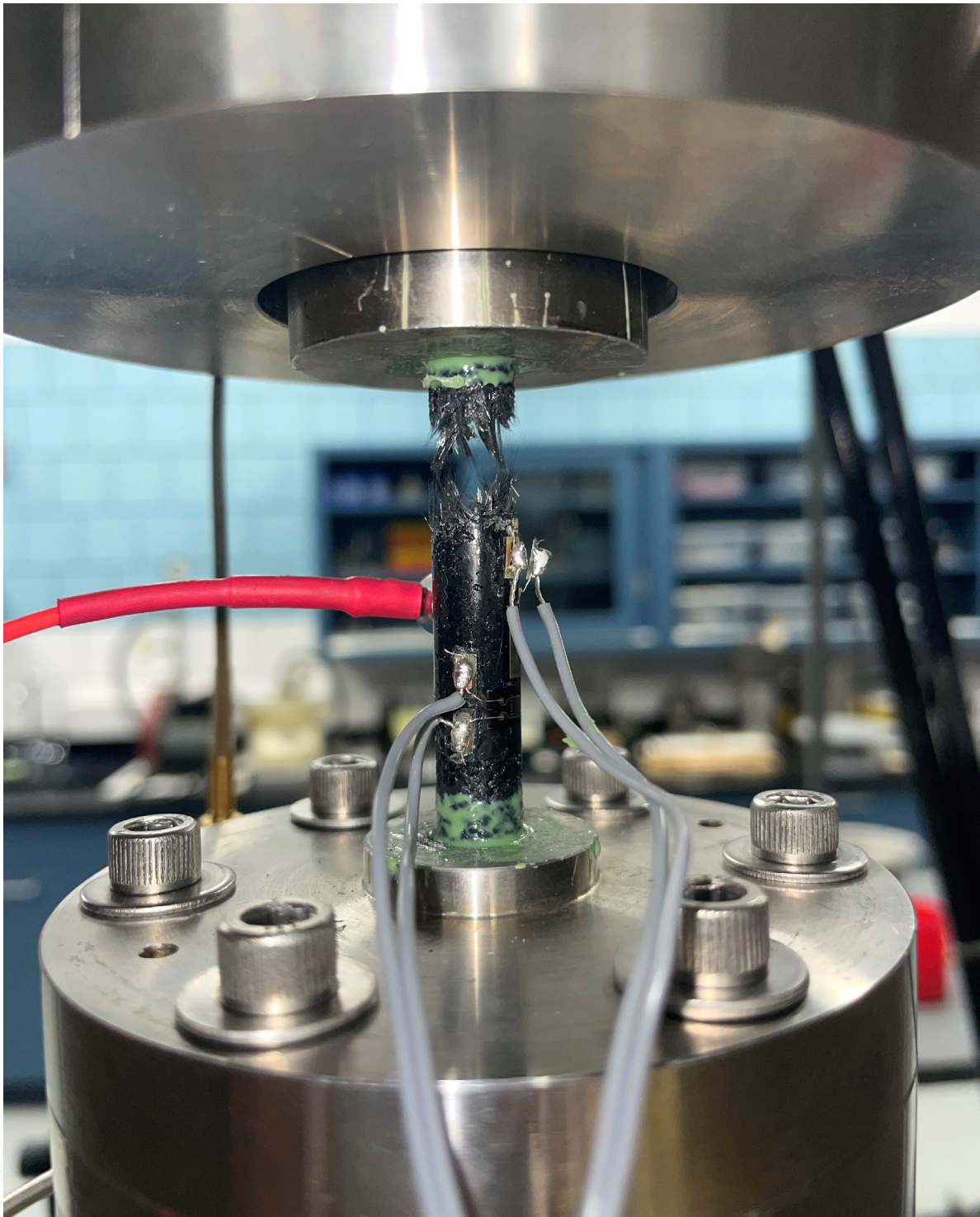


Figure 2. Failure pattern of a SiC/SiC tube specimen in a multi-axial test

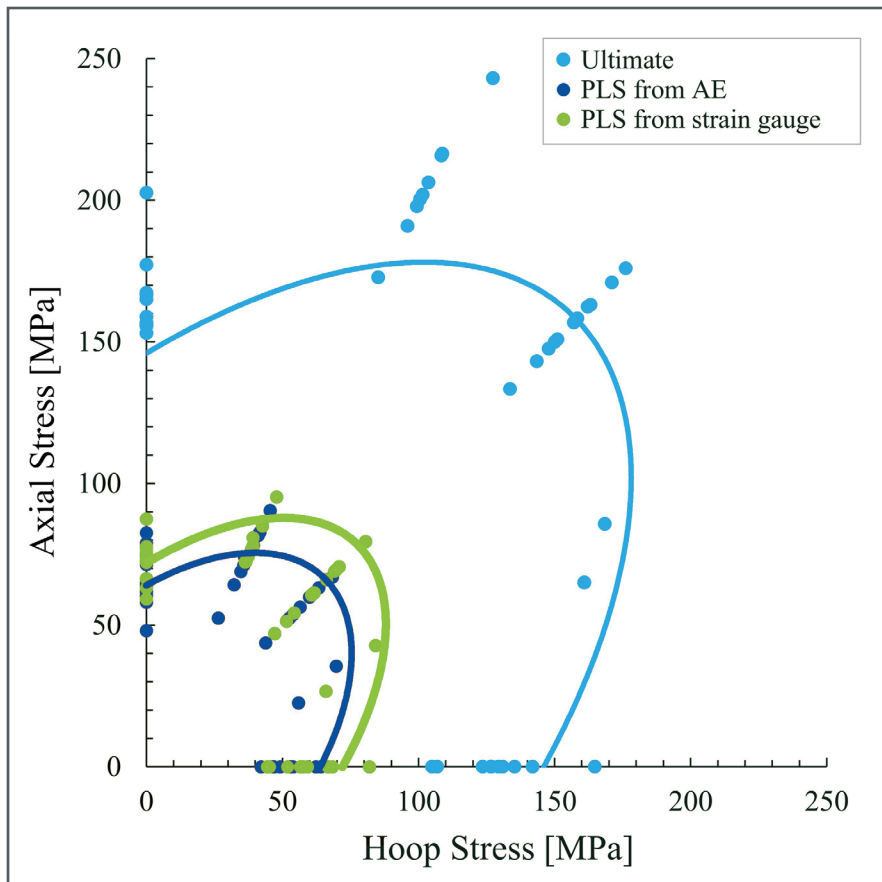


Figure 3. Measured multi-axial failure surface

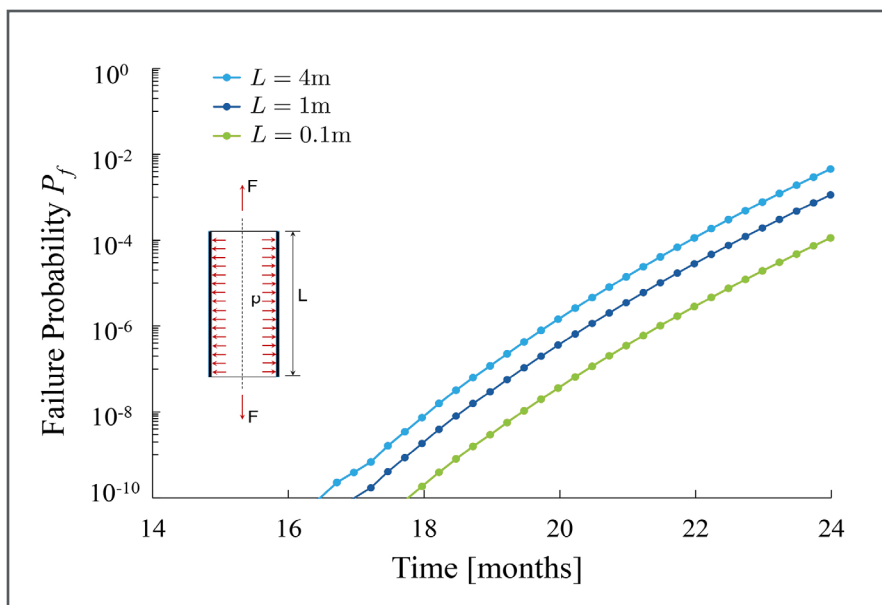


Figure 4. Length effect on the failure probability of SiC/SiC cladding

Development of Multi-Axial Failure Criteria for Nuclear Grade SiC_f-SiC_m Composites

Principal Investigator: Xinyu Huang, University of South Carolina (UofSC)

Team Members/Collaborators: Jingjing Bao, UofSC; George Jacobsen, General Atomics (GA)

The project revealed failure threshold of SiC_f-SiC_m composite cladding under complex loading conditions.

Mechanical strength of silicon carbide (Si)C_f-SiC_m composite tube is typically evaluated under uniaxial tension and internal pressure (burst) loading. Under more complex loading scenarios, such as combined bending and pressurization, the principal stress direction can point to directions off the hoop or the axial direction. Axial tensile and internal burst strength do not provide adequate information to determine mechanical failure threshold for the clad tube. In this project, UofSC utilized five types of tests to help trace out a failure envelope for the SiC_f-SiC_m composite tube. These tests include internal pressure test, combined internal pressure-tension test, torsion test, combined tension-torsion test, and uniaxial tension test. The combined loading conditions can steer the 1st principal stress (highest tensile stress) in between hoop and axial direction thus allowing us to generate a multi-axial failure envelope.

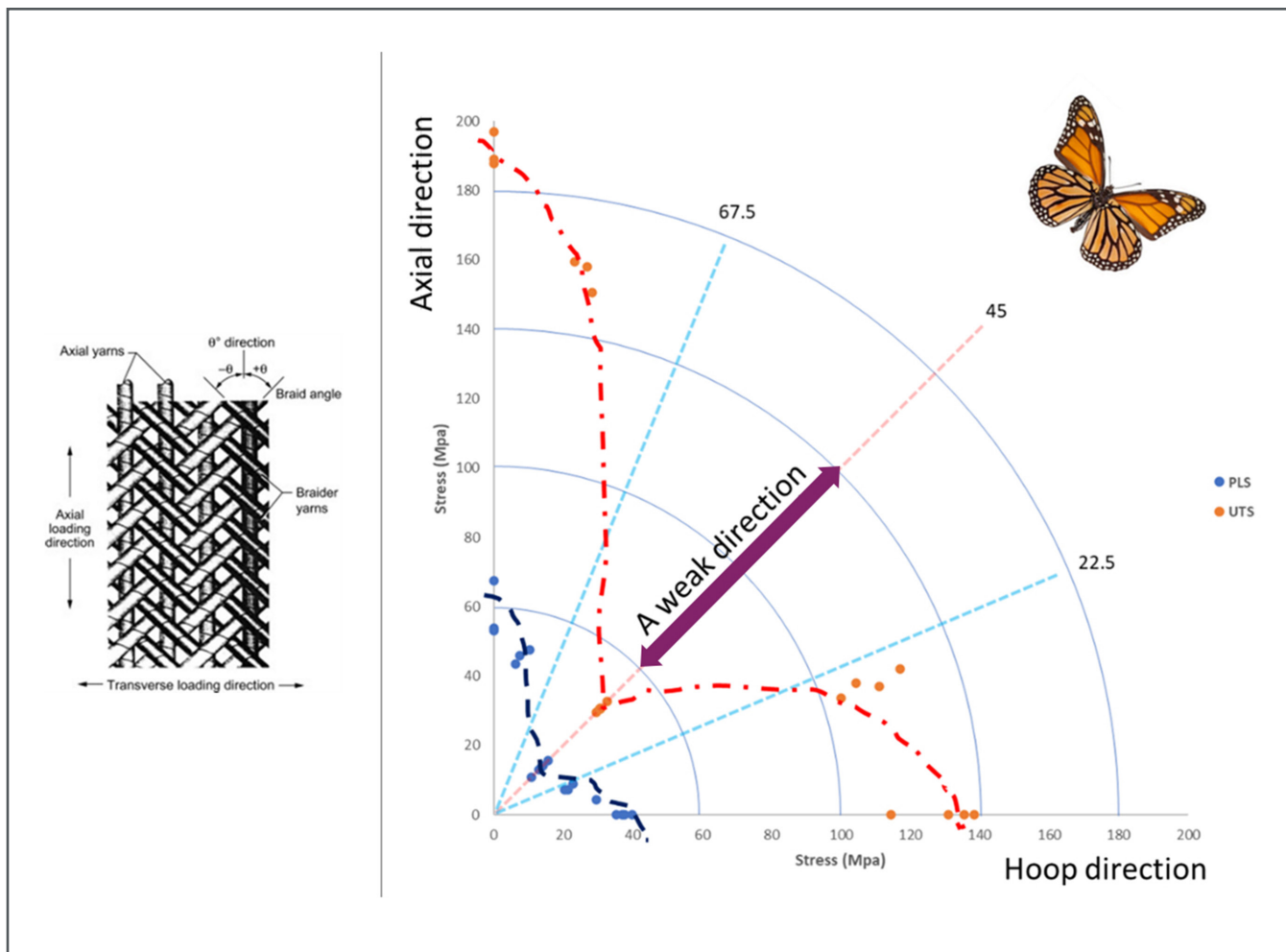
Project Description:

Continuous SiC fiber-reinforced SiC matrix (SiC_f-SiC_m) composite with engineered weak fiber-matrix interphase has demonstrated greatly improved mechanical toughness while preserving other beneficial characteristics of monolithic β-SiC. These attributes can significantly improve the accident tolerance of the light water reactor (LWR), thus making it a highly promising

candidate for numerous core structural components, such as accident tolerant fuel cladding and channel box. Complex state of stress can develop in SiC_f-SiC_m composite fuel cladding. In addition to the self-equilibrated eigenstress due to thermal gradient and irradiation swelling, stresses can be induced by differential pressure loading and other concentrated external loading. It is the objective of this program to develop multiaxial failure criteria for nuclear grade SiC_f-SiC_m composites which will allow more rigorous mechanical failure analysis of fuel rod under complex loading conditions.

Accomplishments:

UofSC developed and validated capabilities to conduct tension, torsion, internal pressure, combined tension-torsion, and combined internal pressure torsion tests. In combined loading tests, proportional load control was implemented with the proportional-integral-derivative controller operating under a master-slave mode. The applied loads (e.g., torsion and pressure, or tension and pressure) are kept proportional during the test. The test rig and its different loading modes were validated by testing aluminum samples and comparing the measured properties with well-known mechanical properties of aluminum. Satisfactory results were obtained. During testing, the applied load (and or pressure) are monitored



together with strain (via traditional resistance foil gage and digital image correlation) and acoustic emission from the samples. X-ray computed tomography was utilized to observe samples after tests. GA fabricated SiCf-SiCm tubes for this project using standard GA-Electromagnetic Systems Group procedures used for the Department of Energy – Nuclear Energy Accident Tolerant Fuel Program. This includes a thin pyrolytic interphase coating deposited directly on the fibers and a crystalline SiC matrix deposited using chemical vapor infiltration. UofSC

conducted several test campaigns on these representative materials and obtained failure multiaxial failure envelope as shown in Figure 1. The failure envelope reveals strong direction-dependence of the mechanical strength. For tri-axial braid composite tube, axial direction turns out the strongest direction due to the set of axial tows in addition to the two sets of bias tows. The hoop direction is the 2nd strongest direction. Surprisingly, a much weaker direction is revealed when the 1st principal direction is at 45 degrees with respect to the hoop direction.

Figure 1. Failure envelope of tri-axial braid SiCf-SiCm composite tube extracted from a large number of combined loading tests. (UTS, ultimate tensile strength; PLS, proportional limit stress.)

Advanced Coating and Surface Modification Technologies for SiC-SiC Composite for Hydrothermal Corrosion Protection in Light Water Reactor

Principal Investigator: Dr. Kumar Sridharan, University of Wisconsin-Madison

Team Members/Collaborators: Dr. Hwasung Yeom, University of Wisconsin-Madison; Dr. Adrien Couet, University of Wisconsin-Madison; Dr. Peng Xu, Westinghouse Electric Company; Dr. Sergey Chemerisov, Argonne National Laboratory

Chromium coating deposited by PVD greatly enhances the feasibility of the use of SiC-SiC composite as an accident tolerant fuel cladding material in light water reactors.

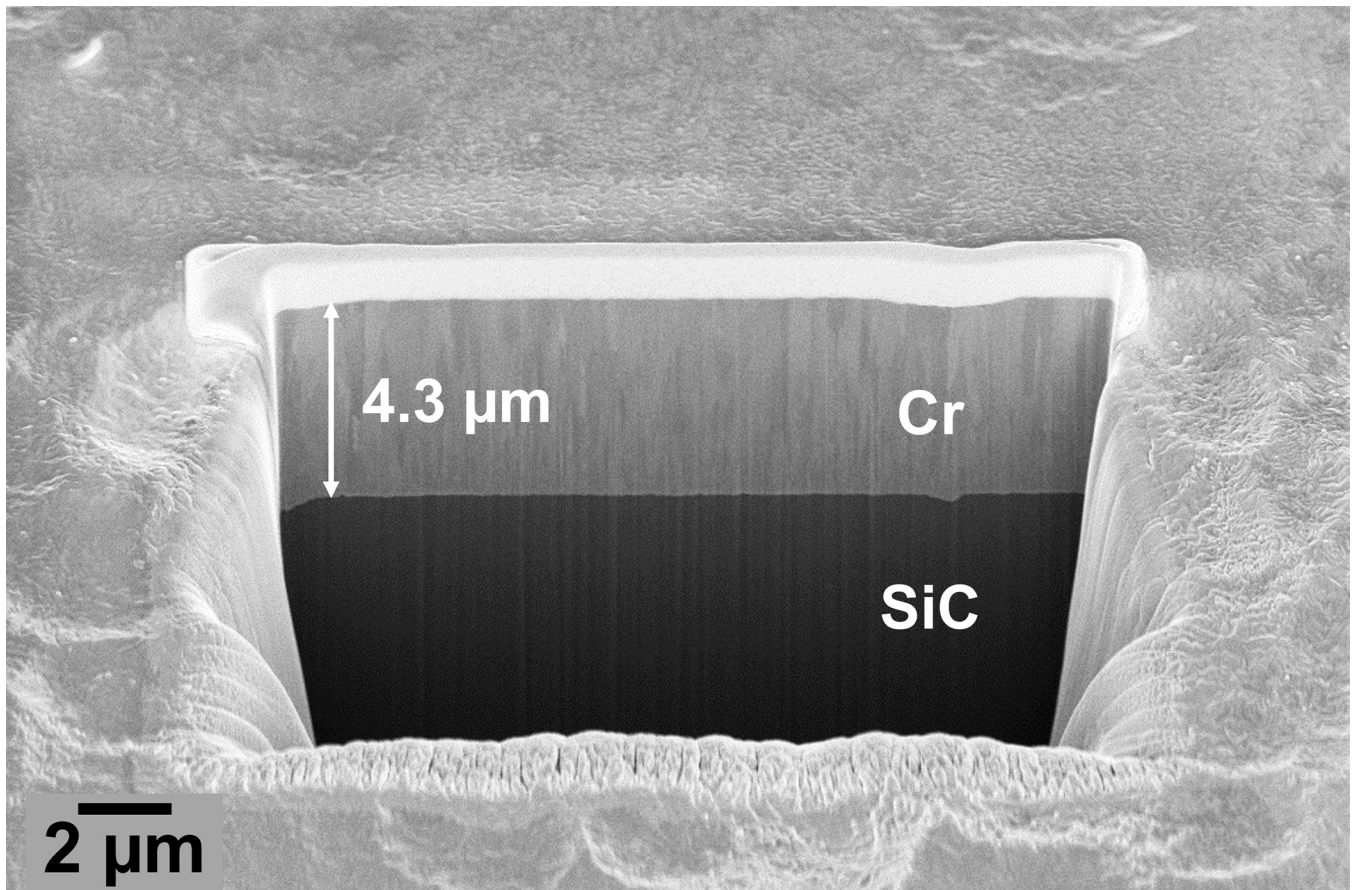
Silicon carbide (SiC)-SiCf composites are being investigated for use as an accident tolerant fuel (ATF) cladding material in light water reactors (LWR). SiC offers greater oxidation resistance and high temperature strength in severe accident conditions ($> 1200^{\circ}\text{C}$ steam) compared to the currently used Zr-alloys. However, SiC experiences corrosion at normal reactor operating conditions (i.e., hydrothermal corrosion) through the reaction of SiO_2 with water at $\sim 300^{\circ}\text{C}$, leading to contamination of the coolant and dimensional changes of the cladding. In this project, surface modification and coating technologies are being developed to protect the SiC-SiCf cladding against hydrothermal corrosion. Cr has been selected as the coating material on account of its outstanding hydrothermal corrosion resistance in pressurized water reactor water conditions. The primary focus of this work has been on physical vapor deposition (PVD) of Cr coatings. Detailed characterization of the coatings has been performed to understand the effect of deposition parameters on the resultant coating

and coating-substrate interfacial microstructures. The mechanical behavior of the coating materials has been investigated using micro- and nano-mechanical test methods. Corrosion performance and thermal stability of the coatings has been investigated with a variety of experimental systems to assess the performance of coatings in a variety of simulated reactor environments.

Project Description:

A central objective of this project is the development and optimization of coating technologies for the SiC-SiCf composites. In particular, coatings produced using state-of-the-art PVD technologies have been studied extensively. The microstructural characterization, mechanical property analysis, and performance testing of these advanced coatings is of great interest to both the nuclear materials and thin film scientific communities.

Pure Cr coatings produced with PVD have been investigated extensively in this project. The evaluation of processing-structure-property relationships for the Cr coatings studied in this project builds upon the body of knowledge of PVD Cr coatings



for nuclear applications and brings value to the ongoing Department of Energy programs on PVD Cr coatings for Zr-alloys as a near-term ATF option. Finally, the existing literature on the behavior of Cr under irradiation is limited, and neutron and ion irradiation experiments conducted as part of this project will help advance

the understanding of the radiation response of pure Cr, specifically when used as a coating material.

Overall, this project seeks to enhance the feasibility of applying SiC-SiCf composite fuel cladding for use in commercial LWRs as an alternative to currently used Zr-alloy. SiC-SiCf

Figure 1. Focused ion beam-milled cross section of the B-HiPIMS Cr coating on SiC

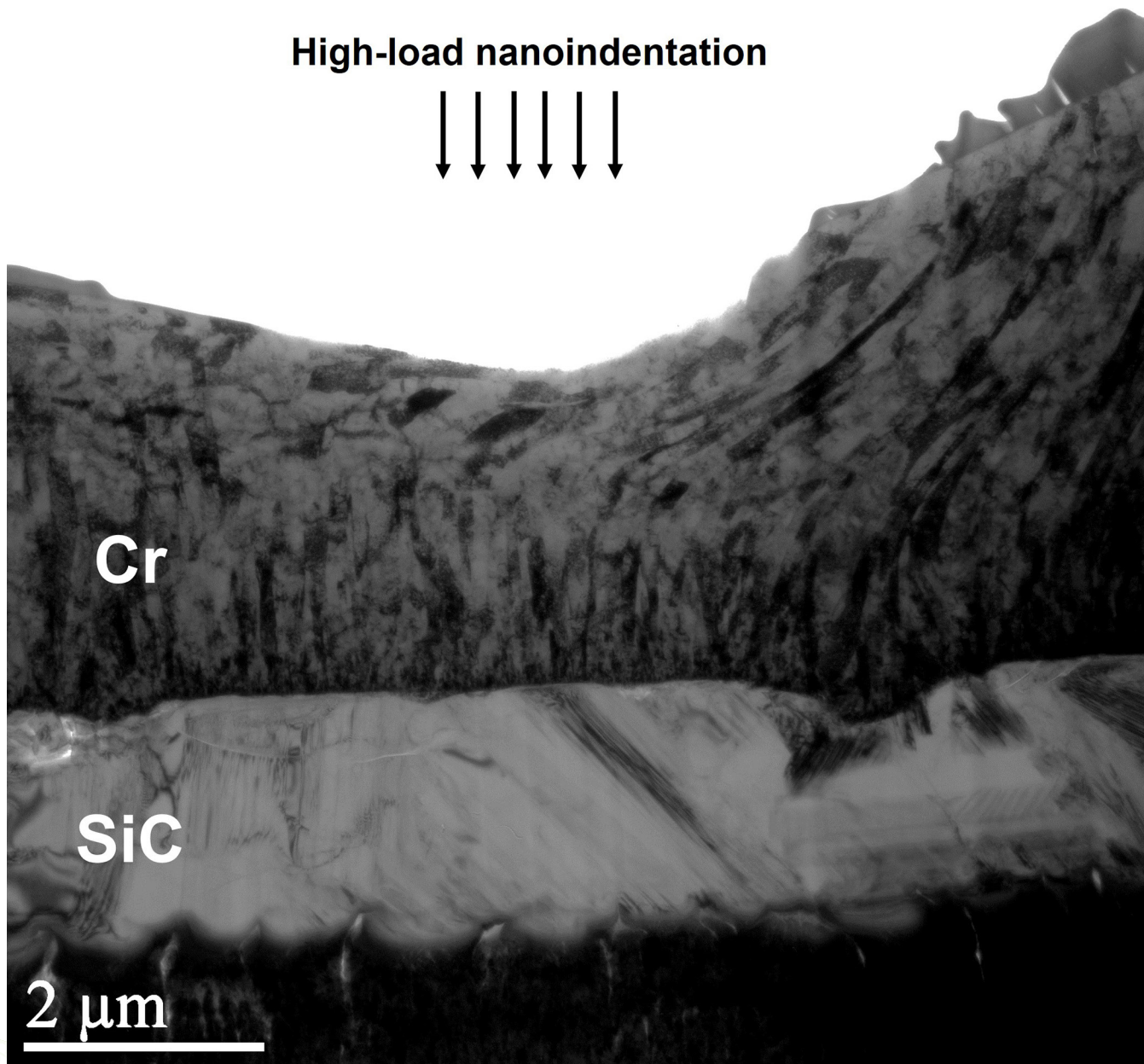


Figure 2. Cross-sectional bright field transmission electron microscopy image of a high-load nanoindentation on the B-HiPIMS coating showing deformation of the columnar grains, as an indication of ductility of the coatings

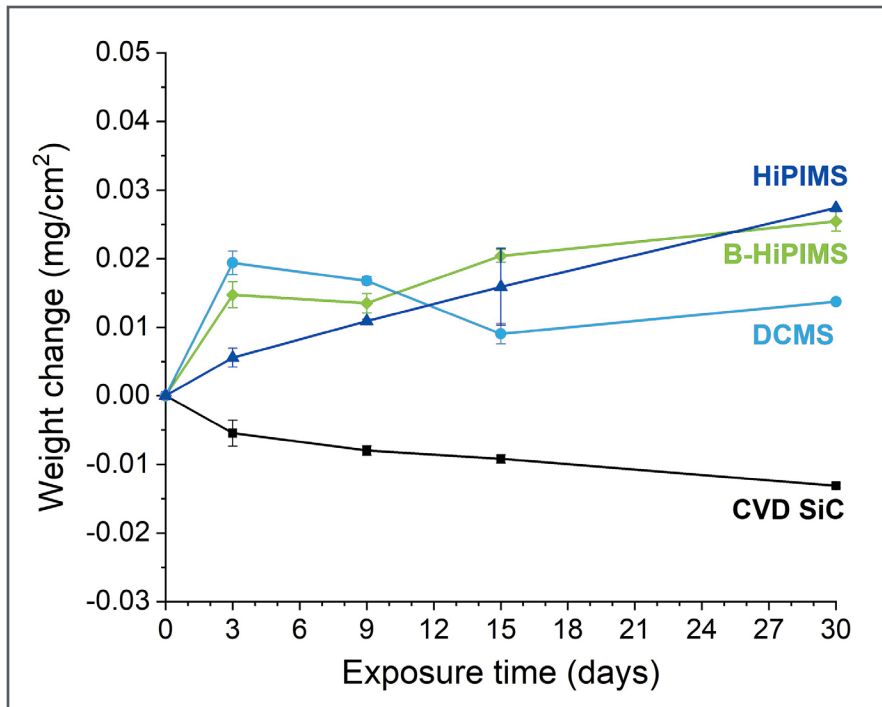


Figure 3. Weight change data for various types of Cr coatings compared to uncoated SiC from a 30-day static pure water hydrothermal corrosion test conducted at 360 °C

cladding offers greatly improved safety performance in severe accident scenarios compared to Zr-alloys and has the potential for use as an ATF design in both existing and future reactors. SiC also offers the potential for improved reactor efficiency based on its lower neutron absorption cross section, good radiation resistance, and ability to withstand higher burn-ups. However, the most significant impediment to the use of SiC-SiCf composite fuel cladding is hydrothermal corrosion, and this project seeks to overcome this challenge by the development of PVD Cr coatings. These coatings may also be

considered for the application of SiC-SiCf composites in steam and high temperature aqueous environments.

Accomplishments:

In the first stage of the project, a variety of coating and surface modification technologies were evaluated, followed by initial performance screening of the resultant samples. Cold spray deposition of Cr and Fe-Cr-Al and a chromizing thermal diffusion treatment demonstrated limited feasibility due to the high hardness and thermal stability of the SiC substrate material. Through collaborations with

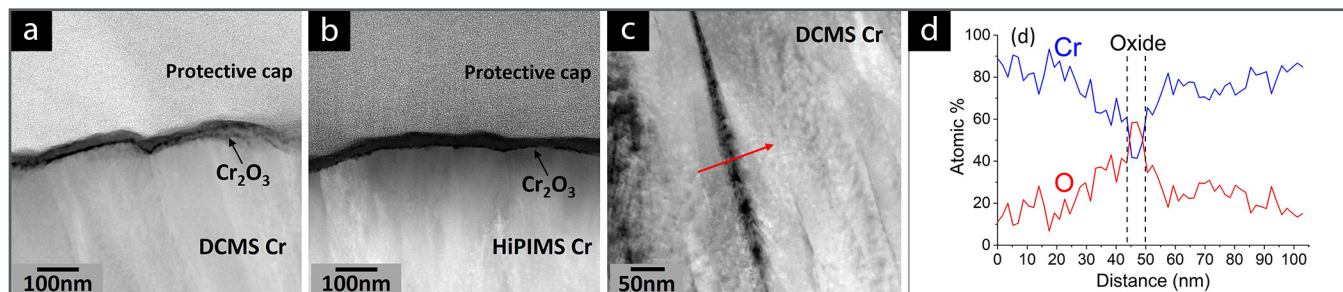


Figure 4. High-angle annular dark-field imaging (HAADF) scanning transmission electron microscopy (STEM) images at the surface of the (a) DCMS Cr and (b) HiPIMS Cr coatings after the 30-day corrosion test; (c) HAADF STEM image below the surface of the DCMS coating showing the location of EDS line scan across an intercolumnar boundary; (d) EDS line scan data showing formation of Cr_2O_3 along the intercolumnar boundary

industrial coating vendors, Cr, CrN, Zr, and CrCxNy coatings 5-10 μm in thickness were deposited using direct current magnetron sputtering (DCMS), high-power impulse magnetron sputtering (HiPIMS), and cathodic arc processes. Among these coating materials, pure Cr coatings produced with magnetron sputtering demonstrated the best mechanical properties as determined by micro- and nano-mechanical testing and scratch tests.

As an initial evaluation of the protective capability of the coating, SiC samples coated with DCMS Cr and HiPIMS Cr were subjected to a 30-day static water corrosion test at 360 $^{\circ}\text{C}$ at the University of Wisconsin. It was found that both types of Cr coatings prevented hydrothermal corrosion of the underlying SiC through the formation of a passive Cr_2O_3 layer 20-30 nm thick on the coating surface. The weight gain (an inverse measure

of oxidation resistance) of the DCMS coating was greater than HiPIMS during the initial stages of oxidation due to the higher surface roughness and presence of nanoscale intercolumnar porosity within the DCMS microstructure.

In the next generation of coating development, the investigation of sputter deposition technologies was expanded to include processes which incorporate secondary ion bombardment and target voltage pulsing. Extensive microstructural characterization using transmission electron microscopy was conducted to understand the influence of these deposition parameters on grain size, morphology, and density. Ion-assisted DCMS was found to enhance densification of the microstructure through atomic peening effects, while pulsed DCMS promoted columnar grain growth. A state-of-the-art bipolar HiPIMS (B-HiPIMS) process was

also developed in collaboration with industrial partners to deposit Cr coatings. The B-HiPIMS process resulted a fully dense coating under compressive residual stress due to the high atomic mobility and ion bombardment effects generated during deposition.

The B-HiPIMS Cr coating demonstrated excellent corrosion performance in hydrothermal corrosion tests with oxidation characteristics similar to that of bulk Cr. Nanoindentation testing of the coating materials showed that coatings which contain fine grains separated by porosity tend to crack during deformation due to weak intercolumnar adhesion. In comparison, the larger, densely packed grains comprising the B-HiPIMS coating are more amenable to plastic deformation and produce a more ductile mechanical response.

In collaboration with Argonne National Laboratory (ANL), a unique corrosion system was designed and fabricated. Designed for use at the Low Energy Accelerator Facility at ANL, the sample capsule is irradiated by 3 MeV electron to generate corrosive water radiolysis products that may be present during reactor operation. In addition, select coatings have been irradiated with heavy ions at ANL and the University of

Wisconsin Ion Beam Laboratory to study defect evolution in the coatings and any mixing effects at the Cr-SiC interface, under irradiation.

Scanning transmission electron microscopy-energy dispersive spectroscopy (STEM-EDS) and HRTEM characterization of the Cr/SiC interface were performed at Idaho National Laboratory (INL) by the University of Wisconsin graduate student to analyze the extent of atomic mixing at the interface produced by different deposition processes. Results showed there may be an intermixed region 5-10 nm in width, but further characterization is necessary. The strength of the Cr/SiC interface will be measured at INL using in situ microcantilever bending at room temperature and 300 °C. In situ high temperature x-ray diffraction measurements were also conducted at INL and showed that at 300 °C, the stress in the B-HiPIMS coating becomes more compressive than at room temperature due to differential thermal expansion effects.

2.3 LWR IRRADIATION TESTING AND PIE TECHNIQUES

Ring Tension Testing

Principal Investigator: Robert Hansen

Team Members/Collaborators: Fabiola Cappia, Philip Petersen, David Kamerman

This project meets the challenge of obtaining accurate hoop strengths from irradiated cladding through the ring tension test by proper configuration selection, increased understanding of experimental uncertainties, and mathematical models to correct data.

The Idaho National Laboratory (INL) Accident Tolerant Fuel (ATF) post-irradiation examination (PIE) program is focused on obtaining accurate data on material behavior of ATF cladding concepts. In anisotropic cladding, hoop direction mechanical properties are vital to qualification efforts. However, accurate hoop measurements are challenging to obtain experimentally, and cannot be replaced by axial mechanical testing. The ring tension test (RTT) is an extremely useful method to determine hoop direction properties in irradiated cladding, requiring only a small amount of irradiated material per test. Several different configurations have been implemented, yet results will either under- or overestimate the cladding hoop strengths, depending on the configuration. Additionally, hot cell testing environments introduce experimental uncertainties which can lead to further errors in property measurement. For hoop direction testing of irradiated cladding using the RTT, it is important to understand these uncertainties and to improve the accuracy of resulting strength measurements.

Project Description:

The purpose of this research can be summarized by three key objectives. First, to compare two leading RTT configurations for accuracy in strength measurements. Second, to understand the effect of uncontrol-

lable test parameter variations in the RTT. And third, to develop processing methods to extract material properties more accurately. To meet these objectives, finite element models of the RTT setup were developed and analyzed, allowing precise replication of the experimental conditions and an in-depth understanding of how the configurations impact property measurements.

While several configurations of the RTT have been proposed and implemented, the results vary between configurations, and property measurements can be significantly inaccurate due to a non-ideal loading state. This project investigated two leading configurations, seen in Figure 1, comparing the measurements made from the raw data. By using finite element models which feature known material properties, the measured properties can be directly compared with material inputs that represent the correct results. This allows a robust evaluation of the accuracy of these two configurations, which can be paired with three-dimensional stress and strain fields to understand discrepancies.

Further complicating matters, several test parameters that can vary uncontrollably when testing irradiated material in a hot cell environment. Deviation of specimens and fixturing from nominal dimensions,

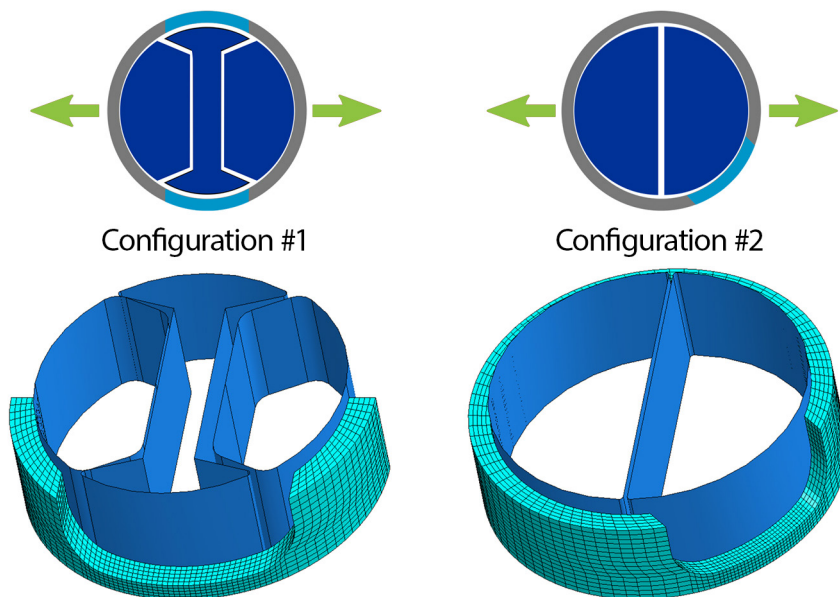


Figure 1. Schematics of the two RTT configurations investigated, with arrows showing the direction of loading. In Configuration #1, the reduced gauge section is supported by a “dogbone” insert; in Configuration #2, the gauge is placed on the mandrel, at a 45° angle

geometries, and orientations have the potential to significantly impact property measurements. Using the finite element models, a wide range of these test parameters were perturbed. Their effect on load-displacement and derived strength measurements was investigated.

Using free body force cuts of the finite element models, hoop tensile load was examined at cross sections throughout the ring during the simulated RTT experiment. Understanding how tensile load varies through the ring allows a robust description of the stress within the gauge region, which can lead to force correction methods for highly accurate property measurement.

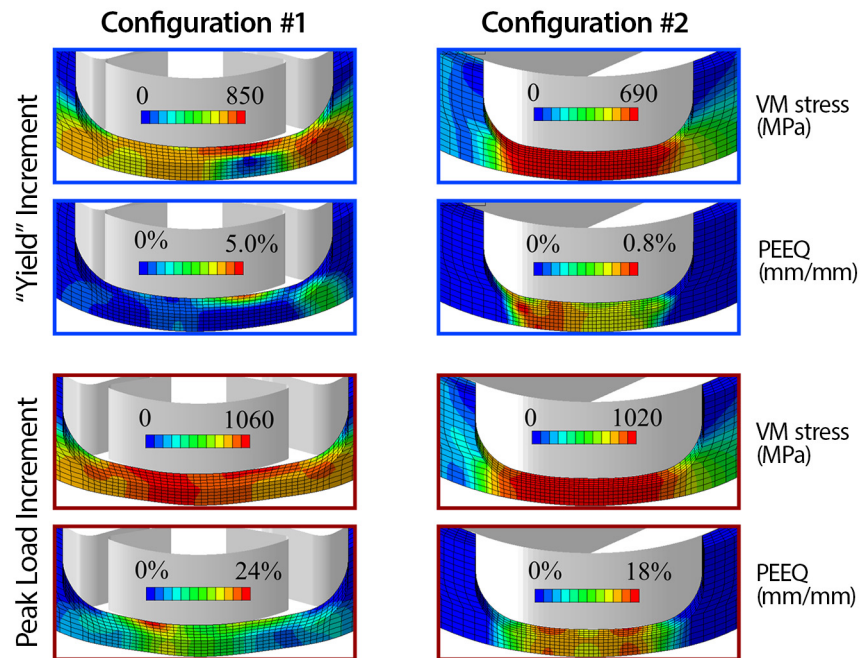
Accomplishments:

The analysis of these key objectives was carried out at INL. Using the finite element models, the ability to accurately measure the material strengths using the two RTT configurations was compared. Using raw

load-displacement data, the yield and ultimate tensile strengths were calculated, resulting in errors on the order of 5-20%. Configuration #1 underpredicted both strengths, while Configuration #2 overpredicted both strengths. The stress and strain fields produced were also analyzed, revealing the presence of key issues. As seen in Figure 2, Configuration #1 was found to produce non-uniform stresses and strains, likely due to a bending stress near a gap between fixturing in the gauge region. However, Configuration #2 produces more uniform results, closely mimicking loading states expected from a traditional tension test. This uniform loading state is ideal for testing coated cladding concepts, where comparable stresses at the outer and inner surface of the ring are desirable.

The sensitivity analysis was also completed, highlighting the challenges of in-cell testing and informing future testing of irradiated

Figure 2. Finite element results, for Configuration #1 (left) and Configuration #2 (right). Both von Mises (VM) stress and equivalent plastic (PEEQ) strain contours are given. Images at the top are from the increment at yield as determined by the stress-strain curve, and images at the bottom are at peak load where ultimate tensile strength occurs



cladding. A wide range of parameters were investigating, systematically varying their values by a series of increments comparable between the two configurations. Those categorized as having a significant impact in at least one of the configurations are summarized in the top of Figure 3. This impact determination was based on significant changes to the strength measurements derived from the load-displacement data. For example, when varying the ring inner diameter from nominal dimensions, the strengths are greatly impacted as seen in the bottom of Figure 3. The compiled sensitivities resulting from this project provides valuable information for future tests of irradiated cladding, allowing tests to both minimize and properly account for measurement uncertainty.

Because of its loading state and reduced sensitivity, Configuration #2 appears an ideal method if the errors identified in the first key objective can be reduced. Using the section cut method described in the third objective, a mathematical model describing the hoop tension load in the Configuration #2 ring as a function of angle was developed. This model closely matched the finite element section cuts. From this model, force correction factors were generated, which reduce the strength measurement errors to less than 1%. The uncorrected, corrected, and actual stress-strain curves are shown in Figure 4. This approach results in highly accurate and robust hoop strength measurements of irradiated cladding.

Sensitive Parameters?



Config. #1



Config. #2

Ring diameter	XX	X
Gauge length	XX	X
Mandrel size	XX	
Dogbone size	XX	
Dogbone angle	XX	
Rotation	XX	X
Eccentricity	XX	X
Ovality	XX	
Friction		XX

Change in Ring-Mandrel Gap	% Change in YS	
	Config. #1	Config. #2
0.14x	-4.1%	
0.25x	-11.1%	-2.5%
0.50x	-12.0%	-2.3%
0.75x	-8.6%	-1.1%
1.5x	+6.3%	+0.6%
2.0x	+10.8%	+1.2%

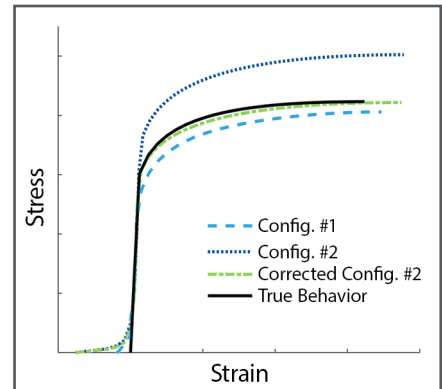


Figure 3. (left) Parameters which demonstrated a significant impact on strength measurements are shown above; two red Xs signify more severe sensitivity. At bottom, the change on measured strength values for the ring inner diameter parameter, reported as a change in the gap between the ring and fixturing mandrel

Figure 4. (above) Plot of engineering stress vs engineering strain for the raw data of both configurations, and with the correction to Configuration #2 using the developed mathematical model for hoop tension load. The true behavior of the modeled material is shown by the black curve

2.4 LWR FUEL SAFETY TESTING

Resumption of Water-based RIA Testing in the U.S.

Principal Investigator: Charles Folsom

Team Members/ Collaborator: David Kamerman, Colby Jensen, Nicolas Woolstenhulme, Jason Schulthess, Leigh Ann Astle

The restart of the Transient Reactor Test (TREAT) facility has renewed the capability for transient testing of nuclear fuels in the United States. This capability is critical to support the mission of the Accident Tolerant Fuels (ATF) campaign and the recent U.S. nuclear energy industries' interest to extend burnup beyond the current limits of 62 GWd/t. Design basis accident testing in TREAT, such as reactivity-initiated accidents (RIA) and Loss of Coolant Accidents, can be performed in TREAT to support these efforts. The development of the Static Environment Rodlet Transient Test Apparatus (SERTTA) experiment capsule provides the capability to test Light Water Reactor (LWR) fuel rods in a static water environment under RIA conditions. A series of six commissioning tests were completed in the SERTTA capsule in TREAT to demonstrate the renewed capability of RIA testing to support U.S. nuclear energy goals. Post-transient characterization of the test specimens has been performed to complete evaluation of the specimen/test system performance.

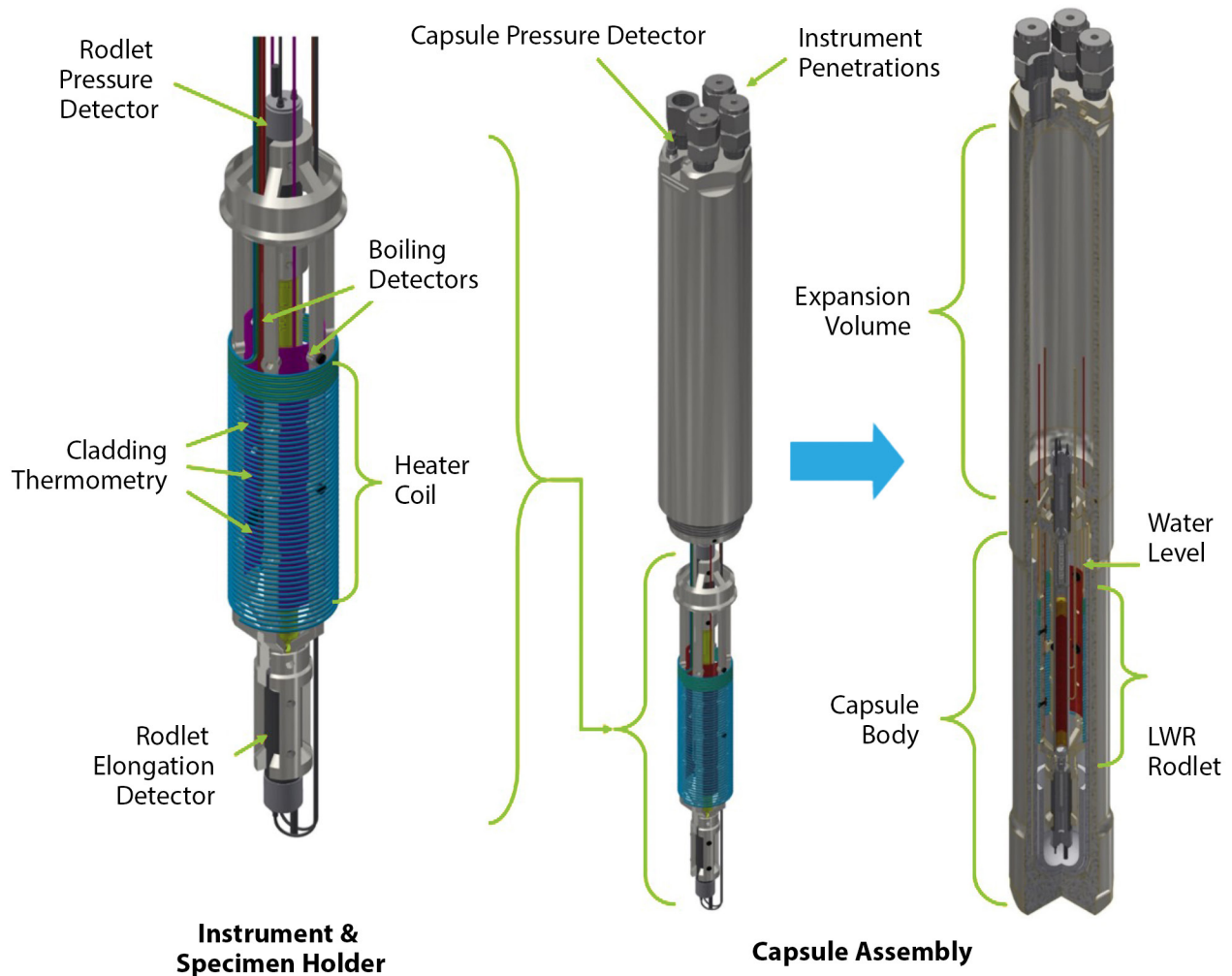
Project Description:

The SERTTA capsule provides a static water environment surrounding the fuel rod with a suite of state-of-the-art and first-of-a-kind instruments to collect relevant data for post-test

A series of commissioning tests for water-based reactivity-initiated accidents have been completed in TREAT to demonstrate the renewed capability of RIA testing to support U.S. nuclear energy goals.

analysis of the experiments (Figure 1). The purpose of the ATF-RIA-1 test campaign was to commission the SERTTA capsule and instrumentation for RIA testing in a static water environment in TREAT. Demonstrating and qualifying the capabilities of the SERTTA capsule is required for planned follow-on testing of ATF as well as high burnup LWR fuels. Therefore, these tests are crucial for meeting industries needs to support licensing these fuels.

Following the irradiations of these experiments in TREAT, post-transient examinations (PTE) of the fuel rodlets were performed as well as post-test fuel performance modeling predictions. PTE included x-ray radiography of the capsules prior to disassembly, visual inspections of the rodlets, high resolution optical profilometry, optical microscopy, and gamma



spectroscopy. The results from the experiment instrumentation as well as post-irradiation examination (PIE) provide valuable data for post-test fuel performance modeling validation. Models using the as-run

experiment conditions for both the BISON fuel performance and RELAP5-3D codes are compared against experimental and PIE results. This provides more data to improve our modeling and predictive capabilities.

Figure 1. SERTTA capsule rendering

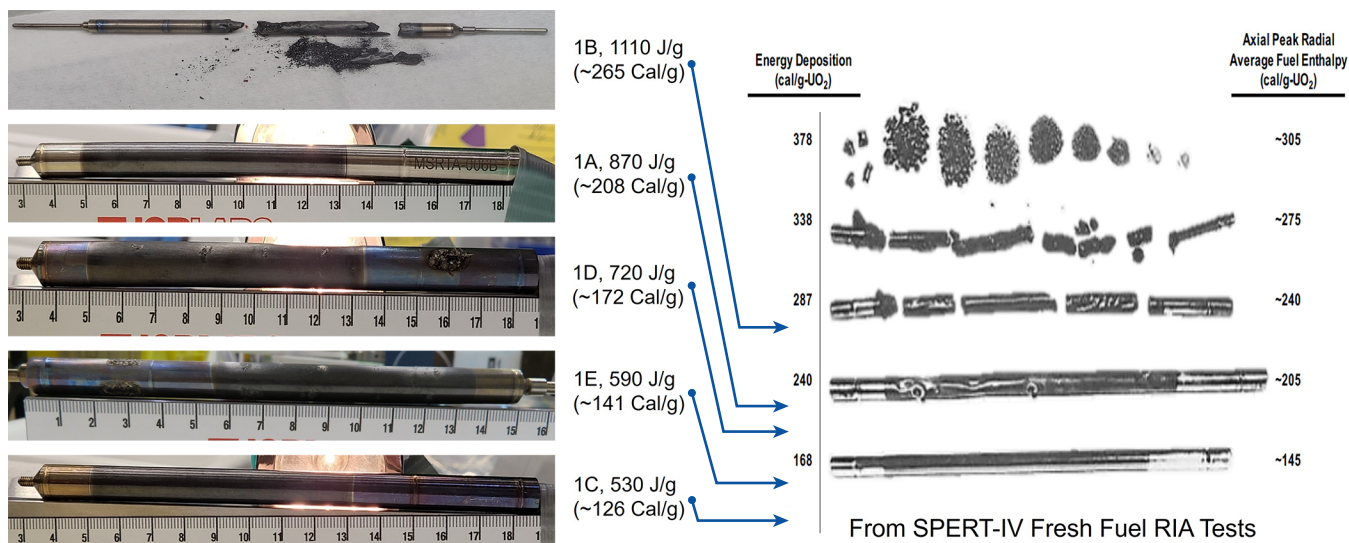


Figure 2. Visual inspections for rodlets A-E compared to historic SPERT-IV fresh fuel RIA tests

Accomplishments:

The completion of the RIA commissioning experiments in the SERTTA capsule demonstrate the renewed capability to perform water-based RIA testing in the U.S. Figure 2 shows images of the rodlets compared to similar historic tests that were performed under the SPERT-IV fresh fuel RIA tests program. In all cases, the condition of the fuel rods shows good agreement with historical observations, providing confidence that testing in the SERTTA capsule will meet RIA testing needs. The following paragraphs highlight a few results from the tests.

Throughout the commissioning tests, many lessons were learned with regards to assembly, operation, and instrumentation performance that allowed for improvements in later tests as well as future test campaigns utilizing the SERTTA capsule. Experiments using different cladding surface thermocouples

were utilized to test the thermocouple performance. The ATF-RIA-1-E test utilized two different types of thermocouples and the results show good agreement to each other, but also revealed challenges of creating reproducible cladding attachment. Figure 3 shows the thermocouple results with best-estimate predictions using a coupled BISON/RELAP5-3D model. The experimental results can be used to improve and validate the BISON models applicable to RIA conditions. Thermocouple attachment and performance understanding remains an active challenge for continued work with hot cell integration.

PTE of the rodlets included high resolution optical profilometry to measure the final cladding diameter. Figure 4 shows the measured and predicted final cladding diameter for the ATF-RIA-1-E experiment. The large spikes in the measured data show the weld locations on the rodlet. This rodlet experienced

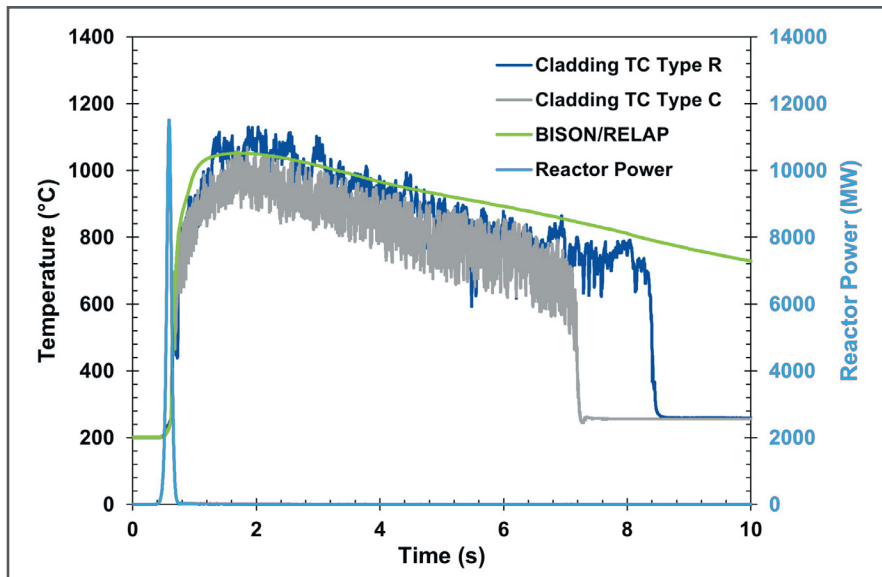


Figure 3. ATF-RIA-1-E cladding temperature measurements compared against coupled BISON/RELAP5-3D predictions

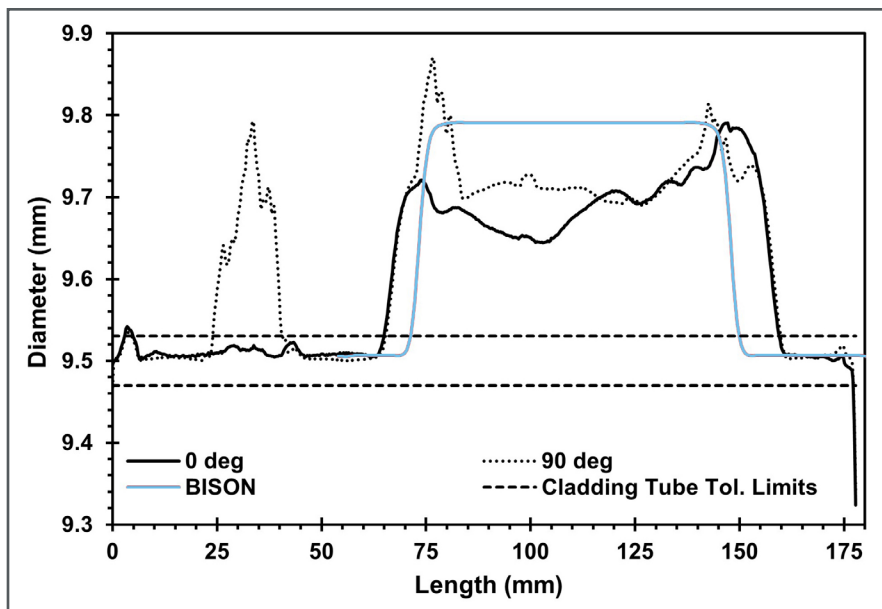


Figure 4. ATF-RIA-1-E optical profilometry cladding diameter measurements compared against BISON predictions

ballooning due to the high cladding temperatures reached (Figure 3) and a large positive pressure differential between the rodlet and capsule. The BISON model predicts similar outward ballooning of the cladding during the test. The profilometry

results for all rodlets show outcomes expected from the test plan. Rodlets with negative pressure differentials experienced cladding creep down during the tests.

Combined TREAT-SATS LOCA Test Plan with Industry Consensus

Principal Investigator: Colby Jensen

Team Members/ Collaborators: Robert Armstrong, Nathan Capps

The AFC combined TREAT and SATS LOCA plan will address cross-cutting industry needs as a first-of-a-kind approach to evaluate High Burnup Fuels during LOCA.

The U.S. nuclear energy industry has goals for licensing fuel burnup beyond current limits of 62 GWd/t, targeting up to ~75 GWd/t. Loss of coolant accident (LOCA) performance of high burnup fuel, in particular fuel fragmentation relocation and dispersal (FFRD), was ranked the top research and development (R&D) priority by the Electric Power Research Institute's (EPRI) Collaborative Research on Advanced Fuel Technologies (CRAFT) Fuel Performance and Testing Technical Experts Group (FPTTEG). To address industry needs, the Advanced Fuels Campaign (AFC) program has developed a combined Transient Reactor Test Facility (TREAT) and Severe Accident Test Station (SATS) LOCA test plan with the support of the Nuclear Energy Institute (NEI) and CRAFT framework. Under the CRAFT framework and the AFC program, the plan is intended to provide stakeholder consensus as a living document and serve as a roadmap for addressing FFRD issues and responding to new findings in the next several years.

Project Description:

LOCA performance of high burnup fuel, in particular FFRD, was ranked the top R&D priority by the CRAFT FPTTEG. The AFC test program was developed with stakeholder input targeting relevant conditions. It relies on a unique combination of

in-pile and out-of-pile experimental approaches to (1) provide clear tieback to the existing integral and semi-integral LOCA experiment database using state-of-the-art facilities. More importantly, this program will systematically investigate the impacts of: (2) prototypic high burnup (HBu) fuel and cladding temperature thermomechanical behaviors under postulated light water reactor (LWR) LOCA conditions never fully investigated before. These conditions correspond with prototypic decay-energy heat up (DEH) and stored-energy heat up (SEH) conditions of HBu fuel during predicted LOCA events. Unique TREAT capability will provide first evaluations of SEH conditions on HBu fuels. The plan includes a description of the problem addressed, key testing capabilities, expected data streams (instrumentation), test matrix, schedule, and experiment model descriptions, enabling stakeholders to contribute to the test program through modeling and simulation informed experiment design. The test plan incorporates stakeholders review input to prioritize and maximize cross-cutting data outcomes. The final plan is to be presented to the FPTTEG and the CRAFT governing board for formal endorsement as the industry-consensus LOCA test plan. Regular review and updates of the plan will be necessary to ensure relevance and impact.

Accomplishments:

The AFC test plan represents the culmination of multiple activities and research teams at Oak Ridge National Laboratory (ORNL) and Idaho National Laboratory (INL) from the past several years including a critical review of FFRD during LOCA. The AFC program has worked internally and with industry and other Department of Energy (DOE) programs to develop a clearer understanding of prototypic LOCA conditions of relevance to high burnup fuel. This work has revealed boundary conditions of potential consequence where temperature evolution and ramp rates have not been explored by any LOCA experiments to date. Meanwhile, the SATS system at ORNL has been developed for several years now with testing already performed on HBU fuels, similar to testing performed by other facilities such as Studsvik. The SATS system is currently undergoing some system upgrades to better address identified data gaps. At the same time, a LOCA test design has been developed at INL within TREAT based on evaluated needs and unique in-pile capability since the closure of the Halden test reactor. Meanwhile, the Nuclear Regulatory Commission published a Research Information Letter on the topic of FFRD during LOCA which has further stirred the community and casts light on further research opportunities. The AFC LOCA plan was drafted early this year as a combined INL and ORNL effort with support from the FPTTEG to provide a point of consensus for cross-cutting research. The plan addresses the testing data gaps and focuses on



experiment drivers, technical objectives, and a description of the means to achieve them.

The draft plan was provided to stakeholders via the FPTTEG members, with significant feedback provided by five non-laboratory organizations. A separate report has been created to document all comments and associated responses, maintaining privacy of the comment source. The plan will undergo final presentation to the FPTTEG and then to the CRAFT governing board for final endorsement and signature, prior to public release. The plan will be reviewed and updated as needed (~ annual basis) with the FPTTEG serving in an advisory role.

Figure 1. AFC combined TREAT and SATS HBU LOCA test plan has been completed with support from stakeholders. The plan leverages the best capabilities in the world at ORNL and INL for testing and characterization

Design of Severe Accident Test Station Fission Gas Release Capability

Principal Investigator: Jason Harp

Team Members/ Collaborator: Yong Yan, Adam James, Chuck Baldwin, Nathan Capps

The available data on transient fission gas release (tFGR) relevant to light water reactors (LWR) is sparse [1–6] and the fuel conditions covered by this data are also limited. Creating additional relevant tFGR data that is applicable to different fuel irradiation histories is complex for several reasons. There is not a viable surrogate for irradiated nuclear fuel that can be used to study this behavior. This limits the study of tFGR to facilities that can safely handle and refabricate irradiated fuel into relevant test items. The available data suggests tFGR testing must be carried out under fuel pin relevant pressure (~10 MPa) to be characteristic of in-pile conditions [2,6]. This increases the complexity of systems designed to capture tFGR because they must handle high pressures. Measurement of tFGR is typically accomplished by measuring the release of the long-lived radioactive fission product Kr-85 with gamma spectrometry. An additional complication to detecting tFGR is the short timescale over which tFGR occurs. The release appears to occur in a burst at certain on-set temperatures [3,4]. Attempts to capture the onset of release at pressure have previously used a stepwise approach to collecting Kr-85 [6]. Given the complexity of this phenomenon, it is doubtful that a perfect experiment can be

performed that results in a mechanistic model for tFGR. Understanding tFGR will require collecting data on a variety of fuel conditions in separate experimental apparatus some of which isolate key variables while some evaluate the integral tFGR response. To this end, ORNL is developing two systems to further study tFGR. One system is designed to focus on visualization and tFGR from small samples of fuel during rapid heating (featured elsewhere in this document). The other system will focus on integral tFGR tests under as representative as possible conditions. It will be coupled with the ORNL Severe Accident Test Station (SATS) and builds upon previous ORNL experience with the Core Conduction Cooldown Test Furnace (CCCTF) [7].

Project Description:

The goal of the integral testing is to capture the onset temperature of tFGR and the amount (moles of gas) of tFGR for a segment experiencing a representative loss of coolant accident (LOCA) transient. This release is also being measured while the fuel is under mechanical constraint by the cladding and under representative fuel pin internal pressure prior to the segment bursting. For the ORNL approach, segments of irradiated fuel will be cut into 15 to 30 cm segments. These segments will be refabricated with end-caps and connected to

This new system will evaluate critical gaps in transient fission gas release behavior for fuel segments experiencing simulated LOCA events

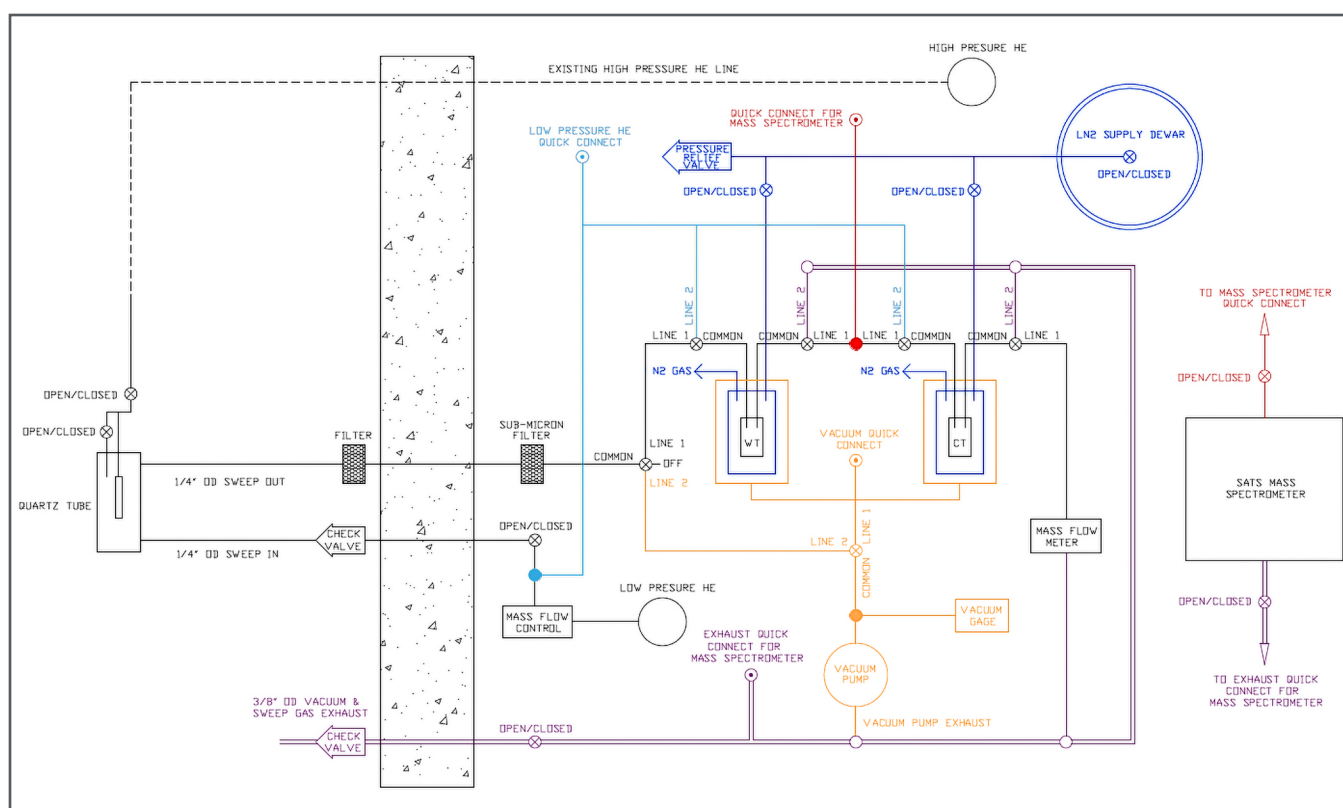


Figure 1. A schematic representation of the designed tFGR system

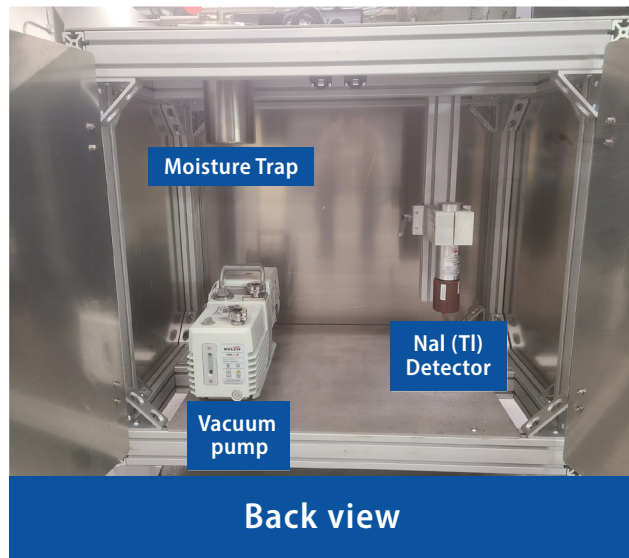
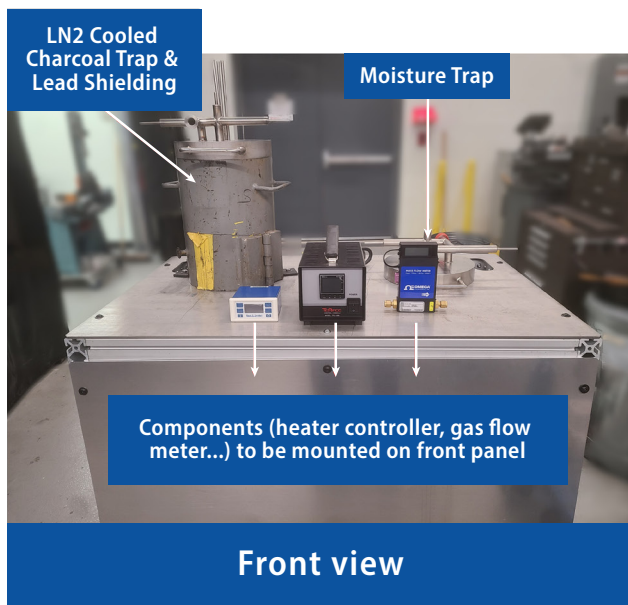


Figure 2. Images of some components of the tFGR system prior to final assembly

a pressurization system. It is not feasible to circulate high pressure gas through the segment and out of the hot-cell into a fission gas trap during a test. During the test, the segment will be stepwise heated to a temperature at a specified ramp rate, the content of the segment will be expanded into a larger volume and sent to the fission gas traps out-of-cell at atmospheric pressure where the content will be evaluated by counting the released Kr-85 content. The test will then proceed on to the next hold temperature until the final temperature is reached. Alternatively, it will be possible to simply heat the fuel segment under representative LOCA ramp and pressure conditions and then capture the total amount of tFGR released by the sample. However, the onset temperature and evolution of tFGR will not be captured in this sort of test.

Accomplishments:

The design of the tFGR system attachment to SATS is complete, components are ordered, and some assembly of the components has begun. The tFGR system consists of a sweep gas system to conduct gases from the SATS in-cell to a fission gas detection system out-of-cell, a series of cold traps to capture off-gas from heating tests, and a gamma spectrometry system to detect Kr-85. In addition to the cold trap system, a mass spectrometry system will also be available to sample the content of the gas exiting the hot-cell. A flow diagram of the system is included in Figure 1. The system table, moisture trap, cold trap, detector system, and some additional components are shown in Figure 2. This system will be assembled for cold testing over the next few months. Testing on irradiated fuel is expected by the end of September 2023.

References:

- [1.] Y. Pontillon, M.P. Ferroud-Plattet, D. Parrat, S. Ravel, G. Ducros, C. Struzik, I. Aubrun, G. Eminet, J. Lamontagne, J. Noirot, A. Harrer, Experimental and theoretical investigation of fission gas release from UO₂ up to 70 GWd/t under simulated LOCA type conditions: The GASPARD program, Proc. 2004 Int. Meet. LWR Fuel Perform. (2004) 490–499.
- [2.] J. Rest, M.W.D. Cooper, J. Spino, J.A. Turnbull, P. Van Uffelen, C.T. Walker, Fission gas release from UO₂ nuclear fuel: A review, J. Nucl. Mater. 513 (2019) 310–345. <https://doi.org/10.1016/j.jnucmat.2018.08.019>.
- [3.] G. Khvostov, A. Pautz, E. Kolstad, G. Ledergerber, Analysis of a Halden LOCA test with the BWR high burnup fuel, LWR Fuel Perform. Meet. Top Fuel 2013. 1 (2013) 644–651.
- [4.] G. Khvostov, Analytical criteria for fuel fragmentation and burst FGR during a LOCA, Nucl. Eng. Technol. 52 (2020) 2402–2409. <https://doi.org/10.1016/j.NET.2020.03.009>.
- [5.] H. Sonnenburg, W. Wiesenack, J. Karlsson, J. Noirot, V. Garat, N. Waeckel, F. Khattout, A. Cabrera-Salcedo, J. Zhang, G. Khvostov, A. Gorzel, V. Brankov, F. Nagase, P. Raynaud, M. Bales, T. Taurines, T. Nakajima, A. Alvestav, Report on Fuel Fragmentation, Relocation and Dispersion, NEA/CSNI/R (2016)16. Organisation (2016). <https://www.oecd-neo.org/nsd/docs/2016/csni-r2016-16.pdf>.
- [6.] J.A. Turnbull, S.K. Yagnik, M. Hirai, D.M. Staicu, C.T. Walker, An Assessment of the Fuel Pulverization Threshold During LOCA-Type Temperature Transients, Nucl. Sci. Eng. 179 (2015) 477–485. <https://doi.org/10.13182/NSE14-20>.
- [7.] C.A. Baldwin, J.D. Hunn, R.N. Morris, F.C. Montgomery, C.M. Silva, P.A. Demkowicz, First elevated-temperature performance testing of coated particle fuel compacts from the AGR-1 irradiation experiment, Nucl. Eng. Des. 271 (2014) 131–141. <https://doi.org/10.1016/j.nuceng-des.2013.11.021>.

Report Summarizing Progress in Digital Image Correlation Analysis of Burst Phenomenon

Principal Investigator: Nathan Capps, Kenneth Kane

Team Members/ Collaborator: Samuel Bell, Benton Garrison, Mackenzie Ridley, Brandon Johnston, Kory Linton

Novel application of digital image correlation and infrared thermography during burst testing provides a robust framework for not only characterizing incumbent materials but also accelerating qualification of Accident Tolerant Fuel cladding concepts.

A novel approach has been developed to measure in-situ temperature profiles, pressure, and strain during burst testing of nuclear fuel claddings. This includes the application of digital image correlation to quantify strain and infrared thermography to determine temperature gradients. Both techniques have never been simultaneously applied during a burst test. The work presented in the report demonstrates the upgraded burst test measurement capabilities on zirconium claddings as a test case, with the long-term goal of developing high fidelity models for Accident Tolerant Fuel (ATF) cladding materials. Quantities such as multi-dimensional strain and strain rate of select cases are presented alongside axial temperature profiles.

Project Description:

Burst testing has long been a reliable method of characterizing fuel cladding materials in accident transients. However, most data generated from these efforts results in end-of-life measurements such as burst temperature and pressure as well as post-test strain. In-situ strain and temperature data linking the as-received and end-of-life conditions was previously not captured. Therefore, a technical goal of this research was to demonstrate a methodology by incorporating modern in-situ experimental techniques, increasing characterization capabilities during burst testing. Specifically,

the intent was to simultaneously incorporate digital image correlation and infrared thermography to completely quantify strain, loading, and axial temperature of zirconium and ATF claddings throughout testing. Successful application of these techniques will address data and modeling gaps, develop new material models, and refine current predictive capabilities. The developed methodologies will be applied beyond incumbent systems to ATF cladding concepts such as Cr coated zirconium and Fecral alloys. This work was largely driven by the need for accelerated qualification of such new cladding materials. Development of in-situ characterization capabilities will lead to better understanding of safety limits and reduce the time and cost of qualification of ATF materials. Additionally, current interest in approval to higher burnup in light-water reactors beyond the current 62 GWd/TU limit will require more detailed characterization of zirconium systems. Such an increase will allow for longer fuel cycles, increasing the efficiency and economics of reactor operations. Before burnup extension can be approved, there are key safety related research areas that need addressing, including improved understanding and modeling capabilities of fuel claddings in loss-of-coolant accident scenarios. Therefore, the main objectives of this research were:

(1) demonstrate the ability of the recently developed framework for reliably measuring in-situ cladding behavior during simulated accident conditions and (2) begin testing of an incumbent zirconium alloy to address community concerns.

Accomplishments:

As accident scenarios place claddings in conditions where creep mechanisms can dominate deformation, simultaneous knowledge of time, temperature, strain, and loading are necessary to characterize behavior. To demonstrate the newly developed framework and to work towards addressing community concerns, digital image correlation and infrared thermography techniques were applied to eight burst tests of zirconium claddings. However, before targeted testing began, several novel challenges were addressed. Typically, the specimens used for burst testing are 30 cm in length. Due to the constraints of the viewport and slight variability in failure location, initial testing focused on finding the optimal cladding length, Figure 1, to ensure ballooning occurred in view of the cameras while maintaining fidelity of experimental conditions. Conventional metrics for the shortened segments such as burst temperature and pressure, Figure 2, agreed with legacy empirical models indicating the tests are representative. Additionally, this work has identified a gap in the historic model requiring additional

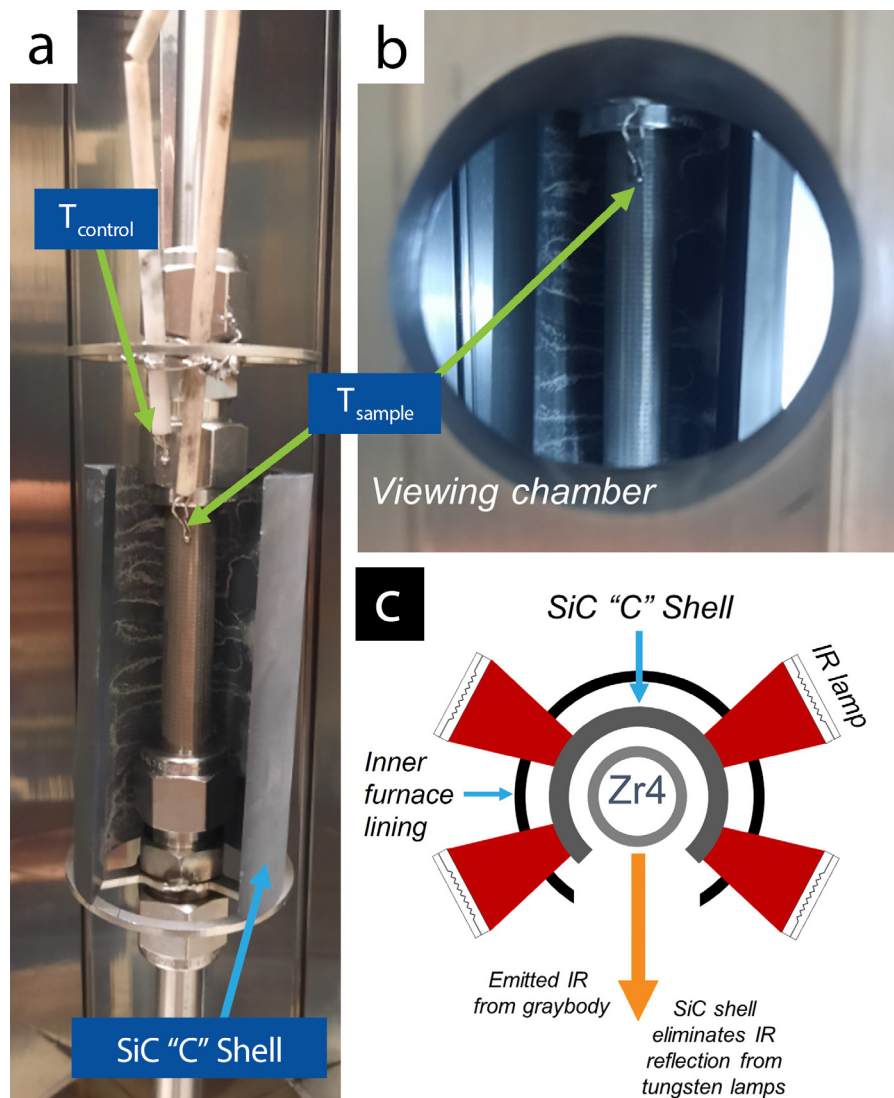
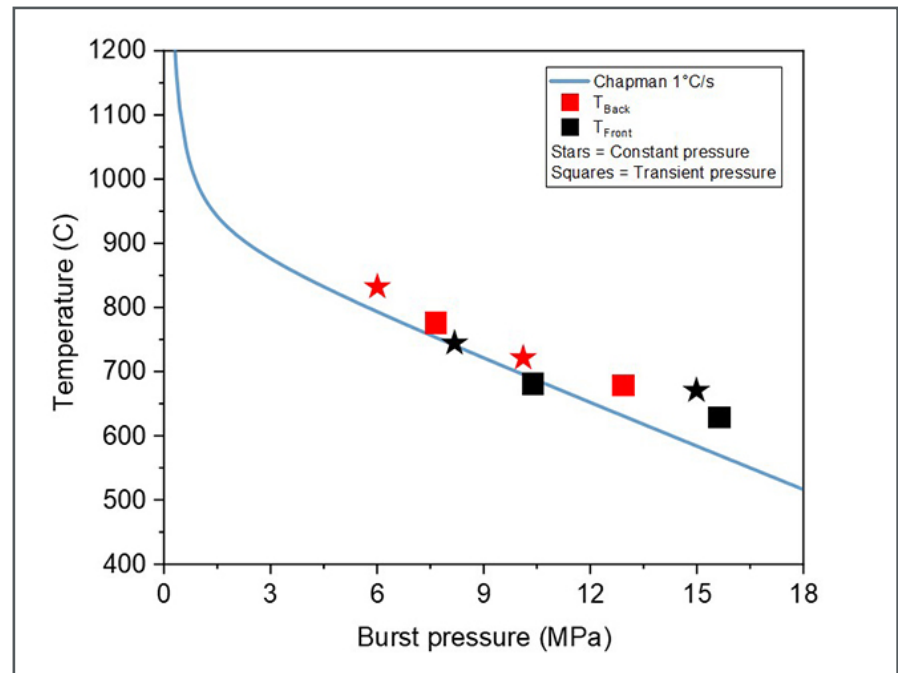


Figure 1. (a) Full cladding train set in the furnace. (b) Perspective of the cladding segment outside the viewport. (c) Diagram illustrating the effect of the silicon carbide shell for improved thermography results

Figure 2. Burst temperature and pressure data from shortened segments demonstrating agreement with historic empirical model



investigation. Another technical challenge addressed was related to thermography measurements. The furnace used in burst testing emits infrared radiation to heat the claddings. This presented a difficulty, as the cladding materials reflect a large portion of infrared radiation leading to measurable reflections of the tungsten lamps and skewed temperatures readings. To mitigate this effect, a 76.2 cm silicon-carbide “shell”, shown in Figure 1, was placed around the cladding segment removing reflections and acted as an intermediate heating element.

The test matrix utilized two distinct loading conditions: (1) transient loading, where the cladding train was sealed and the internal pressure allowed to increase with temperature and (2) constant loading, where the claddings were connected to a fixed pressure reservoir. The former more accurately reflects pressurization

of fuel rods in accident conditions, while the latter seeks to reduce the number of variables for development and validation of material models. Four tests were completed for each loading condition, with initial pressures of 6.2, 8.2, 10.3, and 15.9 MPa at room temperature. This breadth was chosen to preliminarily compare cladding behavior across a range of conditions pertinent to higher burnup fuel. In the report, axial temperature profiles from infrared imaging, Figure 3, are presented as well as strain, Figure 4, and strain rate from several tests are reported, demonstrating successful characterization and integration of experimental techniques. Further work will focus on utilizing the generated data to develop material models, as well as refining the experimental setup.

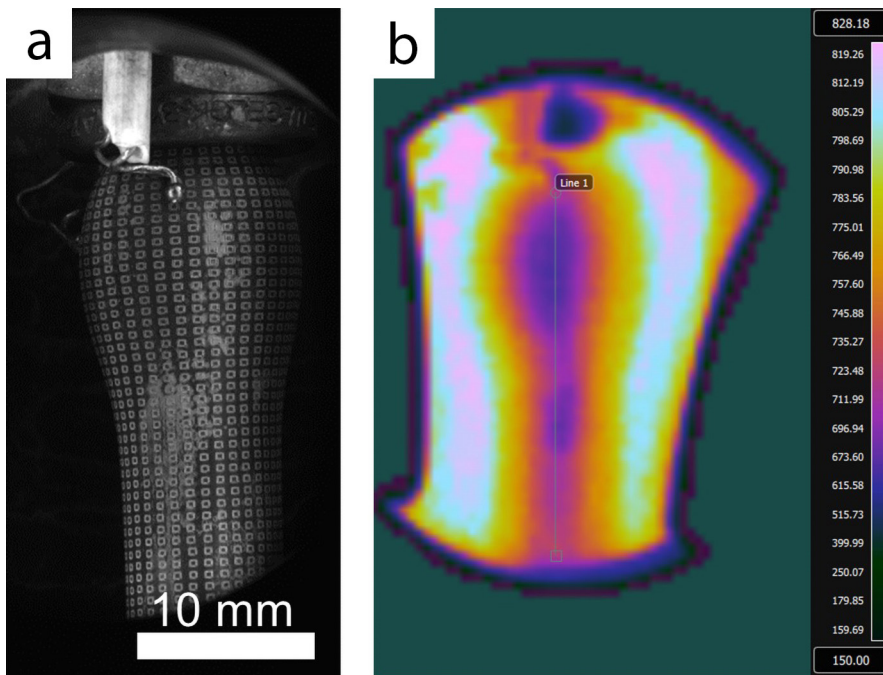


Figure 3. (a) Optical image of cladding during ballooning utilized for digital image correlation. (b) Thermal image with line profile used to extract axial temperature measurements

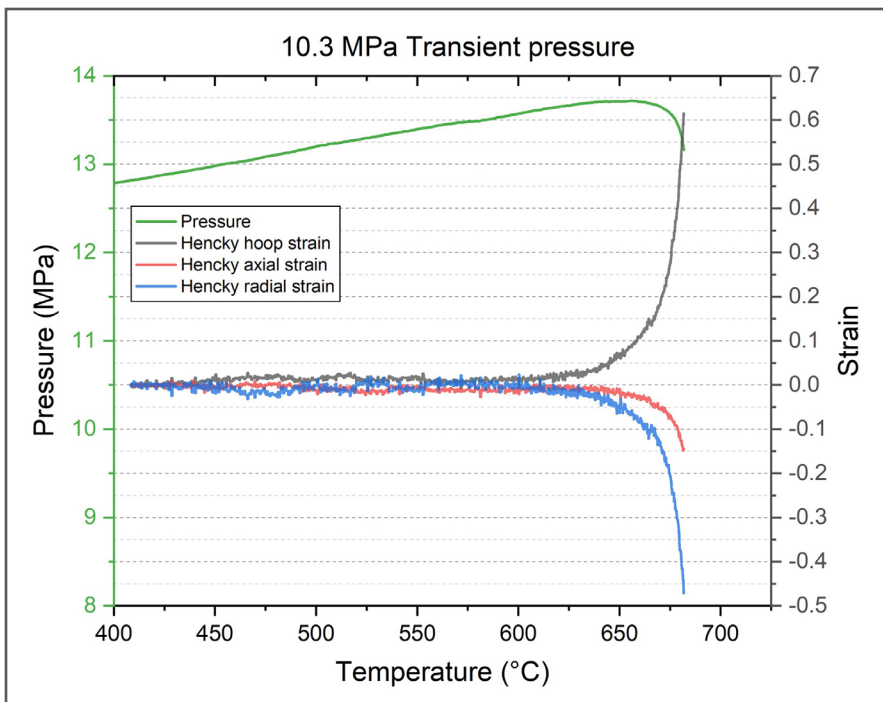


Figure 4. Raw strain data captured by integrating digital image correlation

Demonstration of a Transient Heating and Visualization System to Collect and Characterize Fission Gas Release on Irradiated Nuclear Fuel

Principal Investigator: Peter Doyle

Team Members/ Collaborators: Jason Harp, Ben Garrison, Kory Linton

The Fuel Heating and Visualization System demonstrates a key capability at ORNL to evaluate and observe fission gas release in local sections of nuclear fuel.

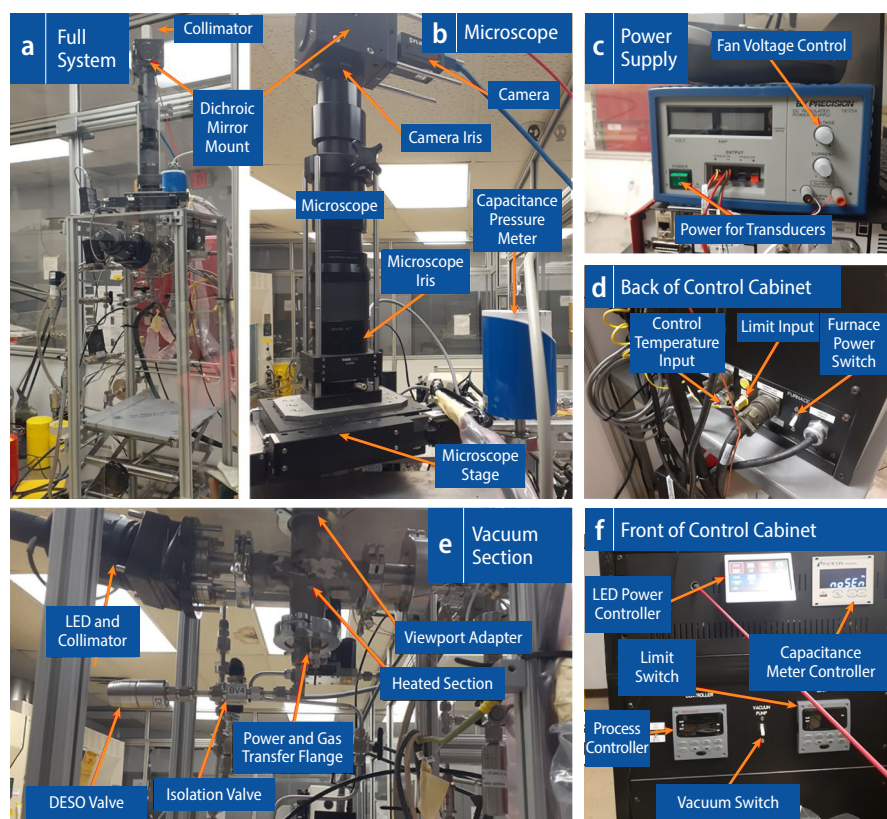
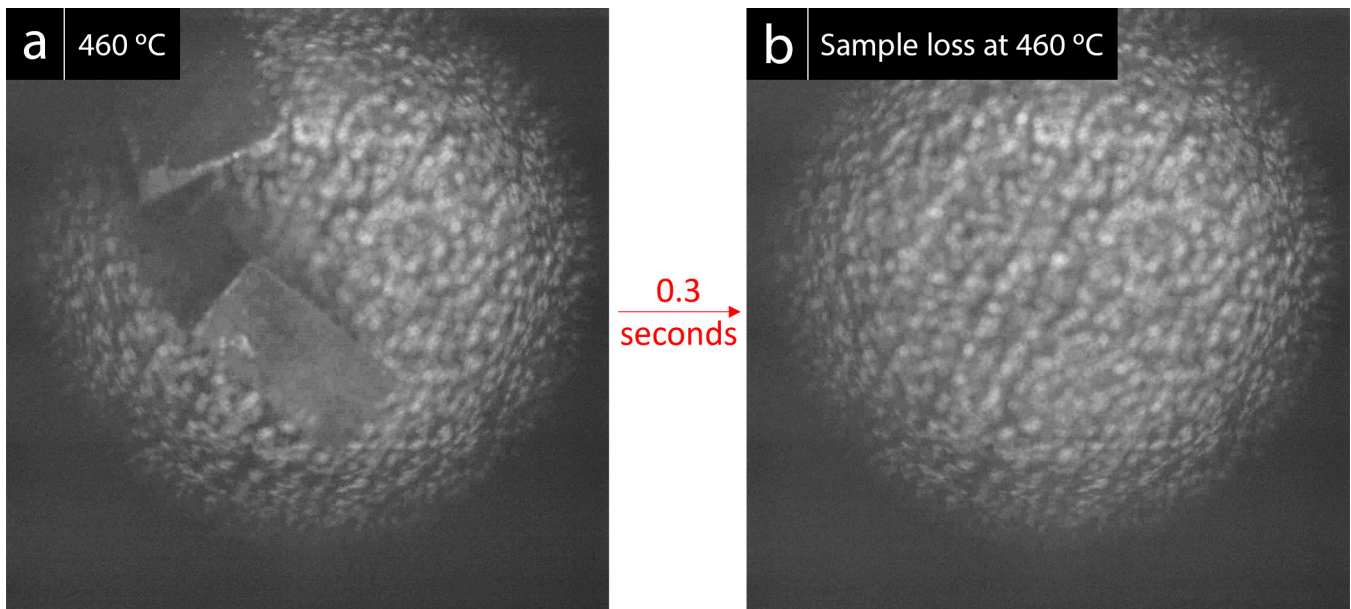


Figure 1. Images of the system and control cabinet. Full testing station, together with major tubing elements (a). Microscope section of the system with important components labeled; capacitance meter shown as it protrudes above the top plate of the frame (b). Power supply used to power the pressure transducers and cooling fans (c). Control cabinet with various components indicated (d and f). Components inside the cabinet — including the serial hub, LabJack, stage motor controller, and spectrometer — are not shown. Test portion of the system's vacuum section, with important features labeled (e)

The kinetics of fission gas release under high temperature transients is an important consideration for increasing burnup of nuclear fuel in Light Water Reactors (LWRs). Several groups have performed experiments to understand different portions of fission gas release [1–3] and others have conducted work to model fission gas release, with a particular focus on gas bubble physics [4,5]. Although many important details regarding mechanisms of gas release have been determined by these efforts [6], several outstanding questions remain to be addressed to aid in modeling fission gas behavior under high-burnup conditions. Additionally, transient fission gas release was identified as a critical gap in data available to support the extension of the burnup limit for commercial light water reactors [7]. A key aspect in addressing these questions is the development of experiments in which several types of information are gathered simultaneously.

Project Description:

The objective of this work was to develop a rapid transient testing technique allowing visual observation of an irradiated fuel sample during a temperature transient while measuring the amount of fission gas released and collecting fission gas for post-test characterization.



Pressure, temperature, and optical measurements are collected to quantitatively determine the kinetics of gas release and correlate this release with visual changes in the fuel. Heating occurs inside a small vacuum system up to 800 °C where the sample temperature is carefully monitored. With the system under 1000 Pa absolute pressure, approximately 0.07 μ moles instantaneously released gas can be resolved during heating. Once released, gas in the chamber is collected in charcoal traps for Kr-85 activity determination, followed by ultimate release into the hot cells. Temperature is measured by

thermocouples in contact with the fuel holder and with additional indirect monitoring via pyrometry.

As this capability is developed, this device provides a significant capability at ORNL to evaluate gas release of small, irradiated fuel samples. Samples can be extracted from commercial or research reactor irradiated fuel samples and be visualized during heating operations. This capability will enable experimental campaigns to evaluate fission gas release for specific radial portions of fuel, which will contribute to the knowledge of accident progression in current commercial light water reactors.

Figure 2. Optical images of the heated TiHx sample at various stages in the test. Images are shown at (a) the start of heating, and at sample temperatures of (b) 400 °C, (c) 500 °C, (d) 600 °C, (e) 700 °C, and (f) 760 °C. Annotations in (a) indicate the foil location, as well as the alumina insulators for the thermocouple wires. The AlN sample plate is holding the TiHx sample and is the only other feature in the images

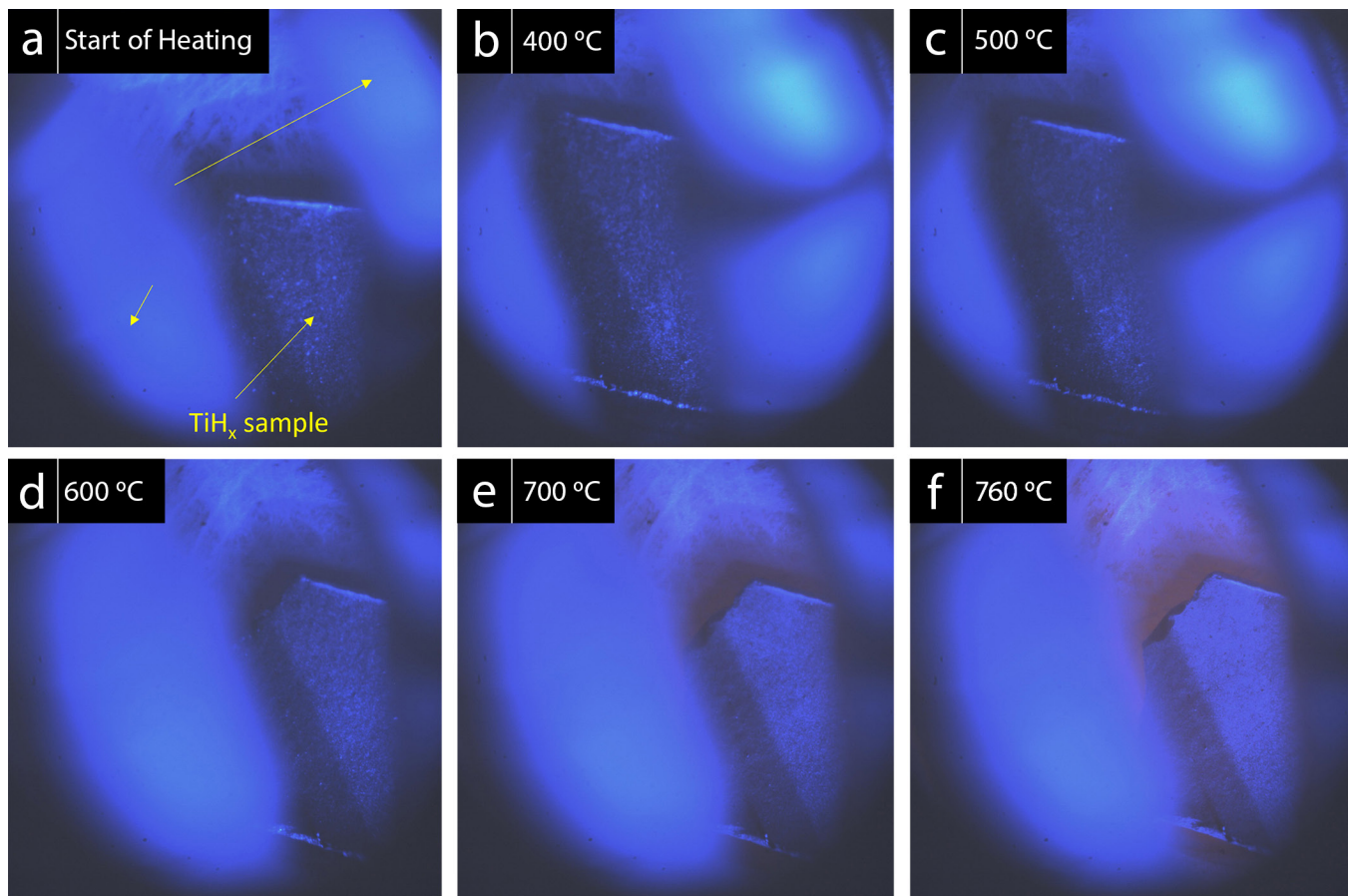


Figure 3. Fuel sample on the SiC holder at a) 460°C and b) 0.3 seconds after showing sample disappearance. The fuel piece is shown in the center of panel a) with the associated cladding segment detached above the fuel to the left

Moreover, as new accident tolerant fuel (ATF) variants of UO_2 and other novel fuel technologies are irradiated and sent of postirradiation examination, this capability will allow detailed examination of off-normal gas release behavior in this fuel as well.

Accomplishments:

The system was successfully built and demonstrated on two different sample sets: a hydrogen-impregnated Ti foil and an irradiated fuel sample. Final instrument configuration is shown in Figure 1. The primary heating chamber consists of a 4-way vacuum cross. On one end of the cross a

light emitting diode (LED) source provides illumination. Opposite the LED is an instrumentation cross that consists of the gas outlet, thermocouple leads, a sample gas chamber for system volume analysis, and two pressure meters (one full range to atmosphere and the other a <1400 Pa capacitance meter). The top of the cross goes to a viewport which is connected to a microscope onto which a camera and spectrometer are attached. The camera views all visible light, and the spectrometer receives infrared light for pyrometric evaluation.

During a test, the bottom of the cross is loaded with a custom flange

with a gas inlet and electric leads. On the vacuum side of this flange, these leads are connected to a microheater onto which is placed a ceramic holder, AlN or SiC, which contains the sample. For the TiHx foil test AlN was used, while the fuel test used a 3D-printed SiC holder. It was found that the AlN holder was more durable but the SiC holder was more readily manufacturable into the required form. Because of cracking concerns in the SiC, the maximum temperature of the initial fuel test was set to 650 °C and the TiHx sample was able to be heated to 760 °C.

To test large gas volume detection, the TiHx sample was prepared with a calculated 0.21 mmol H₂, sufficient to create a pressure change of 900 Pa within the chamber. Heating the sample at rate of 20 °C/min to 760 °C. Optical observation of the sample throughout the test can be seen in Figure 2. In this test, the visible area of the foil sample was partially shielded by the alumina insulated thermocouple wires. Clear gas evolution was found in this test with a calculated gas release of 0.18 mmol H₂, similar to the estimated 0.21 mmol H₂ calculated initially to be in the sample.

The fuel test was accomplished with 0.8 mm³ fuel piece with a burnup of 84 GWd/kgU. This fuel was taken from the same fuel segment that was LOCA tested as NA#2 in Reference [8]. This sample was removed from the outer edge of a fuel pellet by cutting three grooves around the sample normal to the interface and then cutting out a 1 mm thick slice. This piece was loaded onto the SiC holder and heated at 25 °C/

min to 650 °C. At 460 °C the sample disappeared from view. This is shown in Figure 3. Evaluation of the released gases further showed 85Kr had been released during the testing.

This first heating of nuclear fuel in the Fuel Heating and Visualization System demonstrates a key capability at ORNL to evaluate and observe fission gas release in local sections of nuclear fuel. Additional capability improvements are being investigated in data collection and sample retention for future experiments.

References:

- [1.] C. Le Gall, S. Reboul, L. Fayette, T. Blay, I. Zacharie-Aubrun, I. Félines, K. Hanifi, I. Roure, P. Bienvenu, F. Audubert, Y. Pontillon, J.L. Hazemann, MOX fuel microstructural evolution during the VERDON-3 and 4 tests, *J. Nucl. Mater.* 531 (2020). doi:10.1016/j.jnucmat.2020.152015.
- [2.] T. Vidal, L. Gallais, R. Burla, F. Martin, H. Capdevila, S. Clément, Y. Pontillon, Optical system for real-time monitoring of nuclear fuel pellets at high temperature, *Nucl. Eng. Des.* 357 (2020) 110383. doi:10.1016/j.NUCENG-DES.2019.110383.
- [3.] Y. Pontillon, M.P. Ferroud-Plattet, D. Parrat, S. Ravel, G. Ducros, C. Struzik, I. Aubrun, G. Eminet, J. Lamontagne, J. Noirot, A. Harrer, Experimental and theoretical investigation of fission gas release from UO₂ up to 70 GWd/t under simulated LOCA type conditions: The GASPARD program, *Proc. 2004 Int. Meet. LWR Fuel Perform.* (2004) 490–499.
- [4.] M.S. Veshchunov, V.E. Shestak, Modelling of fission gas release from irradiated UO₂ fuel under high-temperature annealing conditions, *J. Nucl. Mater.* 430 (2012) 82–89. doi:https://doi.org/10.1016/j.jnucmat.2012.06.048.
- [5.] L.O. Jernkvist, A review of analytical criteria for fission gas induced fragmentation of oxide fuel in accident conditions, *Prog. Nucl. Energy.* 119 (2020) 103188. doi:10.1016/j.pnucene.2019.103188.
- [6.] M. Tonks, D. Andersson, R. Devanathan, R. Dubourg, A. El-Azab, M. Freyss, F. Iglesias, K. Kulacsy, G. Pastore, S.R. Phillpot, M. Welland, Unit mechanisms of fission gas release: Current understanding and future needs, *J. Nucl. Mater.* 504 (2018) 300–317. doi:10.1016/j.JNUCMAT.2018.03.016.
- [7.] M. Bales, A. Chung, J. Corson, L. Kyriazidis, Interpretation of Research on Fuel Fragmentation, Relocation, and Dispersal at High Burnup, *Res. Inf. Lett. Off. Nucl. Regul. Res.* (2021) RIL 2021-13.
- [8.] N. Capps, Y. Yan, A. Raftery, Z. Burns, T. Smith, K. Terrani, K. Yueh, M. Bales, K. Linton, Integral LOCA fragmentation test on high-burnup fuel, *Nucl. Eng. Des.* 367 (2020) 110811. doi:10.1016/j.nucengdes.2020.110811.

2.5 LWR COMPUTATIONAL ANALYSIS

LWR Computational Analysis

Principal Investigator: Michael Todosow

Team Members/ Collaborator: Arantxa Cuadra

The combination of accident tolerant fuel/cladding and advanced control rods with improved thermo-chemical/ mechanical characteristics enhances the performance and safety of LWRs in normal and accident conditions beyond those achievable by ATF alone and will be an enabler for successfully achieving higher burnups.

The objective of increasing the fuel burnup in current Pressurized Water Reactors (PWRs) requires higher fuel enrichments than the current <5 w/o. The use of higher enrichments reduces the worth of current silver-indium-cadmium (AIC) control rods. An option to address this issue is to explore other control rod materials with the objective to enhance the poisoning effects/requirements while maintaining structural integrity/functionality during normal operation and accident conditions. These objectives are a natural complement to accident tolerant fuel (ATF) concepts which are viewed as enablers to the achievement of higher burnups. The combination of accident tolerant fuel/cladding and advanced control rods enhances the performance and safety of light water reactors (LWRs) in normal/high burnup and accident conditions beyond those achievable by ATF alone.

Project Description:

Requirements and desirable characteristics of advanced/accident tolerant control rods include:

• Options must:

Maintain or exceed absorption capabilities (shutdown, ejected rod worth, etc.) for desired target lifetime

Maintain structural integrity and functionality under operating and accident scenarios (ability to be inserted/withdrawn, handle loads/shocks, such as due to SCRAM)

Be chemically and mechanically “robust” in reactor temperature and radiation environment

High miscibility with fuel materials to avoid possibility of re-criticality

• Desirable characteristics include:

High melting temperature:

Absorber, cladding/sheath

Minimal adverse chemical interactions: Between absorber and cladding/sheath, coolant, etc.

Minimize adverse mechanical interactions, e.g., swelling, wear/fretting, ballooning, bowing

Resource availability, manufacturability, cost

This FY the neutronic performance of hafnium-based control rods that could potentially satisfy the above criteria was evaluated with a focus on implementation in PWRs with fuels with an enrichment of 7 w/o to achieve high burnup. Impacts considered include control rod worth, as well as fuel and moderator temperature coefficients, and soluble boron worth. The present effort is complementary to work performed at Brookhaven National

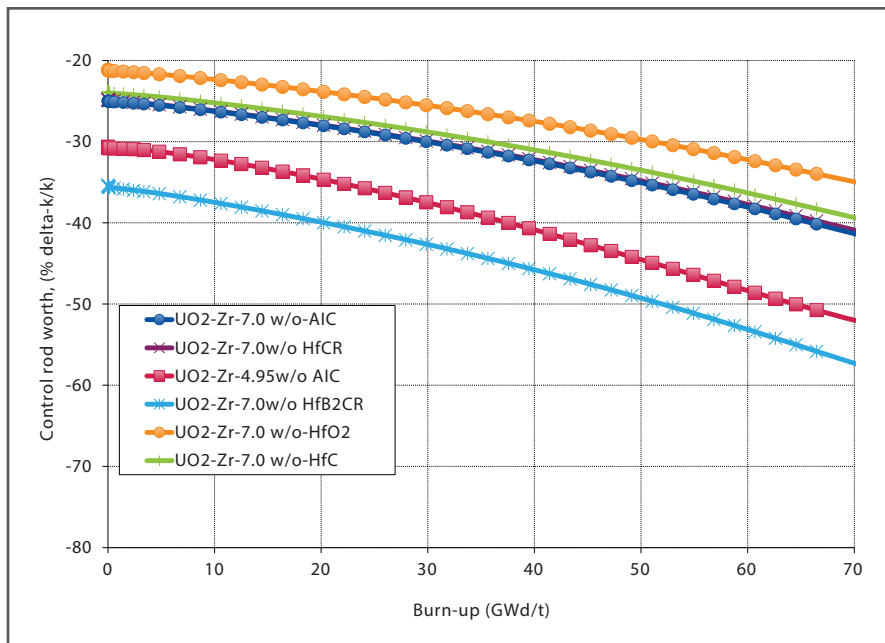


Figure 1. Control Rod Worth vs. Burnup

Laboratory (BNL) in 2019 and an ongoing Nuclear Energy University Project (NEUP) on accident tolerant control rods (ATCR)

Accomplishments:

There are a number of candidate options for more “robust” control rods (higher temperature, reduced hydrogen generation, minimize adverse chemical and mechanical interactions) to complement fuels with enhanced ATF. These include rare-earths (e.g., Re_2O_3 where $\text{Re}=\text{Gd}$, Er , Dy , etc.), hafnium, etc. These have been considered in combination with material other than the stainless steel currently used for the “sheath”/cladding (e.g., SiC , FeCrAl) as well as “bare”. In the present work, options based on hafnium as a replacement for AIC in a stainless steel sheath in the standard PWR

Control rod geometry were evaluated via scoping calculations with a detailed TRITON model of a Westinghouse 17x17 fuel assembly. The standard AIC control rod (24-rodlets) was replaced by selected hafnium-based control rods with: Hf , HfB_2 , HfO_2 , HfC . Control rod worths as a function of fuel burnup are shown in Figure 1 based on “branch calculation” of rod-out/rod-in, i.e., the control rod material remained at its initial composition. Based on these preliminary results only HfB_2 offers the desired increased reactivity worth, recognizing that the boron in the present analyses assumed “natural” boron. These results suggest that hafnium-based control rod material, other than HfB_2 do not provide the desired enhance reactivity worth for fuels with enrichment of 7 w/o.

2.6 ATF INDUSTRY ADVISORY COMMITTEE

Accident Tolerant Fuel Industry Advisory Committee

Committee Chair: Bill Gassmann, Constellation

Collaborators: Daniel Wachs, Ed Mai, and Phyllis King

The Advanced LWR Fuel Advisory Committee was established in 2012 to advise the Advanced Fuel Campaign's (AFC) National Technical Director on the direction, development, and execution of the campaign's activities related to accident tolerant fuels (ATF) for commercial light water reactors (LWRs). This year, the committee

continued to provide an industry perspective on LWR fuels issues that are broader in scope than just ATF. The industry advisory committee (IAC) is comprised of recognized leaders from diverse sectors of the commercial LWR industry. They represent the major suppliers of nuclear steam supply systems, owners/operators of U.S. nuclear

power plants, fuel vendors, advanced reactor representatives, the Electric Power Research Institute (EPRI), and the Nuclear Energy Institute (NEI). Members are invited to participate on the committee based on their technical knowledge of nuclear plant and fuel performance issues as well as their decision-making authority in their respective institutions.



During the past year the committee provided important industry input relative to utility and fuel vendor perspectives on the potential benefits of ATF and extending the burnup and enrichment of current fuels; continued efforts in testing, evaluation and examination of new ATFs, especially relative to the lead test assemblies operating in numerous

commercial plants; steady state/transient testing infrastructure needs and gaps, in particular at Idaho National Laboratory and Oak Ridge National Laboratory; coordination between Department of Energy (DOE) and industry groups such as EPRI and NEI, and DOE assistance with industry responses to proposed Nuclear Regulatory Commission rulemaking.

The IAC meets monthly via teleconference and is currently chaired by William Gassmann of Constellation Nuclear. Additional members represent Framatome, Global Nuclear Fuels, Westinghouse, General Atomics, Terrapower, BWXT Nuclear, Dominion, Duke Energy, Southern Nuclear, EPRI, and NEI.



2.7 ATF INDUSTRY TEAMS

As we look back on the accident tolerant fuel industry accomplishments this year, there is a lot of activity across the nation to support this mission. Lead test rods, and in some cases lead test bundles, are in commercial and research and development (R&D) reactor irradiations now (Vogle, Calvert Cliffs, Byron, Hatch, Clinton, and the Advanced Test Reactor at Idaho National Laboratory).

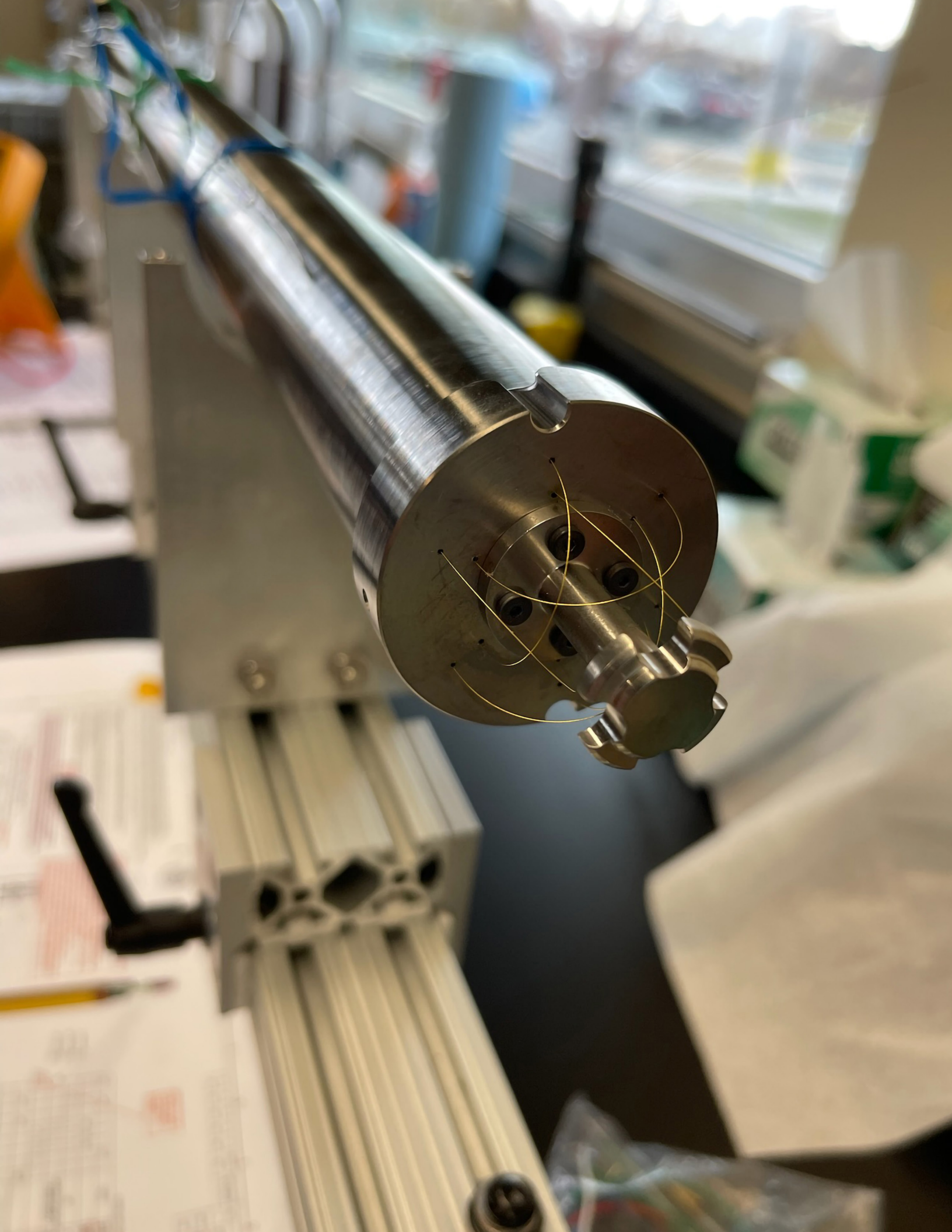
Cladding irradiation planning is also underway for new short term (Cr-coated) and long term (SiC variants) technology approaches in both commercial and R&D facilities, with multiple teams having completed their final designs, initial fabrications, and testing needed to submit for irradiations in FY23.

Industry teams have accelerated their efforts to prepare for a transition to high burnup and longer fuel life. Preparations included topical reports submitted for Cr-coated cladding, burnup limit extensions, and LEU+ implementation; license amendments to start upgrading production facilities for both cladding and enrichment increases; as well as scaling up production

capacity and infrastructure to manufacture industrial quantities of CR-coated cladding to burnups of 75 MWd/kgU. A lead test rod (LTR) program has been defined for Électricité de France (EDF) that will produce further data for licensing Cr coated cladding. Data is also being obtained from the ORNL post irradiation examinations (PIE) on the Byron-2 LTRs (Figure 1), pool-side examination of the Doel-4 LTRs and INL PIEs of cladding from the Advanced Test Reactor (ATR).

Nitrogen cold spray (NCS) was selected as the coating method to be used for Cr coated cladding. The primary basis for this decision was the absence of scratching during loading on the NCS cladding while the physical vapor deposition (PVD) cladding exhibited some scratching. Development work on increasing the density and hardness of PVD coatings is being pursued. Autoclave corrosion testing is continuing for both coating deposition methods.

To validate the accident tolerant benefit of Cr coated cladding, bundle tests were completed at Karlsruhe Institute of Technology (KIT) on



Accident Tolerant Fuel (ATF) Industry Teams – Westinghouse Electric Company LLC

Principal Investigator: E. J. Lahoda

Team Members/ Collaborators: Westinghouse Electric Company LLC (Westinghouse); General Atomics (GA); Bangor University (BU); Idaho National Laboratory (INL); Los Alamos National Laboratory (LANL); Oak Ridge National Laboratory (ORNL); University of Wisconsin (UW); University of South Carolina (USC); North Carolina State University (NCSU); University of Virginia UVa); University of Bristol (UBr); Constellation Energy Corporation (EC) and Southern Nuclear Company (SNC); Rensselaer Polytechnic Institute (RPI), University of Tennessee (UT), University of Texas at San Antonio, Air Liquide (AL), Royal Institute of Technology (Sweden) (KTH), Karlsruhe Institute of Technology (KIT)

Westinghouse EnCore fuel is a gamechanger for the nuclear industry because of significantly increased safety margins in severe accident scenarios, longer fuel cycles and/or large uprates, lower operating costs, and increased flexibility for fuel management.

Westinghouse is working to commercialize unique accident tolerant

EnCore® fuel (ATF) designs which include advanced Cr coatings on cladding and SiGA® silicon carbide (SiC) cladding with the capability of using higher ²³⁵U enriched ADOPT™ fuel (Cr₂O₃+Al₂O₃ doped UO₂) and U¹⁵N fuel (UN) to achieve burnups of around 75 MWd/kgU and/or substantial power uprates.

Project Description:

The Westinghouse ATF program is deploying lead test assemblies (LTAs) of Cr coated cladding with ADOPT and UO₂ pellets with greater than 5% enriched ²³⁵U higher with increased oxidation resistance to steam and air at design basis and beyond design basis accident conditions. The oxidation resistant cladding along with the greater than 5% ²³⁵U fuel and U¹⁵N fuel provide utilities with fuel capable

of supporting economic 24-month cycles and/or significant uprates. This capability significantly lowers the cost of operation of nuclear plants while providing increased accident tolerance.

Accomplishments:

A topical report for burnup extensions of current and ADOPT fuel to 68 MWd/kgU was sent to the Nuclear Regulatory Commission (NRC) December 14, 2021, and the Safety Evaluation Report for ADOPT fuel was issued to Westinghouse June 14, 2022. The Vogtle High Burnup Higher Energy License Amendment Request for the >5% ²³⁵U LTA program was submitted to and accepted by the NRC for review. Manufacturing studies are being completed to support the manufacture of Cr coated cladding for the Vogtle LTA program beginning in 2023. This program will support the final high burnup topical report

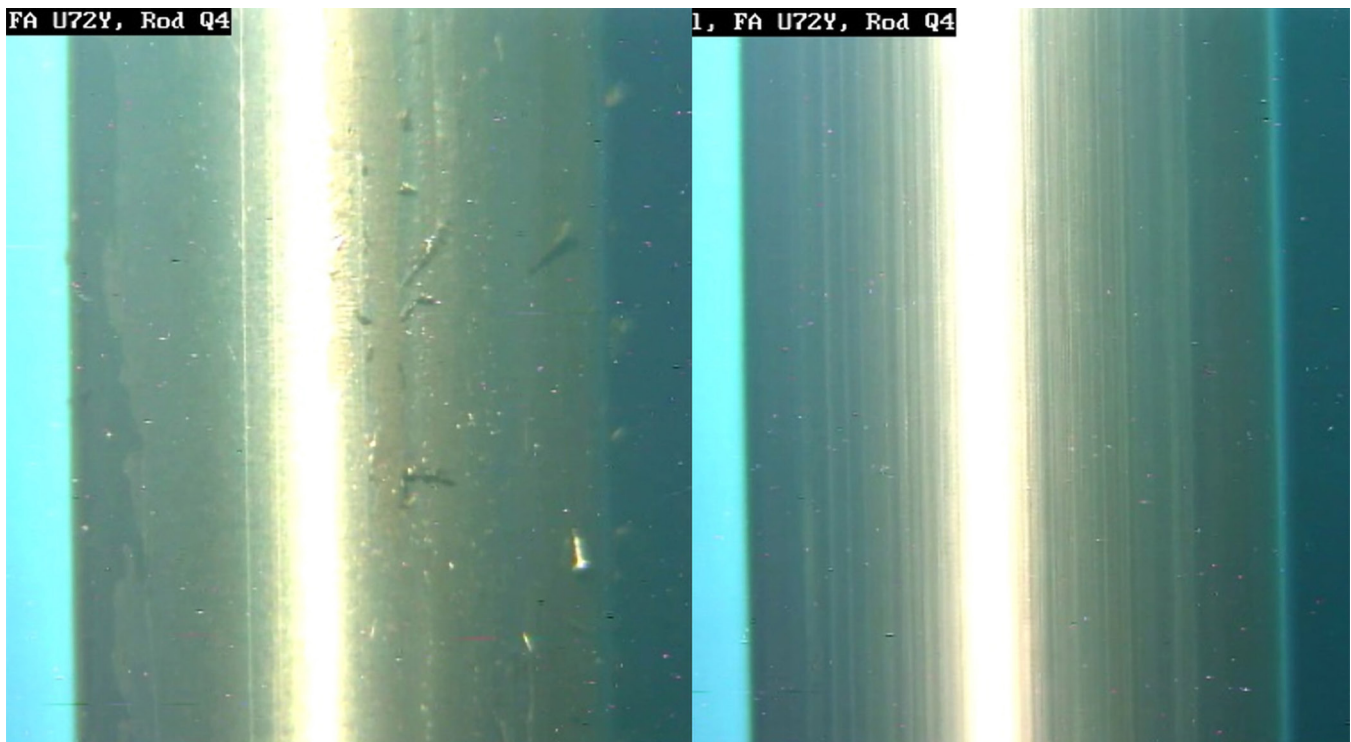


Figure 1. Cr coated rod before and after brushing

to burnups of 75 MWd/kgU. A lead test rod (LTR) program has been defined for Électricité de France (EDF) that will produce further data for licensing Cr coated cladding. Data is also being obtained from the ORNL post irradiation examinations (PIE) on the Byron-2 LTRs (Figure 1), pool-side examination of the Doel-4 LTRs and INL PIEs of cladding from the Advanced Test Reactor (ATR).

Nitrogen cold spray (NCS) was selected as the coating method to be used for Cr coated cladding. The

primary basis for this decision was the absence of scratching during loading on the NCS cladding while the physical vapor deposition (PVD) cladding exhibited some scratching. Development work on increasing the density and hardness of PVD coatings is being pursued. Autoclave corrosion testing is continuing for both coating deposition methods.

To validate the accident tolerant benefit of Cr coated cladding, bundle tests were completed at Karlsruhe Institute of Technology (KIT) on

Figure 2. SiGA metal-bond rodlets with surrogate fuel molybdenum pellets delivered for ATR cycle



Figure 3. Test setup of 7.8 liter recirculating autoclave system at Westinghouse Churchill facility



Westinghouse Cr coated Zr cladding. The test simulated loss of coolant accident (LOCA) conditions (5°C/second temperature rise with rod pressures of ~55 bar) but terminated at 1300°C instead of the current 1204°C LOCA limit. Much lower oxidation was found at the peak temperature of 1300°C as compared to uncoated Zr cladding. These test results will be used to validate the beyond design basis accident (BDBA) performance models in the MAAP5 and MELCOR codes. The results of these codes and probability safety analyses (PSA) which take advantage of FLEX capabilities, will be used as the basis for the NRC to allow downgrading of some equipment classifications, resulting in economic benefits for the utility.

Lower length scale modeling (ASM) is being used to develop ADOPT and UN fuel properties. U15N with 5% enriched has a ²³⁵U content equivalent to ~6.9% enriched UO₂ and a higher thermal conductivity that also aids in reducing or eliminating fuel fragmentation, relocation, and dispersal (FFRD).

GA has advanced SiC microstructure consistency and demonstrated favorable out-of-pile corrosion results of its baseline chemical vapor deposition (CVD) SiC coating and has shown improved hermeticity and yields of the locally heated CVD endcap joining. Demonstration of SiGA cladding irradiation performance is scheduled for the upcoming ATR cycles 171, 173 and

175; starting with unfueled SiGA rodlets, followed by SiGA metal-bond rodlets, and concluding with SiGA UO₂ metal-bond rodlets in ATR cycle 175.

Further, GA is completing fabrication of six SiGA metal-bond rodlets with surrogate fuel (molybdenum pellets) for water loop irradiations in ATR cycles 173A/B (Figure 2). In parallel, GA is collaborating with Westinghouse to demonstrate autoclave robustness of this configuration through 120+ days of Westinghouse autoclave exposure (Figure 3). Previously, GA has delivered six unfueled SiGA rodlets for ATR cycle 171A, currently scheduled to be inserted fall 2022.

Preliminary steam oxidation ultra-high temperature (UHT) testing at Westinghouse Churchill of SiGA cladding resulted in minimal corrosion at 1600°C in a steam environment. ORNL tests showed SiGA cladding survived temperatures and pressures far above other materials and did not burst when to design limits of the test apparatus (up to 1200°C and 15 MPa internal pressure).

GA continues fabrication preparation for batches of 3-foot SiC ceramic matrix composites cladding as a forerunner to fabricating full-length (12-foot) SiGA cladding. Corrosion and irradiation performance of 2-ft SiC metal-bond fuel pins will be demonstrated in future ATR irradiations.

ATF Industry Teams - Framatome

Principal Investigator: Kiran Nimishakavi

Team Members/ Collaborators: Idaho National Laboratory (INL), Oak Ridge National Laboratory (ORNL), Southern Nuclear Operating Company, Kernkraftwerk Gösgen-Däniken, Entergy Nuclear, Constellation Energy, French Alternative Energies and Atomic Energy Commission (CEA).

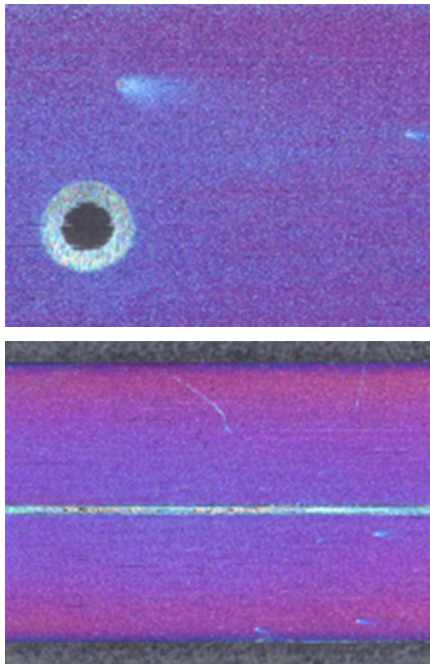


Figure 1. Pre-damaged Cr-coated M5Framatome samples after three cycles of irradiation in the Gösgen reactor.

Framatome's Accident Tolerant Fuel (ATF) strategy relies on a two-phased approach to balance benefits with the anticipated timeline for full-core deployment. PROtect Cr-Cr is Framatome's evolutionary solution which brings incremental benefits compared to standard Zr-UO₂ system. The goal is to deploy this product in commercial reactors by mid-2020s. PROtect SiC is Framatome's breakthrough solution which offers significant benefits during beyond design basis accidents. A progressive implementation is envisioned for SiC-based solution with an initial goal to demonstrate proof-of-concept in test reactors by the mid-2020s.

In response to Department of Energy (DOE) direction, Framatome further expanded the Enhanced Accident Tolerant Fuel (EATF) program to include high burnup and increased enrichment with the objective of increasing energy production and reducing the outage costs by minimizing the number of refueling outages.

Project Description:

The goal of DOE's EATF program is to develop an economical and more robust nuclear fuel design that will reduce or mitigate the consequences of reactor accidents while maintaining or improving existing performance and reliability levels in daily operations. After extensive

testing, evaluation, and down selection, Framatome's technical approach addresses three focus areas: (i) Coatings for pressurized water reactor (PWR) and boiling water reactor (BWR) claddings, (ii) Chromia-doped and Chrome-variant UO₂ fuel pellets, and (iii) Silicon carbide (SiC) composite materials.

A dense Cr-coating on a zirconium-based cladding substrate has the potential for improved high temperature steam oxidation resistance and high temperature creep performance, as well as improved wear behavior. Over the course of the EATF program, extensive processing and testing activities are being carried out on Cr-coated M5Framatome cladding in support of batch implementation by the mid-2020s

Building on both the experience gained and scientific knowledge achieved from the PWR Cr-coated cladding development, a coating material that is suitable for BWR application has been developed. Several out-of-piles tests were performed to ensure adherence and coating quality. Currently, the lead test rods (LTR)s with BWR coating segments are being irradiated in the Monticello reactor and 1st cycle hot cell post irradiation examination (PIE) is planned for 2023.

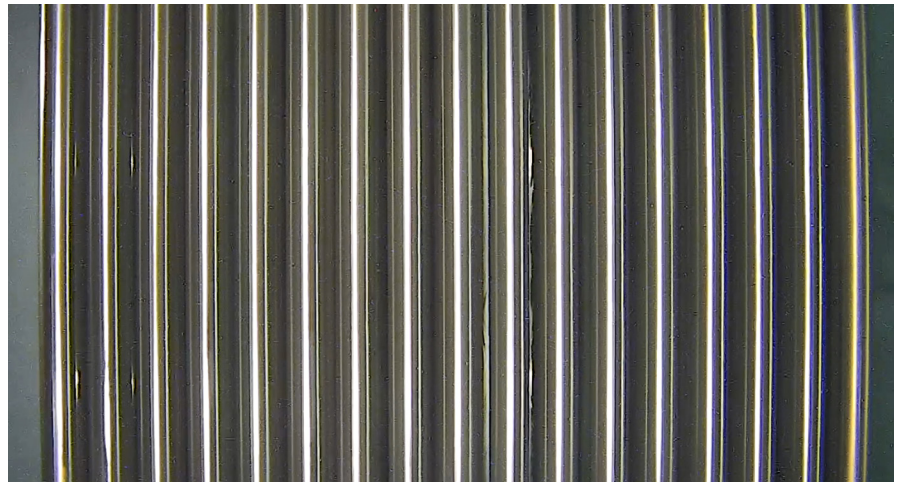
Chromia-doped UO₂ pellets can improve pellet wash-out behavior after cladding breach and reduce

fission gas release. The performance of this fuel has been extensively studied in out-of-pile and in-pile test programs. Chromia-doped fuel topical report for PWR application is currently under Nuclear Regulatory Commission (NRC) review.

Framatome's EATF pellet development is also focused on improving thermal-mechanical properties, especially thermal conductivity. Variants of Cr-doped UO_2 fuel pellets have been developed and out-of-pile testing showed a significant increase in thermal conductivity compared to UO_2 . As part of the proof-of-concept, investigation has been focused on understanding evolution of thermal conductivity and microstructure under irradiation. Framatome fabricated and shipped rodlets containing chromium variant pellets for testing in ATF-1 experiments.

Framatome is also developing a composite cladding comprising a silicon carbide fiber in a silicon carbide matrix (SiCf/SiCm) for revolutionary performance improvements. The objective is to develop a system which does not suffer from the same rapid oxidation kinetics of zirconium-based cladding while having attractive operating features such as reduced neutron absorption cross-section and higher mechanical strength at accident temperatures. Currently, Framatome fabricated test rodlets made of SiC-based composite

Framatome has aggressively pushed the implementation schedule for the DOE EATF project by inserting the first full length fueled coated EATF LTRs into a commercial reactor Vogtle in Spring 2019 and followed that with full length coated LTRs in ANO in Fall 2019 and a full EATF lead test assembly of coated rods at Calvert Cliffs in Spring 2021 on its journey to full batch implementation.



for irradiation in the Massachusetts Institute of Technology Reactor (MITR) and Advanced Test Reactor (ATR).

Framatome's innovative SiC-based cladding design solves critical feasibility issues and NRC concerns such as hydrothermal corrosion, fission gas retention and end plug sealing.

Figure 2. Cr-coated fuel rods after two cycles in Vogtle (left and right corner rods were coated with chromium)

Figure 3. Cr-coated fuel rods after one cycle in ANO (two corner rods on left were coated with chromium)



Accomplishments:

IMAGO was the first irradiation campaign of Framatome's Cr-coated samples in the Gösgen nuclear power plant (NPP). Irradiation was launched in 2016. Several Cr-coated samples were placed in the materials test rods (MTRs) and directly exposed to the reactor coolant and the radiation. Some coated samples were pre-damaged to simulate coating defects and scratches, which could arise during bundle fabrication. Pre-damaged PROtect Cr samples after three cycles of irradiation showed excellent coating adhesion even near the pre-damaged region with no indication of coating degradation. The color of the Cr-oxide is in the blue to purple range and aligns with the expected behavior for undamaged Cr-coatings.

Metallographic analysis did not show increased corrosion of the exposed M5Framatome substrate at the damaged region relative to an uncoated M5Framatome cladding tube.

Framatome with the support of Southern Nuclear installed PROtect Cr fuel rods in the Vogtle Nuclear Power Plant in 2019. This program was the first irradiation of integral Cr-coated M5Framatome cladding with Cr_2O_3 -doped UO_2 fuel ($\text{Cr-Cr}_2\text{O}_3$) in a commercial reactor. Additionally, this was the first irradiation of full-length PROtect Cr fuel rods. Four assemblies each containing four full-length Cr-coated M5Framatome rods were installed in 2019. First cycle visuals were collected in Fall 2020 and the results were reported in the

previous Advanced Fuels Campaign (AFC) report. Second cycle visuals were collected in Spring 2022. The Cr-coated fuel rods are in good shape with no signs of coating delamination. The lustrous golden appearance of Cr-coated rods is not clearly visible due the crud layer, which covered all the fuel rods. Other inspections, such as fuel rod diameter measurements demonstrated the expected behavior.

A limited number of Cr-coated fuel rods were installed in Arkansas Nuclear One (ANO) reactor in 2019. After one cycle, Cr-coated fuel rods showed lustrous-gold appearance indicating a significant reduction in corrosion kinetics compared to uncoated cladding. The coating remained tightly adherent, and there was no sign of coating degradation. These observations are consistent with the findings of other irradiation campaigns.

Framatome is scaling up its production capacity to manufacture industrial quantities of Cr-coated cladding. A more detailed design phase has been launched to flesh out the specifics of the industrial pilot. Fabrication of full-length cladding transportation system has been launched and this mockup system will be tested at the supplier's facility to validate its functionality. Additionally, a scaled down version of the transportation system is being attached to one of the prototype machines at Paimboeuf to test its functionality during the deposition process.



Framatome has developed an innovative SiC-based design which addresses several key issues of SiC/SiC composite cladding. A thin environmental barrier coating on the outer surface protects the cladding against recession under normal operating conditions and a tubular liner inside the composite helps with the hermetic sealing. Framatome manufactured SiC-based rodlets which are ready for irradiation in MITR and ATR.

Figure 4. PROtect SiC rodlets for ATR irradiation

General Electric Progress in Developing Accident Tolerant Fuels

Principal Investigator: Raul B. Rebak

Team Members/ Collaborators: Evan J. Dolley, Russ M. Fawcett, Mason Makovicka, Rich Augi, David Barrientos, Dan Lutz, Tyler Schweitzer, Jason Harp, David Kamerman, Fabiola Cappia, Scarlett Widgeon Paisner

GE is pursuing the development of more robust fuel materials for LWR, both for the shorter term (~5 years) and the longer term (~10 years) commercial implementation.

General Electric (GE) has been working on the development of Accident Tolerant Fuels (ATF) since October 2012. GE is pursuing several concepts to develop a more robust and economically feasible fuel that can withstand accident conditions while generating less hydrogen and maintaining a coolable fuel architecture for longer times. These concepts include the development of; (1) two cladding concepts (ARMOR or coated Zircaloy-2 & monolithic FeCrAl), (2) Fuel with improved thermal and mechanical properties, and (3) fuels with enrichments of fissile uranium higher than 5% & burn up limits higher than 62 GWd/MtU (Figure 1).

Project Description:

The technical objective of the GE-led ATF project is to develop materials that will make fuel rods more reliable to operate in light water reactors (LWRs) both in terms of safety and economics. The use of these materials may also allow for the extension of the life of currently operating reactors and avoid their premature decommissioning. It is projected that nuclear energy will continue to be an important share of clean energy that may alleviate climate change in the next few decades. The newer materials were never used before in LWR; therefore, their suitability needs to be evaluated in the entire fuel cycle, from economical tube and rod fabrication

to final used fuel disposal. GE is currently engaged in evaluating ATF fuel materials in the entire fuel cycle of LWR (Figure 2). For this effect GE is working with utility partners such as Southern Nuclear and Constellation, with national laboratories (such as Idaho National Laboratory (INL), Los Alamos National Laboratory (LANL), and Oak Ridge National Laboratory (ORNL)) and industrial partners such as Alleima AB (formerly Sandvik Materials Technology). The information gathered in the current project for the IronClad or FeCrAl cladding can also be used in near future for the next generation of reactors since FeCrAl alloys possess high strength and oxidation resistance at temperatures higher than 600°C. While doing materials characterization this project is also helping to train the next generation of nuclear materials scientists that will help keeping nuclear energy a consistent source of clean energy.

Accomplishments:

The accomplishments for GE can be summarized in the following areas:

6.1 (by Mason Makovicka) During the fiscal year of 2022 coating cladding work continued research and development activities for an ARMOR 1.0 replacement. The investigation into the causes of the performance miss in reactor of ARMOR 1.0 at Hatch was completed. Both the ARMOR 1.5 and ARMOR 2.0 initiatives were advanced. A large number of

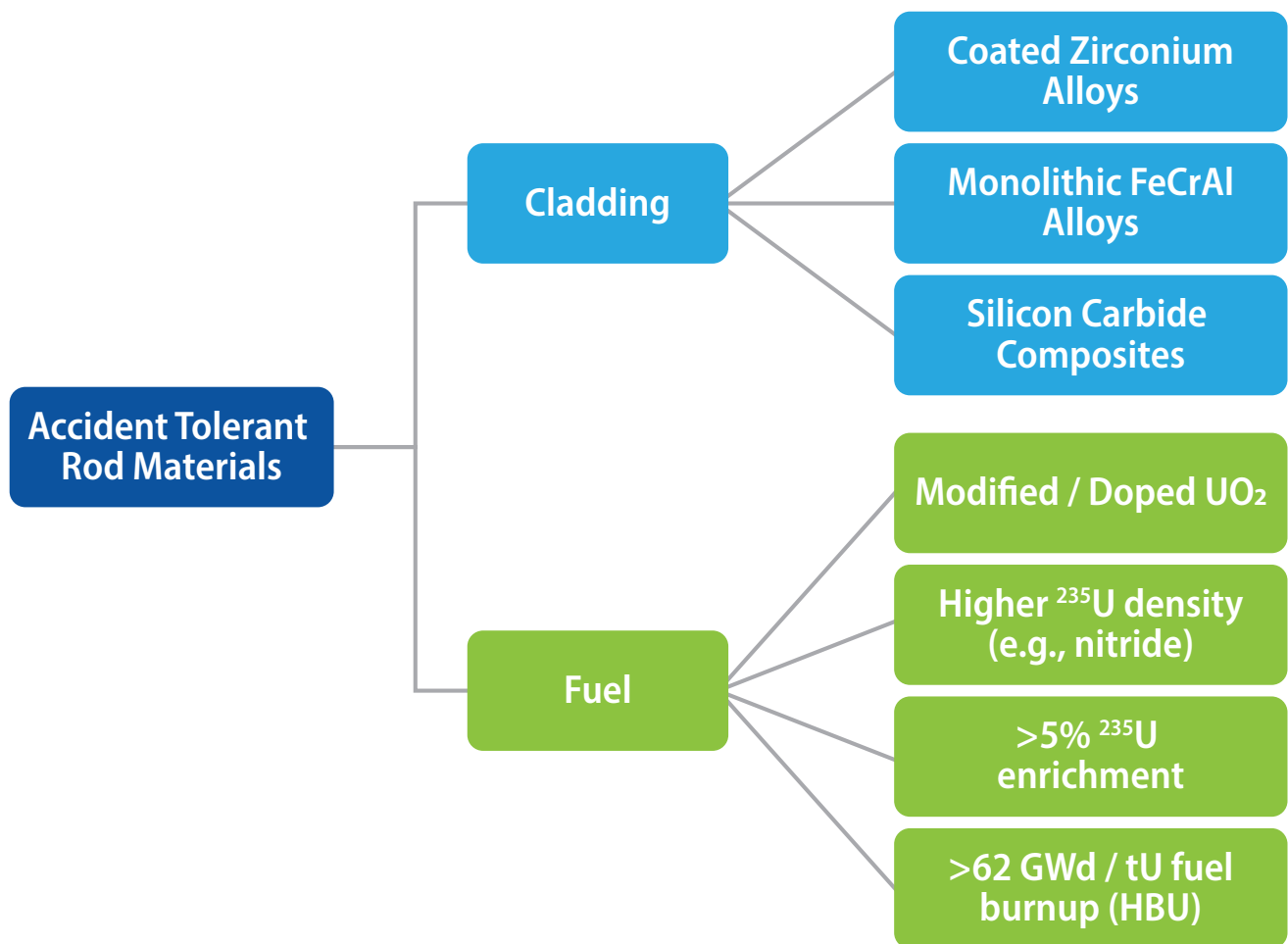


Figure 1. ATF Related Areas of Study under Consideration by General Electric.

screening tests were conducted on multiple ARMOR 1.5 and ARMOR 2.0 concepts with mixed results. The fiscal year will conclude with a down selection of ARMOR 1.5 concepts to move the effort into an optimization phase to focus on the most promising coating architecture. ARMOR 2.0 will similarly go through a down selection that will take place in the next fiscal year.

6.2 The advancements in the characterization of IronClad (FeCrAl) continued during the fiscal year and most of the results were published in more than 15 articles (see publications list). More manuscripts will appear in the following period.

6.3 (by Dan Lutz) Irradiations of ARMOR and IronClad are being conducted in Hatch, Clinton and

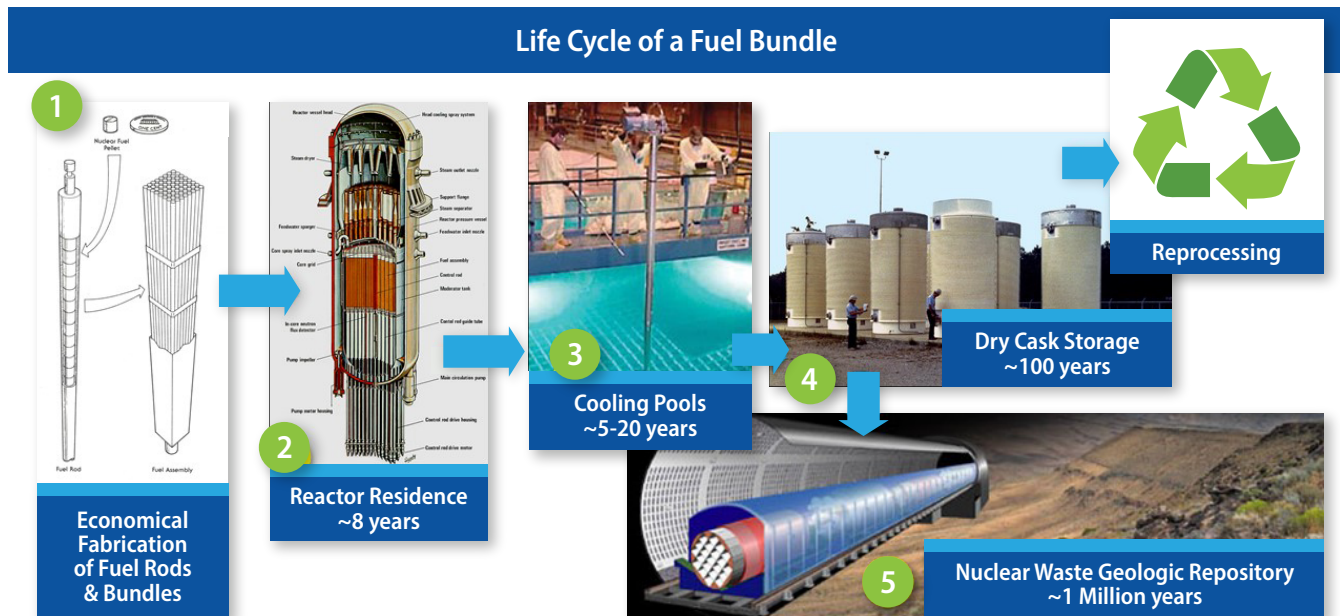


Figure 2. The Newer ATF Materials need to be Evaluated in the Entire Fuel Cycle.

the INL Advanced Test Reactor (ATR). Hatch ARMOR lead test assemblies (LTAs) completed their second cycle of operation in early 2022 and are now all permanently discharged; a single Hatch IronClad Lead Test Rod continued to operate in 2022 in its third cycle in Hatch. All Clinton ARMOR LTA bundles remain discharged after completing one cycle of operation in 2021; two Clinton IronClad LTA bundles have completed their first cycle of operation and are awaiting poolside

inspection that is planned for 2023 while a third IronClad LTA bundle is currently operating in its second cycle. ARMOR and IronClad ATR irradiation under ATF-2 was completed in 2021. Hot cell examinations of ARMOR and IronClad irradiated in Hatch and ATR have been advanced by ORNL and INL, while a shipment of Clinton one-cycle IronClad Lead Test Rods to ORNL is being planned for 2023.

6.4 (by Tyler Schweitzer) Interactions with the Nuclear Regulatory

Commission (NRC) continue to be constant and productive. In December 2021 Global Nuclear Fuels (GNF) submitted three topical reports to the NRC that are needed for low enriched uranium (LEU)+ implementation, including update to Lattice Neutronic Characteristics Evaluation & Research code (LANCR) for LEU+, update to LANCR Model, and LANCR/PANAC (GE 3D core simulator code) Implementation topical reports. Submitted Special Nuclear Materials (SNM)-1097 License Amendment to the NRC to enable the GNF-A fuel fabrication facility to handle LEU+. Pre-submittal meeting with the NRC in July of 2022 for the downstream implementation LTR for LANCR with plans to submit later in 2022. GNF fresh fuel transport container RAJ-II pre-submittal meeting completed and planning to submit by the end of September 2022. GNF updated the NRC in August 2022 with the overall LEU+/high burnup (HBU) licensing plan and program trajectory, and GNF participated in the NRC HBU workshop in August 2022.

6.5 (by Tyler Schweitzer) GNF continues to progress on updating methodologies to enable LEU+ and HBU. After the initial submittal of the LANCR topical reports, GNF began working on implementing LANCR into the downstream methods. GNF is working to prepare

a topical report for HBU licensing and will address the issues raised in NRC RIL-2021-13 as well as hydrogen for higher burnup.

6.6 (by Rich Augi and David Barrientos) GE has had extensive positive interaction with the utilities, mainly Southern Company and Constellation, which have been fully supportive on GE's current direction. The collaborative approach working with these two companies is on the current LTAs (Clinton + Hatch), and the HBU Lead Use Assembly (LUAs; Limerick) to make sure GE can obtain as much valuable information as possible. The utilities have also contributed to conversations with DOE, as we continue progressing through the funding reduction and product trajectory. Deployment for ARMOR and LEU+/HBU will be closer to the end of the decade. IronClad has an estimated deployment date closer to mid-2030s. GE continues working with our utility partners and national labs getting as much information from LTAs and advancing our methods to support the data that's needed for all the licensing topical reports to ultimately deploy each technology.

General Atomics – Electromagnetic Systems (GA-EMS)

Principal Investigator: Ryan Hon

Team Members/ Collaborators: Westinghouse Electric Company LLC, Structural Integrity Associates Inc., Constellation Energy Corporation

The project will accelerate development and licensing of SiGA® SiC-SiC accident tolerant fuel cladding by obtaining representative irradiation and corrosion performance data in a commercial nuclear reactor.

The Irradiation of Silicon Carbide Ceramic Matrix Composite Cladding in a Commercial Nuclear Reactor project will complete all the design, manufacturing, and licensing necessary to irradiate GA-EMS' SiGA® silicon carbide composite (SiC-SiC) cladding in a commercial reactor, helping to drive future development and commercialization.

Project Description:

The SiGA® Commercial Reactor Irradiation Project's objective is to complete all the necessary steps for the irradiation of SiC material in a commercial nuclear reactor. After completion of the project, the SiC samples will undergo one cycle of irradiation in a commercial nuclear reactor from fall 2024 to spring 2026. Subsequent post irradiation examination of the samples will occur in the fall 2026 and will provide SiC performance data under prototypical coolant and irradiation conditions to support future SiGA® development and testing. This data, along with the lessons learned while designing and licensing the irradiation, will enable accelerated implementation of lead test rods, lead tests assemblies, and commercialization of SiGA® cladding.

As lead, GA-EMS will be manufacturing selected silicon carbide samples to obtain data to support

future test programs and validate current and future models. GA-EMS is subcontracting with Westinghouse, who will be designing and manufacturing metallic capsules to house the SiGA® samples, and Structural Integrity (SI), who will be providing modeling support. Constellation, as a partner, will be providing a commercial reactor for the irradiation as well as licensing and analysis support.

This project is part of a larger SiC-SiC cladding development effort at GA-EMS that includes funding via the Accident Tolerant Fuel (ATF) program, the Industry Opportunities for Advanced Nuclear Technology Development program, and internally funded work. Data obtained following this project will be combined and correlated with data obtained through irradiation of SiGA® in test reactors to support follow on commercial reactor irradiations. The project accelerates the development of SiC cladding which has the potential to increase the safety and economics of the current reactor fleet due to its high-temperature strength and irradiation stability enabling high-burnup high-enrichment fuels.

Accomplishments:

In the previous year GA-EMS completed the needed preliminary actions and objectives to position

itself for successful manufacturing of SiGA® test specimens and related design and modeling work required for reactor insertion. This included completing an initial test plan for irradiation detailing the irradiation objectives, requirements, conceptual SiC sample design, and post irradiation planning. The plan aims to capture the details needed to realize the follow-on goal of obtaining post irradiation data that will drive SiGA® development. SiC samples will be unfueled, to avoid the need for a license amendment request, and were selected to investigate corrosion, joint and cladding strength with irradiation, and bowing. A modified guide tube thimble plug assembly was chosen as the vehicle to house and insert the SiC samples into the core to minimize the impact on reactor operations and facilitate licensing through the 10 CFR 50.59 process. Westinghouse has providing initial scoping on the thimble plug assembly irradiation concept and predicts that the fit form and function of the guide tube thimble plug assembly will not change with the addition of the silicon carbide samples. The project has secured approval from Constellation for irradiation of the silicon carbide material in Byron Unit 1 targeting the October 2024 refueling outage.

To fit within the guide tube thimble plug assembly, SiGA® samples need to be manufactured at a smaller diameter than current ATF cladding specifications. GA-EMS has demonstrated the manufacturing of two batches of reduced diameter SiC samples that exceed expected insertion requirements and are representative to the larger diameter accident tolerant fuel cladding in terms of braid geometry, strength, and leak tightness. Samples easily met the leak tightness requirement of $< 1 \times 10^{-7}$ atm*cc/s and strength testing shows ultimate tensile strengths within 10% of ATF cladding values. GA-EMS is confident that the smaller diameter samples will provide representative data to support commercialization of the larger diameter design.

SI has begun modifications on their PEGASUS finite element fuel performance code to model the silicon carbide samples during the irradiation. Silicon carbide properties have been implemented into the code and code validation through test case comparison has begun. The modeling will support performance analysis of the SiC samples performed by GA-EMS.



Figure 1. Comparison of smaller diameter and standard ATF diameter SiGA® cladding





ADVANCED REACTOR FUELS

- 3.1 Fuel Fabrication and Properties
- 3.2 AR Irradiation Testing and PIE Techniques
- 3.3 AR Fuel Safety Testing
- 3.4 AR Computational Analysis
- 3.5 Performance Assessment

3.1 FUEL FABRICATION AND PROPERTIES

Thermal Conductivity of Irradiated Binary Metallic Fuels

Principal Investigator: Cynthia A. Adkins

Team Members/ Collaborators: Chuting Tan, Narayan Poudel, Zilong Hua, Scott Middlemas, Tiankai Yao, INL; Yong Yang, University of Florida

These first of a kind experimental thermal conductivity measurements on irradiated high burn up U-10 wt% Zr will transform the foundation for physics-based fuel performance modeling of thermal conductivity used to develop new metallic fuel forms and reactor designs.

Modeling and simulation tools for predicting the effective thermal conductivity of metallic fuels, particularly U-Zr and U-Pu-Zr alloys, are limited and incomplete. The physics-based tools that do exist in fuel performance codes use assumptions about the pre and post irradiated microstructure of U-Zr fuel that are based on the structure being homogeneous and the Zr redistribution during irradiation following a uniform gradient. As characterization techniques improve for irradiated metallic fuels, it is reported that the microstructure is even more intricate and inhomogeneous than previously reported. Therefore, it becomes even more important to associate local thermal properties with local microstructure. This study produced local thermal diffusivity and thermal conductivity data that supports and improves the calculation of effective thermal conductivity and our understanding of the behavior of U-Zr fuel in-pile.

Project Description:

Microstructural phases in an alloy system have distinct physical and chemical properties, including thermal conductivity. The goal of this study is to show that the different phases present, formed due to Zr migration, in the U-Zr system indeed do have different thermal conductivities. These phases along with the porosity

from fission gas bubble formation can be described by an analytical model that can be used with those individual properties to represent the effective thermal conductivity of the bulk U-Zr alloy system both pre and post irradiation. For materials with simple physical structures, the effective thermal conductivity can be modelled using existing fundamental structural models such as Maxwell-Eucken and Effective Medium Theory (EMT) models. These models are examples of analytical models that have a physical basis in the microstructure of the materials they are used to describe. They can be combined in such a way to account for the volume fraction of phases, pores, and the interaction between them for an effective thermal conductivity calculation. Analytical models are preferred over numerical models to describe the effective thermal conductivity due to their physical basis, rapid and low cost of calculation and reported reasonable accuracy even when the microstructure is uncertain. These models require that the thermal conductivity and volume fraction of each defined phase be known as input parameters to the calculations. This work is the starting point for further development of a robust post-irradiated effective thermal conductivity model of the U-Zr metal fuel system that can be

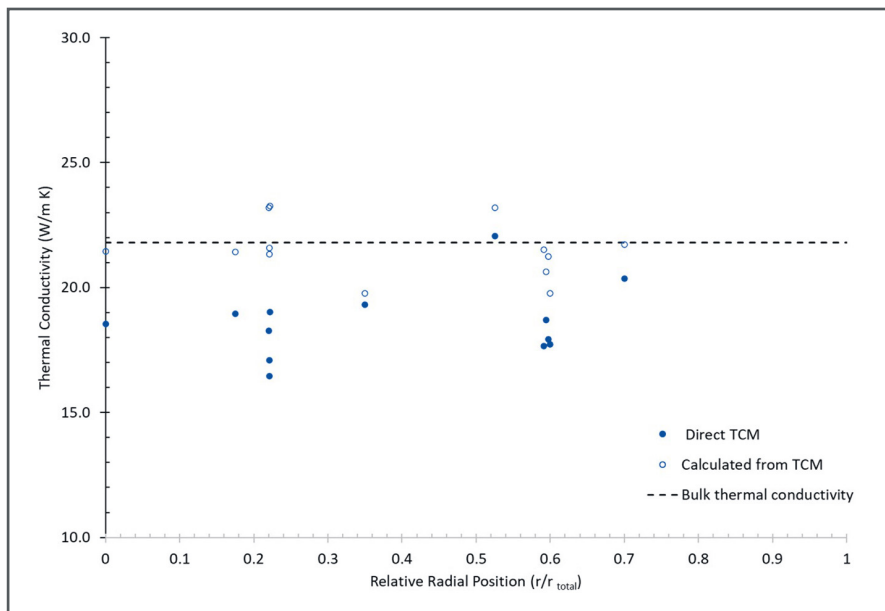


Figure 1. Thermal conductivity as a function of radial location for fresh U-10 wt% Zr. Bulk thermal conductivity from LFA (dashed line), local TCM conductivity (solid circles), and local thermal conductivity calculated from TCM diffusivity (open circles) are compared

used in conjunction with other data leading to a metallic fuel qualification and approved safety analysis for use in the advanced reactor designs being proposed by Department of Energy and TerraPower.

Accomplishments:

This study provides meso-scale (20-100 μm) experimental observations of phase dependent thermal conductivity of Na-bonded legacy FFTF MFF-3 fresh and irradiated U-10 wt% Zr fuel (12 at% burnup). The calculated effective thermal conductivity is compared to the bulk measurements to validate the model assumption. The pre- and post-irradiated microstructure was

also examined to identify the phases and porosity of the U-10 wt% Zr alloy brought on by temperature and neutron flux and correlate it with the thermal conductivity. Bulk thermal properties including thermal diffusivity were measured of a fresh sample of MFF-3 U-10 wt% Zr by traditional measurement techniques (i.e., laser flash analysis (LFA)). Local thermal diffusivity was measured using a thermal conductivity microscope (TCM) designed around the thermoreflectance measurement technique. This measurement is capable of the meso-scale data collection of thermal diffusivity and conductivity directly

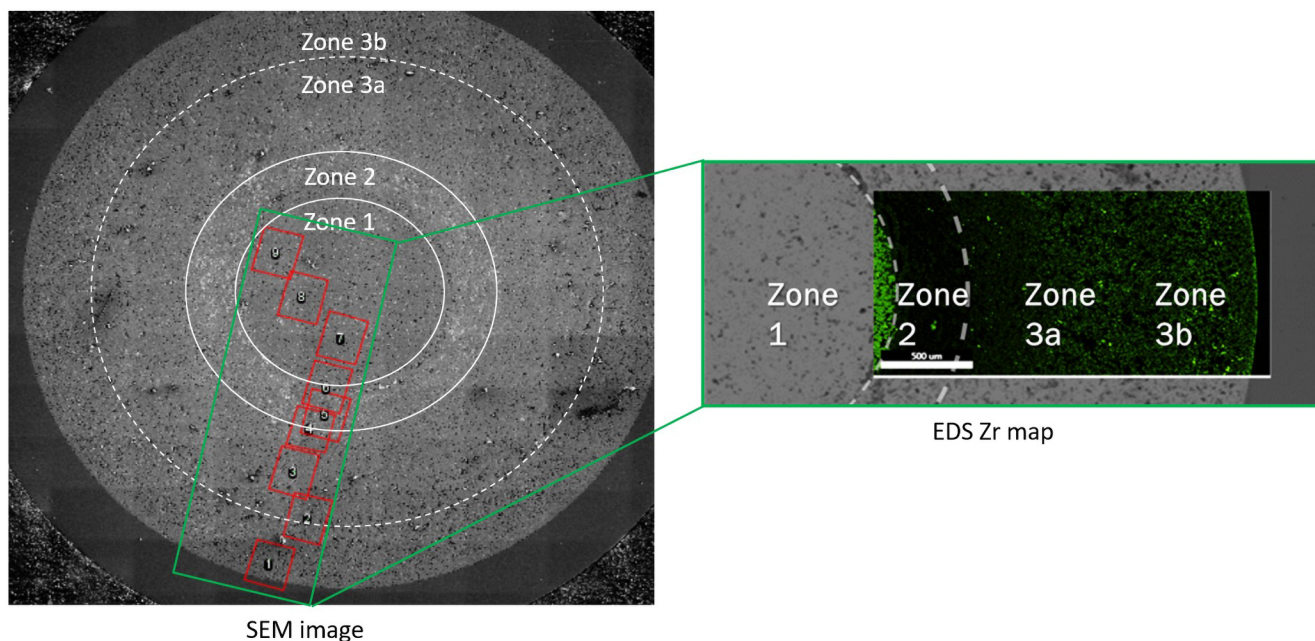


Figure 2. (left) Scanning electron microscopy image of irradiated U-10 wt% Zr with locations of local thermal diffusivity measurements (red squares); (right) EDS image of Zr concentration (green areas)

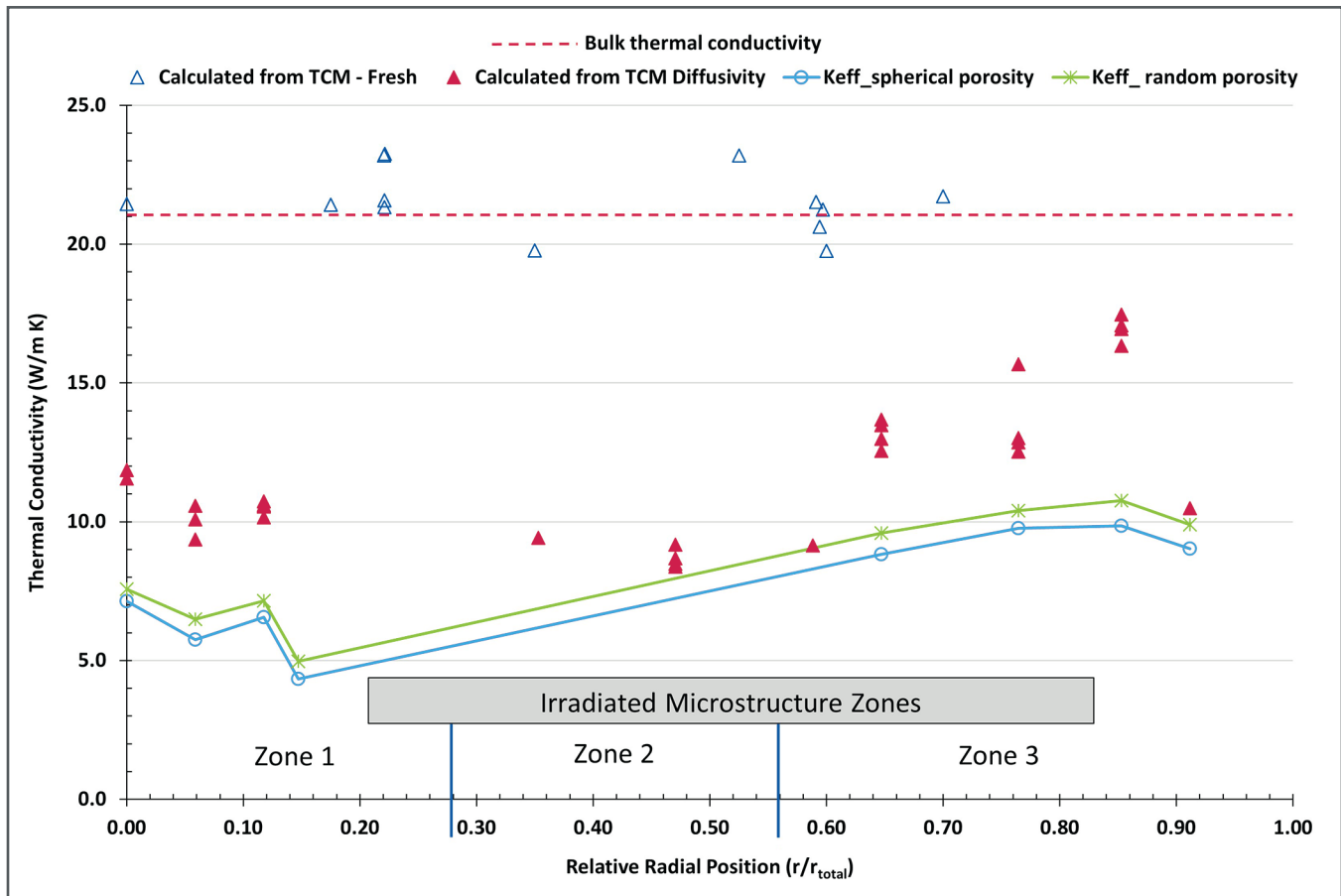
from the surface of a polished sample and its use on the irradiated U-Zr fuel system produced the first of its kind values for local thermal property measurements. Figure 1 compares the bulk thermal conductivity and local thermal conductivity measured across the radius of a fuel slug cross section of a fresh MFF-3 sample. Additionally, it shows a calculation of the local thermal conductivity using Equation 1.

$$k = C_p \cdot \rho \cdot \alpha \quad (1)$$

where k is thermal conductivity, C_p is specific heat at constant pressure, ρ is density, and α is local thermal diffusivity measured on the TCM. This comparison shows that the TCM direct measurement of thermal conductivity is lower

than the corresponding calculated conductivity which matches the bulk value well and is likely due to sample surface preparation and scattering of the instrument lasers by the surface coating and the underlying microstructure. Therefore, local thermal diffusivity data from the TCM is more reliable.

Local thermal diffusivity measurements were collected on an irradiated MFF-3 U-10 wt% Zr sample from pin #193114. Figure 2 shows the location of TCM measurements and the irradiated microstructure zones created by Zr migration and fission gas bubbles. The inset is an energy dispersive spectroscopy (EDS) map showing the concentrations of Zr in green. From transmission electron microscopy data collected for another study, zone 1 is mostly δ -UZr₂ and zone



2 is mostly α -U while zone 3 has a gradient of U and U-Zr phases.

Thermal conductivity as a function of radial location is presented for the irradiated U-Zr in Figure 3 comparing the values for the bulk and local fresh material with the calculated thermal conductivity from the local TCM measurements. The local calculated thermal conductivity comes from the values used in Equation 1. A modified Maxwell-Eucken / EMT equation was used to calculate effective thermal conductivity, k_{eff} , that utilizes the thermal conductivities

of the individual phases, fission gas trapped in the bubbles (here it is Xenon) and a shape factor describing the sphericity of the pores. This factor describes pores from perfectly spherical to completely random shaped. It is shown that the local thermal conductivity of the irradiated U-Zr based solely on volume fraction of phases is approximately 62-74% lower than the fresh material. When accounting for the volume and shape of the porosity, the local thermal conductivity decreases again.

Figure 3. Thermal conductivity as a function of radial location for irradiated U-10 wt% Zr. Bulk fresh thermal conductivity from LFA (dashed line), local TCM conductivity, fresh (open triangles), local irradiated thermal conductivity calculated from TCM diffusivity (solid triangles), and effective thermal conductivity models with spherical (open circles) and random (stars) pores are compared

3.2 AR IRRADIATION TESTING AND PIE TECHNIQUES

AFC-FAST Irradiation and Initial PIE

Principal Investigator: Boone Beausoleil

Team Members/ Collaborators: Luca Capriotti, Kyle Paaren, and Byron Curnutt

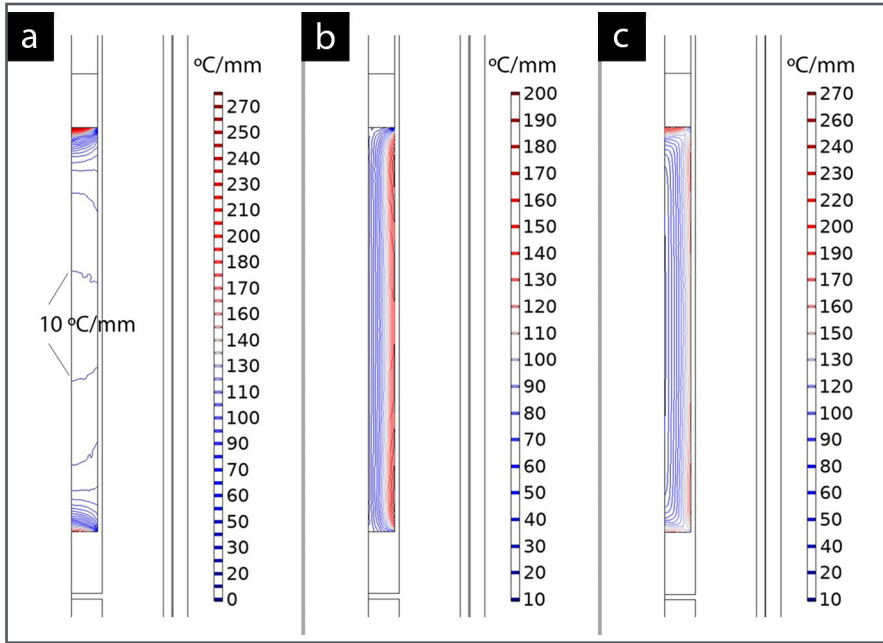


Figure 1. Local temperature gradients for the FAST-007 rodlet. (a) shows the temperature gradient analyzed in the axial direction (dT/dh) and (b) shows the temperature gradient in the radial direction (dT/dr). (c) shows the combined magnitude of gradients. These gradients were similarly assessed for all four rodlets and this is qualitatively representative of all four rodlets

The Advanced Fuels Campaign (AFC) Fission Accelerated Steady-state Testing (FAST) experiments underwent the initial post irradiation examination (PIE) and fuel performance analysis using the BISON code. Examination performed included the standard suite of non-destructive examinations including visual examination, neutron radiography (nRAD), and precision gamma spectroscopy (PGS). Analysis of the fuels included performing

as-run power history neutronic analysis and thermal analysis using COMSOL multi-physics software. Supporting performance modelling was performed using the BISON fuel performance codes as a comparison to the historical Experimental Breeder Reactor (EBR)-II experiments. These results will be used in support of and to guide further destructive PIE efforts in the coming fiscal year.

Project Description:

The objectives of the FAST experiment are, at a basic level, to improve the timeline of advanced fuel research and development (R&D) efforts and to support accelerated qualification methodologies. The project lends itself to support high throughput, rapid prototyping of fuel designs to be able to provide qualitative comparisons to the performance of standard fuel designs. The ability to produce high burnup fuel pins of both a control and novel fuel design within the same capsule and irradiation conditions is critical to the development of next generation reactors. Novel fuel designs can then be paired against controls in post-irradiation furnace tests or transient testing in Transient Reactor Test Facility (TREAT). This allows rapid qualitative comparisons of

This work represents the first look at PIE and as-run analysis of the first AFC FAST tests and the effects from scaled irradiation fuels testing

performance between novel designs against established performance metrics. The solution of simply accelerating irradiation, however, requires consideration of many other phenomena that FAST can provide answers for. Phenomena such as fission product diffusion and alloy re-distribution are heavily influenced by temperature gradients, time at temperature, and concentration gradients. By scaling the geometry to a reduced size and reducing the total time under irradiation, the balance of time and distance for diffusion centric phenomena is tested. This has important implications for developing high burnup alloy fuel as the roles of alloy redistribution and fission product concentrations at the cladding are both important fuel performance metrics. This adds additional value to the use of FAST as it provides critical data to the development and implementation

of physics-based models by virtue of the departure from fully prototypic irradiation and thus an improved, broader basis for validating performance codes against.

Accomplishments:

The power histories of the FAST fueled specimens during irradiation were calculated and used for thermal analysis of the FAST pins. Thermal analysis profiles and contours generated from the as-run power histories are presented in Figure 1 for FAST-007. These contour plots are useful in understanding potential effects from the size of the rodlets and results from PIE, especially during future destructive examination where chemical and microstructural analyses can be performed. Axial and radial gradients are compared within the rodlet as to help understand the impacts of reduced scale testing. Axial thermal gradients existed to some degree in the previous AFC and EBR-II tests, but the fraction

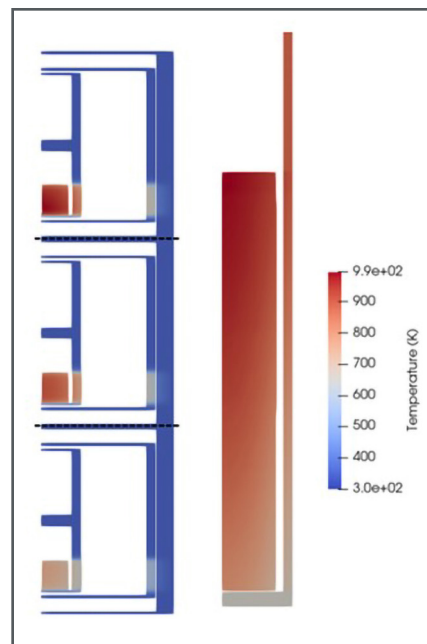


Figure 2. (above) A comparison between EBR-II experiment DP10 (right) and three ½ diameter FAST capsules stacked alongside it (right). The FAST method is shown to adequately represent the bottom, middle, and top portions of the DP10 experiment

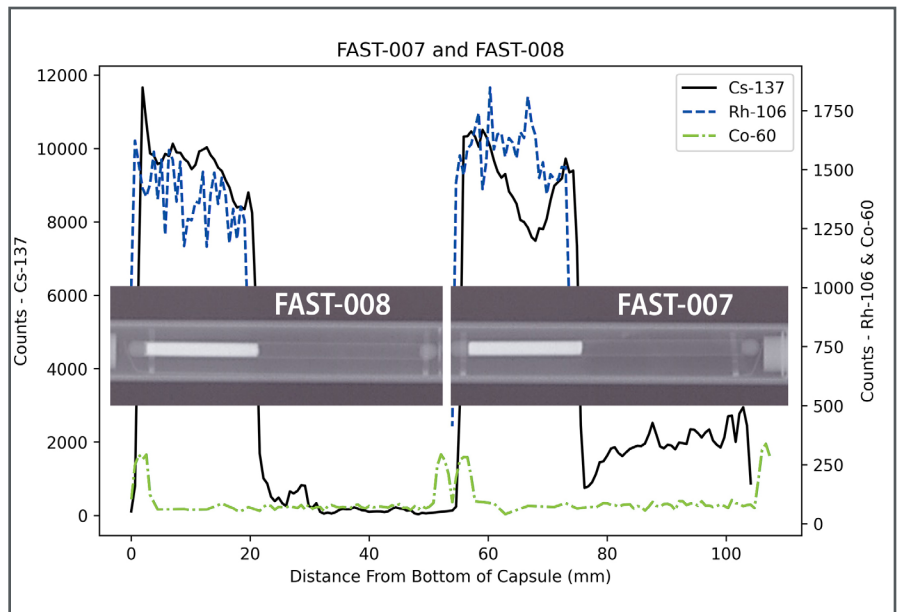


Figure 3. Gamma scan results for the AFC-FAST-005 capsule containing rodlets FAST-007 and FAST-008. The figure shows the axial distribution of fission products for Cs-137, Rh-106, and Co-60

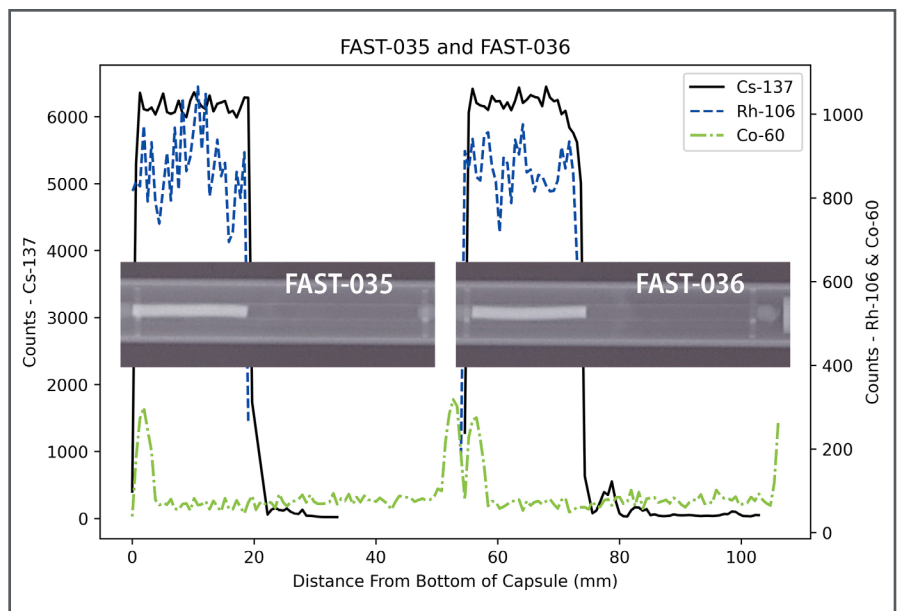


Figure 4. Gamma scan results for the AFC-FAST-016 capsule containing rodlets FAST-035 and FAST-036. The figure shows the axial distribution of fission products for Cs-137, Rh-106, and Co-60

of the fuel rod or rodlet over which they were appreciable was much smaller than for the FAST tests. Regions of significant axial gradients were defined as having a gradient in excess of 10°C/mm. For AFC and FAST tests this represented about 20-25% of the fuel length. For the FAST tests, this represented between 60-80% of the fuel length. This is expected to have significant implications to performance that will require more destructive PIE. (INL, Beausoleil, Curnutt)

FAST experiments were also analyzed as portions of EBR-II experiments using BISON fuel performance codes. It was observed that a FAST rodlet can make a good approximation to different axial positions within an EBR-II pin (Figure 2). Work is on-going to show the difference between EBR-II experiments and FAST experiments and how the PIE data from FAST can be used to augment prototypic fuel performance codes. (INL, Paaren)

Neutron radiography was performed using the Neutron Radiography Reactor located in the basement of the Hot Fuel Examination Facility. The FAST-007 and FAST-008 rodlets appeared to have swelled completely towards their respective cladding, while some space between the fuel and cladding is still visible for the

rodlets FAST-035 and FAST-036. This difference is attributed to the difference in burnup levels reached by the two different capsules, as historical fuel performance data indicates major fuel swelling by about 2-3 %FIMA burnup. (INL, Capriotti)

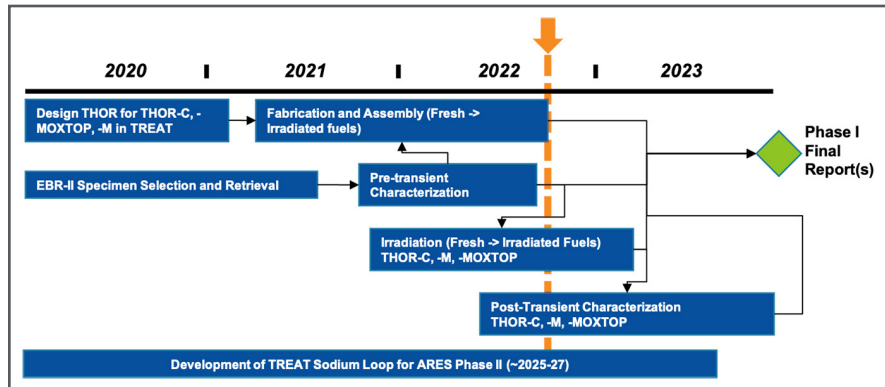
PGS was performed on the capsules and rodlets to monitor the fission products axial distribution (Figures 3 and 4). Rodlets FAST-035 and -036 present an image of “early” life fission product behavior, in which Cs does not seem to have migrated yet to the plenum. This also correlates to the lack of contact between the fuel and cladding that is seen in the radiography. In both rodlets, a small Cs peak is present just above the rodlet. FAST-008, the control rodlet, shows a behavior very similar to the previous tests within AFC. The cesium behavior for FAST-007 was also atypical as it appears to be non-uniform within the fuel (in contrast to the other three rodlets) and has a large amount present along the length of the rodlet plenum. (INL, Capriotti)

3.3 AR FUEL SAFETY TESTING

Initial Fast Reactor Fuel Transient Irradiations: In-Pile Data and Initial Findings

Principal Investigator: Colby Jensen

Team Members/ Collaborators: Klint Anderson, Robert Armstrong, Trevor Smuin



Advanced reactor deployment will be enabled by the results of these transient tests on fast reactor fuels that ensure maximum fuel performance and safety of these systems.

Figure 1. Overview of ARES Phase I project schedule

Advanced Reactor Experiments for Sodium Fast Reactor Fuels (ARES) is a joint project between the U.S. Idaho National Laboratory (INL) and the Japanese Atomic Energy Agency (JAEA) to investigate the transient fuel performance of irradiated advanced metallic and mixed oxide (MOX) fuel designs from Experimental Breeder Reactor (EBR)-II experiment programs. Figure 1 provides an overall view of the ARES project tasks and schedule. Transient fuel performance of fast reactor fuels has been well-established internationally. The continued optimization of fuel designs and associated operational limits to improve performance and economics demands the continued experimental evaluation of these behaviors. These goals require the development of improved fuel performance behavioral models

implemented in advanced modeling and simulation tools, which in turn require modern experiment complements with new data streams. An important step in the ARES project is to establish new sodium capsule testing capability through commissioning testing in the Transient Reactor Test Facility (TREAT) facility. The first experiments and results of these experiments show excellent performance of the test design and show the robust nature of metallic fast reactor fuel.

Project Description:

The ARES project is comprised of the Temperature Heat Sink Overpower Response-Commissioning (THOR-C), THOR-Metallic (THOR-M), and THOR-Mixed Oxide Transient OverPower (MOXTOP) experiments including six fresh metallic fuel capsules, two irradiated metallic fuel capsules, and two irradiated MOX fuel capsules, respectively. A



Figure 2. Final assembly of the THOR-C-2 capsule at the TREAT facility

total of four commissioning experiments for a new TREAT sodium capsule, the THOR capsule, have been completed in this fiscal year using fresh metallic fuel EBR-II driver pins. These experiments are the primary experiments to commission the THOR capsule for multiprogram usage, including testing of high burnup metallic and MOX fuel pins. Remaining commissioning tests will provide further support of hodoscope performance evaluation and explore unique Loss of Flow (LOF) conditions never

before tested in TREAT on metallic fuels. The experiment design and first TREAT experiment on a THOR capsule was completed in 2021. During the past year, fabrication and assembly of multiple THOR capsules has continued, along with design, demonstration, and deployment of remote handling equipment to allow THOR capsules to be loaded with irradiated fuel pins in Hot Fuel Examination Facility (HFEF). Figure 2 shows the final assembly of the THOR-C-2 experiment at the TREAT Facility building.

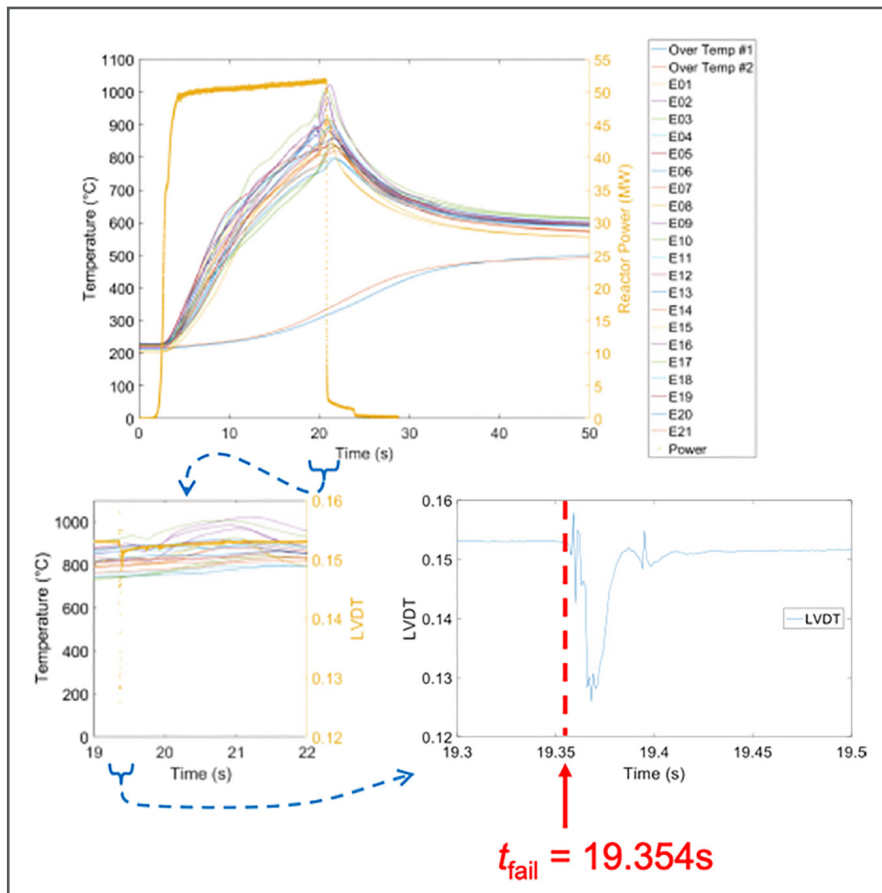


Figure 3. Online data results from the THOR-C-2 experiment. (Top) All heat sink thermocouple data overlaid with reactor power history. (Left) Zoom of thermocouple data overlaid with linear variable differential transformer (LVDT) pressure signal during late state of the experiment showing point of fuel disruption by LVDT signal and showing in thermocouple signal with slight delay. (Right) Zoom of LVDT signal showing clear point of failure where pin pressure is released into the THOR capsule volume

Recently, the THOR-C-2 experiment was irradiated with the objective of failing a fuel pin to demonstrate in-situ diagnostics performance. The THOR-C-3 experiment includes a Na-free annular fuel design to be irradiated by fiscal year end. The annular fuel includes an optical-fiber-coupled infrared pyrometer located in the central hole of the fuel for direct measurement of temperature/power. Fuel performance predictions have been performed to project experiment outcomes and best ensure their success. As-run fuel performance analysis will also be performed and compared with predictions and experiment results.

All specimens will undergo various post-transient characterization over the next year as the THOR-M and THOR-MOXTOP experiments are prepared and irradiated.

Accomplishments:

THOR-C-1: Thermal calorimetry analysis and gamma spectroscopy on the THOR-C-1 specimen. The THOR-C-1 experiment was irradiated in September 2021 with the objective of characterizing the axial reactor-specimen power coupling factor for neutronics model validation. Thermal analysis of the measured temperature histories revealed excellent performance of the capsule design to serve as a calorimeter. Analysis of measured temperatures resulted in a power coupling factor within 6.5% of the calculated value and detailed uncertainty analysis showing 2σ uncertainty of 10%. evaluation of experimental results showed excellent performance of the capsule to provide energy measurement to the test specimen, required for continued testing per reactor safety requirements and to validate modeling predictions of specimen heating rates. Gamma spectroscopy was performed along the axial length of the fuel pin to provide power distribution validation. Results of these measurements is expected shortly to compare with calculated results.

THOR-C-2: The first modern TREAT experiment with precise identification of fuel rod failure time and tracked fuel melting and relocation. THOR-C-2 was irradiated in TREAT in August 2022. The fresh EBR-II driver pin was pressurized and resealed prior to loading in the capsule to mimic high burnup fuel

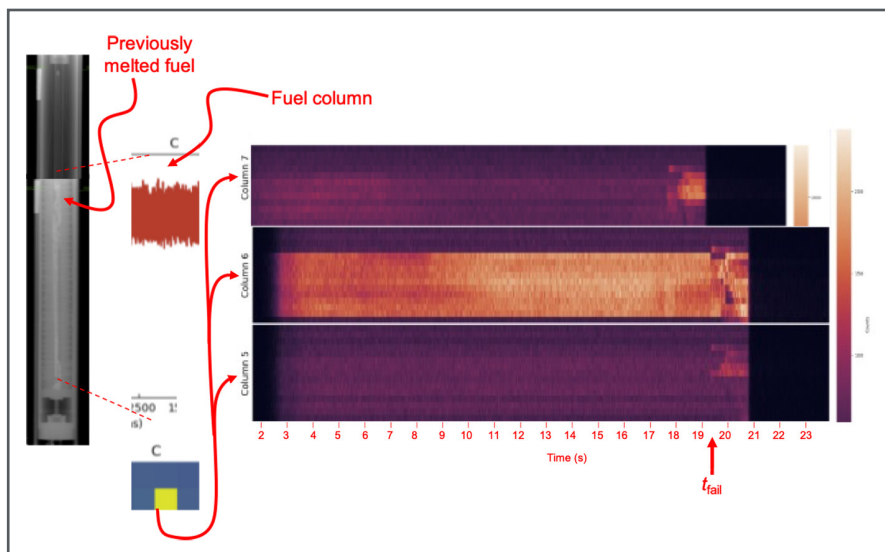


Figure 4. (Left) Post-transient radiography of THOR-C-2 showing clear regions of disrupted fuel. (Middle) Hodoscope view of THOR-C-2 test specimen. (Right) Corresponding waterfall plot of each column during the experiment, again showing the point of failure and the behavior of the fuel during the event

internal pin pressure. The data from the experiment shows excellent performance of the primary in-situ measurements and experiment design goals. Fuel pin failure was detected via the capsule pressure sensor, corroborated by significant fuel motion measured online by the TREAT hodoscope system and seen in post-test radiography at TREAT, and by delayed temperature signals in the heat sink thermocouples. Based on pretest model predictions, the fuel surpassed the liquidus point for the U-10Zr fuel of 1371°C and the fuel-cladding interface surpassed the low U-concentration Fe-U eutectic threshold of approximately 1078°C. X-ray radiography is planned at the TREAT facility. Later, neutron computed tomography will be performed on the capsule using the Neutron Radiography (NRAD) facility. Each test will be analyzed based on as-run data using detailed fuel performance models. Figure 3 and Figure 4 summarize data results collected from THOR-C-2 highlighting

the success of diagnostics to detect and characterize fuel failure behaviors.

THOR-C-3: First experiment on annular, Na-free metallic fuel type with an infrared pyrometer in the fuel center hole. THOR-C-3 is currently assembled ready for irradiation to be completed by the end of September 2022. THOR-C-3 will undergo two distinct experiments, i.e., transients, taking advantage of the in-fuel temperature measurement. The direct fuel temperature measurement will provide further measurement of reactor-specimen energy coupling, using an optical fiber for the first time in fuel in-pile. The first transient will be a sinusoidal power profile to evaluate the ability of the THOR capsule to characterize integral fuel thermal transport. The second transient will push the annular fuel in a severe overpower condition as a direct comparison with THOR-C-4 on a traditional fuel form. This will be the first transient overpower test on annular fuel to observe fuel-cladding mechanical interaction and behavior

of the annulus during the transient.

Completion of design and qualification of THOR capsule remote handling capability for HFEF. This capability builds on the established capability to handle the first TREAT experiment device in HFEF, the Static Environment Rodlet Transient Test Apparatus (SERTTA) capsule, in 2020. The integration of most TREAT designs into HFEF environment is a fundamental need for transient testing nuclear fuels. The engineering team has done a stellar job in meeting project demands and has made significant improvements in the overall experiment integration strategy in HFEF. The increased momentum is encouraging for next steps for other TREAT devices such as the Transient Water Irradiation System in TREAT (TWIST) capsule and the Mk-IIIIR Na loop.

3.4 AR COMPUTATIONAL ANALYSIS

AR Computational Analysis

Principal Investigator: Pavel Medvedev

This effort is an example of how award-winning computational tools are used to advance nuclear fuel technology.

Development of sodium-free metallic fuel design has been postulated as an Advanced Fuel Campaign(AFC) goal. In this regard, one of the design options is annular U10Zr alloy fuel with 75% smeared density and stainless steel cladding. In accomplishing this campaign goal, performance assessment of this design provides basis for down selection decisions, identifies performance benefits or deficiencies, and identifies fuel development and testing needs. Performance assessment includes calculation of fuel temperature, deformation and predicting fuel failures. At Idaho National Laboratory, a fuel performance code BISON has been developed for these purposes by the Nuclear Energy Advance Modeling and Simulation (NEAMS) program. BISON is a winner of the 2021 RD 100 awards.

Project Description:

To fulfill the milestone requirements, the present summary provides a status update for performance assessment of annular metallic fuel using BISON. This effort commenced on 03/02/2022. A generalized plane strain model of annular U10Zr fuel was developed. The model represents a 0.230" diameter fuel pin. Annular fuel slug features 55% smeared density and has an outer diameter of 0.195". In addition to thermoelasticity, the model includes fuel and cladding creep and fuel swelling.

Accomplishments:

Comparison of model results to the metallography of the AFC-3A R4 is shown in Figure 1. Qualitative agreement of the simulation results and the experiment is demonstrated by successful prediction of the fuel annulus closure and apparent absence of cladding strain. Future work will focus on modeling zirconium redistribution and extrapolation of the model to higher burnups and higher smeared densities.

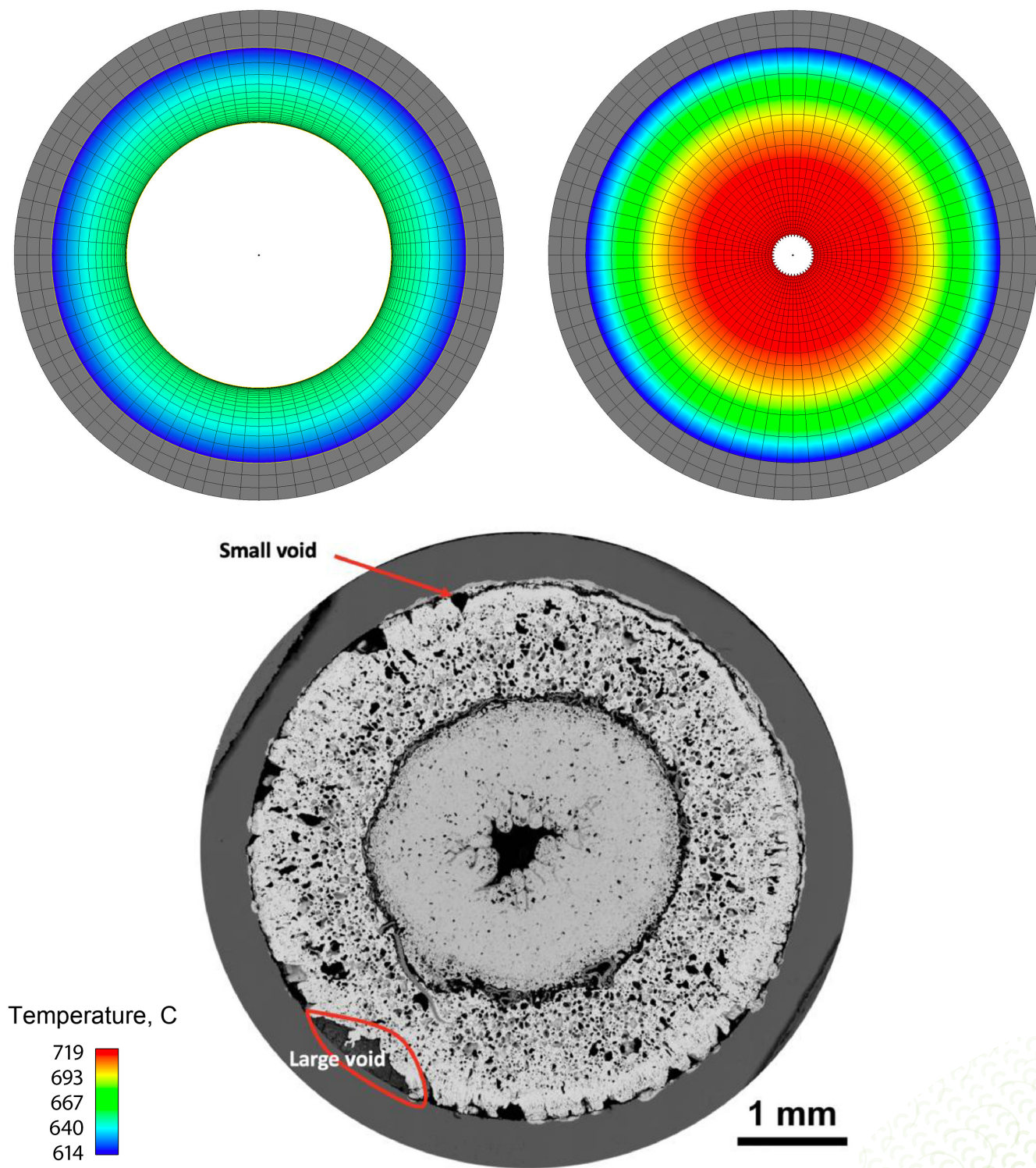


Figure 1. Comparison of model results (BOL-top left, EOL-top right) to the metallography of the AFC-3A R4 (bottom)

3.5 PERFORMANCE ASSESSMENT

Results of a Trade Study on Design and Fabrication Candidates for Sodium Free Metallic Fuel

Principal Investigator: Nicolas Woolstenhulme

Team Members/ Collaborators: Kevan Weaver, Randall Fielding, Douglas Porter, Colby Jensen, Daniel Wachs, Steven Hayes

Metallic fuel systems offer several beneficial features for sodium cooled fast reactors (SFR). The classical metallic fuel design uses an internal liquid sodium bond (between fuel slug and cladding inner diameter) which offers significant thermal fuel performance benefits. However, this design feature has undesirable impacts such as requiring reactive metal handling in fuel fabrication, creating modest detriments to reactor neutronics, and increasing chemical reactivity hazards in shipping/storage scenarios. The latter point is particularly important in SFRs designed for once-through fuel cycles rather than continuous fuel recycle. An engineering trade-off study was undertaken to evaluate fuel design and fabrication process options for developing a so-called sodium-free fuel (SFF) able to eliminate these undesirable features while still retaining many of metallic fuel's most beneficial properties. The primary purpose of this trade study was to rank and prioritize future research tasks in order to accelerate overall development cycle for deploying SFF.

Project Description:

In product development few junctures are as pivotal as design concept selection. An engineering trade study is a structured way of assessing design options and deciding on preferred candidates. Sometimes referred to as "optioneering," a trade study endeavors to reduce subjectivity and avoid classical problems in design decisions such as favoring concepts that just seem better or that are simply preferred by an influential member of the team. In this case a decision matrix method was used where criteria were listed, concepts were generated, and candidates were assessed by expert team ranking. This process was semi-quantitative and required expert judgment, so it was still somewhat subjective, but the various viewpoints expressed and reconciled during the ranking added confidence to the decision reached.

Accomplishments:

The SFF trade study was performed over the course of a few months in 2022 using several team sessions, rather than a single long session, in order to give time in between for team member to generate new concepts. This approach was

Influential Considerations				Category	Functional Need	Importance (Weighting)	Fuel Alloy			Cladding Alloy			Fuel Geometry						FCCI Mitigation			
							U-10Zr	U-10Mo	Low/micro alloy U	F/M steels (HT-9, Gr-92)	Austenitic SST (316, 316L)	ODS	No-Bonded Loose Slag	Annular	Grooved	Split-C*	Particle	Loose	None	Alloy additives	Barrier	
Fabrication	Labor, duration and quantity of processing steps				Baseline	The fuel system must be economic to fabricate in a fresh uranium HALEU licensed fabrication facility	4	3	3	3	3	5	1	4	2	3	2	2	1	5	4	3
	Cap. investment, size/cost of facility and equipment																					
	Utility demand (electricity, natural gas, etc)																					
	Tolerances and repeatability -> yield rate																					
Fabrication	Magnitude and hazard level of waste disposal				Enhanced	The fuel system fabrication processes should be viable for adaptation to include Pu and/or minor actinides	2	3	3	2	3	5	1	3	1	2	2	1	1	5	4	3
	Raw material cost (fuel, cladding, hardware, consumables)																					
	Process continuity and/or batch size (crit. limits)																					
	Ability to recycle/recover scrap																					
Normal Operation	Acceptable range for special process controls				Baseline	The fuel system must perform reliably up to 10% burnup, 100 cladding dpa, and 600 C inner cladding temperature	5	3	2	2	3	3	3	5	4	2	3	1	2	3	3	3
	Ability/difficulty inspecting product characteristics																					
	Isotropy of fuel swelling																					
	Fuel density and swelling free space (mean density)																					
Normal Operation	Cladding mechanical properties evolution				Enhanced	The fuel system should perform reliably up to 20% burnup, 200 cladding dpa, and 650-700 C inner cladding temperature	3	3	2	1	3	2	5	4	3	1	2	1	1	1	2	1
	Strength and defect propensity in end cap weld																					
	Neutron absorption of materials in active core																					
	Cladding/duct atom displacement void swelling/bowing																					
Normal Operation	Constituent redistribution, FCCI, cladding wastage				Enhanced	The fuel system should perform reliably with the addition of plutonium and/or minor actinides	3	3	2	1	3	2	5	4	3	1	2	1	1	1	2	1
	TH performance, heat flux, heat transfer rate																					
	Fuel cladding mechanical interaction																					
	Fission gas release, plenum pressure accumulation																					
Off-Normal Scenarios	Solid fission product driven fuel swelling				Baseline	The fuel system must enable passively safe plant designs (no damage in DBA, no cladding failure in BDBA) for baseline fuel performance requirements	4	3	2	2	3	3	3	5	3	4	3	1	2	3	3	3
	Fission gas driven fuel swelling and pore interconnection																					
	Reactivity change from axial expansion, melt relocation, & sodium expulsion																					
	Fuel thermal conductivity (stored energy) & melting temperature																					
Off-Normal Scenarios	Cladding fuel eutectic penetration				Enhanced	The fuel system must enable passively safe plant designs (no damage in DBA, no cladding failure in BDBA) for opportunity fuel performance requirements	2	4	2	1	3	4	5	5	2	3	2	1	2	1	2	4
	Cladding mechanical properties (resistance to high temperature deformation, fuel thermal expansion, & pressure driven rupture)																					
	Coolant/fuel chemical compatibility, benign behavior in run beyond cladding breach, non-violent behavior in cladding burst																					
	Propensity for fuel particle ejection & channel blockage																					
Back-end	Chemical compatibility of fuel system constituents with air/water				Baseline	The fuel system must be viable for direct disposal in a once-through fuel cycle, i.e. must not create severe chemical interaction hazards in storage, transportation, and disposition or be considered "mixed waste"	3	3	3	3	3	3	1	3	3	3	3	3	3	3	3	3
	Ability to separate constituents and recycle into new fuel pins																					
Baseline Score				48	39	39	48	56	40	64	49	47	44	26	31	56	52	48				
Enhanced Score				25	19	12	24	27	30	31	18	16	17	10	12	18	21	29				
Overall Score				73	58	51	72	83	70	95	67	63	61	36	43	74	73	77				

Figure 1. Design options ranking spreadsheet

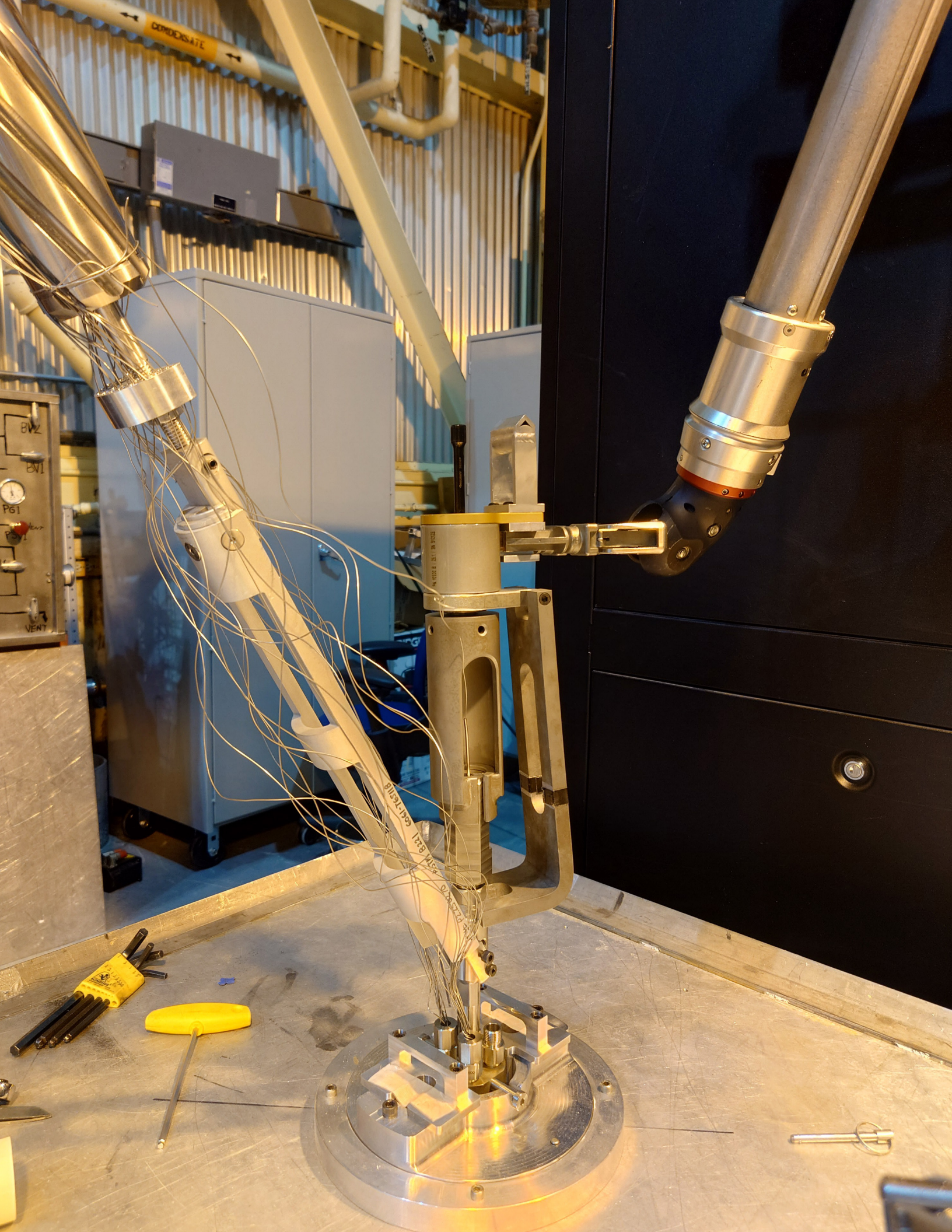
Influential Considerations	Category	Functional Need	Importance (Weighting)	Fuel slug production					FCCI Barrier Application				Slug installation, gap treatment					
				Injection cast into quartz mold	Extrusion w/ heat treat	Continuous casting	Cast into reusable mold	Additive Process	Don't apply barrier	Combined slag barrier production	Deposit barrier onto slug	Deposit barrier in sodium cladding tube	Loose slug fit, sodium bond	Med slug fit, then "sawge down" cladding from	Med slug fit, then "cone down" with external pressure	Med slug fit, then "fill gap" with internal processing		
Labor, duration and quantity of processing steps Cap. investment, size/cost of facility and equipment Utility demand (electricity, natural gas, etc.) Tolerances and repeatability -> yield rate Magnitude and hazard level of waste disposal Raw material cost (fuel, cladding, hardware, consumables) Process continuity and/or batch size (crt. limits) Ability to recycle/recover scrap Acceptable range for special process controls Ability/difficulty inspecting product characteristics	Fabrication	The fuel system must be economic to fabricate in a fresh uranium HALEU licensed fabrication facility	4	2	4	5	3	2	5	4	4	2	3	5	2	2	2	
Enhanced The fuel system fabrication processes should be viable for adaptation to include Pu and/or minor actinides			4	2	3	3	1	5	4	4	2	3	5	1	2	2		
			Baseline The fuel system must perform reliably up to 100% burnup, 100 cladding dips, and 600 C inner cladding temperature	5	4	5	4	3	2	3	3	5	4	2	2			
				Enhanced The fuel system must enable a long reactor operation cycle by between refueling with predictable reactivity evolution using HALEU-based once-through fuel cycles	5	4	5	4	3	2	3	3	5	4	2	2		
					Normal Operation	The fuel system should perform reliably up to 20% burnup, 200 cladding dips, and 700 C inner cladding temperature	3	5	4	5	4	3	1	4	4	5	3	2
Enhanced The fuel system should perform reliably under routine power adjustments (e.g. daily and/or evening cycles)	3	4	5	4			3	1	4	4	5	3	2	2				
	Baseline The fuel system should perform reliably with the addition of plutonium and/or minor actinides	3	5	4			5	4	3	1	4	4	5	3	2	2		
		Enhanced The fuel system must enable passively safe plant designs (no damage in DBA, no cladding failure in BDBA) for baseline fuel performance requirements	4	3			3	3	3	2	3	3	5	4	2	2		
			Off-Normal Scenarios	Cladding mechanical properties (resistance to high temperature deformation, fuel thermal expansion, & pressure driven rupture) Coolant/fuel chemical compatibility, benign behavior in run beyond cladding breach, non-violent behavior in cladding burst Propensity for fuel particle ejection & channel blockage			Enhanced The fuel system must be viable for direct disposal in a once-through fuel cycle, i.e. must not create severe chemical interaction hazards in storage, transportation, and disposition or be considered "mixed waste"	2	3	3	3	3	1	4	4	5	4	2
Baseline The fuel system must perform passively safe plant designs (no damage in DBA, no cladding failure in BDBA) for baseline fuel performance requirements	3	3			3	3		3	2	3	3	5	4	2	2			
	Enhanced The fuel system must enable passively safe plant designs (no damage in DBA, no cladding failure in BDBA) for baseline fuel performance requirements	3			3	3		3	3	2	3	3	5	4	2	2		
		Baseline The fuel system must be viable for direct disposal in a once-through fuel cycle, i.e. must not create severe chemical interaction hazards in storage, transportation, and disposition or be considered "mixed waste"			3	3		3	3	3	3	3	3	5	4	2	2	
					Back-end	Enhanced The fuel system should achieve representing in closed fuel cycles by electromechanical methods		The fuel system must be viable for direct disposal in a once-through fuel cycle, i.e. must not create severe chemical interaction hazards in storage, transportation, and disposition or be considered "mixed waste"	1	3	3	3	3	3	3	3	3	3
Baseline The fuel system must be viable for direct disposal in a once-through fuel cycle, i.e. must not create severe chemical interaction hazards in storage, transportation, and disposition or be considered "mixed waste"	3	3	3	3			3		3	3	3	3	3	3	3	3		
	Enhanced The fuel system must be viable for direct disposal in a once-through fuel cycle, i.e. must not create severe chemical interaction hazards in storage, transportation, and disposition or be considered "mixed waste"	3	3	3			3		3	3	3	3	3	3	3	3	3	
		Baseline The fuel system must be viable for direct disposal in a once-through fuel cycle, i.e. must not create severe chemical interaction hazards in storage, transportation, and disposition or be considered "mixed waste"	3	3			3		3	3	3	3	3	3	3	3	3	3
			Enhanced The fuel system must be viable for direct disposal in a once-through fuel cycle, i.e. must not create severe chemical interaction hazards in storage, transportation, and disposition or be considered "mixed waste"	3			3		3	3	3	3	3	3	3	3	3	3

Figure 2. Fabrication options ranking spreadsheet

This effort is an example of how award-winning computational tools are used to advance nuclear fuel technology.

productive in avoiding meeting fatigue and in spurring new ideas. The main outcome of the study was organized in a spreadsheet where fuel design and fabrication options were ranked relative to impact on fuel fabrication, normal reactor operation, off-normal reactor scenarios, and storage/disposal situations. Within these four categories, each option received two rankings, one each for a “baseline” and an “enhanced” set of performance metrics. The baseline category assumed a once-through uranium-based fuel cycle with state-of-the-art reactor performance needs (10% burnup, 100 dpa cladding, 600C inner cladding temperature). The enhanced category encompassed plutonium and minor actinide bearing fuel designs and strived for more challenging irradiation conditions (20% burnup, 200 dpa cladding, 700C inner cladding temperature). The baseline category was weighted more heavily to help prioritize near term technology options in the grand average ranking, but the baseline and enhanced scores were also tracked discretely to identify candidates which diverge into near-term and long-term development phases.

A full publication is currently under preparation to discuss the findings of this study more fully, but the key findings are summarized here. The highest ranked SFF options identified for the baseline technology would use U-10Zr alloy with additives (e.g., Sn) to mitigate fuel cladding chemical interaction (FCCI), produced in a 75% smear density annular slug geometry by continuous casting, clad in austenitic stainless-steel alloy, and followed by a final step to swage the cladding diameter down slightly to close the slug/cladding gap. The highest ranked SFF options for the enhanced fuel technology would use U-Mo alloy, also produced by continuous casting into an annular geometry, followed by coating/plating with an FCCI barrier (e.g., Zr) on the slug outer diameter, again with a final step to swage the cladding diameter down likely using oxide dispersion strengthened (ODS) steel or advanced ferritic/martensitic if the ODS option cannot tolerate swaging.





CAPABILITY DEVELOPMENT

- 4.1 In-reactor LOCA Testing Capability
- 4.2 Summary of I-Loop Status and Accomplishments
- 4.3 Refabrication of Fuel Rods for Follow-on Testing
- 4.4 Capabilities/Core Functions of R&D Campaign
- 4.5 General

4.1 IN-REACTOR LOCA TESTING CAPABILITY

In-Reactor LOCA Testing Capability

Principal Investigator: Nicolas Woolstenhulme

Team Members/ Collaborators: Colby Jensen, Charlie Folsom, Klint Anderson, Leigh-Ann Astle

TWIST will enable unprecedented in-reactor experiment capabilities in manipulating thermal hydraulic and nuclear heating conditions to simulate LOCA conditions.

The unexpected closure of the Halden Boiling Water Reactor eliminated the only in-reactor Loss of Coolant Accident (LOCA) testing capability available in the western world. This capability would have been key in continued research about Fuel Fragmentation Relocation and Dispersal (FFRD), especially with ongoing efforts to extend the allowable fuel burnup limits in Light Water Reactor (LWR). Thankfully LOCA testing programs, based on hot cell furnace capabilities at Studsvik Sweden and Oak Ridge National Lab, continued to investigate these behaviors alongside various efforts to model LOCA fuel performance and understand its effects. Still, the ability to perform highly representative LOCA testing with nuclear heating was known to be a major capability gap. A few years of engineering studies have investigated options and ultimately produced the design for a new in-reactor LOCA capability in the Transient Reactor Test facility (TREAT). The final design for this device has been completed, out-of-reactor prototype testing is underway, and plans are in place to perform in-reactor commissioning tests next year.

Project Description:

A few design options were investigated via modeling to determine the best path forward for LOCA testing

in TREAT. It was shown that this capability would need to provide adequate heat transfer conditions for a test rod during a brief “part I” power transient in TREAT in order to develop representative pre-LOCA thermomechanical gradients and stored energy in the test rod. Then, this device would need to significantly reduce heat transfer conditions and support a longer “part II” power transient to elevate rod cladding temperature and create balloon, burst, and FFRD behaviors. After comparing options including a flowing water loop, natural circulation capsule, and static water capsule with nucleate boiling, it was found that the latter would provide the most practical approach to supporting part I of the transient. Then, TREAT’s automatic transient control system would be synchronized with a remote actuated valve to allow fast water draining to support part II of the transient. A smaller version of this capsule was conceptualized, but ultimately a larger version termed the Transient Water Irradiation System for TREAT (TWIST) underwent final design and engineering.

An early prototype of the TWIST capsule was constructed and demonstrated the functionality of the remote blowdown valve. As prototype often do, these efforts revealed a glitch with the assembly/

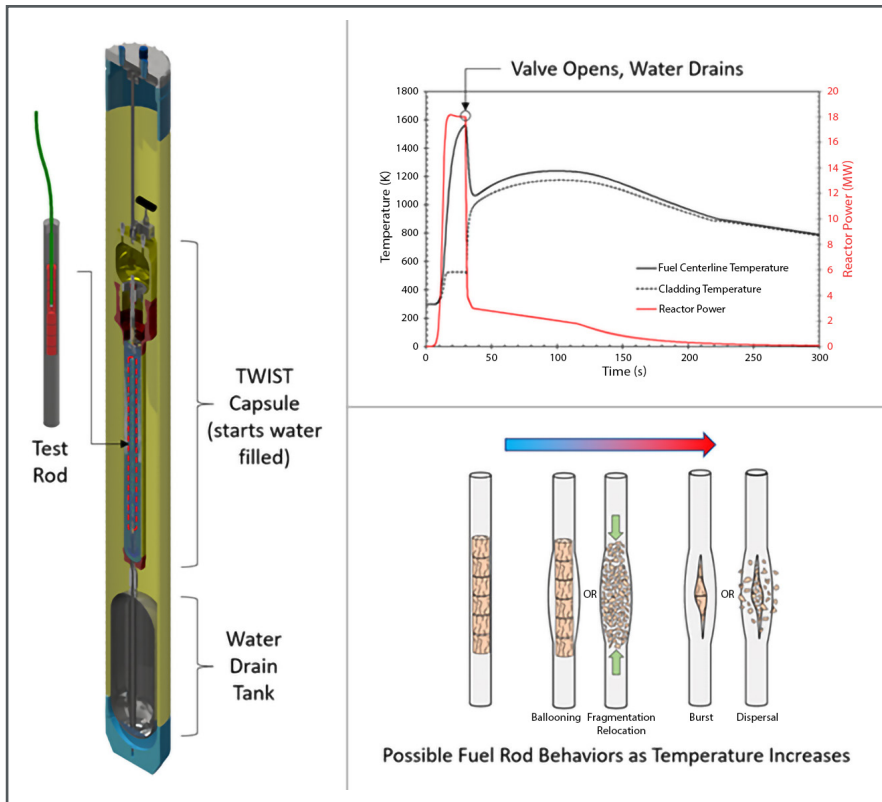


Figure 1. Illustrations of TWIST capability simulating loss of coolant accident conditions on a test rod in TREAT

disassembly sequence which was incorporated into the final in-reactor version of the design. All of the engineering documents and design/safety analysis was completed for the TWIST capsule to encompass the conditions needed for a series of fresh fuel commissioning test rods. These commissioning tests, which are planned to begin next year, encompass some aggressive conditions and thus this safety analysis package is expected to envelope many of the conditions needed for previously irradiated high burnup tests that will follow. The first-generation TWIST instrumentation and analysis package is focused on simulating and measuring behaviors

relevant for FFRD. The capsule is designed with modular adaptability to allow cost effective modifications as needed in the future. A few conceptual-level design efforts are now underway, primarily through student-led senior design projects, to determine the best path for “bolt-on” modifications to TWIST. These adaptations will help simulate other conditions and behaviors of interest such as pre-blowdown forced convection with a small motor/impeller device, post-blowdown steam composition control, and alternate instrumentation packages focused on transient fission gas release.

4.2 SUMMARY OF I-LOOP STATUS AND ACCOMPLISHMENTS

Summary of I-Loop Status and Accomplishments

Principal Investigators: Nate Oldham

Team Members/ Collaborators: Kendell Horman, Vince Tonc, Josh Tonks, Kelly Ellis, Carlos Estrada-Perez, Brian Durtschi, Cody Race, Thomas Berti, R Dale Kepler, and Darrin Steffler

The I-Loop will expand fuel testing capacity, address LWR fuel irradiation testing capability gaps left by the HBWR closure and enhance testing capabilities including ramp testing.

Expand access and capability to the Advanced Test Reactor (ATR) Medium-I position with a flowing water loop, allowing testing of fuels and materials in prototypic light water reactor (LWR) conditions.

Project Description:

The closure of the Halden Boiling Water Reactor (HBWR) and growing demand for extending LWR fuel performance limits, has created urgency to find a testing solution to support near-term fuel testing needs. This need comes at a time when industry, via Electric Power Research Institute (EPRI), and the Department of Energy (DOE), via the Accident Tolerant Fuels (ATF) Program, are pushing for performance and capability increases for new fuels. The I-Loop project aims to fill the gap created by HBWR's closure and provide a similar capability at ATR, by installing a flowing water loop in one Medium-I position and providing access to the other Medium-I positions for future experiments. In order to provide better access to the I-positions of ATR, a new Top Head Closure Plate (Mark II) has been installed, expanding the capabilities of the ATR for continued fuel and materials testing. To support the flowing water loop, the refurbishment of the 1A cubicle will be required including new pumps, piping, heat exchangers,

and other equipment. In order to provide the neutronics to approximate prototypic LWR heating rates, nuclear grade Zr-2.5Nb will be used for the experiment tubes. The improvements will enable advanced fuel qualification to continue at the Idaho National Laboratory (INL) and support the industry and DOE's desire for these capabilities in the United States, support the continued safe use of existing LWR reactors, and provide for future fuel testing for next generation reactors.

Accomplishments:

After a brief funding hiatus, the I-Loop project restarted in March 2022. The project team replanned the entire work baseline structure to account for newly discovered scope and additional cost due to supply chain uncertainty. The project expected completion of an operational I-Loop in ATR is early 2026. The design team was reassembled with the addition of ATR project engineers. ATR project engineering is fresh off of an extensive ATR project that occurs every couple of decades called ATR Core Internal Changeout (CIC). The I-Loop project is excited to have the expertise of this talented design group. The success of the I-Loop project requires a team with experience in modifying a complex test reactor such as ATR.

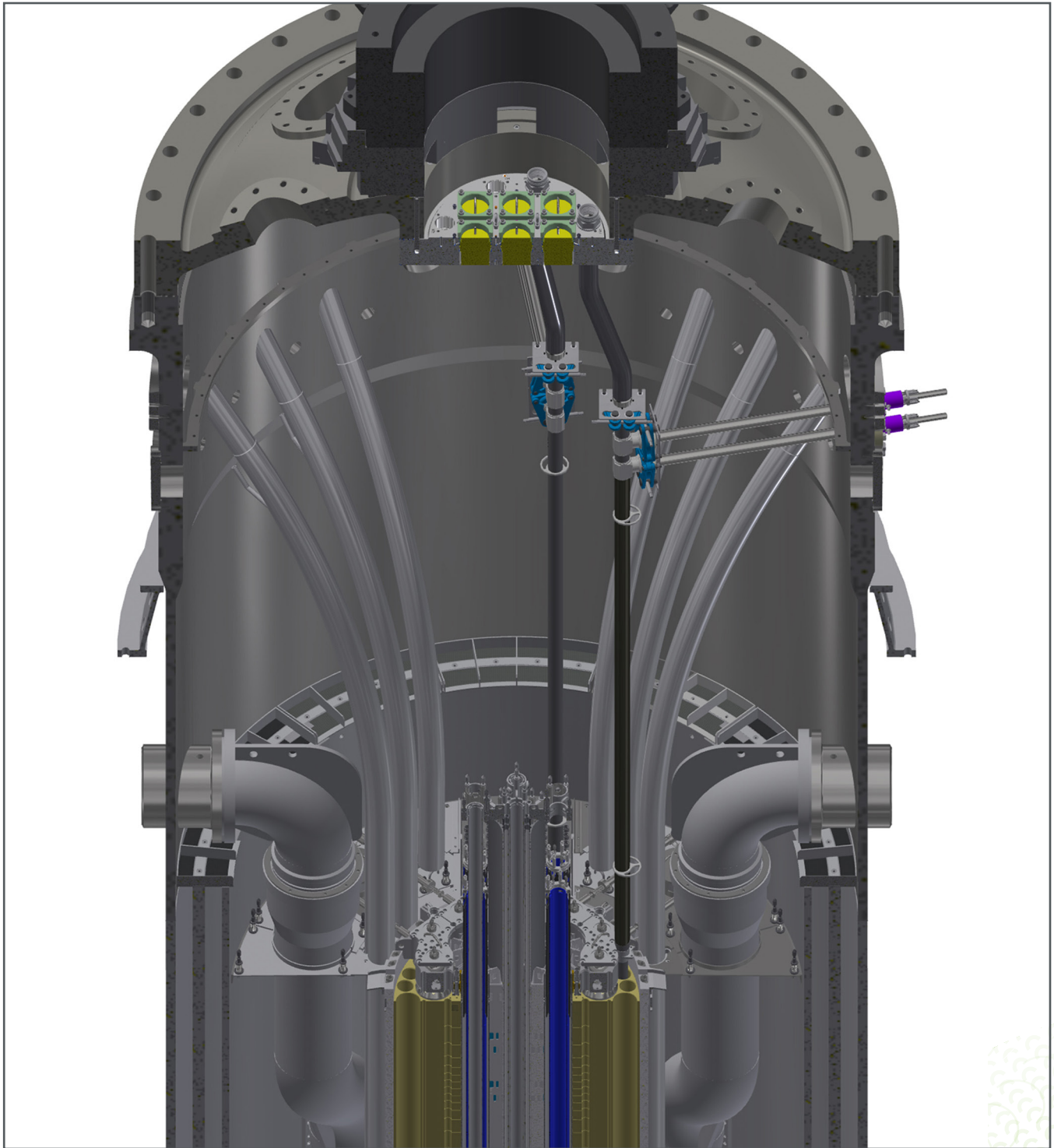


Figure 1. 3D model of i-loop tube with quick-connect flanges

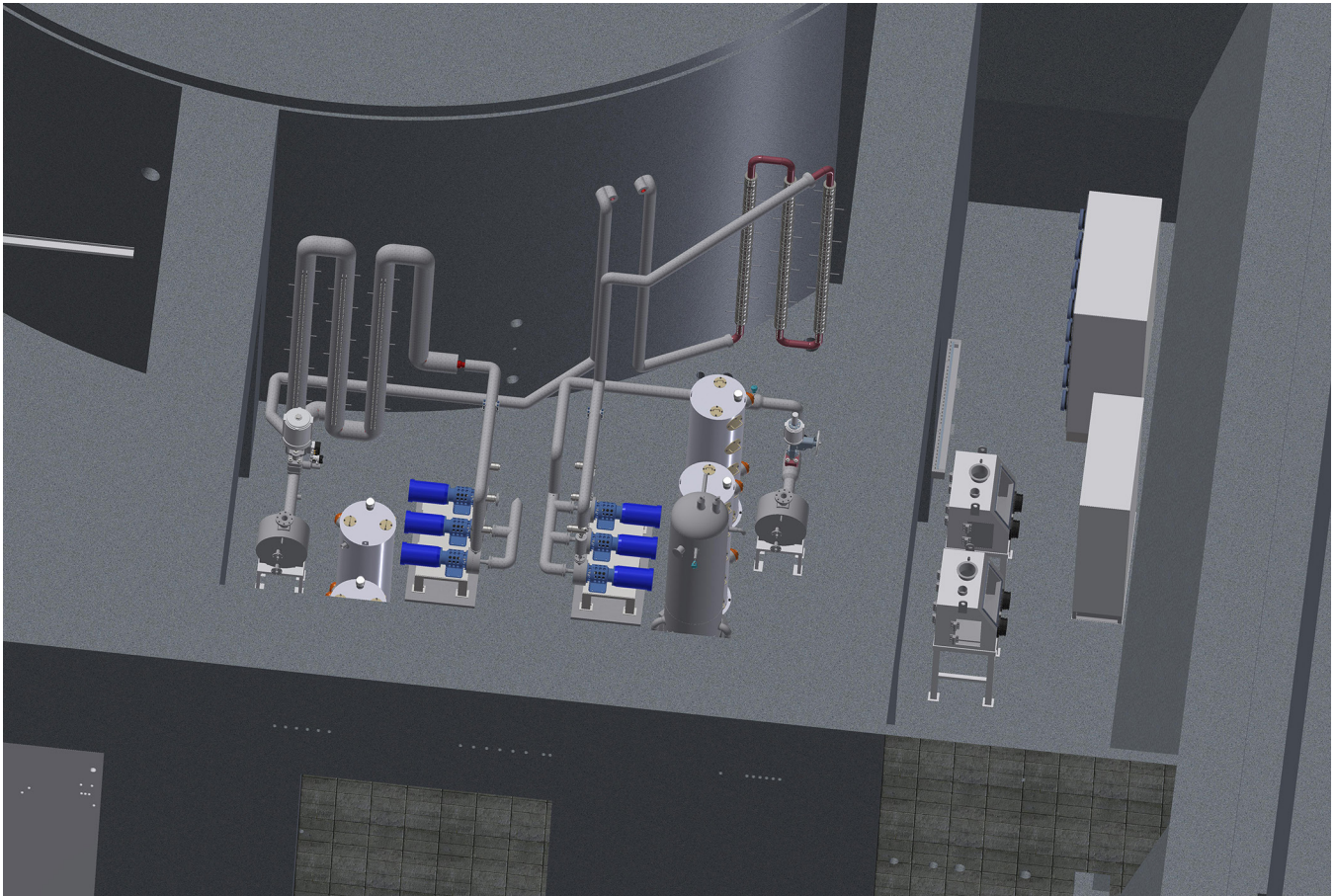


Figure 2. I-loop system equipment layout in 1A primary and secondary cubicle

The I-Loop project is large in scope which requires many sub-teams working on discrete tasks. The main project areas are as follows: (1) I-Loop Tube, (2) I-Loop System, and (3) Transfer Shield Plate.

1. The I-Loop Tube serves as the primary component within the ATR vessel (I-Loop Figure 1). Its purpose is to contain the experiment in a separate environment at prototypic LWR fluid conditions. This includes the ability to perform two-phase flow similar to a boiling water reactor (BWR). The I-Loop Tube has completed the conceptual design and moved to the

preliminary design phase. A finite element analysis was performed to identify the high stress areas. Those areas were modified to add additional thickness and supports through iterative changes. The design now passes an ASME Boiler and Pressure Vessel Code Section III design criteria. Additionally, the team has been in contact with vendors/fabricators to determine optional features to ensure a successful fabrication.

2. The I-Loop System is all the equipment outside of the reactor vessel, e.g., pumps, heat exchangers, valves, and piping (I-Loop

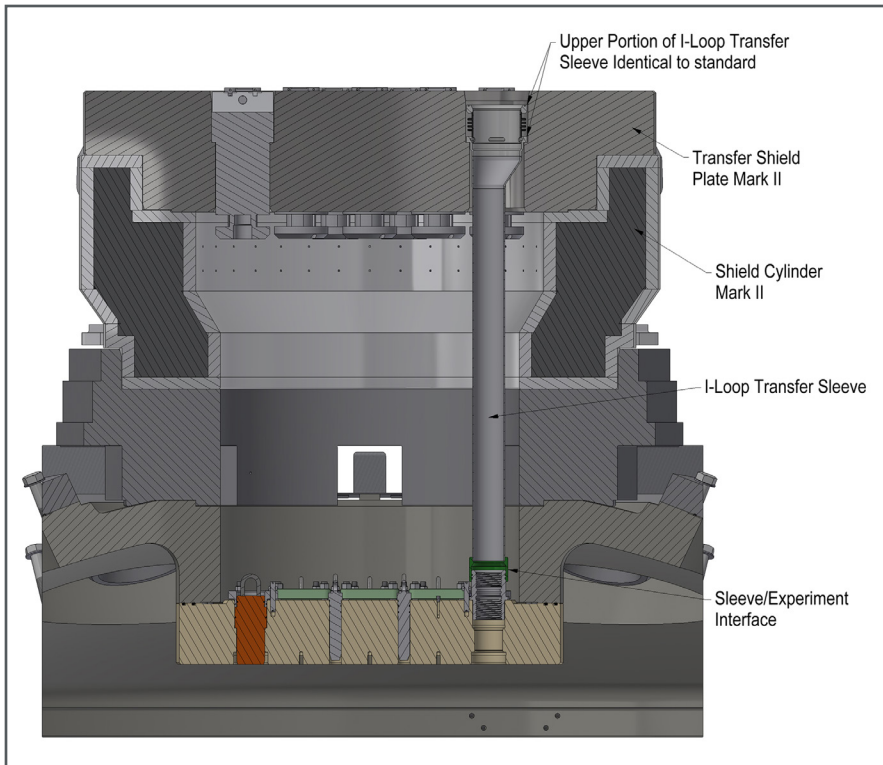


Figure 3. Transfer Shield Plate – Mark II Conceptual Design

Figure 2). This system includes a series of sub-systems such as loop makeup, ion exchange/filtrations, sampling, and loop chemistry. A team of experienced ATR project engineers are leading this effort. A major accomplishment has been evaluating primary coolant pump options and selection of the optimal pump for the I-Loop. This evaluation has resulted in a \$2.5 million cost savings to the project compared to other ATR loops. The team has also designed a component to maintain loop pressure known as a pressurizer. This new pressurizer design is unique to ATR because it is designed to modern seismic design criteria which allows the I-Loop to be the safest loop in the ATR facility.

- I-Loop is well positioned to begin several long-lead procurements e.g., pumps, pressurizers, control system, purification systems, and Helium-3.
3. In FY 2021, the I-Loop project completed a modification to the ATR reactor vessel pressure boundary with a new Top Head Closure Plate. The main design benefit is the addition of eight new penetrations that can be utilized for irradiation testing. Access to these new penetrations requires modification to the shielding known as the Transfer Shield Plate. A conceptual design is completed for the Transfer Shield Plate – Mark II (I-Loop Figure 3).

4.3 REFABRICATION OF FUEL RODS FOR FOLLOW-ON TESTING

Refabrication of Fuel Rods for Follow-On Testing

Principal Investigator: Jason Schulthess

Team Members/ Collaborators: Justin Yarrington, Spencer Parker, Joe Palmer, James Zillinger, Clayton Turner, Connor Woolum, Mark Cole

Advanced refabrication capability will support using instrumented fuel rodlets in follow on experiments.

Irradiated fuel rod refabrication is a crucial enabling capability that bridges between base reactor irradiation and subsequent experimentation and/or re-irradiation. It is key to performing meaningful research and development (R&D) on fuels with any level of burnup, especially at the Transient Reactor Test (TREAT) Facility and opens the door to R&D for materials tested in commercial nuclear power plants. Refabrication allows access to fuel at any point in its lifetime, allowing opportunity to apply instrumentation and perform experiments to measure performance under a variety of specified conditions. Secondly, the ability to repackage previously irradiated fuel into experiment vehicles is an enabling capability that ensures experiments are instrumented and contain desired boundary conditions for experiment objectives. Measurements on high burnup fuels are impractical, if not impossible, without refabrication and experiment preparation capability.

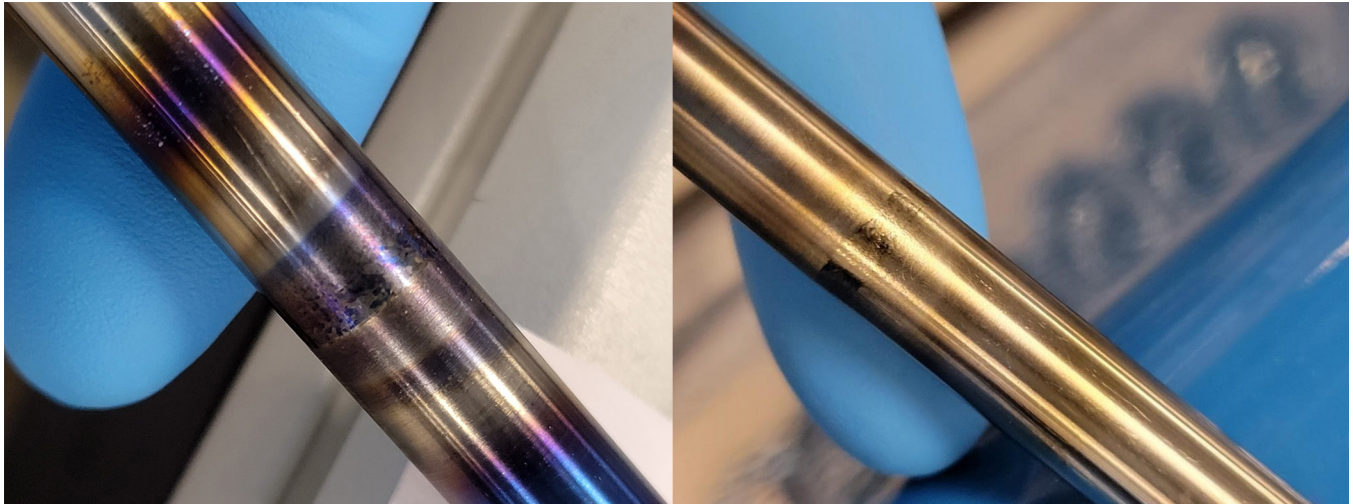
Project Description

Basic refabrication capability was established in FY2021 and included the ability to section rods, defuel the ends to create space for new end caps, weld new end caps in place, and finally seal weld under pressure and leak check. Objectives in FY2022 included evaluation of advanced refabrication

capability and benchmarking against capabilities that had been previously available at the Halden reactor project. Specific objectives included performing evaluations of the Halden drilling and welding modulus using surrogate materials, evaluating the potential engineering needs and facility requirements for establishing a cryogenically cooled fuel drilling system in a hot cell environment, evaluating alternative fuel drilling methods that do not require cryogenically cooling the fuel, and options for remotely welding/attaching thermocouples to the outer surface of fuel cladding both in the remote environment and in a manner compatible with the current design of the transient water irradiation system for TREAT (TWIST) irradiation device. These advanced refabrication capabilities are necessary to support experiments using highly instrumented rodlets.

Accomplishments

Halden had developed separate defueling, fuel drilling and welding modules over the course of thirty+ years of refabrication development. To rapidly gain experience with refabrication, Idaho National Laboratory (INL) procured a defueling, fuel drilling and welding module from Halden. The Halden fuel drilling module utilizes a cryogenic system to stabilize the fuel during drilling operations, while the welding



system uses a large weld chamber with a moveable Tungsten Inert Gas welding tip to allow for welding at nearly any location within the weld chamber. INL received these systems and completed set up and initial functional testing during FY2022. Initial experiential trials with these systems were performed using surrogate materials as they are currently installed in a non-radiological laboratory. These trials are providing a firm basis for comparison to developing an advanced drilling and welding system for use in a hot cell at INL. Figure 1 shows successful welding trials performed using the Halden welding module.

To support further development of welding parameters and fixtures necessary for advanced refabrication and instrumentation including welding thermocouples to the cladding surface of a previously

irradiated fuel pin, a duplicate of the remote circumferential weld system was fabricated and installed into the Advanced Fuel Fabrication Facility at INL's Materials and Fuels Complex (MFC).

A preliminary engineering evaluation was conducted to establish functions, requirements, and limitations for safety and facility infrastructure for installation of a Halden type cryogenic drilling system into a generic hotcell environment. This was conducted to help establish design inputs, and preliminary cost estimates for future use and decision making. The evaluation proved quite useful in establishing requirements for the system to minimize potential impacts to hotcell facility safety basis. For example, it was established that cryogenic liquids would be delivered through a feed through rather than via bottles transferred into the

Figure 1. Successful circumferential welds joining non-fueled zirconium cladding tubes using the Halden welding module. In the left image, a system leak allowed oxygen into the chamber resulting in the discoloration. In the right image, the weld was made after correction of the leak, and successful purge of oxygen

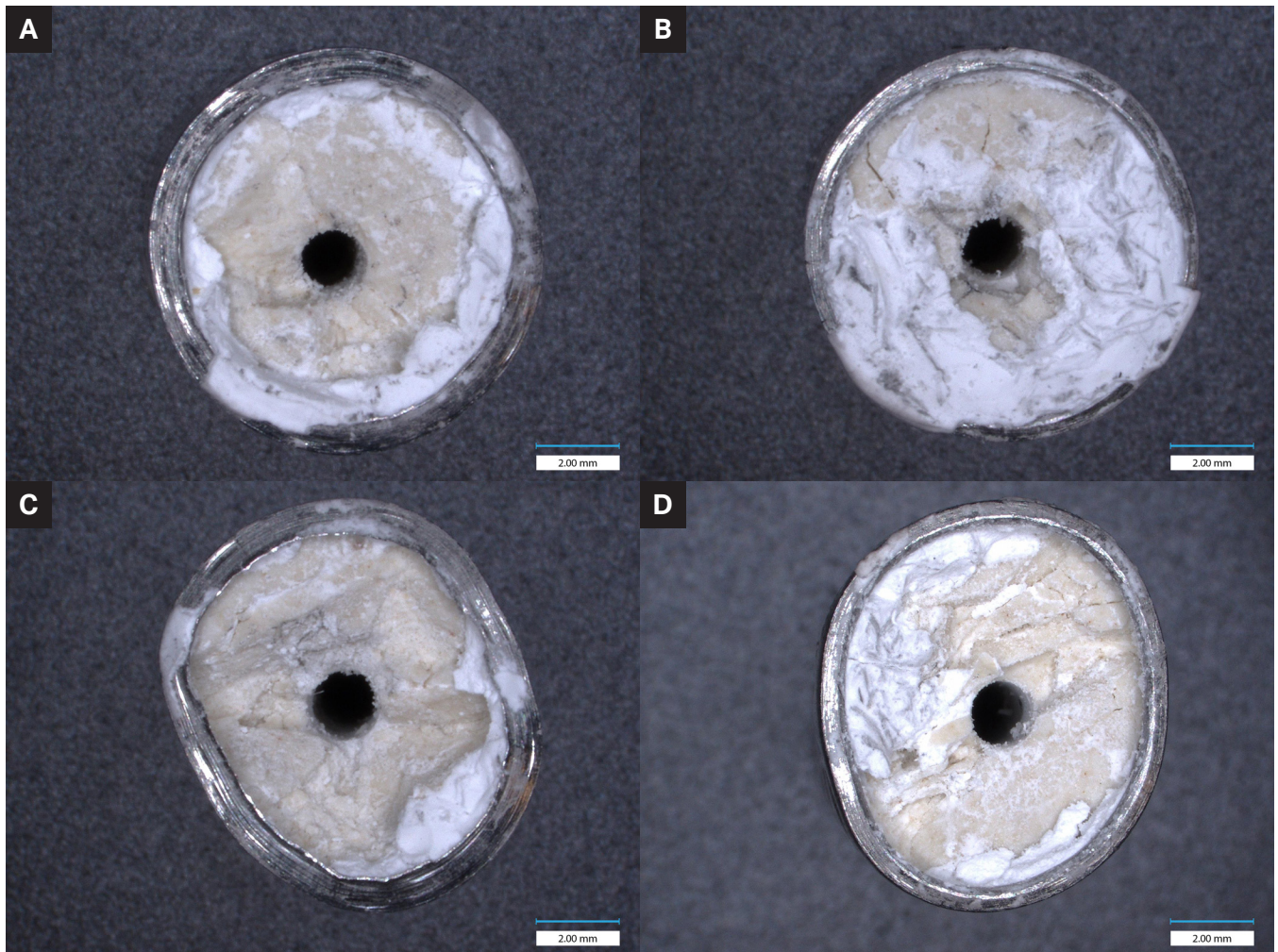


Figure 2. Top and bottom surfaces of sample 15 (A&B, respectively) and sample 16 (C&D, respectively) post-drilling. Both samples were two pellet stacks glued inside of stainless steel tubing. Sample 15 was only moderately crushed, while sample 16 was heavily crushed, as noted by its visible deformation. Both samples were re-glued after crushing activities to re-bond the outer pellet surface with the cladding tube

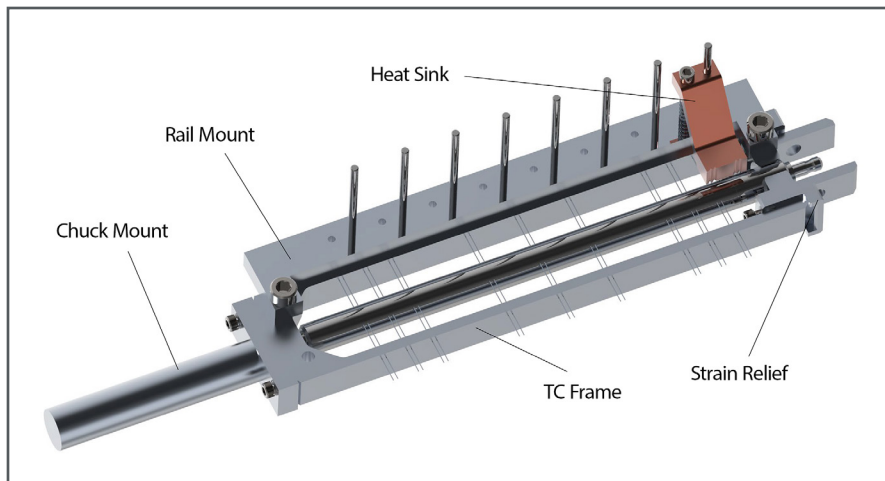


Figure 3. Rendering of the prototype fixture concept to weld thermocouples to the surface of rodlet cladding

cell, to mitigate the risk of a depressurization event within the cell.

As a potential alternative to the methods developed by Halden to cryogenically stabilize the fuel for drilling operations, INL in FY2021 began developing a methodology to drill centerline holes without cryogenic stabilization. Originally this methodology was developed and is still in use today by the Commissariat à l'énergie atomique (CEA) in France. In FY2021, INL successfully developed a method to drill centerline holes in fresh sintered UO_2 fuel pellets. In FY2022, efforts were made to adapt this methodology to drilling fresh pre-cracked pellets in an attempt to simulate cracked irradiated fuel. Optimization was performed using cordierite as a surrogate fuel pellet, which was bonded to a tube, and then pre-cracked in a vice to a pre-determined force. Optimization of the method included variation of the feedrates,

spindle speeds, and drilling bit profile. Holes were successfully drilled in a two-pellet stack with the diameter of the hole being approximately 0.063" (See Figure 2).

A conceptual design of a modular fixture to enable welding of thermocouples to the cladding surface was completed. This is a critical step due to the difficulty of handling loose wires remotely in the hotcell environment. The conceptual fixture, shown in Figure 3. This design allows for the wires to be pre-placed in the holder prior to entry to the hotcell and is also compatible with the remote circumferential weld system previously installed. This design incorporates a heat sink to minimize weld affected area and enables accurate angular positioning of the thermocouple-rodlet interface relative to the tungsten electrode. A prototype is currently being fabricated and testing will begin in FY2023.

4.4 CAPABILITIES/CORE FUNCTIONS OF R&D CAMPAIGN

Final Design of the LOCA Test Commissioning Series in TREAT

Principal Investigators: Klint Anderson

Team Members/ Collaborators: Charles Folsom, Clinton Wilson, Changhu Xing, Kelly Ellis, Robert Armstrong, Leigh Ann Astle, Nicolas Woolstenhulme, Colby Jensen

The completed design of the LOCA test device will allow the U.S. to perform critical safety testing for studying and advancing LWR fuel for the U.S. nuclear energy fleet.

The unexpected closure of the Halden Boiling Water Reactor (HBWR) eliminated the only in-reactor Loss of Coolant Accident (LOCA) testing capability available in the western world. This capability would have been key in continued research about Fuel Fragmentation Relocation and Dispersal (FFRD). To help eliminate this major capability gap, and ultimately support the light water reactor (LWR) Industry's goal for achieving higher burnups and evaluating new fuel design at various development stages, a LOCA testing device is critical. After a few years of engineering studies, a new in-reactor LOCA testing device for the Transient Reactor Test facility (TREAT) was developed. The final design for this device has been completed, out-of-reactor prototype testing is underway, and plans are in place to perform in-reactor commissioning tests next year.

Project Description:

The Transient Water Irradiation System in TREAT (TWIST) capsule provides a controlled environment in which a blow-down event can be simulated by actuating a valve

to release water from the upper capsule containing a fuel specimen into an expansion tank below (Figure 1). The approach will fill the in-pile LOCA testing gap left by HBWR and adds capability to study stored-energy heating effects resulting in temperature ramp rate effects, never evaluated before on irradiated LWR fuels. These behaviors are expected to play important roles in FFRD, the primary challenge to extending the regulatory burnup limit beyond 62 GWd/t. The TWIST capsule design provides a state-of-the-art instrumentation package to collect relevant time-dependent data for post-test analysis of the experiment. Figures 2 and 3 show the instrumentation package included in the commissioning test design including options to measure either the fuel centerline temperature or rodlet pressure. The design accommodates rodlets with fueled lengths ranging from 25 to 50 cm. An out-of-reactor prototype was designed as a part of this same effort and is being utilized to inform fabrication, assembly, and testing conditions for future LOCA tests in TWIST (Figure 4). Final design of the

TWIST capsule and its associated commissioning tests was completed this year. In-reactor testing of the commissioning series is planned to start next year. Testing of high burnup fuels is expected to begin in the year thereafter. Also, the TWIST device is planned to be used for reactivity-initiated accident experiments for the High burnup Experiments for Reactivity initiated Accidents (HERA) project.

Accomplishments:

The completion of the final design for the TWIST device and associated commissioning tests officially provides the US with a testing capability for simulated LOCA events. It also provides needed new capability to test larger fuel segments than TREAT capsules used to date since restart. A commissioning LOCA test plan using fresh fuel has been carefully developed to efficiently demonstrate and qualify the TWIST system. Key data objectives will be evaluation of in-situ instrumentation and the entire extensive experimental infrastructure required to execute TWIST tests. The final design package of the TWIST device includes completed full mechanical design and associated

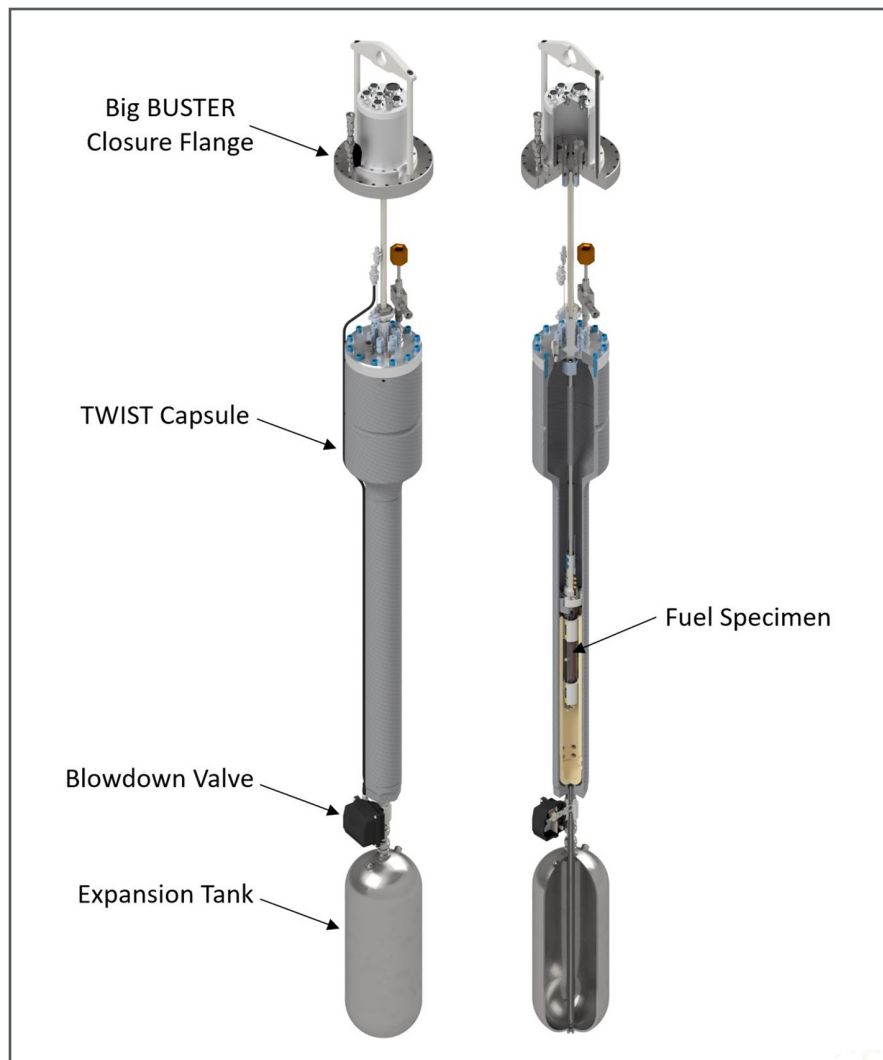
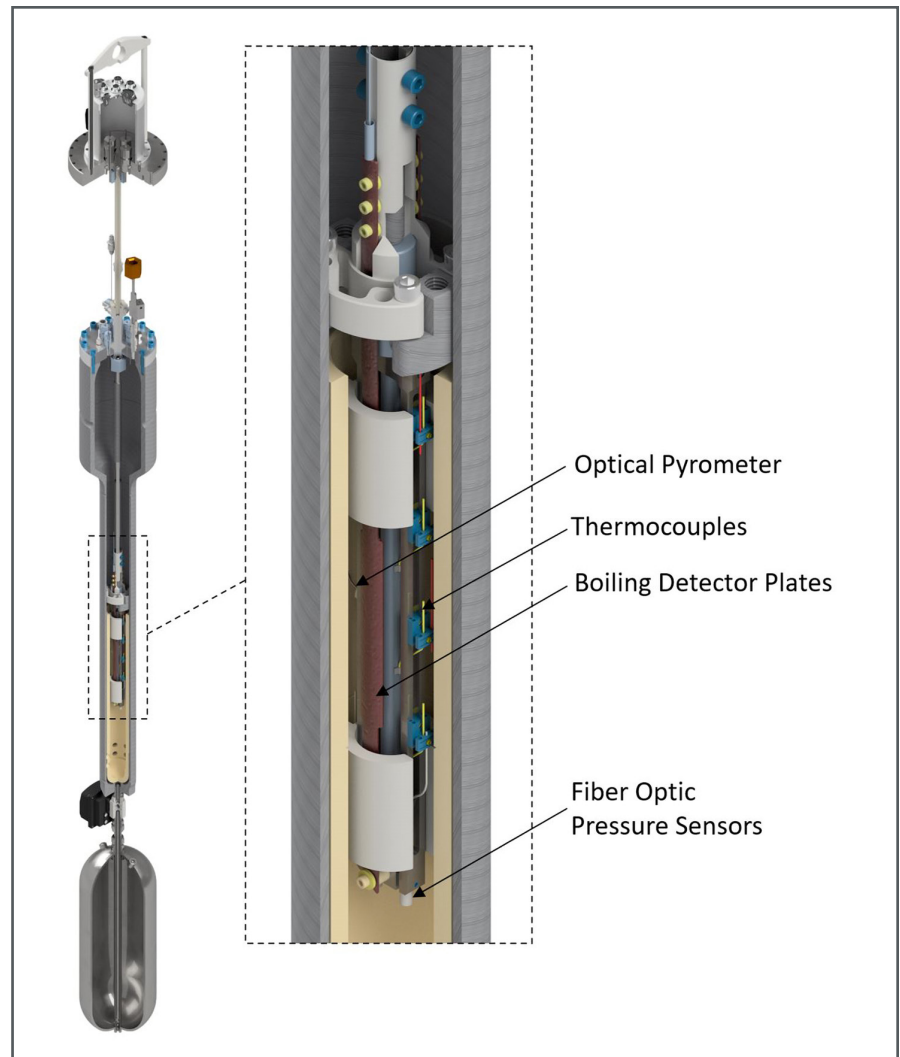


Figure 1. TWIST capsule rendering

Figure 2. TWIST instrumentation



drawings, comprehensive neutronic, heat transfer, thermal-hydraulic, and structural analysis of the test device to meet all associated testing requirements. This milestone represents the culmination of several years of work by a large multidisciplinary and multifacility team. The renewed in-pile LOCA capability in the world

and unique blow-down design in TREAT is expected to fill a critical gap in testing for both extended burnup and new fuel designs. To date, the out-of-reactor demonstration of the LOCA device has provided valuable lessons learned regarding fabrication and assembly of the TWIST capsule.

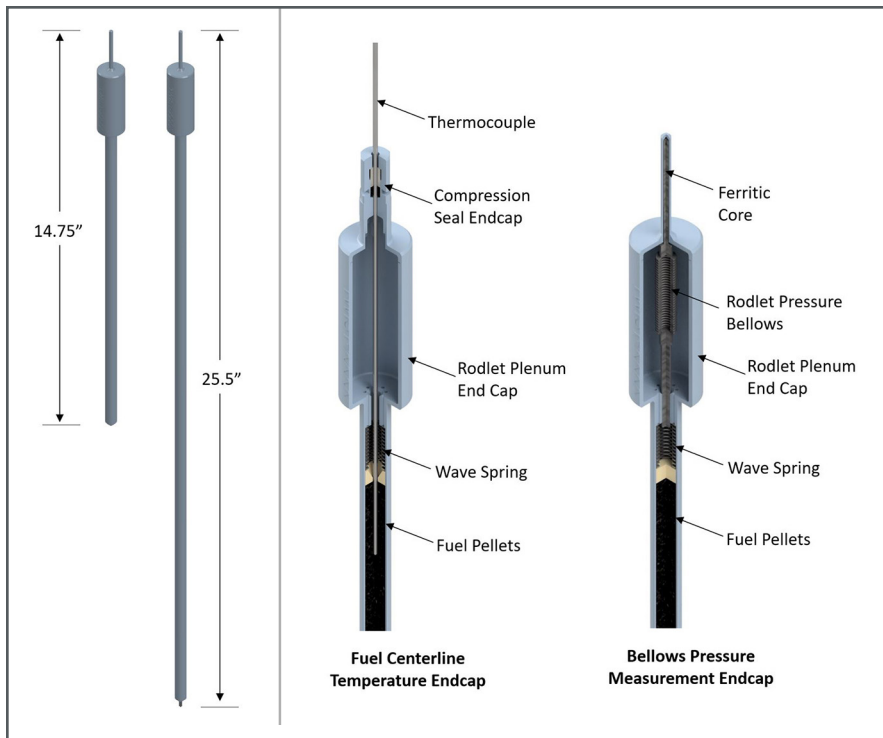


Figure 3. TWIST specimen designs



Figure 4. TWIST prototype test rig

Remote Handling and Assembly of the THOR Capsule for Transient Testing Irradiated Fast Reactor Fuels

Principal Investigators: Philip Petersen

Team Members/ Collaborators: Philip Petersen, Jordan Argyle, Justin Yarrington, Clayton Turner, James Chandler, John Stinger, Chase Christen, Klint Anderson, JD Kelly, Jason Schulthess

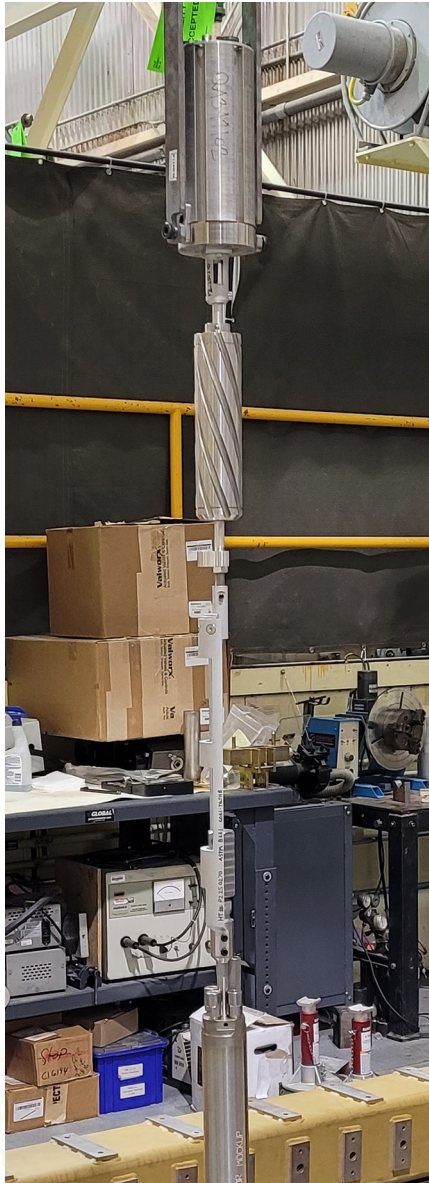


Figure 1. THOR capsule mock-up hanging from electro-mechanical manipulator (EM) showing strain relief fixture and new EM grapple

The Temperature Heat Sink Overpower Response-Metallic (THOR-M) Capsule is loaded with pre-irradiated Experimental Breeder Reactor (EBR-II) pins and due to the pre-irradiated nature of the fuel this loading process must be accomplished within the Hot Fuel Examination Facility (HFEF) hot-cell environment. Remote handling tools, fixturing and processes have been developed to accomplish the complicated handling, loading, bonding, and sealing process in HFEF prior to being irradiated in Transient Reactor Test Facility (TREAT). The effort has involved a team of remote engineers, Post-irradiation examination (PIE) researchers, experiment engineers, project support staff and operators. More than 10 separate pieces of equipment had to be developed, analyzed, and fabricated to accomplish the loading process to have the capsule prepared for irradiation.

Project Description:

Our objectives were to understand the experiment hardware and desired test outcomes and use those to develop a process to load and unload the fuel in HFEF. Once a process flow chart was developed, the tooling, fixtures or modifications needed to accomplish each step of the process were identified. From there each individual piece

of equipment could be designed, drafted, fabricated, and qualified for in-cell use. Adding to the design challenge each piece of equipment incorporated flexibility to function with, or with only slight modification, function with future THOR capsules variations. This equipment development undergirds the critical testing done at the TREAT facility. No pre-irradiated capsules can be loaded outside of HFEF and downstream; no PIE of these experiments can be performed outside HFEF making it a critical link in the completion of the TREAT tests. We are focusing on THOR-M but also are using it as a springboard to equip HFEF, programmatically and physically, to handle TREAT experiment capsule on a regular basis. The data produced by the THOR campaign from TREAT and HFEF is highly valuable to developing advanced fuels for the next generation of reactors that are accident-tolerant, reliable, and economical for future use.

Accomplishments:

The development of this equipment required a coordinated effort from three primary groups – Material Fuels Complex (MFC's) Nuclear Remote Systems Group, MFC's Advanced Characterization and PIE, and the Experiment Design Group. The development of the assembly

process required input from all three groups so that the experiment objectives, PIE objectives, and handling could all be accomplished simultaneously. The initial development of the process resulted in PLN-6325, a plan document. This document served as a convenient place to collect important assembly information. It was written to be a living document that would be revised as the assembly process changed and progressed. This document also served as a foundation for HFEF-LI-0214, the actual work control document for performing the assembly. Progressing from this, equipment was identified, and the engineering process could be initiated. Functional and Operational Requirements (FOR)-662, was then written to formally document all the engineering requirements needed. This document is the primary document used in the design process and all of the engineering process builds on this, so it was a major pillar to put in place. With these foundational documents in place, design and development of the equipment could begin. Preliminary designs were reviewed on 11/17/2021, three months ahead of schedule and just four months after completion of the process plan (PLN-6325), completing a M2 milestone due to the direct efforts of the nuclear remote systems design group. Drafting then commenced with the mechanical drafting done solely by Cory Conway from MFC's drafting department with collectively over 50 drawings. Fabrication followed with a huge effort from MFC's machine shop. Fabrication started in

the height of COVID complications, staffing issues and supply chain shortages. These complications were expertly handled by Derek Sommer, MFC's machine shop supervisor. The project still being on schedule is direct evidence of his leadership and the craftsmanship of the MFC machinists. The completed equipment then started its equipment qualification process (EQP) in MFC's mock-up area. Many important changes and additions resulted from mock-up testing with the operators. Some equipment was found unnecessary, an additional stand was developed, and a variety of supplementary hand tools were procured and modified for use with master slave manipulators (MSMs) to further aid the operators. All the developed equipment was successfully demonstrated and functioned as intended, during Phase I. Currently the mechanical portion of Phase I and II of the EQP have been completed and just the electrical/instrumentation and controls (I&C) portion remains. By completing Phase II, all the equipment not only functioned as intended, but each step of the THOR assembly was accomplished with the equipment remotely. This shows that in theory assembly of the THOR capsule in HFEF can be accomplished with the current equipment. The final phase (Phase III) of the EQP (actual in-cell practice) and closeout of the engineering process is all that remains before all the needed equipment can be implemented in-cell and the first THOR-M capsule can be assembled.

The THOR Capsule remote handling equipment has made it possible for pre-irradiated transient test capsule assembly, and disassembly PIE, leading the way to further capsule handling capabilities in HFEF to support advanced fuels development.



Figure 2. THOR capsule top cap torque multiplier used to seal the capsule at 120ft-lbf

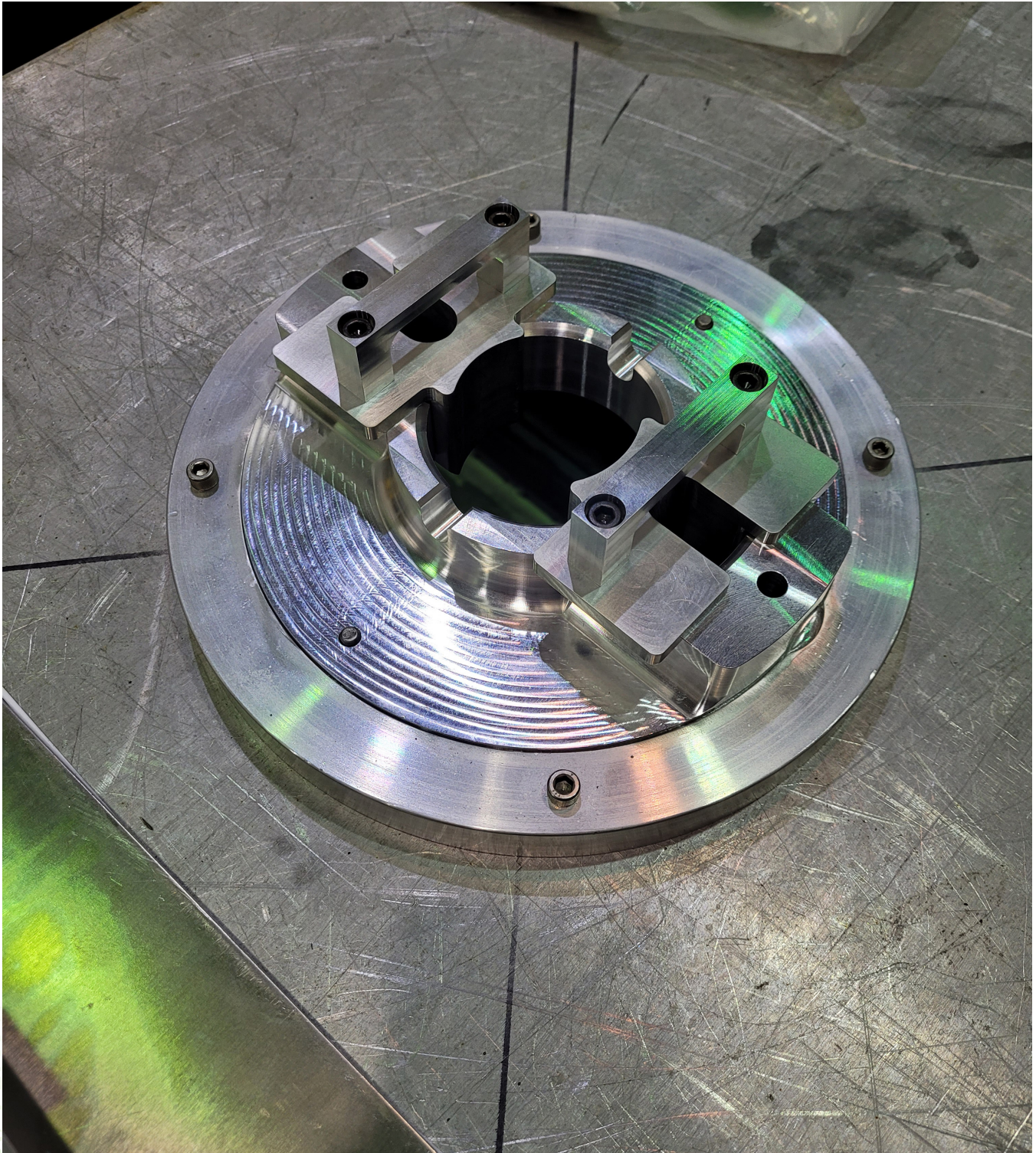


Figure 3. THOR 5D table insert used to hold the capsule at the 5D worktable while it is loaded and sealed

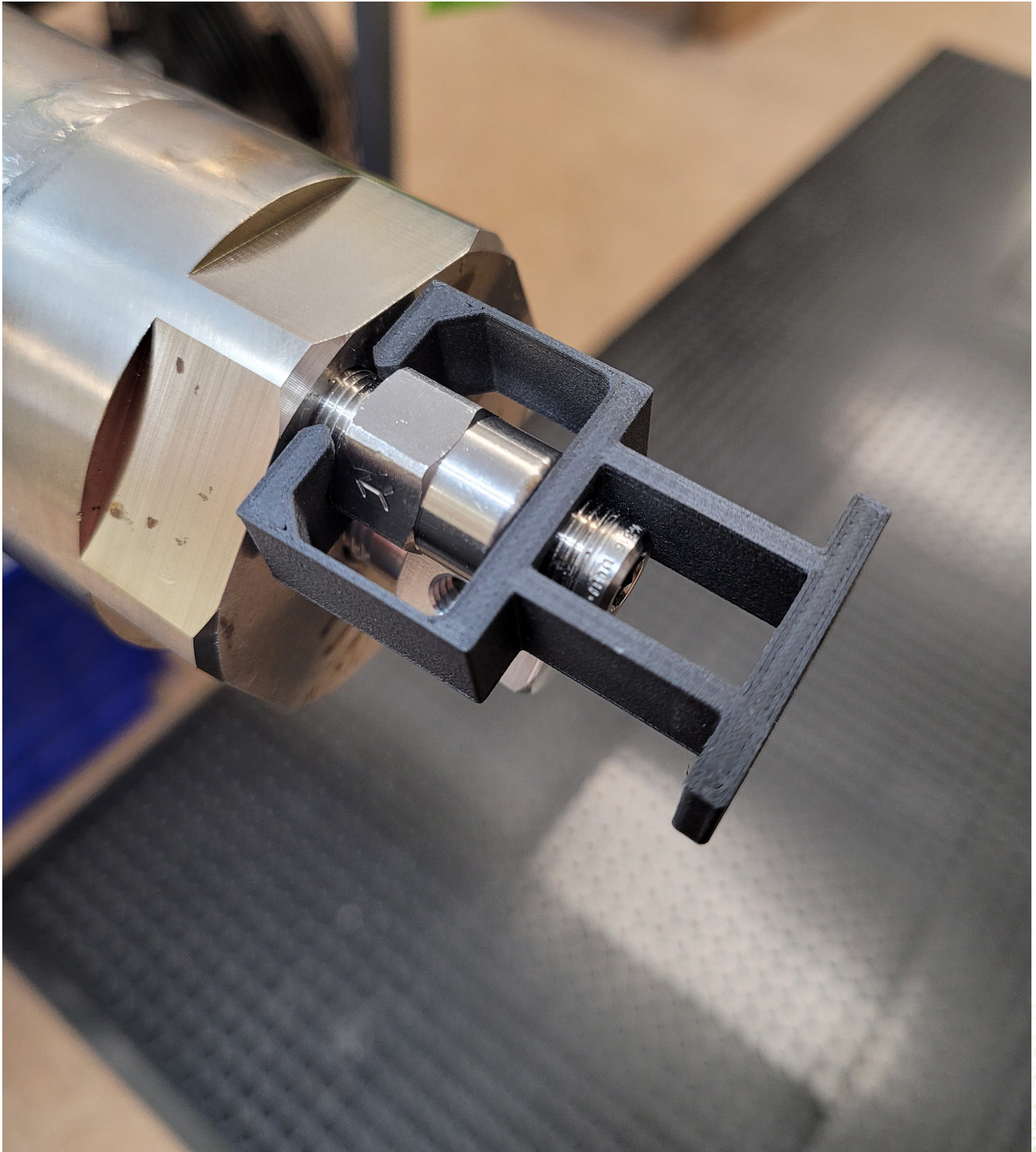


Figure 4. THOR disposable check valve plug clip used to position the plug to be threaded into the check valve, one of the first 3D printed tools slated to be used in-cell

4.5 GENERAL

A Strategy for Establishing a Fast Reactor Testbed without a Domestic Fast Spectrum Test Reactor

Principal Investigators: Nicolas Woolstenhulme

Team Members/ Collaborators: Colby Jensen, Casey Jesse, Austin Carter

The BEAST design will enable ATR-based irradiation of advanced fuel designs in prototypic-length fuel pins and representative flux environment to support post irradiation exams, enable transient testing, and permit LTA irradiations in true sodium fast reactors.

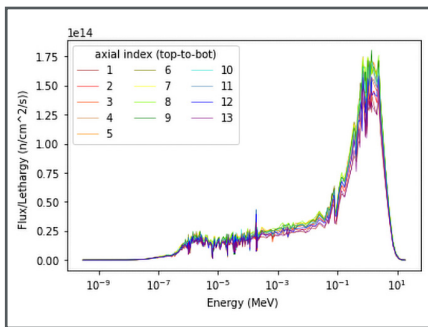


Figure 1. Neutron flux spectrum in test pins

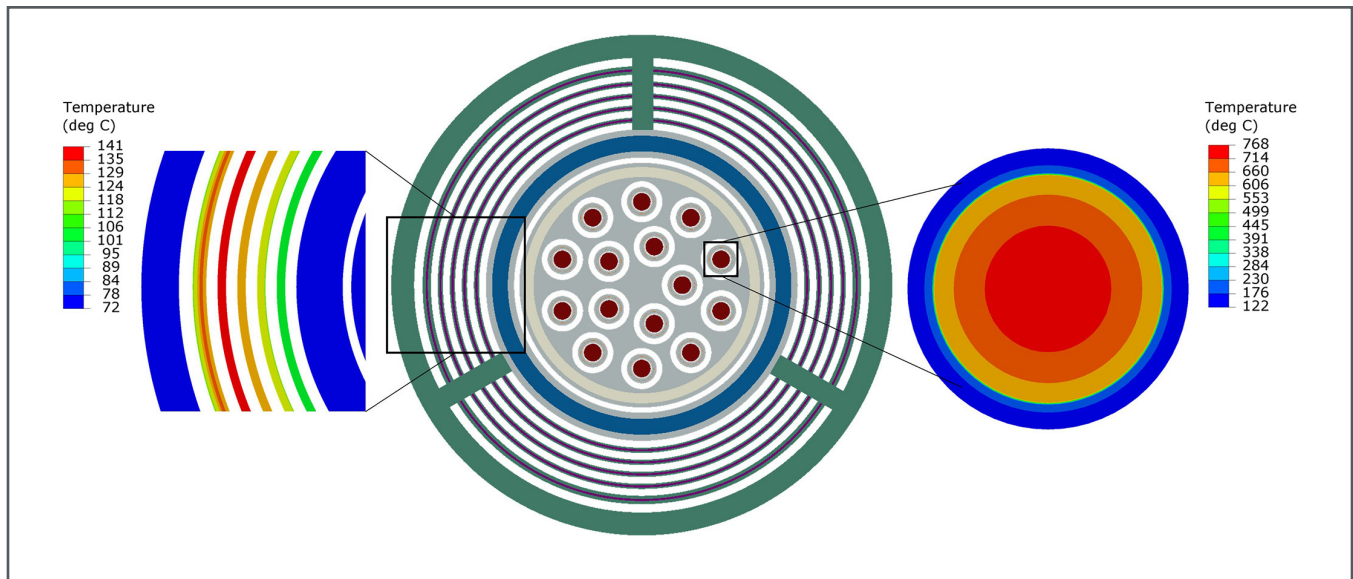
Advanced reactor researchers rallied at the prospect of a much-needed fast spectrum test reactor in the United States, but enthusiasm is beginning to wane for the Versatile Test Reactor (VTR) as meaningful congressional budget support continues to be deferred. The future is uncertain, and hope still endures for the VTR, but at this time it is clear that Advanced Fuels Campaign (AFC) must formulate a success strategy without a fast spectrum test reactor in the United States. Recent developments for transient testing capabilities in the Transient Reactor Test facility (TREAT) and investigations into flux hardening capabilities in the Advanced Test Reactor (ATR) lend credence to a fuel maturation pathway which culminates in fuel performance data adequate to enable lead test assembly irradiations in Sodium Fast Reactors (SFR) licensed by the Nuclear Regulatory Commission (NRC) and/or foreign regulators.

Project Description:

The capability for safety testing SFR fuels in TREAT has been recently revived with sodium heat sink capsules while other projects continue to press forward with deployment of a flow sodium loop

for TREAT and transient furnace capabilities in collocated hot cells. In just a few years a full suite of SFR transient testing capabilities will be established. Irradiated specimens retained from the historic Integral Fast Reactor program will support many valuable tests, but these specimens do not represent modern fuel design modifications and advancements of interest to the community.

There are currently no operating fast spectrum reactors available in the US or countries where collaborations are politically feasible. However, TerraPower continues to move forward with their plans to construct the Sodium reactor in Wyoming and efforts are underway to resume operation of the Joyo reactor in Japan. Either of these reactors could offer a prototypic environment for lead test assembly (LTA) irradiations on advanced SFR fuel designs, but neither of these reactors will be licensed in the same way as DOE's test reactors. It is expected that a higher level of performance data (e.g., license amendment request) will be needed to enable LTA irradiations in these reactors, especially for highly novel fuel designs. Thus, the key gap is the ability to accumulate burnup on full-size SFR fuel pins in



a fast flux environment in order to prepare specimens for post irradiation exams and transient tests.

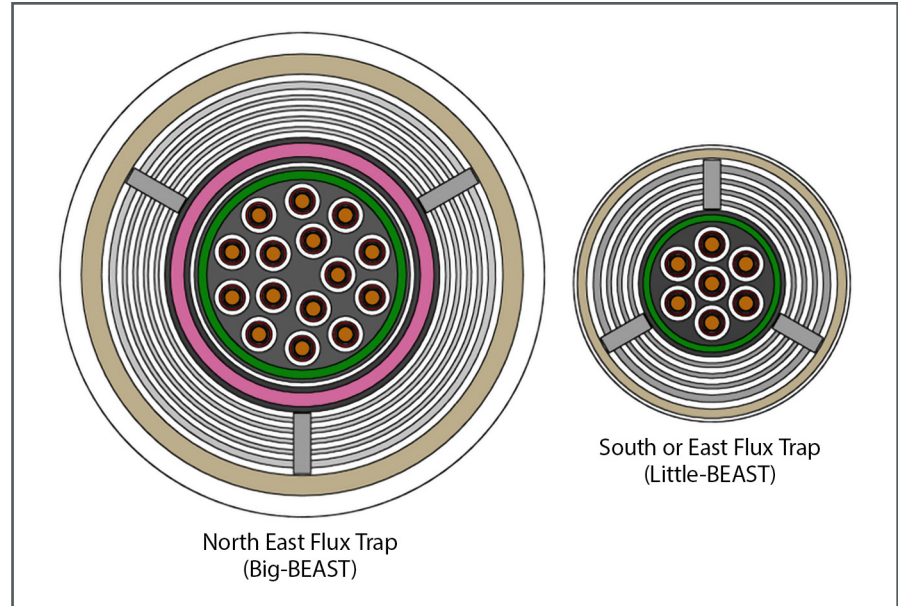
A previous scoping study investigated use of the existing Belgium Reactor 2 (BR2) fuel assembly in an ATR flux trap as a fast-flux converter booster. These results were promising, but it was recognized that that the BR2 assembly was not optimized for this purpose. Investigations into a new design, termed the Boosted Energy Advanced Spectrum Test (BEAST), was undertaken under AFC funding in 2022.

Accomplishments:

A model of BEAST was developed in the Monte Carlo N-Particle (MCNP) code in the Northeast Flux Trap (NEFT) of ATR. The model incorporated explicit representations of the BEAST booster fuel element, thermal neutron filtering, and 15 SFR test pin locations in the center (EBR-II U-10Zr fuel pins were modeled). Significant reductions in the amount of moderating coolant water were made in the design to harden the spectrum as much as possible. Flux levels, neutron energy spectrum, and heating rates

Figure 2. Depiction of thermal model and temperature estimates

Figure 3. Scale representation of Big-BEAST and Little-BEAST options



were predicted. The test pins were shown to have minimal thermal neutron flux, a strong fast flux, and to achieve prototypic linear heating rates ranging from 300-400 W/cm. The heat rate in the booster fuel was found to significantly decrease with each ring toward the experiment center showing that it converts most of thermal neutrons to fission reactions.

A finite element analysis model developed using Abaqus was utilized to provide preliminary temperature predictions. Simple hand calculations estimated the hydraulic characteristics of BEAST and showed that total flow through the test is within the flow limit currently imposed by ATR (~500 gpm). These preliminary

results demonstrate that it should be feasible to irradiate BEAST in the NEFT from a thermal-hydraulic perspective. Future modeling is needed to optimize the design further and explore other irradiation positions such as ATR's smaller flux traps (south or east flux traps). It is presumed that the NEFT option will be ideal since it can accommodate more booster fuel, thicker thermal neutron filters, and more test specimens (Big-BEAST). The NEFT, however, it is a hotly contested position among ATR users and forthcoming studies will determine if other flux traps will be adequate (Little-BEAST).



APPENDIX

- 5.1 Publications
- 5.2 FY-22 Level 2 Milestones
- 5.3 AFC Nuclear Energy University
Projects (NEUP) Grants
- 5.4 Acronyms
- 5.5 Divider Photo Captions

5.1 PUBLICATIONS

Author	Title	Publication
Adkins, C. A.	Effective Thermal Conductivity of Irradiated Uranium-Zirconium Alloy	Materials Science and Engineering Department. Gainesville, FL, University of Florida. Doctor of Philosophy Dissertation: 87. 2022
Adorno Lopes, D., Claisse, A., Limbäck, M., Metzger, K., Lahoda, E., Sivack, M., Boylan, F., McDaniel, Z. & R. Terry.	Atomistic Modeling at Westinghouse: From Design to Performance of Fuel Compounds	Proceedings of TopFuel21 Conference, Santander, Spain. October 2021
Beausoleil, G., Capriotti, L., Curnutt, B., Fielding, R. Hayes, S. & D. Wach.	FAST Irradiations and Initial Post Irradiation Examinations – Part I	Nuclear Engineering and Technology, 2022
Cantonwine, P. Schneider, R. Lutz, D. McCumbee, P. Fawcett, R. Swan, M. & Y.-P. Lin.	GNF Fuel Performance and Continuing Innovation	Proceedings of TopFuel21 Conference, Santander, Spain. October 2021, https://www.euronuclear.org/scientific-resources/conference-proceedings/#1559592636459-42447d8c-0fcc
Cocke, C.K., Rollett, A.D., Lebensohn, R.A. et al.	The AFRL Additive Manufacturing Modeling Challenge: Predicting Micromechanical Fields in AM IN625 Using an FFT-Based Method with Direct Input from a 3D Microstructural Image	Integr Mater Manuf Innov Volume 10 (2021) 157, https://doi.org/10.1007/s40192-021-00211-w
Copeland-Johnson, T.M., Nyamekye, C.K.A., Ecker, L., Bowler, N., Smith, E.A., Rebak, R.B. & S. K. Gill.	Analysis of Inconel 600 Oxidized under Loss-of-Coolant Accident Conditions: A Multi-modal Approach	Corrosion Science Volume 195 (2022) 109950, https://doi.org/10.1016/j.corsci.2021.109950
Dolley, E.J., Rebak, R.B., Buresh, S.J., Huang, S., Soare, M., Fawcett, R.M. & P. P. McCumbee.	Development of IronClad Accident Tolerant Fuel Cladding	Proceedings of TopFuel21 Conference, Santander, Spain. October 2021. https://www.euronuclear.org/scientific-resources/conference-proceedings/#1559592636459-42447d8c-0fcc
Evans, K.J. & R. B. Rebak.	Hydrogen Permeation in FeCrAl APMT Alloy for Accident Tolerant Fuel Cladding	Corrosion Journal, Volume 78 (May 2022) 449, https://doi.org/10.50064018
Garud, Y.S., Hoffman, A.K. & R. B. Rebak.	Hydrogen Isotopes Permeation in Clean or Unoxidized FeCrAl Alloys: A Review	Metallurgical and Materials Transactions A, https://doi.org/10.1007/s11661-021-06535-8

Author	Title	Publication
Gavalek, M., Giho, A., Lam, H.Q., & B. Zhang.	Development of Cross-Section Data Set Repository and Interpolation Code System, LOCUS	Proceedings of the PHYSOR Conference, Pittsburgh, Pennsylvania, USA. May 2022
Grosse, M., Steinbrueck, M., Stuckert, J., Yanga, J., Sevecek, M. & L. Czerniak.	High-temperature Behaviour of Chromium Coated Zirconium-based Fuel Cladding Materials	Proceedings of TopFuel21 Conference, Santander, Spain. October 2021
Hilton, P.A., Sung, X., Akdeniz, B., Snider, S., Salazar, D.A. & M. Gavalek.	Westinghouse Simplified RAVE™ Approach to PWR OTΔT/OPΔT Event Analyses	Proceedings of the PHYSOR Conference, Pittsburgh, Pennsylvania, USA. May 2022
Hoffman, A. K., Cappia, F., Burns, J., He, L., Umretiya, R., Gupta, V., Massey, C., Harp, J. & R. B. Rebak.	FeCrAl Fuel Clad Chemical Interaction in Light Water Reactor Environment	Transactions of the ANS Winter 2021 meeting, Washington DC, USA. December 2021 Volume 125 (2021) 515, https://www.ans.org/pubs/transactions/article-50579/
Hoffman, A. K., Nag, S., Shen, C., Lutz, D.R., Jiang, C. & R. B. Rebak.	Effects of Aluminum on Alpha Prime Formation in FeCrAl Alloys	Proceedings of TopFuel21 Conference, Santander, Spain. October 2021. https://www.euronuclear.org/scientific-resources/conference-proceedings/#1559592636459-42447d8c-0fcc
Hoffman, A.K., Umretiya, R.V., Gupta, V.K., Larsen, M., Graff, C., Perlee, C., Brennan, P. & R. B. Rebak.	Oxidation Resistance in 1200°C Steam of a FeCrAl Alloy Fabricated by Three Metallurgical Processes	JOM https://doi.org/10.1007/s11837-022-05209-z
Huang, S., Dolley, E., An, K., Yu, D., Crawford, C., Othon, M.A., Spinelli, I., Knussman, M.P. & R. B. Rebak.	Microstructure and Tensile Behavior of Powder Metallurgy FeCrAl Accident Tolerant Fuel Cladding	Journal of Nuclear Materials Volume 560 (2022) 153524, https://doi.org/10.1016/j.jnucmat.2022.153524
Kamerman, D., Cappia, F., Wheeler, K., Petersen, P., Rosvall, E., Dabney, T., Yeom, H., Sridharan, K., Ševeček, M. & J. Schulthess.	Development of Axial and Ring Hoop Tension Testing Methods for Nuclear Fuel Cladding Tubes	Nuclear Materials and Energy, Volume 31 (2022) https://doi.org/10.1016/j.nme.2022.101175
Kane et al.	Quantifying deformation during Zry-4 burst testing: A Comparison of BISON and an In-situ Digital Image Correlation and Infrared Thermography Methods	Accepted with revisions – Journal of Nuclear Materials

Author	Title	Publication
Karoutas, Z., Metzger, K., Olson, L., Hallman, L., Lahoda, E., Sivack, M., Lyons, J., Czerniak, L., Boylan, F., McDaniel, Z., Terry, R., Claisse, A., Adorno Lopes, D. & J. Wright.	Westinghouse Encore® Accident Tolerant Fuel and High Energy Program	Proceedings of TopFuel21 Conference, Santander, Spain. October 2021
Kocevski, V., Cooper, M.W.D., Claisse, A.J., Andersson & D.A. Hide.	Development and Application of a Uranium Mononitride (UN) Potential: Thermomechanical Properties and Xe Diffusion	Journal of Nuclear Materials, Volume 562 (April 2022) https://doi.org/10.1016/j.jnucmat.2022.153553
Koyanagi, T. Wang, H., Arregui Mena, J.D., Petrie, C.M., Deck, C.P., Kim, W-J., Kim, D., Sauder, D., Braun, J. & Y. Katoh.	Thermal Diffusivity and Thermal Conductivity of SiC Composite Tubes: The Effects of Microstructure and Irradiation	Journal of Nuclear Materials, Volume 557 (December 2021) https://doi.org/10.1016/j.jnucmat.2021.153217
Kumagai, T., Pachaury, Y., Maccione, R., Wharry, J.P & A. El-Azab.	An Atomistic Investigation of Dislocation Velocity in Body-centered Cubic FeCrAl Alloys	Materialia Volume 18 (2021) 101165 https://doi.org/10.1016/j.mtla.2021.101165
Liu, J. et al.	Structural and Phase Evolution in U3Si2 During Steam Corrosion	Corrosion Science, Volume 204 (2022) 110373 https://doi.org/10.1016/j.corsci.2022.110373
Macisaac, M. Bavdekar, S. Subhash, G. Nance, J. Sankar, B. V., Kim, N-H. & G. Subhash.	A Novel Rotating Flexure-Test Technique for Brittle Materials with Circular Geometries	Experimental Techniques Volume 12 (2022) https://doi.org/10.1007/s40799-022-00565-6
Mirmohammad, H., Gunn, T. & O.T. Kingstedt.	In-Situ Full-Field Strain Measurement at the Sub-grain Scale Using the Scanning Electron Microscope Grid Method	Exp Tech Volume 45 (2021) 109. https://doi.org/10.1007/s40799-020-00402-8
Mirmohammad, H. & O. Kingstedt.	Theoretical Considerations for Transitioning the Grid Method Technique to the Microscale	Exp Mech Volume 61 (2021) 753. https://doi.org/10.1007/s11340-020-00684-4
Nagaraju, H. T., Subhash, G., Kim, N-H, Haftka, R. & B. Sankar.	Effect of Curvature on Extensional Stiffness Matrix of 2-D Braided Composite Tubes	Composites Part A: Applied Science and Manufacturing Volume 147(2021) 106422 https://doi.org/10.1016/j.compositesa.2021.106422
Nance J.R., Subhash, G. Sankar, B., Haftka, R., Kim, N-H, Deck, C. & S. Oswal.	Measurement of Residual Stress in Silicon Carbide Fibers of Tubular Composites Using Raman Spectroscopy	Acta Materialia Volume 217(2021) 117164 https://doi.org/10.1016/j.actamat.2021.117164

Author	Title	Publication
Nance J.R., Subhash, G. Sankar, B., Kim, N-H, Deck C. & S. Oswald.	Influence of Weave Architecture on Mechanical Response of SiCf-SiCm Tubular Composites	Materials Today Communications Volume 33(2022) 104206 https://doi.org/10.1016/j.mtcomm.2022.104206
Oh, S., Andersen, J.G.M, Trofimova, A.V., Kang, K.M., Fawcett, R.M., Swan, M., Sugawara, M. & J. Lamy.	Thermal Hydraulic Performance of GNF Fuels with ARMOR Coating	in Proceedings of TopFuel21 Conference, Santander, Spain. October 2021. https://www.euronuclear.org/scientific-resources/conference-proceedings/#1559592636459-42447d8c-0fcc
Pachauri, Y., Kumagai, T., Wharry, J.P. & A. El-Azab.	A Data Science Approach for Analysis and Reconstruction of Spinodal-like Composition Fields in Irradiated FeCrAl Alloys	Acta Materialia Volume 234 (2022) 118019 https://doi.org/10.1016/j.actamat.2022.118019
Quillin, K., Yeom, H., Dabney, T., McFarland, M. & K. Sridharan.	Experimental Evaluation of Direct Current Magnetron Sputtered and High-power Impulse Magnetron Sputtered Cr Coatings on SiC for Lightwater Reactor Applications	Thin Solid Films Volume 716 (2020) 138431 https://doi.org/10.1016/j.tsf.2020.138431
Quillin, K., Yeom, H., Dabney, T., Willing, E. & K. Sridharan.	Microstructural and Nanomechanical Studies of PVD Cr coatings on SiC for LWR Fuel Cladding Applications	Surface and Coatings Technology Volume 441 (2022) 128577 https://doi.org/10.1016/j.surfcoat.2022.128577
Ratnayake, R. K. Hussey, D. F. Olson, L. Wang, G. Byers W. & R. Becker.	ATF Coating Response in KOH Adjusted PWR Water	Proceedings of TopFuel21 Conference, Santander, Spain. October 2021
Rebak, R.B.	Innovative Accident Tolerant Nuclear Fuel Materials Will Help Extending the Life of Light Water Reactors	KOM – Corrosion and Material Protection Journal Volume 66 (2022) 36. https://doi.org/10.2478/kom-2022-0006
Rebak, R.B., Dolley, E.J., Zhang, W., Umretiya, R.V. & A. K. Hoffman.	Enhanced Mechanical Properties of Iron-Chromium-Aluminum Cladding for Light Water Reactor Fuels	Proceedings of ASME 2022 PVP Conference, Las Vegas, US. July 2022
Rebak, R.B., Jurewicz, T.B., Hoffman, A.K., Yin, L., Amroussia, A., Umretiya, R.V. & R. M. Fawcett.	Zinc Additions Reduces Dissolution Rate of FeCrAl Fuel Cladding	Transactions of ANS Winter 2021 meeting, Washington DC, US. December 2021. Volume 125 (2021) 513.



Foreign Material

FLUX WIRE
REMOVAL
SHIELD PLUG

Author	Title	Publication
Rebak, R.B., Jurewicz, T.B., Larsen, M. & L. Yi.	Zinc Water Chemistry Reduces Dissolution of FeCrAl for Nuclear Fuel Cladding	Corrosion Science 198 (2022) 110156. https://doi.org/10.1016/j.corsci.2022.110156
Rebak, R.B., Umretiya, R.V., Hoffman, A.K., Dolley, E.J. & R. M. Fawcett.	Characterization of FeCrAl Cladding Tubes in the Entire Fuel Cycle	Proceedings of Global 2022 Conference, Reims (July 2022)
Rebak, R.B., Umretiya, R.V., Hoffman, A.K., Yin, L., Amroussia, A. & D. R. Lutz.	Reprocessing Capabilities of FeCrAl-Clad Used Fuel	Transactions of the ANS Winter 2021 meeting, Washington DC, December 2021, Volume 125 (2021) 181. https://www.ans.org/pubs/transactions/article-50500/
Rebak, R.B., Yin, L., Jurewicz, T.B. & A. K. Hoffman.	Acid Dissolution Behavior of Ferritic FeCrAl Tubes Candidates for Nuclear Fuel Cladding	Corrosion Journal, Volume 77 (2021) 1321. https://doi.org/10.5006/3965
Rebak, R.B., Yin, L., Larsen, M., Umretiya, R.V. & A. K. Hoffman.	Mitigating LWR IronClad Fuel Cladding Dissolution Using Zinc Water Chemistry	Paper PVP2022-80559 in Proceedings of ASME 2022 PVP Conference, July 2022, Las Vegas
Roache, D.C., Bumgardner, C.H., Harrell, T.M., Price, M.C., Jarama, A., Heim, F.M., Walters, J., Maier, B. & X.Li.	Reprocessing Capabilities of Accident Tolerant Fuels Clad in FeCrAl Alloys	Proceedings of TopFuel21 Conference, Santander, Spain. October 2021. https://www.euronuclear.org/scientific-resources/conference-proceedings/#1559592636459-42447d8c-0fcc
Sankar, B. V., Thandaga Nagaraju, H., Kim, N-H. & G. Subhash.	An Extrapolation Method to Remove Spurious Stress Concentration in Pixel-based Meshes	Composite Structures Volume 290 (2022) 115522 https://doi.org/10.1016/j.compstruct.2022.115522
Schoell, R., Kabel, J., Lam, S., Sharma, A., Michler, J., Hosemann, P. & D. Kaoumi.	Corrosion Behavior of a Series of Combinatorial Physical Vapor Deposition Coatings on SiC in a Simulated Boiling Water Reactor Environment	Journal of Nuclear Materials (2022) https://doi.org/10.1016/j.jnucmat.2022.154022
Ševeček, M., Chalupová, A., Čech, J., Walters, J., Maier, B. & J. Krejčí.	Experimental Evaluation of Chromium Cold-Spray Coated Cladding	Proceedings of TopFuel21 Conference, Santander, Spain. October 2021
Shockling, M.A., Everhard, A.M., Lam, H.Q. & U. Bachrach.	Assessment of Loss-Of-Coolant Accident Fuel Dispersal for High Burnup Core Designs	Proceedings of TopFuel21 Conference, Santander, Spain. October 2021

Author	Title	Publication
Smith, A. J., Maxwell, H. L., Mirmohammad, H., Kingstedt, O. T. & R.B. Berke.	A Novel Variable Extensometer Method for Measuring Ductility Scaling Parameters from Single Specimens.	ASME. J. Appl. Mech, Volume 89 (2022) 031006, https://doi.org/10.1115/1.4053034
Sooby, E.S. et al.	Steam Oxidation of Uranium Mononitride in Pure and Reducing Steam Atmospheres to 1200 °C	Journal of Nuclear Materials Volume 560 (2022) 153487 https://doi.org/10.1016/j.jnucmat.2021.153487
Steinbrueck, M., Grosse, M., Stegmaier, U., Braun, J. & C. Lorrette.	High-Temperature Oxidation of Silicon Carbide Composites for Nuclear Applications	Proceedings of TopFuel21 Conference, Santander, Spain. October 2021
Sun, T.Y., Shang, Z.X., Cho, J., Ding, J., Niu, T.J., Zhang, Y.F., Yang, B., Xie, D.Y., Wang, J., Wang, H.Y. & X.H. Zhang.	Ultra-Fine-Grained and Gradient FeCrAl Alloys with Outstanding Work Hardening Capability	Acta Materialia Volume 215 (2021) 117049 https://doi.org/10.1016/j.actamat.2021.117049
Sun, T.Y., Cho, J., Shang, Z.X., Niu, T.J., Ding, J., Wang, J., Wang, H.Y. & X.H. Zhang	Deformation Mechanism in Nanolaminate FeCrAl Alloys by In Situ Micromechanical Strain Rate Jump Tests at Elevated Temperatures	Scripta Materialia Volume 215 (2022) 114698 https://doi.org/10.1016/j.scriptamat.2022.114698
Warren, P., Warren, G., Wu, Y.Q., Burns, J., Dubey, M. & J.P. Wharry.	Method for Fabricating Depth-Specific TEM In Situ Tensile Bars	JOM Volume 72 (2020) 2057 https://link.springer.com/article/10.1007/s11837-020-04105-8
Wei, B.Q., Xie, D.Y., Wu, W.Q. Shao, L & J. Wang.	Quantifying the Glide Resistance to Dislocations in Proton-Irradiated FeCrAl Alloy	JOM (2022) DOI: https://doi.org/10.1007/s11837-022-05350-9
Xi, J., Liu, C., Morgan, D. & I. Szlufarska	Deciphering Water-Solid Reactions During Hydrothermal Corrosion of SiC	Acta Materialia Volume 209 (2021) 116803 https://doi.org/10.1016/j.actamat.2021.116803
Xi, J., Liu, C., Morgan, D. & I. Szlufarska	An Unexpected Role of H During SiC Corrosion in Water	Journal Phys. Chem. C, Volume 124 (2020) 9394 https://pubs.acs.org/doi/10.1021/acs.jpcc.0c02027
Xie, D.Y., Wei, B., Wu, W.Q. & J. Wang.	Crystallographic Orientation Dependence of Mechanical Responses of FeCrAl Micropillars	Crystals Volume 10 (2020) 943 https://www.mdpi.com/2073-4352/10/10/943
Xu, S., Xie, D., Liu, G., Ming, K. & J. Wang.	Quantifying the Resistance to Dislocation Glide in Single Phase FeCrAl Alloy	International Journal of Plasticity Volume 132 (2020) 102770 https://doi.org/10.1016/j.ijplas.2020.102770

Author	Title	Publication
Yang, K., Kardoulaki, E., Zhao, D., Broussard, A., Metzger, K., White, J.T., Sivack, M.R., McClellan, K.J., Lahoda, E.J. & J. Lian	Uranium Nitride (UN) Pellets with Controllable Microstructure and Phase – Fabrication by Spark Plasma Sintering and their Thermal-Mechanical and Oxidation Properties	Journal of Nuclear Materials Volume 557 (2021) https://doi.org/10.1016/j.jnucmat.2021.153272
Yang, K., Kardoulaki, E., Zhao, D., Gong, B., Broussard, A., Metzger, K., White, J.T., Sivack, M.R., McClellan, K.J., Lahoda, E.J. & J. Lian	Cr-Doped Uranium Nitride Composite Fuels with Enhanced Mechanical Performance and Oxidation Resistance	Journal of Nuclear Materials Volume 559 (2022) https://doi.org/10.1016/j.jnucmat.2021.153486
Yang, K., Kardoulaki, E., Zhao, D., Gong, B., Broussard, A., Metzger, K., White, J.T., Sivack, M.R., McClellan, K.J., Lahoda, E.J. & J. Lian	UN and U ₃ Si ₂ Composites Densified by Spark Plasma Sintering for Accident-Tolerant Fuels	Ceramic International (December 2021) https://doi.org/10.1016/j.ceramint.2021.12.292
Yang, K., Zhao, D., Broussard, A., Lian, J., Kardoulaki, E., White, J.T., McClellan, K.J., Metzger, K., Sivack, M.R. & E. J. Lahoda	Fabrication of High-Density Uranium Nitride-Based Accident Tolerant Fuels by Spark Plasma Sintering and Thermal-Mechanical Properties	Proceedings of TopFuel21 Conference, Santander, Spain. October 2021
Yarrington, J., Schulthess, J., Parker, S., Argyle, J., Turner, C., Stanek, J. & C. Christensen	Advanced Autonomous Welding for Refabrication and Follow-On Testing of Previously Irradiated Nuclear Fuel	Accepted in Nuclear Technology, 2022
Yuan, G., Kreutzer, P.F., Xu, P., Olson, L., Lahoda, E.J. & D. Liu	In Situ High Temperature X ray Tomography of SiC/SiC Composites Under C Ring Compression Test	Proceedings of TopFuel21 Conference, Santander, Spain. October 2021
Zhang, B.	Study of Reference Burnup Steps Optimization in Fuel Segment Data File Generation for NEXUS/ANC9 Code System	Proceedings of 2022 PHYSOR Conference, Pittsburgh, Pennsylvania, US. May 2022
Zhang, J., Vermeeren, B., Schinazi, C., Schneidesch, C., Meert, A., Doncel, N., Martinez, L. & J.L. Walters	Design and Safety Evaluation of Cr-Coated Lead Test Rods for Doel Nuclear Power Plant Unit 4	Proceedings of TopFuel21 Conference, Santander, Spain. October 2021

5.2 FY-22 LEVEL 2 MILESTONES

Work Package Title	Site	Work Package Manager	Level 2 Milestone
Interface Mechanical Property Testing for Coated Zircaloy - LANL	LANL	Eftink, Ben	Issue report on bulge testing and microscale testing on coated zircaloy
Integral Irradiation Testing - INL	INL	Hoggard, Gary	ATF-2C test train top tier assembled and ready for insertion
HERA - INL	INL	Astle, Leigh Ann	First two experiments on pre-hydrided cladding ready for irradiation
Accelerated Irradiation and Qualification of Ceramic Nuclear Fuels - LANL	LANL	Paisner, Scarlett	Status report on test matrix for irradiation tests
ATF Post Irradiation Examination - INL	INL	Cappia, Fabiola	Draft manuscript on optimized tensile testing of irradiated cladding
Integral Transient Testing - INL	INL	Astle, Leigh Ann	Draft manuscript on the resumption of water capsule RIA testing at TREAT
Accelerated Ceramic Fuel Development - LANL	LANL	White, Josh	Status report on doped UO ₂ properties and performance
Develop HBU Transient FGR Capability - ORNL	ORNL	Linton, Kory	Report summarizing design for SATS fission gas release capability and proof of concept experiment demonstration
Characterization of High Burnup Fuel Samples - ORNL	ORNL	Capps, Nathan	Report summarizing high burnup microstructural data of commercially irradiated fuel
ARES - Joint Work with JAEA to Study Off-normal Behavior of Fast Reactor Fuels - INL	INL	Smuin, Trevor	Conduct preliminary design review for THOR remote handling and process equipment
ARES - Joint Work with JAEA to Study Off-normal Behavior of Fast Reactor Fuels - INL	INL	Smuin, Trevor	Complete THOR commissioning test plan in BUSTER (nominally 3 transients)



TOP RAY
1700 LB
DWG 73250

HFEF-15

TREAT ME-W
LOOP CASE

DWG 73250

HySecurity
Circuit Breaker
Class 2 & 3
To operate this gate

5.3 AFC NUCLEAR ENERGY UNIVERSITY PROJECTS (NEUP) GRANTS

Active Projects Awarded in 2017

Nuclear Energy University Cooperative Agreements

Lead University	Title	Principal Investigator
University of Wisconsin, Madison	Extreme Performance High Entropy Alloys (HEAs) Cladding for Fast Reactor Applications	Adrien Couet
University of Wisconsin, Madison	Critical Heat Flux Studies for Innovative Accident Tolerant Fuel Cladding Surfaces	Michael Corradini
Colorado School of Mines	Development of Advanced High-Cr Ferritic/Martensitic Steels	Kester Clarke
Massachusetts Institute of Technology	Determination of Critical Heat Flux and Leidenfrost Temperature on Candidate Accident Tolerant Fuel Materials	Matteo Bucci
Virginia Commonwealth University	Evaluation of Accident Tolerant Fuels Surface Characteristics in Critical Heat Flux Performance	Jessika Rojas
University of New Mexico	Nanostructured Composite Alloys for Extreme Environments	Osman Anderoglu
University of New Mexico	An Experimental and Analytical Investigation into Critical Heat Flux (CHF) Implications for Accident Tolerant Fuel (ATF) Concepts	Youho Lee

Active Projects Awarded in 2018

Nuclear Energy University Cooperative Agreements

Lead University	Title	Principal Investigator
University of California, Berkeley	Understanding of Degradation of SiC/SiC Materials in Nuclear Systems and Development of Mitigation Strategies	Peter Hosemann
University of California, Berkeley	Bridging the Length Scales on Mechanical Property Evaluation	Peter Hosemann
University of Minnesota, Twin Cities	Probabilistic Failure Criterion of SiC/SiC Composites Under Multi-Axial Loading	Jialiang Le
University of Wisconsin-Madison	Advanced Coating and Surface Modification Technologies for SiC-SiC Composite for Hydrothermal Corrosion Protection in LWR	Kumar Sridharan
University of Michigan	Mechanistic Understanding of Radiolytically Assisted Hydrothermal Corrosion of SiC in LWR Coolant Environments	Peng Wang
Purdue University	Microstructure-Based Benchmarking for Nano/Microscale Tension and Ductility Testing of Irradiated Steels	Janelle Wharry
University of Florida	Multiaxial Failure Envelopes and Uncertainty Quantification of Nuclear-Grade SiCf/SiC Woven Ceramic Matrix Tubular Composites	Ghatu Subhash
University of Notre Dame	Radiolytic Dissolution Rate of Silicon Carbide	David Bartels
University of Utah	Benchmarking Microscale Ductility Measurements	Owen Kingstedt
University of Nebraska, Lincoln	Bridging Microscale to Macroscale Mechanical Property Measurements and Predication of Performance Limitation for FeCrAl Alloys Under Extreme Reactor Applications	Jian Wang
University of South Carolina	Development of Multi-Axial Failure Criteria for Nuclear Grade SiCf-SiCm Composites	Xinyu Huang

Active Projects Awarded in 2019

Nuclear Energy University Cooperative Agreements

Lead University	Title	Principal Investigator
University of Pittsburgh	Thermal Conductivity Measurement of Irradiated Metallic Fuel Using TREAT	Heng Ban
The Ohio State University	Neutron Radiation Effect on Diffusion between Zr (and Zircaloy) and Cr for Accurate Lifetime Prediction of ATF	Wolfgang Windl
North Carolina State University	Novel Miniature Creep Tester for Virgin and Neutron Irradiated Clad Alloys with Bench-marked Multiscale Modeling and Simulations	Korukonda Murty
University of South Carolina	Remote Laser Based Nondestructive Evaluation for Post Irradiation Examination of ATF Cladding	Lingyu Yu
University of Tennessee at Knoxville	Radiation-Induced Swelling in Advanced Nuclear Fuel	Maik Lang
University of Minnesota, Twin Cities	High Throughput Assessment of Creep Behavior of Advanced Nuclear Reactor Structural Alloys by Nano/Microindentation	Nathan Mara

Active Projects Awarded in 2020

Nuclear Energy University Cooperative Agreements

Lead University	Title	Principal Investigator
University of Wisconsin-Madison	Investigation of Degradation Mechanisms of Cr-coated Zirconium Alloy Cladding in Reactivity Initiated Accidents (RIA)	Hwasung Yeom
University of Wisconsin-Madison	Maintaining and Building Upon the Halden Legacy of In-situ Diagnostics	Michael Corradini
University of California, Berkeley	Femtosecond Laser Ablation Machining & Examination - Center for Active Materials Processing (FLAME-CAMP)	Peter Hosemann
Rensselaer Polytechnic Institute	Chemical Interaction and Compatibility of Uranium Nitride with Liquid Pb and Alumina-forming Austenitic Alloys	Jie Lian
Georgia Institute of Technology	Linear and Nonlinear Guided Ultrasonic Waves to Characterize Cladding of Accident Tolerant Fuel (ATF)	Laurence Jacobs

Active Projects Awarded in 2021

Nuclear Energy University Cooperative Agreements

Lead University	Title	Principal Investigator
University of Tennessee at Knoxville	Safety Implications of High Burnup Fuel for a 2-Year PWR Fuel Cycle	Nicholas Brown
University of Tennessee at Knoxville	Fuel-to-Coolant Thermomechanical Behaviors Under Transient Conditions	Nicholas Brown
University of Florida	High-Fidelity Modeling of Fuel-to-Coolant Thermomechanical Transport Behaviors Under Transient Conditions	Justin Watson
University of Wisconsin-Madison	Post-DNB Thermo-mechanical Behavior of Near-term ATF Designs in Simulated Transient Conditions	Hwasung Yeom
University of Tennessee at Knoxville	Modeling High-Burnup LWR Fuel Behavior Under Normal Operating and Transient Conditions	Giovanni Pastore
Massachusetts Institute of Technology	Experimental Investigation and Development of Models and Correlations for Cladding-to-Coolant Heat Transfer Phenomena in Transient Conditions in Support of TREAT and the LWR Fleet.	Matteo Bucci
Oregon State University	Characterizing Fuel Response and Quantifying Coolable Geometry of High-Burnup Fuel	Wade Marcum
University of Pittsburgh	Fragmentation and Thermal Energy Transport of Cr-doped Fuels under Transient Conditions	Heng Ban
Texas A&M University	Multiscale Modeling and Experiments for Investigating High Burnup LWR Fuel Rod Behavior Under Normal and Transient Conditions	Karim Ahmed
Pennsylvania State University	Estimation of Low Temperature Cladding Failures During an RIA Transient	Arthur Motta

Active Projects Awarded in 2022

Nuclear Energy University Cooperative Agreements

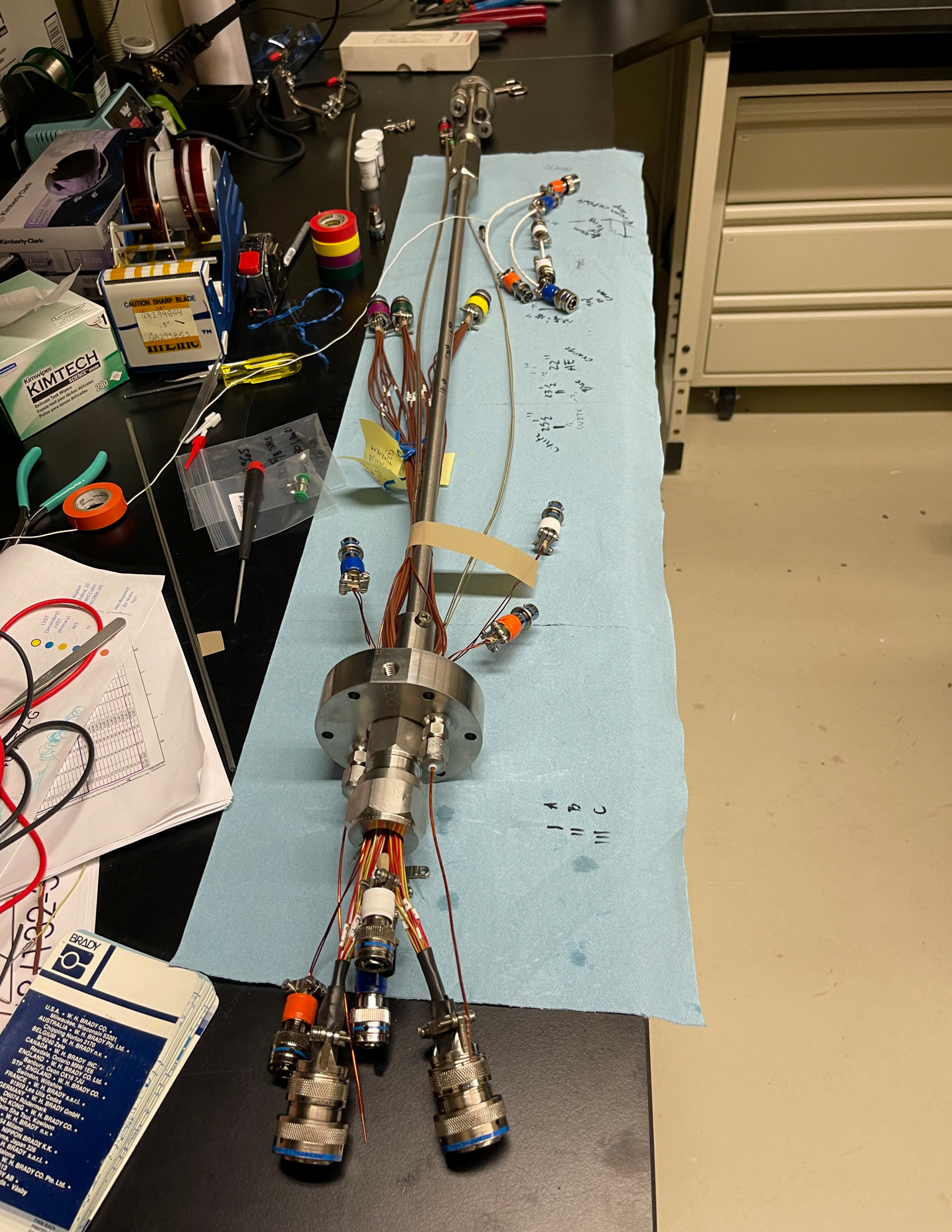
Lead University	Title	Principal Investigator
Massachusetts Institute of Technology	Understanding of ATF Cladding Performance under Radiation using MITR	David Carpenter
University of Texas at San Antonio	International Collaboration to Advance the Technical Readiness of High Uranium Density Fuels and Composites for Small Modular Reactors	Elizabeth S. Sooby
University of Wisconsin-Madison	Development of Advanced Control Rod Assembly for Improved Accident Tolerance and High Burnup Fuel Cycle	Kumar Sridharan
Purdue University	Physics-guided Smart Scaling Methodology for Accelerated Fuel Testing	Hany Abdel-Khalik
Massachusetts Institute of Technology	ATF Solutions to Light Water-Cooled SMRs	Koroush Shirvan

5.4 ACRONYMS

AE.....	Acoustic Emission
AFC	Advanced Fuels Campaign
AIC.....	Silver-Indium-Cadmium
AIMD	Ab Initio Molecular Dynamics
AL.....	Air Liquide
ANL.....	Argonne National Laboratory
ANO	Arkansas Nuclear One
ARES	Advanced Reactor Experiments for Sodium Fast Reactor Fuels
ASI.....	Advanced Sensors and Instruments
ATCR.....	Accident Tolerant Control Rods
ATF.....	Accident Tolerant Fuel
ATR	Advanced Test Reactor
BDBA	Beyond Design Basis Accident
BEAST	Boosted Energy Advanced Spectrum Test
B-HiPIMS.....	Bipolar Hybrid High Power Impulse Magnetron Sputtering
BSDs.....	Black Spot Defects
BNL	Brookhaven National Laboratory
BR2.....	Belgium Reactor - 2
BU	Bangor University
BWR.....	Boiling Water Reactor
CCCTF.....	Core Conduction Cooldown Test Furnace
CDM.....	Continuum Damage Mechanics
CEA	Commissariat à l'Énergie Atomique
CHF.....	Critical Heat Flux
CIC	Core Internal Change-out
CLP.....	Constitutive Law for Polycrystals
COV.....	Coefficient of Variation



CRAFT	Collaborative Research on Advanced Fuel Technologies
CVD.....	Chemical Vapor Deposition
DCMS.....	DC Magnetron Sputtering
DEH	Decay-energy Heat Up
DFT	Density Functional Theory
DIC.....	Digital Image Correlation
DMM	Direct Micromechanics Method
DNB	Departure from Nucleate Boiling
DOE.....	Department of Energy
dpa	Displacements per Atom
EATF	Enhanced Accident Tolerant Fuel
EBR	Experimental Breeder Reactor
EBSD	Electron Backscatter Diffraction
EC.....	Constellation Energy Corporation
EDF	Électricité de France
EDS	Energy Dispersive Spectroscopy



Kimberly-Clark
Kimtech
CAUTION SHARP BLADE
48299854
04299853
MEMO

UTV
(Secondary)
(Primary)
ALS
TC
No. 100
No. 101
No. 102
No. 103
No. 104
No. 105
No. 106
No. 107
No. 108
No. 109
No. 110
No. 111
No. 112
No. 113
No. 114
No. 115
No. 116
No. 117
No. 118
No. 119
No. 120
No. 121
No. 122
No. 123
No. 124
No. 125
No. 126
No. 127
No. 128
No. 129
No. 130
No. 131
No. 132
No. 133
No. 134
No. 135
No. 136
No. 137
No. 138
No. 139
No. 140
No. 141
No. 142
No. 143
No. 144
No. 145
No. 146
No. 147
No. 148
No. 149
No. 150
No. 151
No. 152
No. 153
No. 154
No. 155
No. 156
No. 157
No. 158
No. 159
No. 160
No. 161
No. 162
No. 163
No. 164
No. 165
No. 166
No. 167
No. 168
No. 169
No. 170
No. 171
No. 172
No. 173
No. 174
No. 175
No. 176
No. 177
No. 178
No. 179
No. 180
No. 181
No. 182
No. 183
No. 184
No. 185
No. 186
No. 187
No. 188
No. 189
No. 190
No. 191
No. 192
No. 193
No. 194
No. 195
No. 196
No. 197
No. 198
No. 199
No. 200
No. 201
No. 202
No. 203
No. 204
No. 205
No. 206
No. 207
No. 208
No. 209
No. 210
No. 211
No. 212
No. 213
No. 214
No. 215
No. 216
No. 217
No. 218
No. 219
No. 220
No. 221
No. 222
No. 223
No. 224
No. 225
No. 226
No. 227
No. 228
No. 229
No. 230
No. 231
No. 232
No. 233
No. 234
No. 235
No. 236
No. 237
No. 238
No. 239
No. 240
No. 241
No. 242
No. 243
No. 244
No. 245
No. 246
No. 247
No. 248
No. 249
No. 250
No. 251
No. 252
No. 253
No. 254
No. 255
No. 256
No. 257
No. 258
No. 259
No. 260
No. 261
No. 262
No. 263
No. 264
No. 265
No. 266
No. 267
No. 268
No. 269
No. 270
No. 271
No. 272
No. 273
No. 274
No. 275
No. 276
No. 277
No. 278
No. 279
No. 280
No. 281
No. 282
No. 283
No. 284
No. 285
No. 286
No. 287
No. 288
No. 289
No. 290
No. 291
No. 292
No. 293
No. 294
No. 295
No. 296
No. 297
No. 298
No. 299
No. 300
No. 301
No. 302
No. 303
No. 304
No. 305
No. 306
No. 307
No. 308
No. 309
No. 310
No. 311
No. 312
No. 313
No. 314
No. 315
No. 316
No. 317
No. 318
No. 319
No. 320
No. 321
No. 322
No. 323
No. 324
No. 325
No. 326
No. 327
No. 328
No. 329
No. 330
No. 331
No. 332
No. 333
No. 334
No. 335
No. 336
No. 337
No. 338
No. 339
No. 340
No. 341
No. 342
No. 343
No. 344
No. 345
No. 346
No. 347
No. 348
No. 349
No. 350
No. 351
No. 352
No. 353
No. 354
No. 355
No. 356
No. 357
No. 358
No. 359
No. 360
No. 361
No. 362
No. 363
No. 364
No. 365
No. 366
No. 367
No. 368
No. 369
No. 370
No. 371
No. 372
No. 373
No. 374
No. 375
No. 376
No. 377
No. 378
No. 379
No. 380
No. 381
No. 382
No. 383
No. 384
No. 385
No. 386
No. 387
No. 388
No. 389
No. 390
No. 391
No. 392
No. 393
No. 394
No. 395
No. 396
No. 397
No. 398
No. 399
No. 400
No. 401
No. 402
No. 403
No. 404
No. 405
No. 406
No. 407
No. 408
No. 409
No. 410
No. 411
No. 412
No. 413
No. 414
No. 415
No. 416
No. 417
No. 418
No. 419
No. 420
No. 421
No. 422
No. 423
No. 424
No. 425
No. 426
No. 427
No. 428
No. 429
No. 430
No. 431
No. 432
No. 433
No. 434
No. 435
No. 436
No. 437
No. 438
No. 439
No. 440
No. 441
No. 442
No. 443
No. 444
No. 445
No. 446
No. 447
No. 448
No. 449
No. 450
No. 451
No. 452
No. 453
No. 454
No. 455
No. 456
No. 457
No. 458
No. 459
No. 460
No. 461
No. 462
No. 463
No. 464
No. 465
No. 466
No. 467
No. 468
No. 469
No. 470
No. 471
No. 472
No. 473
No. 474
No. 475
No. 476
No. 477
No. 478
No. 479
No. 480
No. 481
No. 482
No. 483
No. 484
No. 485
No. 486
No. 487
No. 488
No. 489
No. 490
No. 491
No. 492
No. 493
No. 494
No. 495
No. 496
No. 497
No. 498
No. 499
No. 500
No. 501
No. 502
No. 503
No. 504
No. 505
No. 506
No. 507
No. 508
No. 509
No. 510
No. 511
No. 512
No. 513
No. 514
No. 515
No. 516
No. 517
No. 518
No. 519
No. 520
No. 521
No. 522
No. 523
No. 524
No. 525
No. 526
No. 527
No. 528
No. 529
No. 530
No. 531
No. 532
No. 533
No. 534
No. 535
No. 536
No. 537
No. 538
No. 539
No. 540
No. 541
No. 542
No. 543
No. 544
No. 545
No. 546
No. 547
No. 548
No. 549
No. 550
No. 551
No. 552
No. 553
No. 554
No. 555
No. 556
No. 557
No. 558
No. 559
No. 560
No. 561
No. 562
No. 563
No. 564
No. 565
No. 566
No. 567
No. 568
No. 569
No. 570
No. 571
No. 572
No. 573
No. 574
No. 575
No. 576
No. 577
No. 578
No. 579
No. 580
No. 581
No. 582
No. 583
No. 584
No. 585
No. 586
No. 587
No. 588
No. 589
No. 590
No. 591
No. 592
No. 593
No. 594
No. 595
No. 596
No. 597
No. 598
No. 599
No. 600
No. 601
No. 602
No. 603
No. 604
No. 605
No. 606
No. 607
No. 608
No. 609
No. 610
No. 611
No. 612
No. 613
No. 614
No. 615
No. 616
No. 617
No. 618
No. 619
No. 620
No. 621
No. 622
No. 623
No. 624
No. 625
No. 626
No. 627
No. 628
No. 629
No. 630
No. 631
No. 632
No. 633
No. 634
No. 635
No. 636
No. 637
No. 638
No. 639
No. 640
No. 641
No. 642
No. 643
No. 644
No. 645
No. 646
No. 647
No. 648
No. 649
No. 650
No. 651
No. 652
No. 653
No. 654
No. 655
No. 656
No. 657
No. 658
No. 659
No. 660
No. 661
No. 662
No. 663
No. 664
No. 665
No. 666
No. 667
No. 668
No. 669
No. 670
No. 671
No. 672
No. 673
No. 674
No. 675
No. 676
No. 677
No. 678
No. 679
No. 680
No. 681
No. 682
No. 683
No. 684
No. 685
No. 686
No. 687
No. 688
No. 689
No. 690
No. 691
No. 692
No. 693
No. 694
No. 695
No. 696
No. 697
No. 698
No. 699
No. 700
No. 701
No. 702
No. 703
No. 704
No. 705
No. 706
No. 707
No. 708
No. 709
No. 710
No. 711
No. 712
No. 713
No. 714
No. 715
No. 716
No. 717
No. 718
No. 719
No. 720
No. 721
No. 722
No. 723
No. 724
No. 725
No. 726
No. 727
No. 728
No. 729
No. 730
No. 731
No. 732
No. 733
No. 734
No. 735
No. 736
No. 737
No. 738
No. 739
No. 740
No. 741
No. 742
No. 743
No. 744
No. 745
No. 746
No. 747
No. 748
No. 749
No. 750
No. 751
No. 752
No. 753
No. 754
No. 755
No. 756
No. 757
No. 758
No. 759
No. 760
No. 761
No. 762
No. 763
No. 764
No. 765
No. 766
No. 767
No. 768
No. 769
No. 770
No. 771
No. 772
No. 773
No. 774
No. 775
No. 776
No. 777
No. 778
No. 779
No. 780
No. 781
No. 782
No. 783
No. 784
No. 785
No. 786
No. 787
No. 788
No. 789
No. 790
No. 791
No. 792
No. 793
No. 794
No. 795
No. 796
No. 797
No. 798
No. 799
No. 800
No. 801
No. 802
No. 803
No. 804
No. 805
No. 806
No. 807
No. 808
No. 809
No. 810
No. 811
No. 812
No. 813
No. 814
No. 815
No. 816
No. 817
No. 818
No. 819
No. 820
No. 821
No. 822
No. 823
No. 824
No. 825
No. 826
No. 827
No. 828
No. 829
No. 830
No. 831
No. 832
No. 833
No. 834
No. 835
No. 836
No. 837
No. 838
No. 839
No. 840
No. 841
No. 842
No. 843
No. 844
No. 845
No. 846
No. 847
No. 848
No. 849
No. 850
No. 851
No. 852
No. 853
No. 854
No. 855
No. 856
No. 857
No. 858
No. 859
No. 860
No. 861
No. 862
No. 863
No. 864
No. 865
No. 866
No. 867
No. 868
No. 869
No. 870
No. 871
No. 872
No. 873
No. 874
No. 875
No. 876
No. 877
No. 878
No. 879
No. 880
No. 881
No. 882
No. 883
No. 884
No. 885
No. 886
No. 887
No. 888
No. 889
No. 890
No. 891
No. 892
No. 893
No. 894
No. 895
No. 896
No. 897
No. 898
No. 899
No. 900
No. 901
No. 902
No. 903
No. 904
No. 905
No. 906
No. 907
No. 908
No. 909
No. 910
No. 911
No. 912
No. 913
No. 914
No. 915
No. 916
No. 917
No. 918
No. 919
No. 920
No. 921
No. 922
No. 923
No. 924
No. 925
No. 926
No. 927
No. 928
No. 929
No. 930
No. 931
No. 932
No. 933
No. 934
No. 935
No. 936
No. 937
No. 938
No. 939
No. 940
No. 941
No. 942
No. 943
No. 944
No. 945
No. 946
No. 947
No. 948
No. 949
No. 950
No. 951
No. 952
No. 953
No. 954
No. 955
No. 956
No. 957
No. 958
No. 959
No. 960
No. 961
No. 962
No. 963
No. 964
No. 965
No. 966
No. 967
No. 968
No. 969
No. 970
No. 971
No. 972
No. 973
No. 974
No. 975
No. 976
No. 977
No. 978
No. 979
No. 980
No. 981
No. 982
No. 983
No. 984
No. 985
No. 986
No. 987
No. 988
No. 989
No. 990
No. 991
No. 992
No. 993
No. 994
No. 995
No. 996
No. 997
No. 998
No. 999
No. 1000

BRADY
U.S.A. • W. H. BRADY CO.
AUSTRALIA • W. H. BRADY CO.
BELGIUM • W. H. BRADY CO.
CANADA • W. H. BRADY CO.
ENGLAND • W. H. BRADY CO.
FRANCE • W. H. BRADY CO.
GERMANY • W. H. BRADY CO.
HOLLAND • W. H. BRADY CO.
INDONESIA • W. H. BRADY CO.
JAPAN • W. H. BRADY CO.
MALAYSIA • W. H. BRADY CO.
NETHERLANDS • W. H. BRADY CO.
NEW ZEALAND • W. H. BRADY CO.
NORWAY • W. H. BRADY CO.
POLAND • W. H. BRADY CO.
PORTUGAL • W. H. BRADY CO.
ROMANIA • W. H. BRADY CO.
RUSSIA • W. H. BRADY CO.
SCOTLAND • W. H. BRADY CO.
SOUTH AFRICA • W. H. BRADY CO.
SPAIN • W. H. BRADY CO.
SWEDEN • W. H. BRADY CO.
SWITZERLAND • W. H. BRADY CO.
TAIWAN • W. H. BRADY CO.
THAILAND • W. H. BRADY CO.
UNITED STATES • W. H. BRADY CO.
UNITED KINGDOM • W. H. BRADY CO.
WEST GERMANY • W. H. BRADY CO.
YUGOSLAVIA • W. H. BRADY CO.

Handwritten notes on blue paper:
1. 22
2. 22
3. 22
4. 22
5. 22
6. 22
7. 22
8. 22
9. 22
10. 22
11. 22
12. 22
13. 22
14. 22
15. 22
16. 22
17. 22
18. 22
19. 22
20. 22
21. 22
22. 22
23. 22
24. 22
25. 22
26. 22
27. 22
28. 22
29. 22
30. 22
31. 22
32. 22
33. 22
34. 22
35. 22
36. 22
37. 22
38. 22
39. 22
40. 22
41. 22
42. 22
43. 22
44. 22
45. 22
46. 22
47. 22
48. 22
49. 22
50. 22
51. 22
52. 22
53. 22
54. 22
55. 22
56. 22
57. 22
58. 22
59. 22
60. 22
61. 22
62. 22
63. 22
64. 22
65. 22
66. 22
67. 22
68. 22
69. 22
70. 22
71. 22
72. 22
73. 22
74. 22
75. 22
76. 22
77. 22
78. 22
79. 22
80. 22
81. 22
82. 22
83. 22
84. 22
85. 22
86. 22
87. 22
88. 22
89. 22
90. 22
91. 22
92. 22
93. 22
94. 22
95. 22
96. 22
97. 22
98. 22
99. 22
100. 22

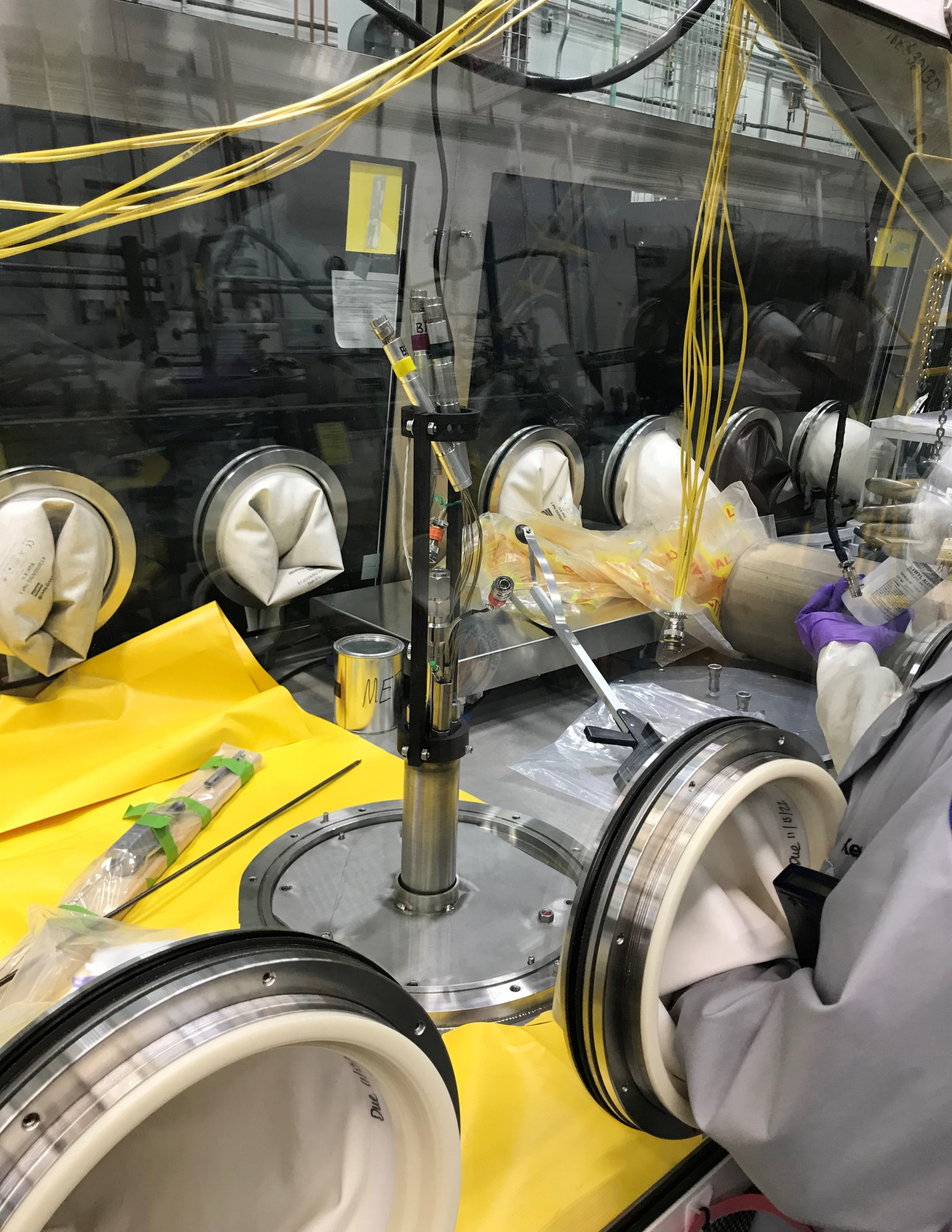
Handwritten notes on blue paper:
A
B
C
D
E
F
G
H
I
J
K
L
M
N
O
P
Q
R
S
T
U
V
W
X
Y
Z
AA
AB
AC
AD
AE
AF
AG
AH
AI
AJ
AK
AL
AM
AN
AO
AP
AQ
AR
AS
AT
AU
AV
AW
AX
AY
AZ
BA
BB
BC
BD
BE
BF
BG
BH
BI
BJ
BK
BL
BM
BN
BO
BP
BQ
BR
BS
BT
BU
BV
BW
BX
BY
BZ
CA
CB
CC
CD
CE
CF
CG
CH
CI
CJ
CK
CL
CM
CN
CO
CP
CQ
CR
CS
CT
CU
CV
CW
CX
CY
CZ
DA
DB
DC
DD
DE
DF
DG
DH
DI
DJ
DK
DL
DM
DN
DO
DP
DQ
DR
DS
DT
DU
DV
DW
DX
DY
DZ
EA
EB
EC
ED
EE
EF
EG
EH
EI
EJ
EK
EL
EM
EN
EO
EP
EQ
ER
ES
ET
EU
EV
EW
EX
EY
EZ
FA
FB
FC
FD
FE
FF
FG
FH
FI
FJ
FK
FL
FM
FN
FO
FP
FQ
FR
FS
FT
FU
FV
FW
FX
FY
FZ
GA
GB
GC
GD
GE
GF
GG
GH
GI
GJ
GK
GL
GM
GN
GO
GP
GQ
GR
GS
GT
GU
GV
GW
GX
GY
GZ
HA
HB
HC
HD
HE
HF
HG
HH
HI
HJ
HK
HL
HM
HN
HO
HP
HQ
HR
HS
HT
HU
HV
HW
HX
HY
HZ
IA
IB
IC
ID
IE
IF
IG
IH
II
IJ
IK
IL
IM
IN
IO
IP
IQ
IR
IS
IT
IU
IV
IW
IX
IY
IZ
JA
JB
JC
JD
JE
JF
JG
JH
JI
JJ
JK
JL
JM
JN
JO
JP
JQ
JR
JS
JT
JU
JV
JW
JX
JY
JZ
KA
KB
KC
KD
KE
KF
KG
KH
KI
KJ
KK
KL
KM
KN
KO
KP
KQ
KR
KS
KT
KU
KV
KW
KX
KY
KZ
LA
LB
LC
LD
LE
LF
LG
LH
LI
LJ
LK
LL
LM
LN
LO
LP
LQ
LR
LS
LT
LU
LV
LW
LX
LY
LZ
MA
MB
MC
MD
ME
MF
MG
MH
MI
MJ
MK
ML
MM
MN
MO
MP
MQ
MR
MS
MT
MU
MV
MW
MX
MY
MZ
NA
NB
NC
ND
NE
NF
NG
NH
NI
NJ
NK
NL
NM
NN
NO
NP
NQ
NR
NS
NT
NU
NV
NW
NX
NY
NZ
OA
OB
OC
OD
OE
OF
OG
OH
OI
OJ
OK
OL
OM
ON
OO
OP
OQ
OR
OS
OT
OU
OV
OW
OX
OY
OZ
PA
PB
PC
PD
PE
PF
PG
PH
PI
PJ
PK
PL
PM
PN
PO
PP
PQ
PR
PS
PT
PU
PV
PW
PX
PY
PZ
QA
QB
QC
QD
QE
QF
QG
QH
QI
QJ
QK
QL
QM
QN
QO
QP
QQ
QR
QS
QT
QU
QV
QW
QX
QY
QZ
RA
RB
RC
RD
RE
RF
RG
RH
RI
RJ
RK
RL
RM
RN
RO
RP
RQ
RR
RS
RT
RU
RV
RW
RX
RY
RZ
SA
SB
SC
SD
SE
SF
SG
SH
SI
SJ
SK
SL
SM
SN
SO
SP
SQ
SR
SS
ST
SU
SV
SW
SX
SY
SZ
TA
TB
TC
TD
TE
TF
TG
TH
TI
TJ
TK
TL
TM
TN
TO
TP
TQ
TR
TS
TU
TV
TW
TX
TY
TZ
UA
UB
UC
UD
UE
UF
UG
UH
UI
UJ
UK
UL
UM
UN
UO
UP
UQ
UR
US
UT
UU
UV
UW
UX
UY
UZ
VA
VB
VC
VD
VE
VF
VG
VH
VI
VJ
VK
VL
VM
VN
VO
VP
VQ
VR
VS
VT
VU
VV
VW
VX
VY
VZ
WA
WB
WC
WD
WE
WF
WG
WH
WI
WJ
WK
WL
WM
WN
WO
WP
WQ
WR
WS
WT
WU
WV
WW
WX
WY
WZ
XA
XB
XC
XD
XE
XF
XG
XH
XI
XJ
XK
XL
XM
XN
XO
XP
XQ
XR
XS
XT
XU
XV
XW
XX
XY
XZ
YA
YB
YC
YD
YE
YF
YG
YH
YI
YJ
YK
YL
YM
YN
YO
YP
YQ
YR
YS
YT
YU
YV
YW
YX
YY
YZ
ZA
ZB
ZC
ZD
ZE
ZF
ZG
ZH
ZI
ZJ
ZK
ZL
ZM
ZN
ZO
ZP
ZQ
ZR
ZS
ZT
ZU
ZV
ZW
ZX
ZY
ZZ

EDX.....	Energy Dispersion X-Ray
EM.....	Electro-mechanical Manipulator
EMPA	Swiss Federal Laboratories for Materials Science and Technology
EMT	Effective Medium Theory
EPRI	Electric Power Research Institute
EQP	Equipment Qualification Process
ESM.....	Electromagnetic Systems Group
F&OR	Functional and Operational Requirements
FAST	Fission Accelerated Steady-state Testing
FCCI	Fuel Cladding Chemical Interaction
FCRD.....	Fuel Cycle Research and Development
FE	Finite Element
FFRD	Fuel Fragmentation, Relocation, and Dispersal
FFT	Fast Fourier Transformation
FGR	Fission Gas Release
FIB.....	Focused Ion Beam
FLAME-CAMP	Femtosecond Laser Ablation Machining & Examination - Center for Active Materials Processing
FMP.....	Five Metal Precipitates
FOR	Functional and Operational Requirements
FPTTEG.....	Fuel Performance and Testing Technical Experts Group
GA	General Atomics
GA-EMS.....	General Atomics – Electromagnetic Systems
GE.....	General Electric
GM	Grid Method
GNF	Global Nuclear Fuels
HAADF	High Angle Annular Dark Field
HBFF.....	High Burnup Fuel Fragmentation
HBu.....	High Burnup

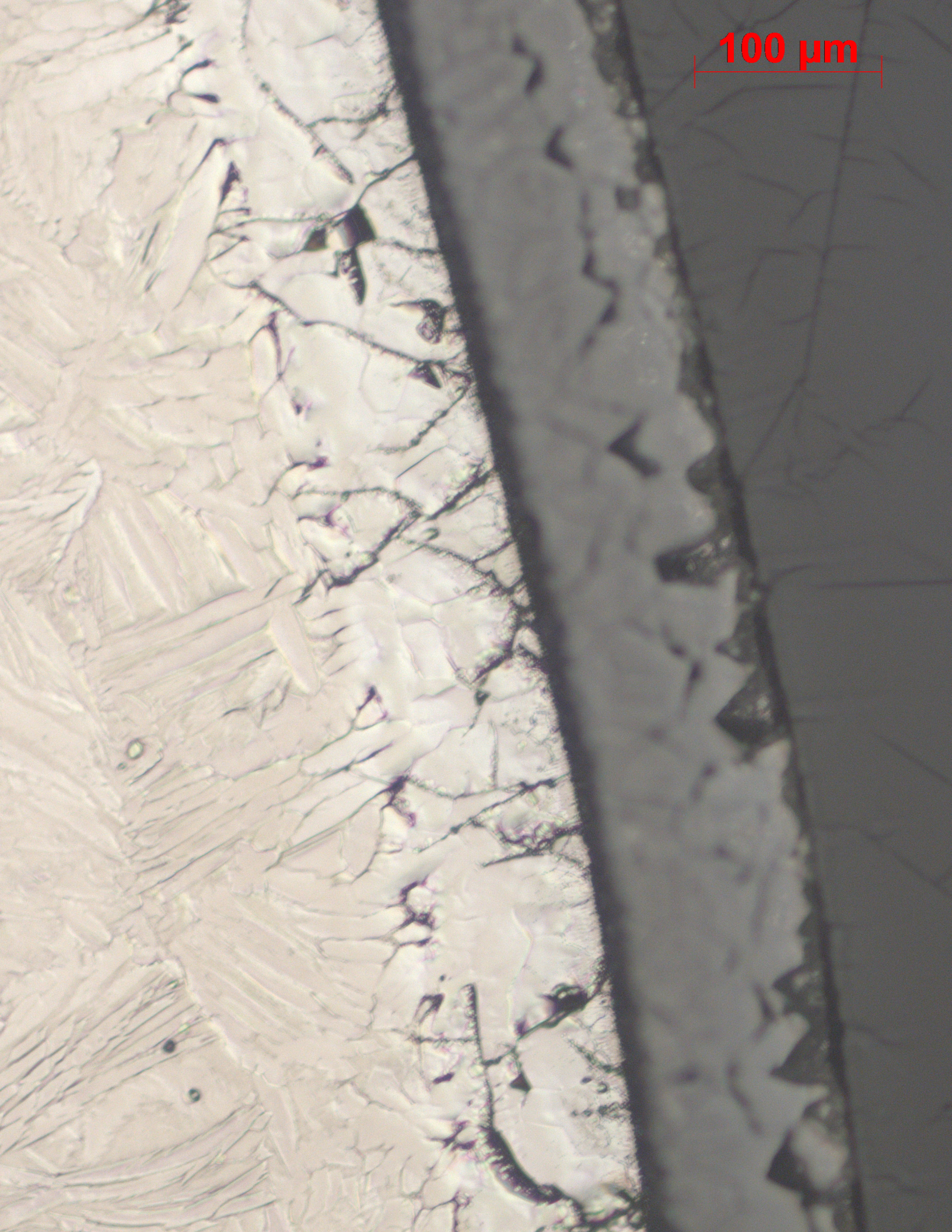
HBWR	Halden Boiling Water Reactor
HEA.....	High Entropy Alloy
HERA	High Burnup Experiments in Reactivity initiated Accidents
HFEF	Hot Fuel Examination Facility
HFIR	High Flux Isotope Reactor
HiPIMS.....	Hybrid High Power Impulse Magnetron Sputtering
HRTEM	High Resolution Transmission Electron Microscopy
IAC	Industry Advisory Committee
ICP-MS.....	Inductively Coupled Plasma Mass Spectrometry
INL	Idaho National Laboratory
JAEA.....	Japanese Atomic Energy Agency
KIT	Karlsruhe Institute of Technology
KTH	Royal Institute of Technology
LAGB.....	Low Angle Grain Boundaries
LANCR.....	Lattice Neutronic Characteristics Evaluation & Research
LANL.....	Los Alamos National Laboratory
LED	Light Emitting Diode
LEXA	Long-term Exposure Autoclave
LFA	Laser Flash Analysis
LOCA.....	Loss of Coolant Accident
LOF.....	Loss of Flow
LS-EVP-FFT	Large Strain Elasto-viscoplastic Fast Fourier Transform
LTA	Lead Test Assembly
LTR.....	Lead Test Rod
LUA.....	Lead Use Assembly
LVDT	Linear Variable Differential Transformer
LWR	Light Water Reactor
MCNP	Monte Carlo N-Particle
MCS	Monte Carlo Simulations

MD	Molecular Dynamics
MFC	Materials and Fuels Complex
MIT	Massachusetts Institute of Technology
MITR.....	Massachusetts Institute of Technology Reactor
MOX.....	Mixed Oxide
MOXTOP.....	Mixed Oxide Transient OverPower
MSCP	Mechanisms-based Single Crystal Plasticity
MSM	Master Slave Manipulator
MTR	Material Test Rod
NCS	Nitrogen Cold Spray
NCSU	North Carolina State University
NE	Nuclear Energy
NEA.....	Nuclear Energy Agency
NEAMS	Nuclear Energy Advanced Modeling and Simulation
NEFT.....	Northeast Flux Trap
NEI.....	Nuclear Energy Institute
NEUP	Nuclear Energy University Project
nRAD	Neutron Radiography
NRC.....	Nuclear Regulatory Commission
ODS.....	Oxide Dispersion Strengthened
OECD	Organisation for Economic Co-operation and Development
OFHC	Oxygen-free High Thermal Conductivity
ORNL	Oak Ridge National Laboratory
OSU	Oregon State University
PEEQ.....	Equivalent Plastic
PGS.....	Precision Gamma Spectroscopy
PI.....	Principal Investigator
PID	Proportional-Integral-Derivative
PIE.....	Post-irradiation Examination

PLS	Proportional Limit Stress
PSA	Probability Safety Analysis
PTE	Post-transient Examinations
PVD	Physical Vapor Deposition
PWR	Pressurized Water Reactor
R&D	Research & Development
RD&D	Research, Development, and Demonstration
RIA	Reactivity-Initiated Accident
RPI	Rensselaer Polytechnic Institute
RTT	Ring Tension Test
RUC	Repeatable Unit Cell
RVE	Representative Volume Element
SATS	Severe Accident Test Station
SEH	Stored-energy Heat Up
SEM	Scanning Electron Microscopy
SERTTA	Static Environment Rodlet Transient Test Apparatus
SFF	Sodium Free Fuel
SFR	Sodium Fast Reactor
SI	Structural Integrity
SiC	Silicon Carbide
SMR	Small Modular Reactor
SNC	Southern Nuclear Company
SNM	Special Nuclear Materials
STEM	Scanning Transmission Electron Microscopy
TCM	Thermal Conductivity Microscope
TD	Theoretical Density
TEM	Transmission Electron Microscopy
tFGR	Transient Fission Gas Release
THOR	Temperature Heat Sink Overpower Response



100 μm



THOR-C	THOR Commissioning
THOR-M	THOR Metallic
TREAT.....	Transient Reactor Test Facility
TWIST	Transient Water Irradiation System in TREAT
UBr.....	University of Bristol
UCB.....	University of California Berkeley
UHT	Ultra-high Temperature
ULS.....	Ultimate Limit States
UN	Uranium Nitride
USC	University of South Carolina
UT.....	University of Tennessee
UTA	University of Texas-Austin
UVa.....	University of Virginia
UW.....	University of Wisconsin
VM	von Mises
VPSC	Visco-Plastic Self-Consistent
VTR	Versatile Test Reactor
WEC.....	Westinghouse Electric Company
XPS.....	X-ray Photoelectron Spectroscopy
XRD.....	X-Ray Diffraction

5.5 DIVIDER PHOTO CAPTIONS



Page 2

SIRIUS-3 in TREAT neutron radiography stand in using the Loop Handling Cask.



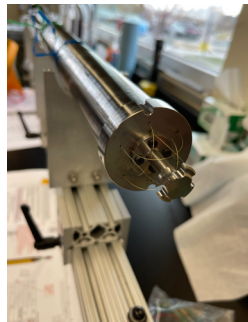
Page 22

Kelly McCary threads the optical fiber for the distributed temperature sensor in the THOR heat sink.



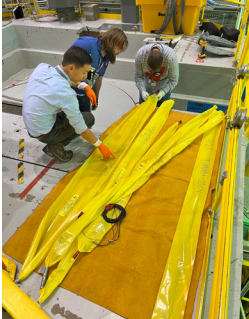
Page 4

THOR-C-2 Assembly in TREAT.



Page 105

Heat sink assembly for the TREAT THOR capsule which was recently irradiated in TREAT to show overpower limits for advanced metallic fuel.



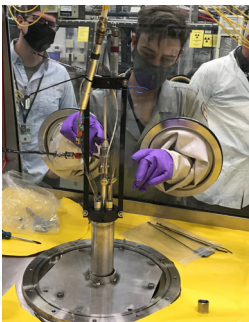
Page 8

Concurrent Testing going into TREAT.



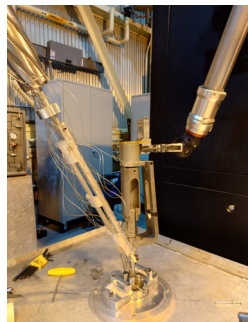
Page 120

THOR-C-3 repair work in progress.



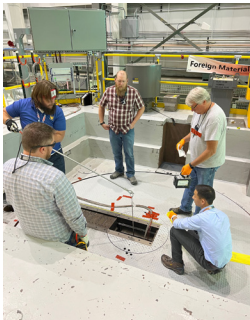
Page 19

Loading sodium into the THOR-C-2 capsule during assembly.



Page 140

Working on mockup testing of remote handling for assembly and disassembly of the THOR experiment capsule.



Page 168

Concurrent Testing going into TREAT.



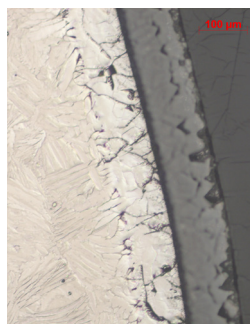
Page 187

THOR-C-2 Assembly in FASB glovebox.



Page 173

ATF-R shipment from TREAT to HFEF.



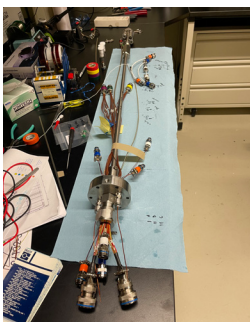
Page 188

Optical microscopy of the ATF-RIA-1-B irradiation experiment tested to failure under RIA conditions in TREAT reveals oxidation and phase transformation of the cladding.



Page 181

Receiving new glove box for TREAT Experiment Support Building (TESB).



Page 182

THOR-C-2 Assembly in HTTL-Instrumentation.

